

Distribution and habitat use of fish in the nearshore ecosystem in the Beaufort and Chukchi Seas.

Johanna J. Vollenweider¹, Ron A. Heintz¹, Kevin M. Boswell², Brenda L. Norcross³, Chunyan Li⁴, Mark B. Barton², Leandra Sousa⁵, Craig George⁵

¹ Auke Bay Laboratories Alaska Fisheries Science Center National Marine Fisheries Service, NOAA Ted Stevens Marine Research Institute, 17109 Point Lena Loop Road Juneau, AK 99801-8626

² Florida International University, 3000 NE 151st St., MSB 359, North Miami, FL 33181

³ University of Alaska, Fairbanks, Institute of Marine Science, School of Fisheries and Ocean Sciences, P.O. Box 757220, Fairbanks, AK 99775-7220

⁴ Louisiana State University, Coastal Studies Institute, 331 Howe-Russell Geocomplex, Baton Rouge, LA, 70803

⁵ North Slope Borough, Department of Wildlife Management, 1795 Ahkovak Street, Barrow, AK, 99723

* Corresponding author: Johanna.Vollenweider@noaa.gov



Prepared under BOEM Award
Award # M12PG00024
Alaska OCS Region
Final Report
January 2017

DISCLAIMER

This study was funded, in part, by the US Department of the Interior, Bureau of Ocean Energy Management, Environmental Studies Program, Washington, DC, through Inter-Agency Agreement Number M12PG00024 with the National Marine Fisheries Service, Alaska Fisheries Science Center. This report has been technically reviewed by BOEM and it has been approved for publication. The views and conclusions contained in this document are those of the authors and should not be interpreted as representing the opinions or policies of the US Government, nor does mention of trade names or commercial products constitute endorsement or recommendation for use.

REPORT AVAILABILITY

To download a PDF file of this Environmental Studies Program report, go to the US Department of the Interior, Bureau of Ocean Energy Management, Environmental Studies Program Information System website and search on OCS Study BOEM 2016-066.

BOEM Environmental Studies Program Office
US Department of the Interior
Bureau of Ocean Energy Management
Environmental Studies Program
Attn: Chief, Division of Environmental Sciences
381 Elden Street, MS HM 3115
Herndon, VA 20170
<http://www.boem.gov/Environmental-Stewardship/Environmental-Studies-Program-Information-System.aspx>

US Department of the Interior
Bureau of Ocean Energy Management
Alaska OCS Region
3801 Centerpoint Drive, Suite 500
Anchorage, AK 99503-5820
Phone: (907) 334-5200
Fax: (907) 334-5202

CITATION

Vollenweider, J. J., R. A. Heintz, K. M. Boswell, B. L. Norcross, C. Li, M. B. Barton, Sousa, L, George, C. 2016. Arctic coastal ecosystems: Evaluating the functional role and connectivity of lagoon and nearshore habitats. Final Report, December 2016, BOEM OCS Study 2016-066.

Table of Contents

Abstract	13
1.0 Introduction.....	13
2.0 Setting the Scene: Habitat Descriptions.....	17
2.1 Geomorphology and Currents	17
2.2 Environmental Parameters	18
2.2.1 Atmospheric Conditions.....	18
2.2.2 Oceanographic Conditions	19
2.2.3 Ice Conditions	19
2.3 References.....	20
3.0 Mesoscale Weather System Induced Flushing of a Multi-inlet Arctic Lagoon in Summer.....	33
3.1 Introduction	33
3.2 Study Area and Instrumentation	34
3.3 Weather Conditions.....	34
3.4 Data Processing and Analysis	35
3.4.1 Correction of Water Level for Air Pressure Effect.....	35
3.4.2 Low Pass Filtering of the ADCP Velocity Data	36
3.4.3 Regression Analysis	36
3.5 Results and Discussion.....	37
3.6 Summary.....	38
3.7 Acknowledgements	39
3.8 References.....	39
A3.0 Chapter 3 Appendix. Supporting Information for “Mesoscale Weather System Induced Flushing of a Multi-inlet Arctic Lagoon in Summer”	45
A3.1 Introduction	45
A3.2 Weather Station Time Series Data	45
A3.3 The WRF Model	57
A3.4 References for the Supplemental Materials	57
4.0 Patterns in Arctic Nearshore Communities Across Multiple Spatial and Temporal Scales	58
4.1 Introduction	58
4.2 Methods.....	58
4.2.1 Study Area	58
4.2.2 Sample Collection.....	58
4.2.3 Determination of Sampling Frequency.....	59
4.2.4 Analytical Approach.....	59
4.4 Results and Discussion.....	60
4.4.1 Spatial Variation in Catch	60
4.4.2 Temporal variation in catch	60
4.4.3 Scales of fish community dynamics	61
4.5 Acknowledgements	62
4.6 References.....	62
5.0 Variance Partitioning for Environmental, Spatial, and Temporal Drivers of Community Structure	101
5.1 Introduction	101
5.2 Methods.....	102
5.2.1 Study Area	102
5.2.2 Sample Collection.....	102

5.2.3 Canonical Correspondence Analysis.....	102
5.2.4 Variance Partitioning.....	103
5.2.5 Explanatory Model Variables.....	103
5.3 Results	105
5.3.1 Forward Selection of Variables	105
5.4 Discussion	106
5.4.1 Environmental Variables	106
5.4.2 Spatial Variables	107
5.4.3 Temporal Variables	107
5.5 References.....	108
6.0 Fish Life History Characteristics: Age, Length, Weight	114
6.1 Introduction	114
6.2 Methods.....	114
6.3 Results and Discussion.....	116
6.3.1 Length-Weight Relationships	116
6.3.2 Length-Age	118
6.4 References.....	122
7.0 Fish Diets.....	151
7.1 Introduction	151
7.2 Methods.....	151
7.2.1 Laboratory methods	151
7.2.2 Descriptive diet analyses	152
7.2.3 Statistical methods	152
7.3 Results and Discussion.....	153
7.4 References.....	157
8.0 Prey Quality of Arctic Marine Fish	194
8.1 Introduction	194
8.2 Methods.....	194
8.2.1 Fish Collections	194
8.2.2 Fish Condition Analyses.....	195
8.3 Results	195
8.4 Discussion	196
8.5 Acknowledgements	197
8.6 References.....	197
9.0 Food Web Analysis (Isotopes)	211
9.1 Introduction	211
9.2 Methods.....	212
9.2.1 Study Area	212
9.2.2 Sample Collection.....	212
9.2.3 Analytical Approach.....	212
9.3 Results	212
9.4 Discussion	213
9.5 References.....	215
10.0 Latitudinal dependence of body condition, growth rate, and stable isotopes of juvenile capelin (<i>Mallotus villosus</i>) in the Bering and Chukchi Seas	221
10.1 Introduction.....	221
10.2 Materials and Methods	222
10.2.1 Fish Collections.....	222
10.2.2 Bomb Calorimetry.....	223
10.2.3 RNA/DNA Analysis	223
10.2.4 Stable Isotopes Analysis.....	224

10.2.5 Stomach Contents.....	224
10.2.6 Data Analysis	224
10.3 Results	224
10.3.1 Energy Allocation	224
10.3.3 Stable Carbon and Nitrogen Isotopes.....	225
10.3.4 Stomach Contents.....	225
10.4 Discussion.....	226
10.4.1 Energy Allocation	226
10.4.2 Stable Carbon and Nitrogen Isotopes.....	227
10.4.3 Stable Carbon Isotopes	227
10.4.4 Stable Nitrogen Isotope	228
10.5 Conclusions	230
10.6 Acknowledgements.....	231
10.7 References.....	231
11.0 Patterns in Basal Resources and Suspended Particulate Matter Compositions in Arctic habitats	245
11.1 Introduction.....	245
11.2 Methods.....	246
11.2.1 Study Area.....	246
11.2.2 Sample Collection and Lab Processing.....	246
11.3 Results	247
11.4 Discussion.....	247
11.5 References.....	248
12.0 Conclusions.....	255
13.0 Synthesis.....	258
13.1 Summary.....	258
13.2 Study area.....	258
13.3 The Point Barrow Ecotone	259
13.3.1 The Alaska Coastal Current connects the Chukchi Sea to the Beaufort Sea	259
13.3.2 Species composition and ages reveal connections between nearshore and offshore	259
13.3.3 Feeding histories through diet analysis and isotopes reveal large scale spatial trends.....	260
13.4 Sources of change	261
13.5 References.....	265
14.0 Management and Policy Implications.....	267
14.0 References.....	268

List of Figures

Figure 1.1 Map of beach seine sites near Point Barrow, Alaska.	15
Figure 2.1 Example of complex habitat deposits from eroded tundra from the DIDSON near the channel between Elson Lagoon and North Salt Lagoon, Barrow, AK.....	21
Figure 2.2 Multibeam (left panel) and DIDSON (right panel) imagery illustrating ice scour marks from the Elson Lagoon- Plover Point sampling station.	22
Figure 2.3 Ice scour in the Chukchi nearshore. Image near Napa Boat Ramp in Barrow	22
Figure 2.4 Multibeam derived imagery of the bathymetric features of sample stations at Plover Point in both the Beaufort Sea and Elson Lagoon.....	23
Figure 2.5 Yearly averaged air temperature at Wiley Post- Will Rogers Memorial Airport.	24
Figure 2.6 Yearly averaged air wind speed at Barrow Airport. The blue line is the mean wind speed in mph averaged through the whole year of each year between 1948 and 2015.....	25
Figure 2.7 Averaged air temperature at Barrow Airport for July and August.....	26
Figure 2.8 Averaged air wind speed at Barrow Airport for July–August.....	27
Figure 2.9 2013 Weekly average wind velocities in Barrow, Alaska. Speed is measured in $m s^{-1}$	28
Figure 2.10 2014 Weekly average wind velocities in Barrow, Alaska. Speed is measured in $m s^{-1}$	29
Figure 2.11 2015 Weekly average wind velocities in Barrow, Alaska. Speed is measured in $m s^{-1}$	30
31	
Figure 2.12 Average weekly surface salinity (PPT) of sample sites by year. Horizontal line represents average salinity across the weeks.	31
Figure 2.13 Average weekly surface temperature ($^{\circ}C$) of sample sites by year.	32
41	
Figure 3.1 Study area.	41
Figure 3.2 Time series of rotated wind components during the study period.....	42
Figure 3.3 Comparison of observed and regression model produced subtidal flows in and out of the lagoon (positive out of the lagoon onto the shelf).....	43
Figure 3.4 Schematic snapshots of the wind vectors based on the WRF model results showing the two wind conditions resulting in two different flow conditions	44
Figure A1. Weather data.	46
Figure A2. Weather map 1 at 0000Z, Aug. 19, 2013.....	47
Figure A3. Weather map 2 at 0000Z, Aug. 20, 2013.....	48
Figure A4. Weather map 3 at 0300Z, Aug. 21, 2013.....	49
Figure A5. Weather map 4 at 0000Z, Aug. 22, 2013.....	50
Figure A6. The velocity profiles time series from the ADCP.....	51
Figure A7. The velocity time series from the ADCP	52
Figure 4.1 2013 Arctic cod catch by week.	64
Figure 4.2 2013 capelin catch by week.	65
Figure 4.3 2013 fourhorn sculpin catch by week.	66
Figure 4.4 2013 Pacific sand lance catch by week.....	67
Figure 4.5 2013 saffron cod catch by week.....	69
Figure 4.6 2014 Arctic cod catch by week.	70
Figure 4.7 2014 capelin catch by week.	72
Figure 4.8 2014 fourhorn sculpin catch by week.....	73
Figure 4.9 2014 Pacific sand lance catch by week.....	74
Figure 4.10 2014 saffron cod catch by week.	75
Figure 4.11 2015 Arctic cod catch by week.	76
Figure 4.12 2015 capelin catch by week.....	77
Figure 4.13 2015 fourhorn sculpin catch by week.	78
Figure 4.14 2015 Pacific sand lance catch by week.....	79
Figure 4.15 2015 saffron cod catch by week.....	80
Figure 4.16 A Non-parametric Dimensional Scaling model representing Bray-Curtis dissimilarity in a two dimensional space.	81

Figure 4.17 Community composition of all beach seine samples broken down by water body (x-axis) represented by relative abundance of all species caught.	82
Figure 4.18 Community composition of all beach seine samples broken down by year (x-axis) represented by relative abundance of all species caught.	83
Figure 4.19 Weekly species richness of beach seine catches by year and water body.....	84
Figure 4.20 Pie charts of community composition of all beach seine samples broken down by water body and year (x-axis) and week (y-axis) represented by relative abundance of all species caught.	85
Figure 4.21 Community composition of all beach seine samples broken down by water body and year (x-axis) represented by relative abundance of all species caught.	86
Figure 5.1 A theoretical representation of variance partitioning among three explanatory variable matrices (Environmental, Spatial, and Temporal).	111
Figure 5.2 A diagrammatical representation of Beach Oriented Wind Direction (BOWD).	112
Figure 5.3. A proportional representation of partitioned variance explained by ENV (green), SPT (grey) and TMP (blue) of the total variance in the community composition matrix (ASP, orange).	113
Figure 6.1 Salmonidae: <i>Coregonus sardinella</i> (Least Cisco).	124
Figure 6.2 Salmonidae: <i>Coregonus sardinella</i> (Least Cisco).	124
Figure 6.3 Salmonidae: <i>Coregonus sardinella</i> (Least Cisco).	125
Figure 6.4 Osmeridae: <i>Mallotus villosus</i> (Capelin).	125
Figure 6.5 Osmeridae: <i>Mallotus villosus</i> (Capelin).	126
Figure 6.6 Osmeridae: <i>Mallotus villosus</i> (Capelin).	126
Figure 6.7 Osmeridae: <i>Mallotus villosus</i> (Capelin).	127
Figure 6.8 Osmeridae: <i>Osmerus mordax</i> (Rainbow Smelt).	127
Figure 6.9 Osmeridae: <i>Osmerus mordax</i> (Rainbow Smelt).	128
Figure 6.10 Osmeridae: <i>Osmerus mordax</i> (Rainbow Smelt).	128
Figure 6.11 Osmeridae: <i>Osmerus mordax</i> (Rainbow Smelt).	129
Figure 6.12 Gasterosteidae: <i>Pungitius pungitius</i> (Ninespine Stickleback).	129
Figure 6.13 Gasterosteidae: <i>Pungitius pungitius</i> (Ninespine Stickleback).	130
Figure 6.14 Gadidae: <i>Boreogadus saida</i> (Arctic Cod).	130
Figure 6.15 Gadidae: <i>Boreogadus saida</i> (Arctic Cod).	131
Figure 6.16 Gadidae: <i>Boreogadus saida</i> (Arctic Cod).	131
Figure 6.17 Gadidae: <i>Boreogadus saida</i> (Arctic Cod).	132
Figure 6.18 Gadidae: <i>Eleginus gracilis</i> (Saffron Cod).	132
Figure 6.19 Gadidae: <i>Eleginus gracilis</i> (Saffron Cod).	133
Figure 6.20 Gadidae: <i>Eleginus gracilis</i> (Saffron Cod).	133
Figure 6.21 Gadidae <i>Eleginus gracilis</i> (Saffron Cod).	134
Figure 6.22 Cottidae: <i>Megalacottus platycephalus</i> (Belligerent sculpin).	134
Figure 6.23 Cottidae: <i>Megalacottus platycephalus</i> (Belligerent sculpin).	135
Figure 6.24 Cottidae: <i>Megalacottus platycephalus</i> (Belligerent sculpin).	135
Figure 6.25 <i>Myoxocephalus</i> spp. (sculpin).	136
Figure 6.26 Cottidae: <i>Myoxocephalus</i> spp. (sculpin).	136
Figure 6.27 Cottidae: <i>Myoxocephalus</i> spp. (sculpin).	137
Figure 6.28 Cottidae: <i>Myoxocephalus</i> spp. (sculpin).	137
Figure 6.29 Agonidae: <i>Aspidophoroides monopterygius</i> (Alligatorfish).	138
Figure 6.30 Stichaeidae: <i>Lumpenus fabricii</i> (Slender eelblenny).	138
Figure 6.31 Stichaeidae: <i>Lumpenus fabricii</i> (Slender eelblenny).	139
Figure 6.32 Stichaeidae: <i>Lumpenus fabricii</i> (Slender eelblenny).	139
Figure 6.33 Stichaeidae: <i>Lumpenus fabricii</i> (Slender eelblenny).	140
Figure 6.34 Stichaeidae: <i>Stichaeus punctatus</i> (Arctic Shanny).	140
Figure 6.35 Stichaeidae: <i>Stichaeus punctatus</i> (Arctic Shanny).	141
Figure 6.36 Stichaeidae: <i>Stichaeus punctatus</i> (Arctic Shanny).	141
Figure 6.37 Stichaeidae: <i>Stichaeus punctatus</i> (Arctic Shanny).	142
Figure 6.38 Ammodytidae: <i>Ammodytes hexapterus</i> (Pacific Sand Lance).	142
Figure 6.39 Ammodytidae: <i>Ammodytes hexapterus</i> (Pacific Sand Lance).	143

Figure 6.40 Ammodytidae: <i>Ammodytes hexapterus</i> (Pacific Sand Lance).....	143
Figure 6.41 Ammodytidae: <i>Ammodytes hexapterus</i> (Pacific Sand Lance).....	144
Figure 6.42 Pleuronectidae: <i>Limanda aspera</i> (Yellowfin sole).....	144
Figure 6.43 Pleuronectidae: <i>Liopsetta glacialis</i> (Arctic Flounder).....	145
Figure 6.44 Pleuronectidae: <i>Liopsetta glacialis</i> (Arctic Flounder).....	145
Figure 6.45 Pleuronectidae: <i>Liopsetta glacialis</i> (Arctic Flounder).....	146
Figure 6.46 Pleuronectidae: <i>Limanda proboscidea</i> (Longhead dab).....	146
Figure 7.1 Percent mean weight (%MW) of major prey groups (including unidentified prey) consumed by nine fish species collected from Beaufort Sea, Chukchi Sea, and Elson Lagoon regions during ACES 2013 and 2014.....	160
Figure 7.2 Cumulative prey curves summarizing the diet compositions of nine fish species throughout the Beaufort Sea, Chukchi Sea, and Elson Lagoon regions during ACES 2013 and 2014.	161
Figure 7.3 Nonmetric multidimensional scaling (nMDS) ordination showing the diet compositions of nine fish species within the Beaufort Sea during ACES 2013 and 2014.....	162
Figure 7.4 Percent mean weight (%MW) of major prey groups (including unidentified prey) consumed by nine fish species collected from the Beaufort Sea during ACES 2013 and 2014.	163
Figure 7.5 Nonmetric multidimensional scaling (nMDS) ordination showing the diet compositions of eight fish species within the Chukchi Sea during ACES 2013 and 2014.	164
Figure 7.6 Percent mean weight (%MW) of major prey groups (including unidentified prey) consumed by eight fish species collected from the Chukchi Sea during ACES 2013 and 2014.	165
Figure 7.7 Nonmetric multidimensional scaling (nMDS) ordination showing the diet compositions of nine fish species within Elson Lagoon during ACES 2013 and 2014.	166
Figure 7.8 Percent mean weight (%MW) of major prey groups (including unidentified prey) consumed by eight fish species collected from Elson Lagoon during ACES 2013 and 2014.	167
Figure 7.9 <i>M. villosus</i> diet composition plotted by 10 to 100 mm size bins to visualize changes in diet with increasing body size.	168
Figure 7.10 <i>O. mordax</i> diet composition plotted by 10 to 100 mm size bins to visualize changes in diet with increasing body size.	169
Figure 7.11 <i>B. saida</i> diet composition plotted by 10 mm size bins to visualize changes in diet with increasing body size.	170
Figure 7.12 <i>Myoxocephalus</i> spp. diet composition plotted by 10 to 100 mm size bins to visualize changes in diet with increasing body size.	171
Figure 7.13 <i>A. hexapterus</i> diet composition plotted by 10 mm size bins to visualize changes in diet with increasing body size.	172
Figure 8.1 Station design of the projects from which samples were obtained.....	199
Figure 8.2 Average energy density (kJ/g wet mass) of all sampled Arctic fish species.....	200
Figure 8.3 Average energy density (kJ/g wet mass) by family of Arctic fish species.	201
Figure 8.4 Energy density (ED; kJ/g) as a function of length for Arctic fish species.....	202
Figure 8.5 Length-energy density relationship of Pacific herring and capelin collected in the summer (July–September) from two Large Marine Ecosystems, the Arctic and the Gulf of Alaska.	203
Figure 8.6 Average total energy content (kJ) of all sampled Arctic fish species.....	204
Figure 8.7 Average total energy (kJ) by family of Arctic fish species.....	205
Figure 8.8 Individual value plot of lengths (mm) of Arctic fish evaluated for energetics.....	206
Figure 8.9 Energy density (kJ/g wet mass) in relation to length (mm) (top panel) and total energy content (kJ) in relation to length (bottom panel) of all Arctic species.	207
Figure 9.1 Stable isotope biplots of all samples.....	219
Figure 10.1 Map of Alaskan waters showing sampling locations of juvenile capelin collected.....	235
Figure 10.2 Linear regression between energy density and RNA/DNA ratios.....	236
Figure 10.3 General Additive Models for energy density.....	237
Figure 10.4 Linear regressions of energy density.....	239
Figure 10.5 General Additive Models for energy density.....	240
Figure 10.6 GAM of surface temperature with a smoothing function on latitude.....	242
Figure 10.7 Average contributions by weight of prey type in the stomach contents of the analyzed capelin for 6 of the 7 regional groups identified in Table 1.....	243
Figure 11.1 Graphical representation of CPUE for each size class separated by week.	252

Figure 11.2 Relative abundance of Suspended Particulate Matter (SPM) 253
Figure 13.1 Schematic of ocean currents converging at Point Barrow 264

List of Tables

Table 1.1 Sampling station names and locations surveyed during summer 2013, 2014 and 2015. * indicates sites historically sampled by Johnson and Thedinga from 2004–2009.....	16
Table A1. Regression of subtidal velocity with wind components for the time period when the southern station using HOBO was measuring water level.....	53
Table A2. Regression of subtidal velocity with pressure difference and wind components for the time period when the southern station using HOBO was measuring water level.....	54
Table A3. Regression of subtidal velocity with wind velocity components for the entire time period when the ADCP was measuring velocity.	55
Table A4. Regression of subtidal velocity with wind velocity components and their squares for the entire time period when the ADCP was measuring velocity.	56
Table 4.1 Fish caught by sampling method.....	87
Table 4.2 Productivity in the three water bodies and three years from beach seine sampling.	89
Table 4.3 Frequency of occurrence (%) of fish in beach seine catches throughout 2013-2015 field seasons.	90
Table 4.4 Frequency of occurrence (%) of fish in beach seine catches throughout 2013-2015 field seasons.	91
Table 4.5 2013 average catch per unit effort (CPUE) of the Chukchi Sea by sampling week.....	92
Table 4.6 2013 average catch per unit effort (CPUE) of the Beaufort Sea by sampling week.....	93
Table 4.7 2013 average catch per unit effort (CPUE) of Elson Lagoon by sampling week.	94
Table 4.8 2014 average catch per unit effort (CPUE) of the Chukchi Sea by sampling week.....	95
Table 4.9 2014 average catch per unit effort (CPUE) of the Beaufort Sea by sampling week.....	96
Table 4.10 2014 average catch per unit effort (CPUE) of Elson Lagoon by sampling week.	97
Table 4.11 2015 average catch per unit effort (CPUE) of the Chukchi Sea by sampling week.	98
Table 4.12 2015 average catch per unit effort (CPUE) of the Beaufort Sea by sampling week.	99
Table 4.13 2015 average catch per unit effort (CPUE) of Elson Lagoon by sampling week.	100
Table 5.1 A summary of the variables that were entered into the forward selection process.	110
Table 6.1 Number of species or genera measured in the laboratory by region (Chukchi Sea, Beaufort Sea, Elson Lagoon) or without a known station location for ACES 2013-2014.....	147
Table 6.2 Length-weight relationships for 14 species and one genus.....	148
Table 6.3 Number of species or genus (denoted with *) estimated for age in the laboratory by region (Chukchi Sea, Beaufort Sea, Elson Lagoon) or without a known station location for ACES 2013-2014.....	150
Table 7.1 Common prey items of <i>C. sardinelli</i> , <i>M. villosus</i> , <i>O. mordax</i> , <i>B. saida</i> , <i>E. gracilis</i> , <i>Myoxocephalus</i> spp., <i>L. fabricii</i> , <i>S. punctatus</i> , and <i>A. hexapterus</i> as detailed by historical sources.	173
Table 7.2 Common predators of <i>C. sardinelli</i> , <i>M. villosus</i> , <i>O. mordax</i> , <i>B. saida</i> , <i>E. gracilis</i> , <i>Myoxocephalus</i> spp., <i>L. fabricii</i> , <i>S. punctatus</i> , and <i>A. hexapterus</i> as detailed by historical sources.	174
Table 7.3 Percent mean weight (%MW) of prey consumed by nine fish species throughout the Beaufort Sea, Chukchi Sea, and Elson Lagoon regions during ACES 2013 and 2014.....	175
Table 7.4 Counts of prey eaten by nine fish species throughout the Beaufort Sea, Chukchi Sea, and Elson Lagoon regions during ACES 2013 and 2014.	177
Table 7.5 Results from overall permutational multivariate analysis of variance (PERMANOVA) relating fish species and region (Beaufort Sea, Chukchi Sea, Elson Lagoon) to fish diet compositions.	179
Table 7.6 Results from PERMANOVA and post-hoc comparisons exploring the interaction between regions and species (see Table 6.5).....	180
Table 7.7 Percent mean weight (%MW) of prey consumed by nine fish species in the Beaufort Sea during ACES 2013 and 2014.	185
Table 7.8 Percent mean weight (%MW) of prey consumed by nine fish species in the Chukchi Sea during ACES 2013 and 2014.	187
Table 7.9 Percent mean weight (%MW) of prey consumed by nine fish species in Elson Lagoon during ACES 2013 and 2014.....	189

Table 7.10 Results from PERMANOVA and post-hoc comparisons exploring the interaction between species and regions (see Table 6.5).....	191
Table 7.11 Results from PERMANOVA, used to examine the effect of fish body size on diet composition.	193
Table 8.1 Survey details of the projects from which samples were obtained	208
Table 8.2 Values indicate mean + standard error, (sample size).....	209
Table 8.3 Correlation of energy density (ED; kJ/g) to fish length from linear regression for 5 species of Arctic fish.....	210
Table 9.1 A summary of isotopic data by species or species group.....	220
Table 10.1 Details of sample sizes and regional group differentiation.	244
Table 11.1 Physical attributes used to categorize particles in the Flowcam images.	254

Abstract

The Arctic nearshore is a habitat expected to be impacted differently from offshore, pelagic regions from the effects of changing sea ice conditions, coastal erosion, increased ship traffic and infrastructure, and oil development. Much work has been done to inventory fish communities in the coastal region where fish and their predators are known to be important resources for subsistence users. The environmental conditions structuring nearshore fish community composition is less understood but critical in understanding and predicting future scenarios. This study was a collaborative effort from a group of scientists with expertise in various marine fields. We characterized nearshore fish communities in three converging waterbodies in the area adjacent to Point Barrow, Alaska, including the Chukchi and Beaufort Seas, and Elson Lagoon. Fish were sampled using beach seines at 12 sites on a weekly basis throughout the summer, ice-free season from July – August in two years, 2013-2014, under funding provided by the Bureau of Ocean Energy Management and the North Pacific Research Board. We enumerated seasonal changes in fish community composition and connectivity between the three water bodies in relation to oceanographic conditions, and described fish diet (stomach content analysis and isotope analysis of the fish), size, age, and body condition. In 2015 we augmented the study with funding provided by the North Slope Borough (NSB) to use a fully integrated ecosystem survey approach, with the addition of offshore oceanography and zooplankton availability. This final report details the findings from 2013-2014, with some inclusions of data from 2015. Full synthesis of 2015 findings will be documented in a final report to the NSB in 2018. This report is structured in a series of chapters written by different authors describing background information, habitat descriptions of the study area, chapters describing the study components, and an overall synthesis with conclusions.

1.0 Introduction

The goal of this project is to develop a detailed characterization of nearshore Arctic fish communities and their habitats in order to better understand the ecological function of the coastal habitats fringing the Northern Bering Chukchi Sea and Beaufort Sea Arctic Large Marine Ecosystems. Nearshore habitats and lagoon systems in the Chukchi and Beaufort Seas are characteristically low relief and shallow (< 20 m) with coarse to fine sediments. Episodic storms and waves can restructure the benthos in water depths to 15 m while seasonal ice scouring can have effect in water depth of more than 40 m (Barnes et al. 1984). Despite the value of nearshore habitats as fish nurseries at lower latitudes, there is little information about nearshore fish communities and habitat in the Arctic. The value of these habitats to Arctic fish is unclear because ice scour remodels much of the nearshore each spring. Regardless, more than 30 fish species have been identified using lagoons and their environs including all life stages of forage fish species (Logerwell et al. 2015). Freshwater inputs to lagoons may foster spawning by Arctic cod (*Boreogadus saida*), provide a prolonged growing season (Bouchard and Fortier 2011) and thereby link lagoon systems to the productivity of offshore habitats. Also important, nearshore habitats and lagoons are focal areas for subsistence harvest by local hunters.

The objective of this study was to characterize Arctic fish communities in nearshore habitats by observing seasonal changes in communities in a variety of habitats near Point Barrow, Alaska, including the Chukchi Sea, Beaufort Sea, and Elson Lagoon (Figure 1). Additionally, we sought to understand habitat quality of the different water bodies through the analysis of energy content of fish. To this end, nearshore fish were sampled at multiple beach seine sites within each water

body on a weekly basis during the ice-free period in 2013 and 2014 (Table 1). Fish from catches were identified, enumerated, measured, and retained for analysis of energetic content. To augment this study with an integrated ecosystem approach, funding was received from the North Pacific Research Board to include 1) a more thorough characterization of fish utilizing the different habitats by aging the fish 2) additional measures of habitat quality including fish diet, and isotopic composition, and 3) environmental and oceanographic currents structuring variability in fish communities. Additional funding was received from the North Slope Borough to continue a third year of sampling in 2015 to examine annual variability, as well as trawl sampling immediately offshore of the beach seine sites.

The combination of these funding sources and areas of expertise promoted the evaluation of three main hypotheses:

H₁: There will be no difference in the spatial patterns or habitat association of fish communities as a function of habitat designation or along functional habitat gradients (depth, salinity, temperature).

H₂: Size, energy content, feeding ecology, and age structure of targeted species will not vary among habitats.

H₃: There will be no detectable linkages in productivity pathways between lagoon and nearshore habitats based on energetics, growth, and isotopic composition of fishes.

We anticipated that differences in the characteristics of water in lagoons and coastal currents would provide nearshore fishes with a range of habitats and movement of water in and out the lagoons would create a mosaic of these habitats. Consequently, our analyses included efforts to characterize habitats and their dynamics. Ultimately, we related fish community structure and population data to these habitat characteristics. Finally, we considered the importance of these habitats to fish productivity in the Northern Bering Chukchi Sea and Beaufort Sea Arctic Large Marine Ecosystems.

This report includes results from the other funding sources to provide a more synoptic understanding of Arctic nearshore fish communities. The report is structured into chapters authored by different researchers describing the specific components of the project. Some of the chapters have been published, submitted to publication or are sections of PhD or masters dissertations. The first two chapters set the scene of the study area, describing the characteristics of the habitats we sampled and their dynamics in relation to local meteorological conditions. Chapters 3 and 4 describe the fish communities and relate community structure to habitat features to test hypothesis H₁. Data for testing hypothesis H₂ are found in Chapters 5-9 where characteristics of the fish populations such as fish age, length and weight, diet, energy content, and trophodynamics are related to habitat features. Chapter 10 is an initial summarization and synthesis of the project components. Further synthesis efforts are underway as part of the North Slope Borough-funded project, with incorporation of oceanographic data in the region between the very nearshore (evaluated here) and offshore fish assessments to examine the connectivity between these regions, as well as characterization of the nearshore zooplankton prey field.

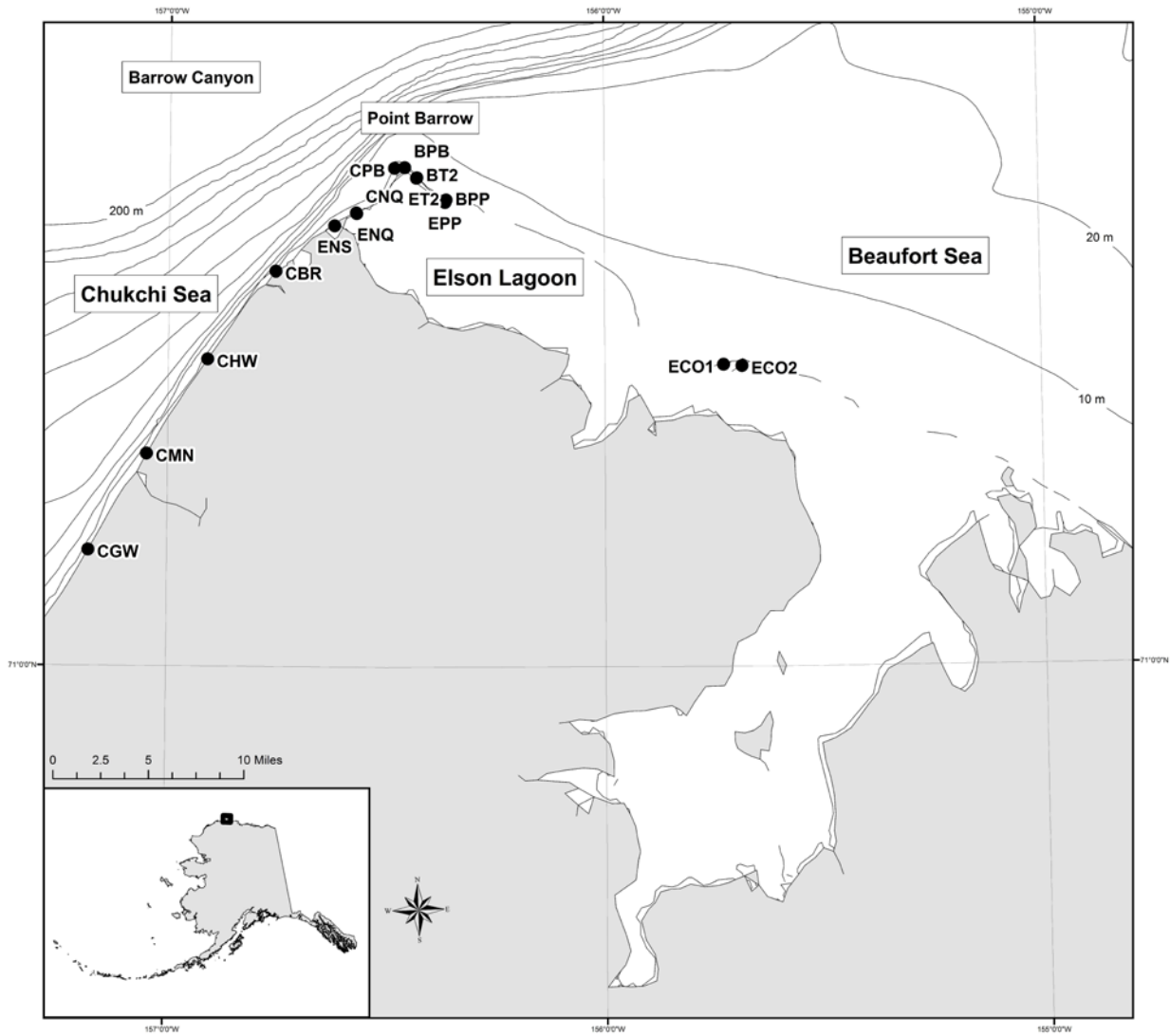


Figure 1.1 Map of beach seine sites near Point Barrow, Alaska.

Table 1.1 Sampling station names and locations surveyed during summer 2013, 2014 and 2015. * indicates sites historically sampled by Johnson and Thedinga from 2004–2009.

Water Body	Site Code	Site Name	Latitude	Longitude
Beaufort Sea	BPB	Beaufort Point Barrow	71.3861	-156.4595
Beaufort Sea	BPP	Beaufort Plover Point	71.3612	-156.3642
Beaufort Sea	BT2	Beaufort Transect 2	71.3783	-156.4314
Chukchi Sea	CBR	Chukchi Boat Ramp*	71.3056	-156.7550
Chukchi Sea	CGW	Chukchi Gray Whale*	71.0897	-157.1791
Chukchi Sea	CHW	Chukchi Hollywood*	71.2375	-156.9101
Chukchi Sea	CMN	Chukchi Monument*	71.1644	-157.0481
Chukchi Sea	CNQ	Chukchi Niksiraq*	71.3510	-156.5706
Chukchi Sea	CPB	Chukchi Point Barrow*	71.3856	-156.4830
Elson Lagoon	ECO1	Elson Cooper Island	71.2333	-155.7281
Elson Lagoon	ECO2	Elson Cooper Island	71.2322	-155.6858
Elson Lagoon	ENQ	Elson Niksiraq	71.3504	-156.5697
Elson Lagoon	ENS	Elson North Salt Lagoon	71.3409	-156.6203
Elson Lagoon	EPP	Elson Plover Point	71.3592	-156.3665
Elson Lagoon	ET2	Elson Transect 2	71.3779	-156.4324

2.0 Setting the Scene: Habitat Descriptions

K. Boswell, J. Vollenweider, R. Heintz

The Arctic is among the most dynamic ecosystems on the globe, experiencing pervasive seasonal changes in temperature and sea ice coverage, with the potential for colonization of new species through range extensions (Rand and Logerwell 2011). It is a region in which there are increasing potential threats from oil and gas exploration, shipping and infrastructure development. An important, yet not well studied component of this dynamic ecosystem, is the coastal zone, comprised of estuarine lagoons and nearshore coastal habitats. These coastal ecosystems are generally characterized by a matrix of shallow lagoons and barrier islands on the edge of an expansive shallow shelf bordered by the Chukchi and Beaufort Seas. For the purposes of this project, the study area is the nearshore region within 30 km of Barrow, Alaska. In this region we identified three main habitat types which represent the main water bodies including the Chukchi Sea, Beaufort Sea, and Elson Lagoon, where sampling effort was focused and are described below (Figure 1.1).

2.1 Geomorphology and Currents

The coastal plain near Barrow, Alaska is generally comprised of Quaternary deposits and range from gravel to sand, with a progression to fining silty sand deposits offshore mixed with gravel (Phillips and Reiss 1985). In the lagoon habitats, which are protected by a barrier-island complex, the dominant substrate is silt, mud and clay (Dasher et al. 2016; Naidu et al. 1982), often with a flocculant layer of organic material from nearby eroded tundra. In areas very near the vegetated edge, large complex features were detected where eroded tundra was released into the shallow water margins (Figure 2.1). These deposits are often reworked by physical processes, largely mediated by meteorological events through storm surge and wave activity or by active gouging from ice in the coastal zone (Phillips and Reiss 1985). The impacts of ice have been documented as deep as 52 m (Phillips and Reiss 1985), and were often seen in multibeam data collected during our study with the autonomous vessel in much shallower waters (Figures 2.2 and 2.3 and Supplementary data). Thus this region and the substrates which comprise the sampling area where our study was focused is inherently variable and emphasizes the overall importance of understanding how the dominant processes act to structure the physical and biological attributes in the nearshore.

Near Point Barrow, a complex hydrodynamic interaction occurs between the Chukchi and Beaufort Seas, and their respective coastal currents, and results in a physically and biologically dynamic environment. In this area, the Alaska Coastal Current (ACC) is compressed along the Chukchi coast and transports water and material northward toward Point Barrow and intersects the westward flowing Beaufort gyre near Barrow Canyon (Phillips and Reiss 1985; Aagaard and Roach 1990; Ashjian et al. 2010). Adjacent to this is the strong tidally and storm driven flow between the Beaufort Sea and the Elson Lagoon system (see Chapters 2 and 3) which is connected to the Beaufort Sea via a deep inlet near Barrow (Figure 2.4).

In this study, we examined the how meteorological forcing and variation in currents structure the biological processes in the Arctic nearshore. We selected stations that represented these three distinct water bodies, allowing for the examination of the linkages between lagoons and nearshore habitats across the ice free period (July–August). Sample stations along the Chukchi

Sea were historically visited annually in 2007-2009 by Thedinga et al. (2013) and were sampled again in 2012 by Boswell and Heintz. In addition, stations along the Beaufort Sea and the western margin of Elson Lagoon were added to the survey design. The climactic variation in the Alaskan Arctic manifests in 'warm' and 'cold' thermal regimes as a result of Pacific water through the Bering Strait as well as atmospheric temperature (Thedinga et al. 2013, Luchin and Panteleev 2014). Therefore, we consider temperature as an important factor structuring the nearshore communities.

2.2 Environmental Parameters

2.2.1 Atmospheric Conditions

Atmospheric conditions were measured throughout the duration of the study period (wind speed m s^{-1} , air temperature $^{\circ}\text{C}$) from a weather station installed near the Barrow Arctic Research Center facility which is 1 km distant from the nearest beach seine site and 11 km distant from Point Barrow. In addition, we reference the atmospheric data collected at the Wiley Post-Will Rogers Memorial Airport, in Barrow (<http://www.wrcc.dri.edu/cgi-bin/cliMAIN.pl?akbarr>) to compare the recent measures with the historical trends.

The historical annual mean air temperature ranged between -15 and -7 $^{\circ}\text{C}$ with an overall mean of -11.4 $^{\circ}\text{C}$ for the time period of 1948 to 2015 (Figure 2.5). The record shows almost no trend between 1948 and 1980, however a clear rapid increasing trend was observed following 1980. The average air temperature of all three study years, 2013 (-8.4 $^{\circ}\text{C}$), 2014 (-8.0 $^{\circ}\text{C}$), and 2015 (-8.9 $^{\circ}\text{C}$), were above 1.5 standard deviations (SD) of the mean of the entire record between 1948 and 2015.

The historical annual mean wind speed at the airport ranged between 10 and 14 mph with an overall mean of 12.3 mph for the time period of 1948 to 2015. The record indicated fluctuations in wind speed between 1948 and 2015. The average wind speeds in two of the study years, 2013 (13.4 mph) and 2014 (13.5 mph), were above 1 SD of the mean for the entire record while the wind speed in 2015 (12.9 mph) was slightly less and within 1 SD of the time series (Figure 2.6).

The July-August mean air temperature at Barrow airport (Figure 2.7) ranges between 0.5 and 7.8 $^{\circ}\text{C}$ with a mean of 3.9 $^{\circ}\text{C}$ for the time period of 1948 to 2015. It is interesting to note that the 2013 mean air temperature for July - August was about 1.5 $^{\circ}\text{C}$ higher than the average of the whole record (+1 SD) while that of 2014 was about 1.5 $^{\circ}\text{C}$ lower (-1 SD) than the average of the whole record (the July-August mean air temperature for 2013 was 5.3 but 2.6 $^{\circ}\text{C}$ for 2014). The mean summer temperature of 2015 (3.8 $^{\circ}\text{C}$) was nearly the mean of the last 68 years summer temperatures.

The July-August mean wind speed at Barrow airport (Figure 2.8) ranges between 9 and 15 mph with a mean of ~ 12 mph for the time period of 1948 to 2015. The record shows fluctuation in wind speed between 1948 and 2015. The 2013 value is lower while the 2014 value is higher than the average of the whole record. Therefore, 2013 was warmer and calmer than the climatological mean while 2014 was colder and windier than the climatological mean.

Average weekly wind velocities in July and August were relatively consistent in 2013-2015 (Figures 2.9 – 2.11). Wind speeds ranged from 3.4 – 8.8 m s⁻¹ across all summers, averaging 5.1, 5.7, and 5.4 m s⁻¹ in 2013, 2014, 2015 respectively. Average weekly wind direction was predominantly from the south, with only one occurrence of wind direction coming from the north during week 30 of 2015. In 2013 wind direction was most consistently from the south (44% of the weeks), southwest in 2014 (56% of the weeks), and southeast in 2015 (67% of the weeks).

2.2.2 Oceanographic Conditions

Oceanographic conditions were measured during each fish sampling event. After each beach seine was completed, a YSI EXO2 Data Sonde was placed in the water 5 meters upcurrent of the location where the beach seine was performed. The sonde was placed on the substrate with the assumption that water chemistry is homogenous at such shallow depths and near to the shore where wave action keeps the water column well-mixed. The sonde remained in the water recording temperature (°C) and salinity (ppt) while the catch was processed to allow the probes to equilibrate (at least 10 minutes).

Across all water bodies, water temperatures were significantly colder in the summer of 2014 (3.3 °C) than 2013 and 2015 (5.7 °C each year) (ANOVA $p = 0.003$; Figures 2.12 – 2.15). Elson Lagoon was consistently warmer than the two marine water bodies, particularly in the summer of 2014 when the lagoon (5.3 °C) was more than twice as warm as the Chukchi (2.6 °C) and Beaufort (2.0 °C) Seas. Water temperature fluctuated significantly from week to week within a given year/water body without a consistent pattern.

Elson Lagoon was significantly fresher (22.1 ppt across all weeks and years) in the summer than the Chukchi Sea (30.0 ppt) and Beaufort Sea (28.0 ppt) (ANOVA $p < 0.000$). The Chukchi Sea was generally more saline than the Beaufort Sea (66% of the time). Interestingly, in each water body there was a pattern of increasing salinity from the summer of 2013 to 2015 to 2014, though not significantly so. No consistent pattern in weekly average salinity was observed within a given year/water body.

2.2.3 Ice Conditions

Though not measured in this study, ice conditions would certainly effect nearshore fish communities. Impacts of ice on the benthos have been documented as deep as 52 m (Phillips and Reiss 1985) likely precluding fish in nearshore habitats during the winter. Across a 30 year time series from 1986 to the present, freeze-up date in the vicinity of Barrow has become later in the Chukchi Sea by nearly a month (Craig George¹ personal communication, George et al. 2004). Ice break-up, in contrast, has only gotten earlier by several days. Timing of ice formation and break-up differs between the Chukchi and Beaufort Sea, as well as Elson Lagoon partially resulting from varying bathymetry. These observations are consistent with other accounts (Johnson and Eicken 2016, Mahoney et al. 2014). In the three years of our study, George¹ documented similar freeze-up dates in the Chukchi in 2013 and 2014 (December 1 and 2, respectively) but an earlier freeze-up in Elson Lagoon in 2013 (September 25) relative to 2014 and 2015 (October 10 and 7, respectively). George also observed a delayed ice break up in the Chukchi by 2 weeks in 2014 (July 8) relative to 2013 and 2015 (June 24 23, respectively). Similarly, Elson Lagoon was ice free nearly 2 weeks earlier in 2015 (June 26) than 2013 or 2014

¹ North Slope Borough, Division of Wildlife, 1274 Agvik Street, Barrow, Alaska.

(July 11 and 15, respectively). Cold air temperature and water temperatures were coincidental with increased ice duration in 2014.

2.3 References

- Aagaard K, Roach AT. 1990. Arctic ocean-shelf exchange: Measurements in Barrow Canyon. *J Geophys Res* 95(C10): 18163–18175. doi: 10.1029/JC095iC10p18163
- Ashjian CJ, Braund SR, Campbell RG, George JC, Kruse J, Maslowski W, Moore SE, Nicolson CR, Okkonen SR, Sherr BF, et al. 2010. Climate variability, oceanography, bowhead whale distribution, and Iñupiat subsistence whaling near Barrow, Alaska. *Arctic*. 63(2): 179–194.
- Dasher, D, Lomax T, Bethé A, Hoberg M, Naidu S, Jewett S. 2016. Offshore oil/gas wastewater study: 2014 assessment of Simpson Lagoon. University of Alaska Fairbanks, Fairbanks, Alaska. Final Report to Coastal Impact Assistance Program, Fish and Wildlife Service, US Department of Interior. 35 p.
- George, JC, Huntington HP, Brewster K, Eicken H, Norton DW, Glenn R. 2004. Observations on shorefast ice dynamics in Arctic Alaska and the responses of the Inupiat hunting community. *Arctic* 54(4):363-374.
- Johnson M, Eicken H. 2016. Estimating Arctic sea-ice freeze-up and break-up from the satellite record: A comparison of different approaches in the Chukchi and Beaufort Seas. *Elementa Science of the Anthropocene*. <http://doi.org/10.12952/journal.elementa.000124>
- Luchin V, Panteleev G. 2014. Thermal regimes in the Chukchi Sea from 1941 to 2008. *Deep Sea Research II*. 109:14-26.
- Mahoney AR, Eicken H, Gaylord AG, Gens R. 2014. Landfast sea ice extent in the Chukchi and Beaufort Seas: The annual cycle and decadal variability. *Cold Regions Science and Technology*, 103:41-56.
- Naidu AS, Larsen LH, Mowatt TC, Sweeney MD, Weiss HV. 1982. Aspects of size distributions, clay mineralogy, and geochemistry of sediments of the Beaufort Sea and adjacent deltas, North Arctic Alaska. Institute of Marine Science, Fairbanks, Alaska. Final Report to the Outer Continental Shelf Environmental Assessment Program, Research Unit 529. 113 p.
- Phillips RL, Reiss TE. 1985. Nearshore marine geologic investigations, Point Barrow to Skull Cliff, northeast Chukchi Sea. No. 85-50. US Geological Survey.
- Rand KM, Logerwell EA. 2011. The first demersal trawl survey of benthic fish and invertebrates in the Beaufort Sea since the late 1970s. *Polar Biol*. 34(4): 475. doi:10.1007/s00300-010-0900-2
- Thedinga JF, Johnson SW, Neff AD, Hoffman CA, Maselko JM. 2013. Nearshore fish assemblages of the northern Chukchi Sea, Alaska. *Arctic*. 66(3): 257–268

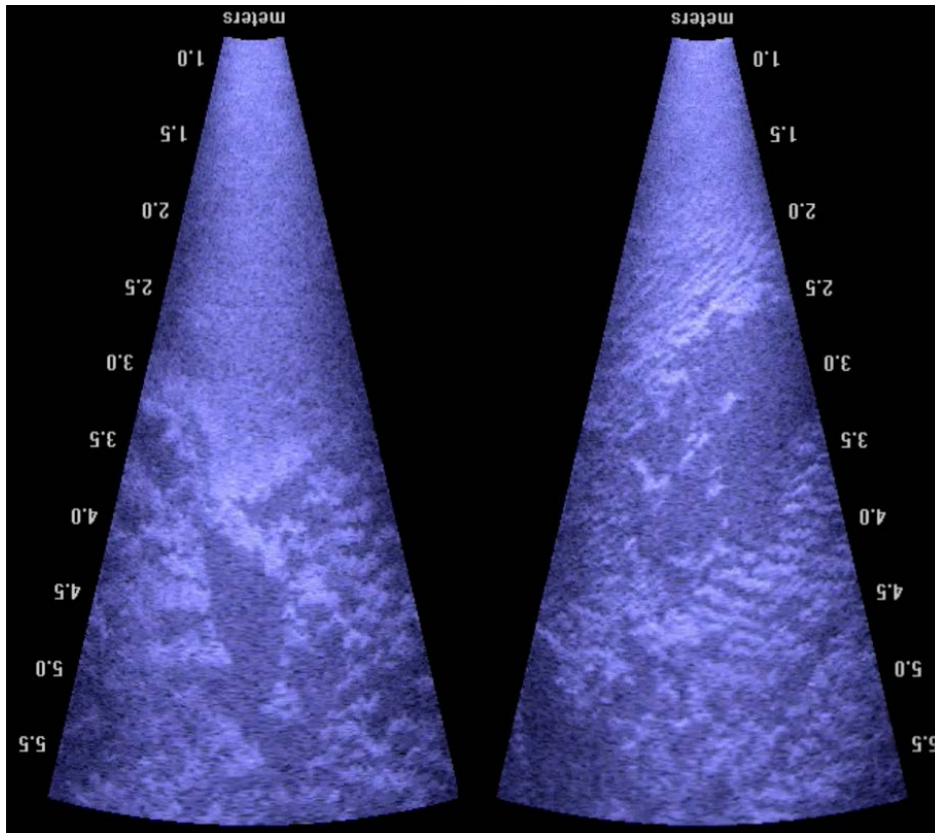


Figure 2.1 Example of complex habitat deposits from eroded tundra from the DIDSON near the channel between Elson Lagoon and North Salt Lagoon, Barrow, AK. See supplementary data for accompanying video.

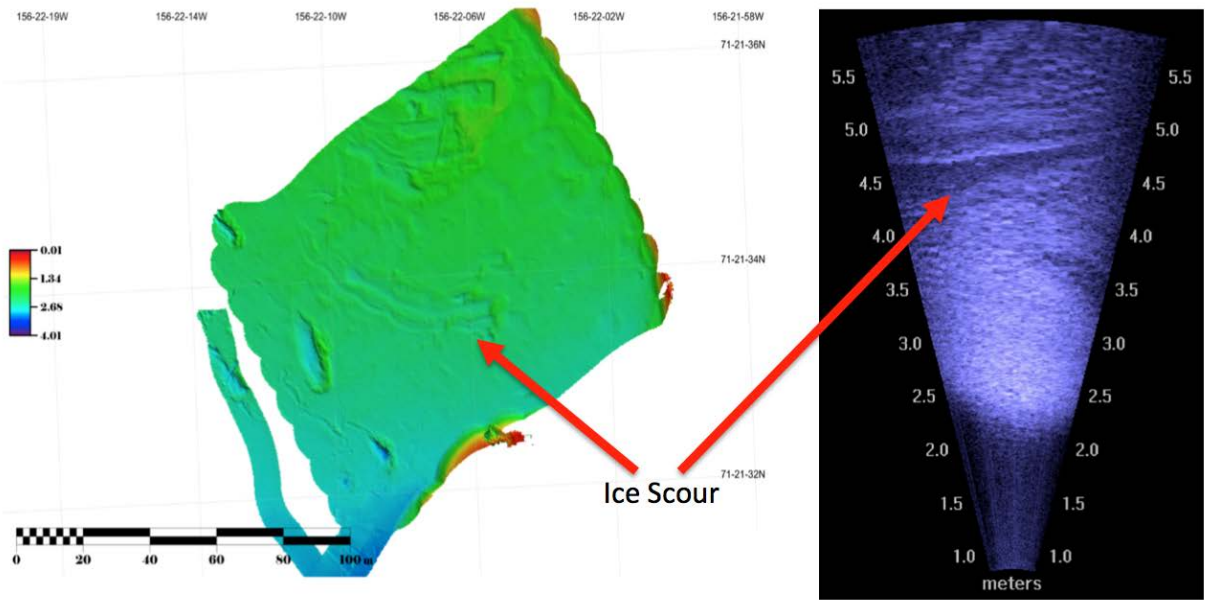


Figure 2.2 Multibeam (left panel) and DIDSON (right panel) imagery illustrating ice scour marks from the Elson Lagoon- Plover Point sampling station.

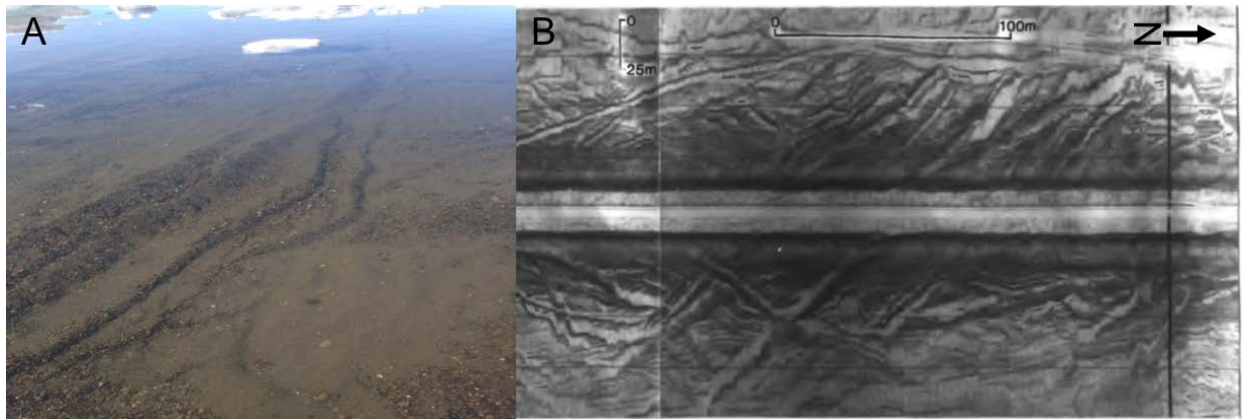


Figure 2.3 Ice scour in the Chukchi nearshore. Image near Napa Boat Ramp in Barrow (A). Side scan image (B) illustrating multiple ice gouges on the shelf near Barrow (10.5 m depth). Major gouge trends northwest-southeast and northeast-southwest (Northwest is upper right corner). Figure B reproduced from (Phillips and Reiss 1985).

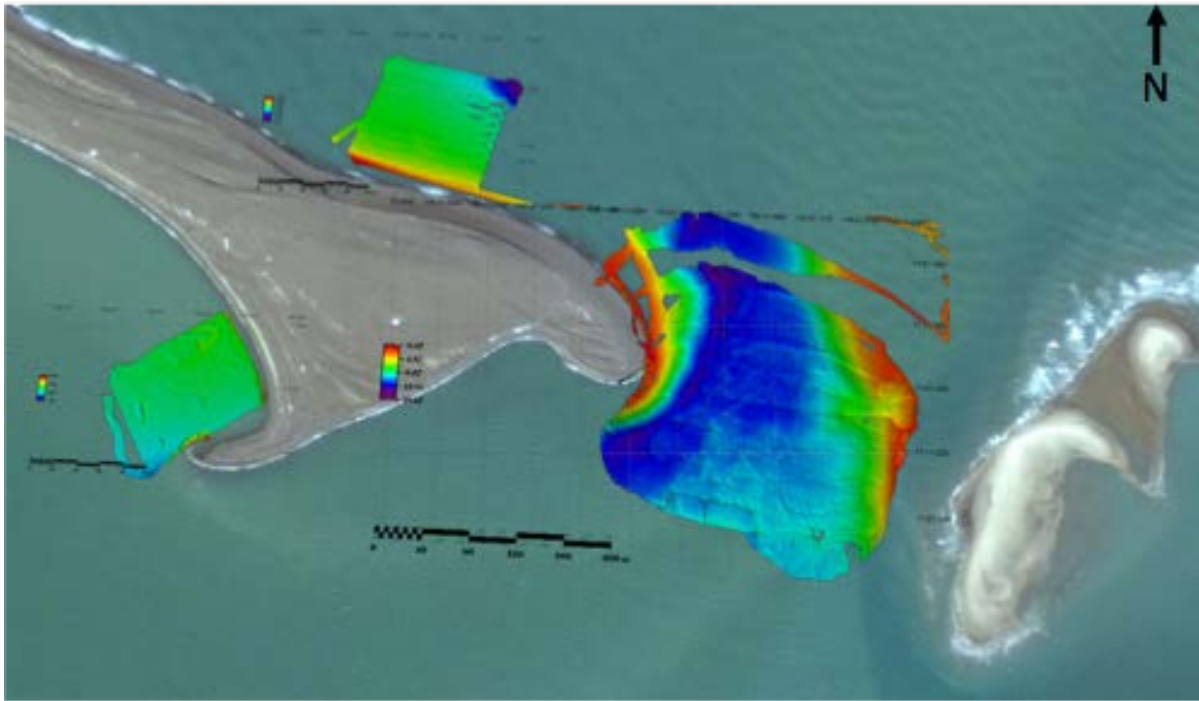


Figure 2.4 Multibeam derived imagery of the bathymetric features of sample stations at Plover Point in both the Beaufort Sea and Elson Lagoon. Note color scales are variable between the three sites, and the features illustrated here represent relative depth differences and should not be used for navigation purposes. High-resolution Geotiff is available in supplementary data. Satellite image courtesy of Google Earth (2016).

Yearly Averaged Temperature at Barrow Airport

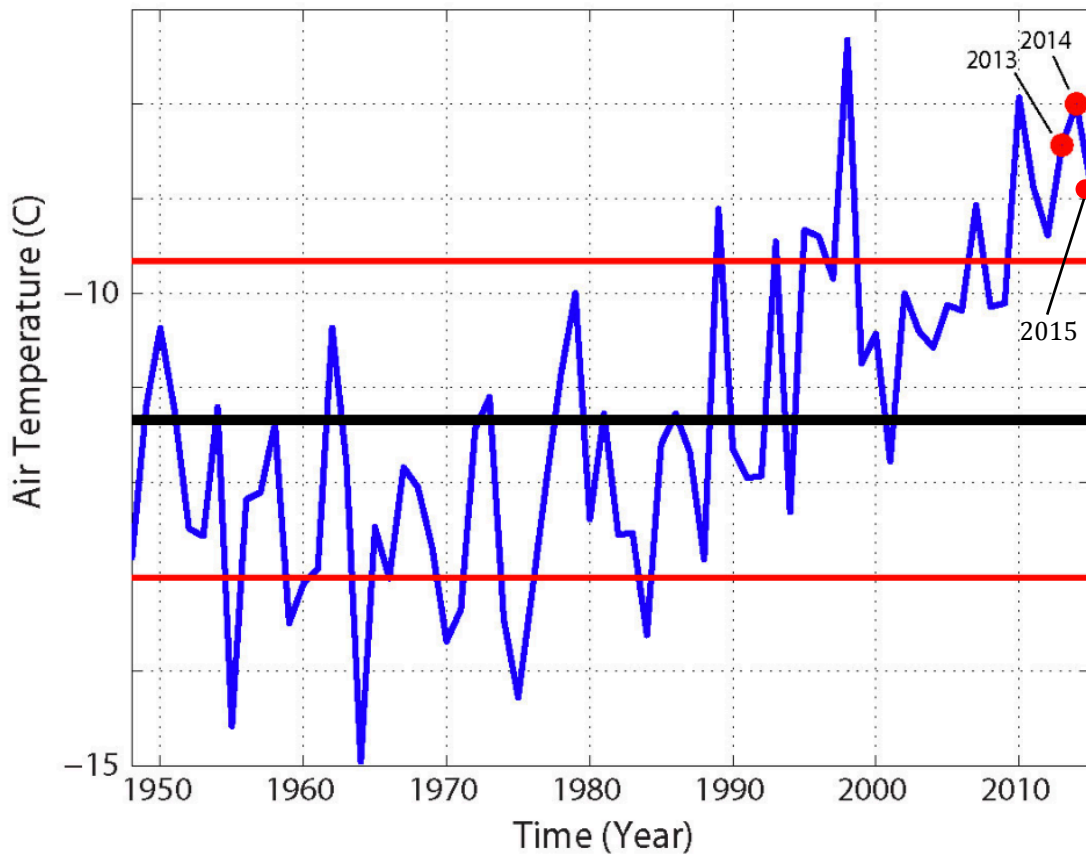


Figure 2.5 Yearly averaged air temperature at Wiley Post- Will Rogers Memorial Airport. The blue line represents mean wind speed (mph) averaged through the whole year of each year between 1948 and 2015. The black line represents the mean of all the years, with red lines being +/- 1 SD from the overall mean. The red dots are the averaged wind speed of 2013, 2014 and 2015, respectively.

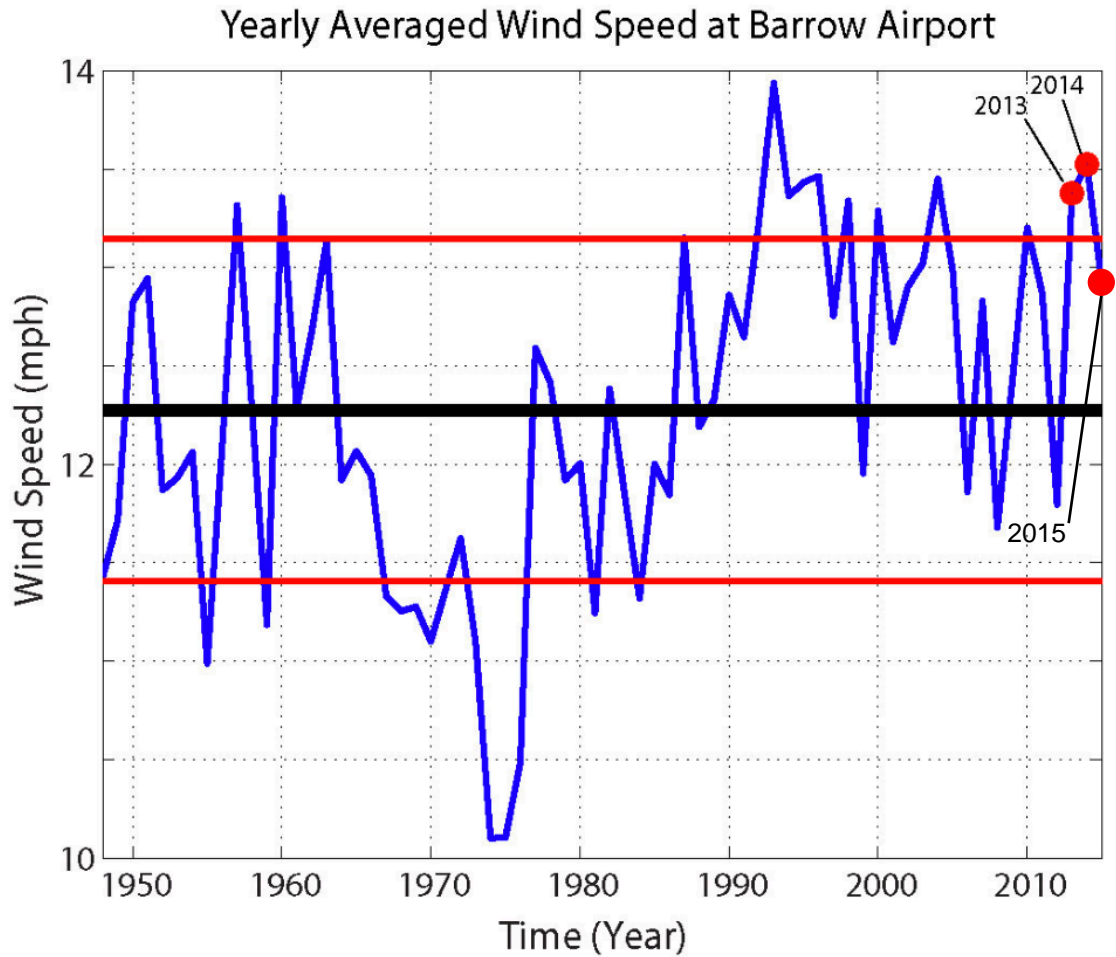


Figure 2.6 Yearly averaged air wind speed at Barrow Airport. The blue line is the mean wind speed in mph averaged through the whole year of each year between 1948 and 2015. The black line is the mean of all the years. The red lines are one standard deviation away from the overall mean. The red dots are the averaged wind speed of 2013, 2014 and 2015, respectively.

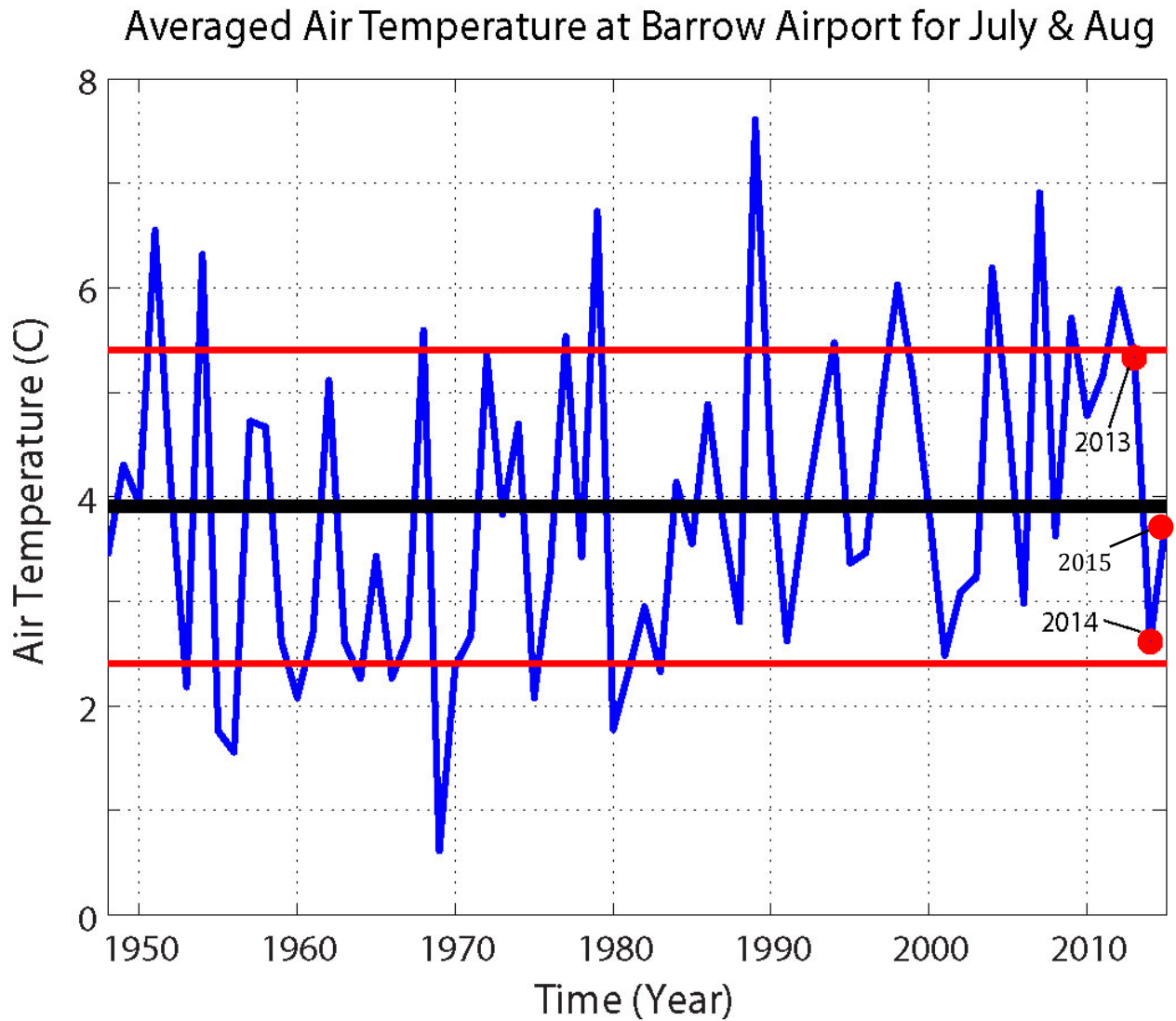


Figure 2.7 Averaged air temperature at Barrow Airport for July and August. The blue line is the mean air temperature averaged through all time during July and August of each year between 1948 and 2015. The black line is the mean of July–August of all the years. The red lines are one standard deviation away from the overall mean. The red dots are the averaged temperature of 2013, 2014 and 2015, respectively.

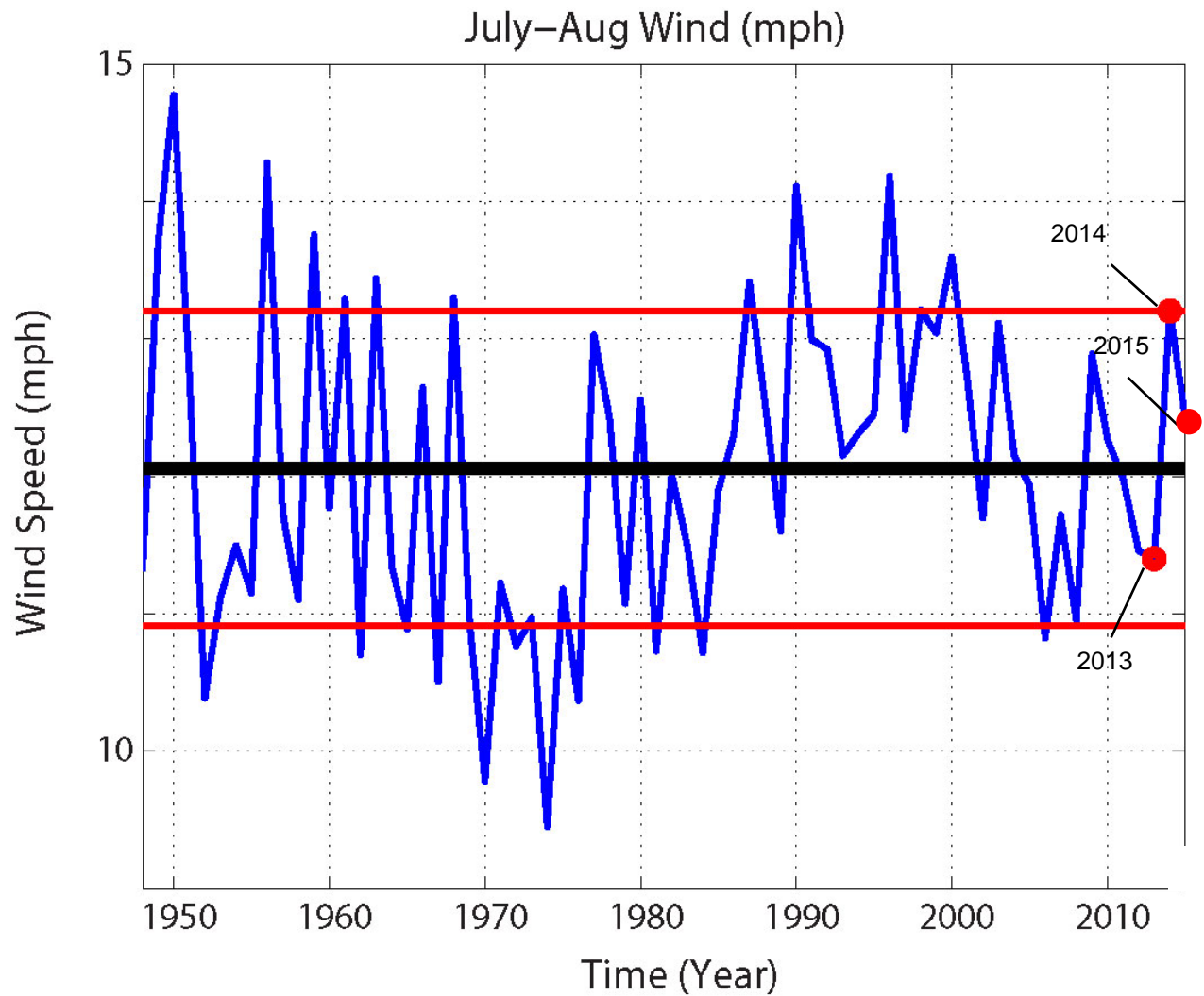


Figure 2.8 Averaged air wind speed at Barrow Airport for July–August. The blue line is the mean wind speed in mph averaged through July and August of each year between 1948 and 2015. The black line is the mean of July–August of all the years. The red lines are one standard deviation away from the overall mean. The red dots are the averaged wind speed of July–August of 2013, 2014 and 2015, respectively.

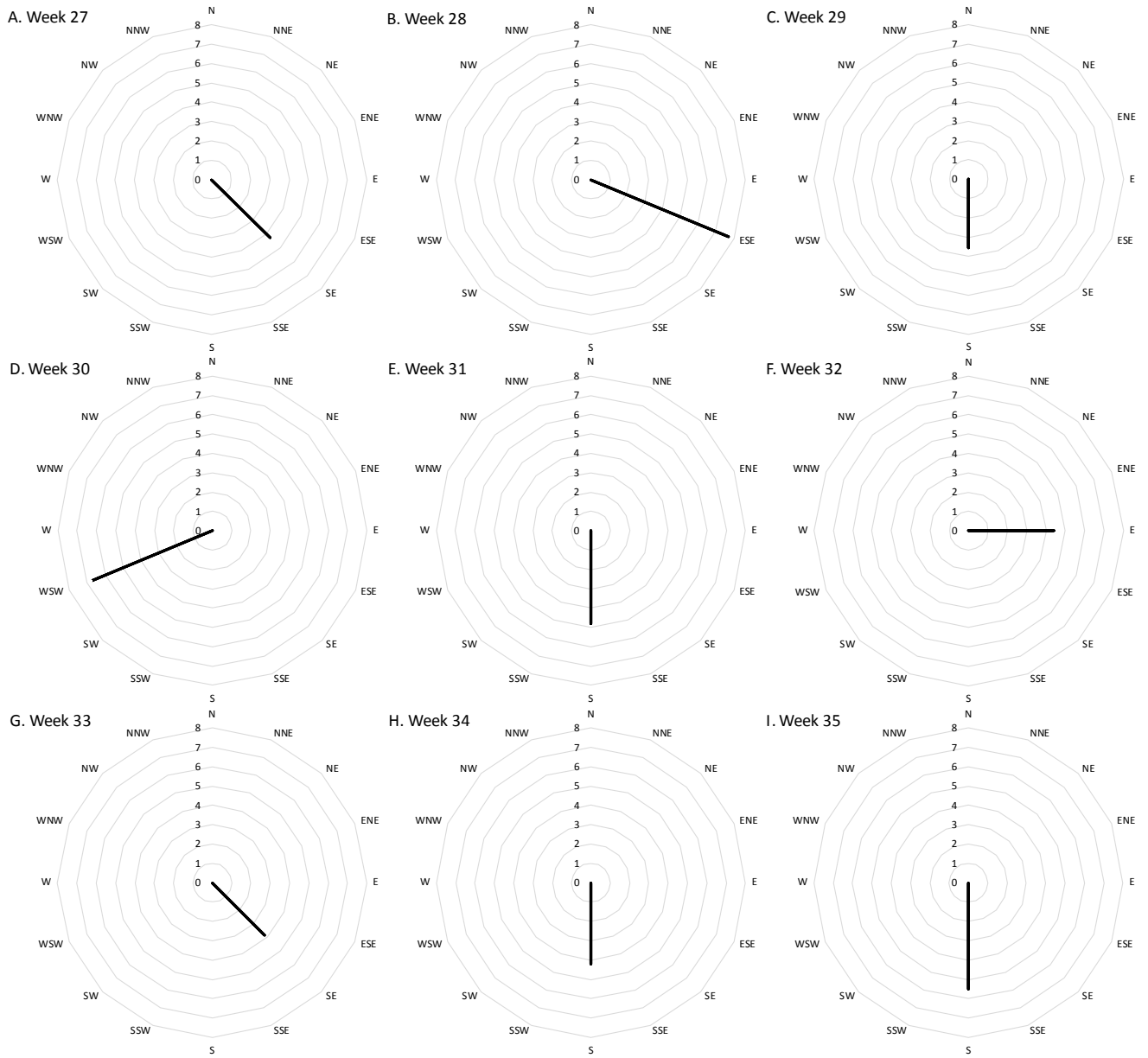


Figure 2.9 2013 Weekly average wind velocities in Barrow, Alaska. Speed is measured in $m\ s^{-1}$.

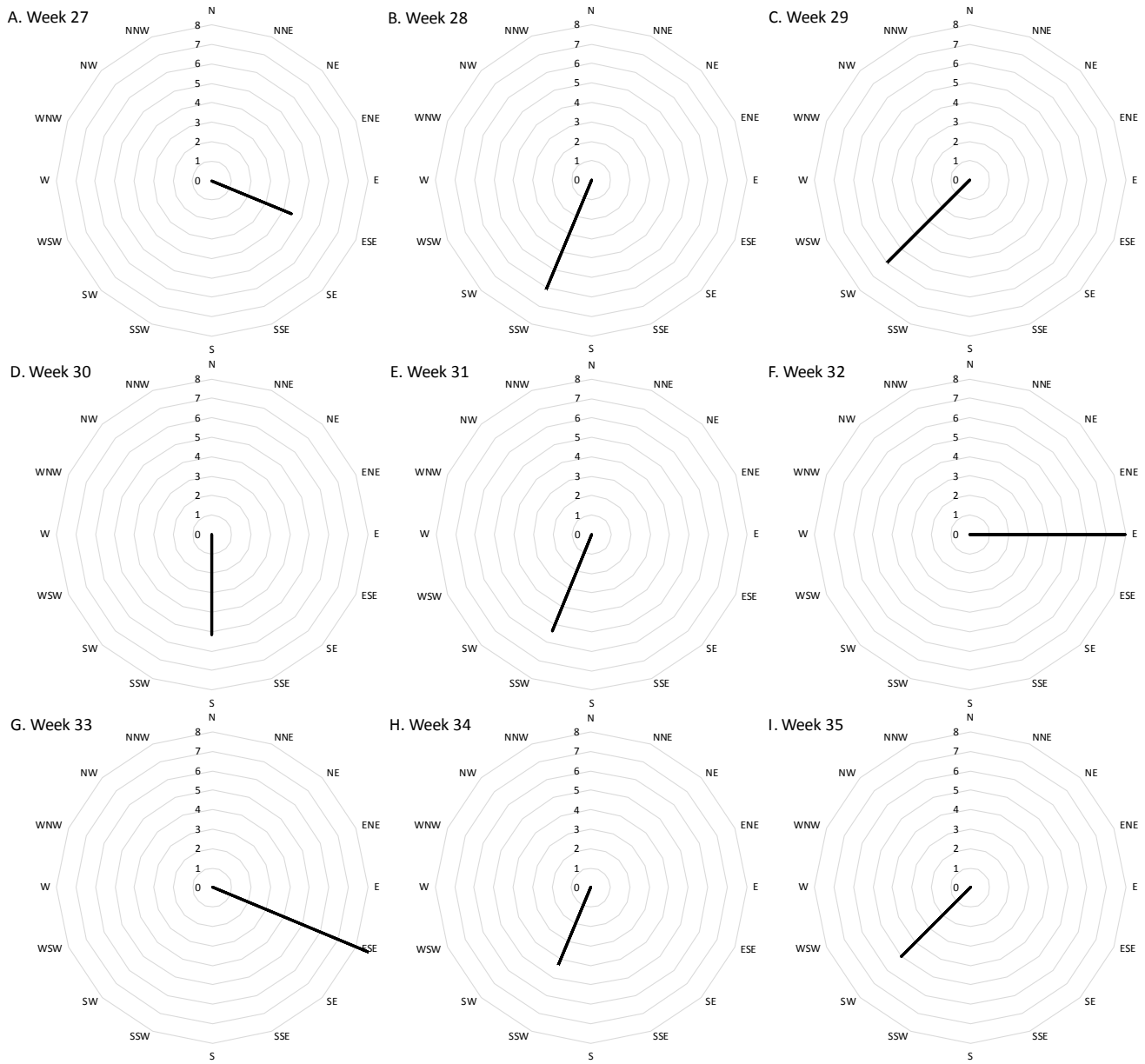


Figure 2.10 2014 Weekly average wind velocities in Barrow, Alaska. Speed is measured in m s^{-1} .

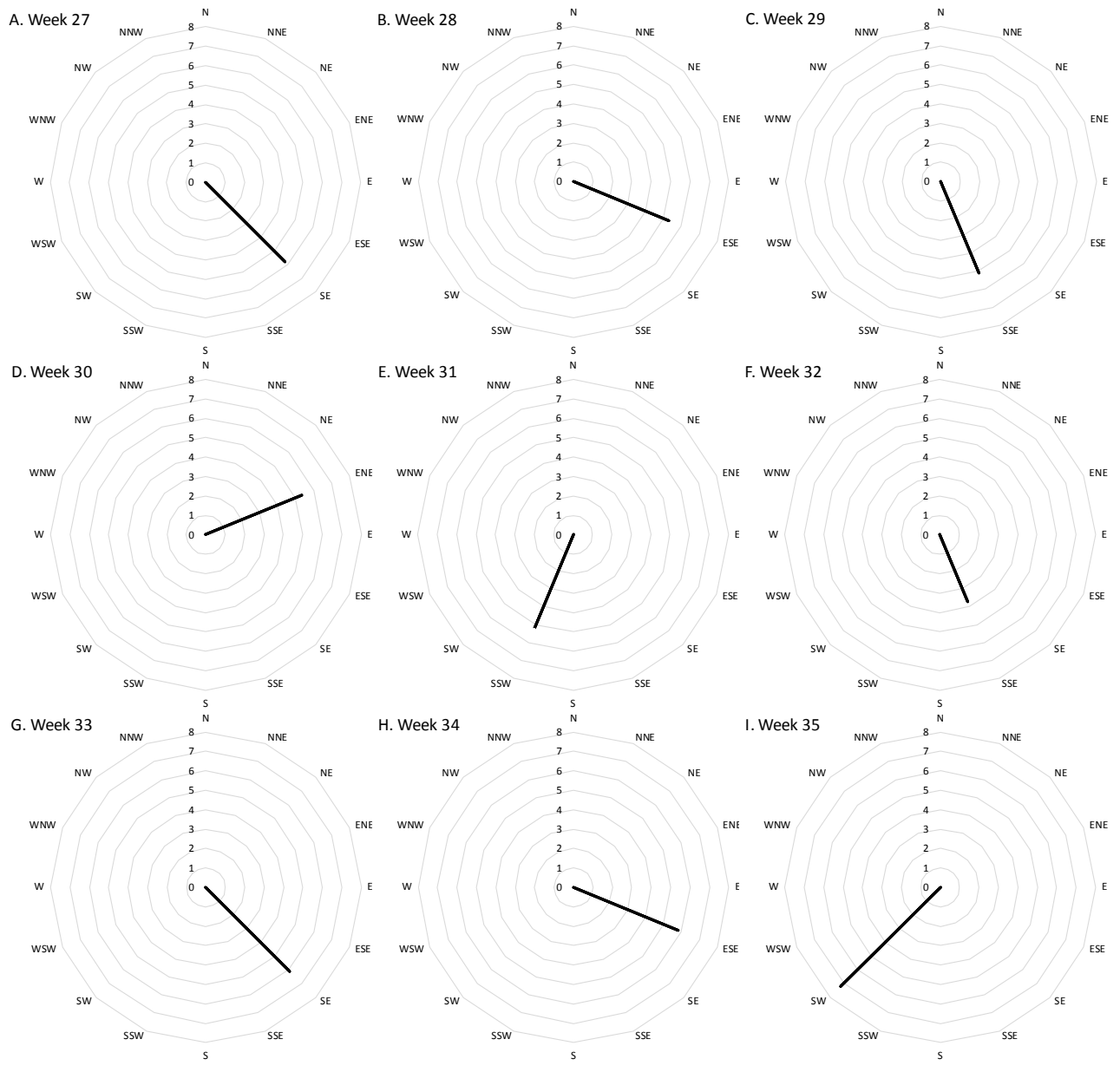


Figure 2.11 2015 Weekly average wind velocities in Barrow, Alaska. Speed is measured in $m s^{-1}$.

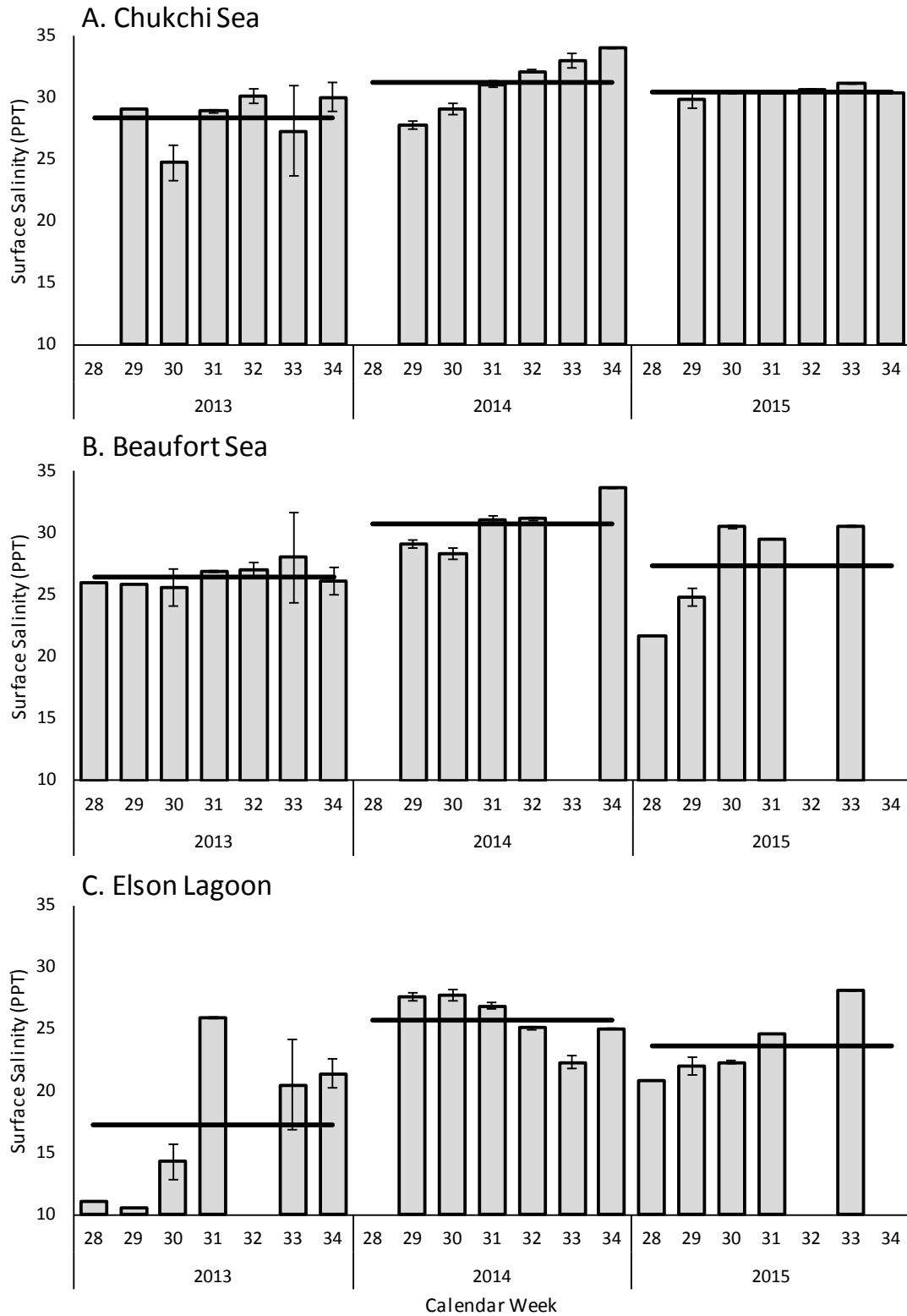


Figure 2.12 Average weekly surface salinity (PPT) of sample sites by year. Horizontal line represents average salinity across the weeks. Error bars represent % Error from the mean.

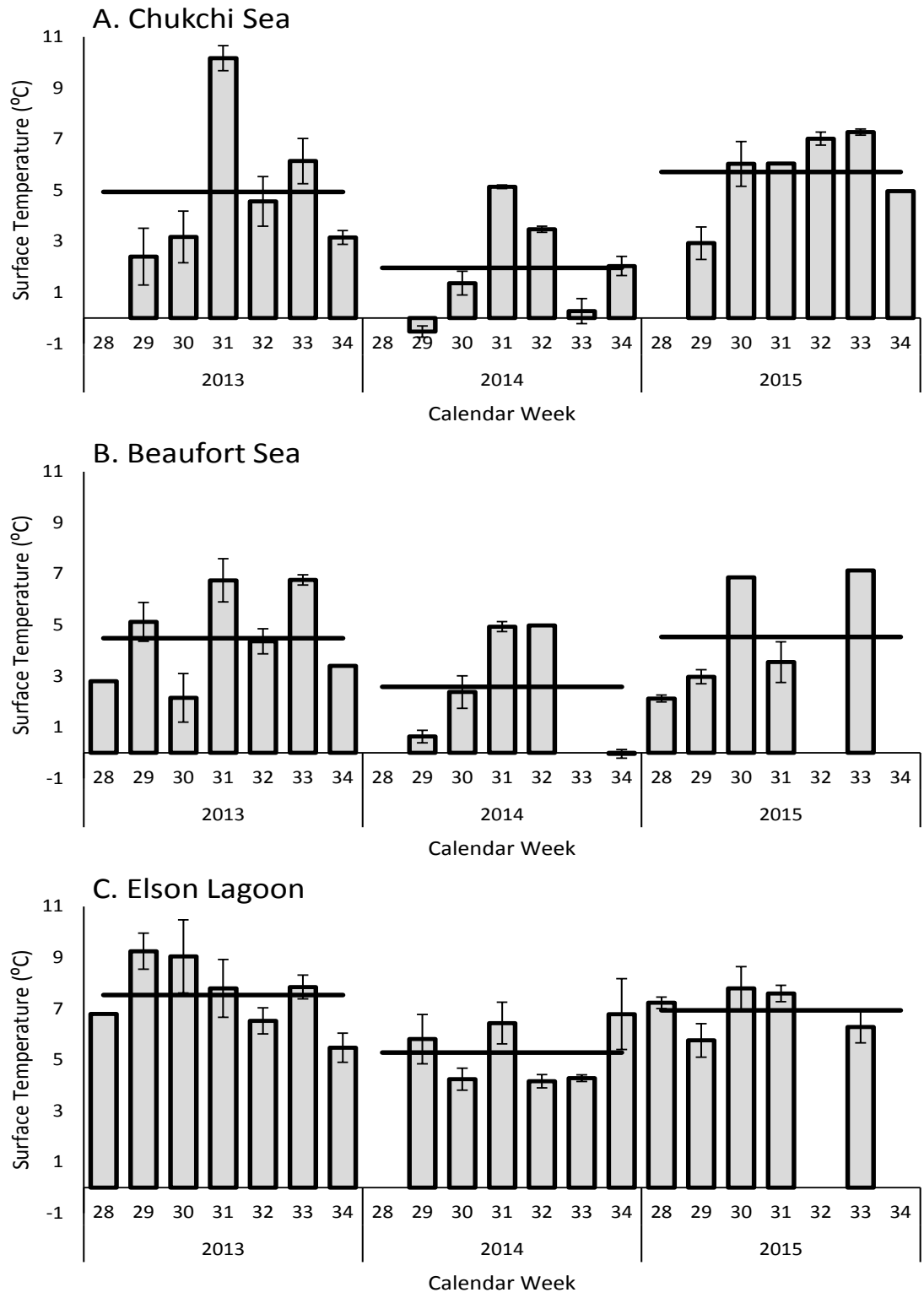


Figure 2.13 Average weekly surface temperature (°C) of sample sites by year. Horizontal line represents average temperature across the weeks. Error bars represent % Error from the mean.

3.0 Mesoscale Weather System Induced Flushing of a Multi-inlet Arctic Lagoon in Summer

C. Li, W. Huang

3.1 Introduction

A coastal lagoon or estuarine embayment with barrier islands often connects to the coastal ocean through multiple tidal inlets (van de Kreeke 1984, 1985, 1990; Aubrey and Giese 1993; Janzen and Wong 1998; Pacheco et al. 2010). The exchange of water between the coastal ocean and these lagoons can be very different from a conventional coastal plain estuary with a single opening, the latter of which have been the focus of study for more than a half century (e.g. Pritchard 1956). Observations in lagoons on the Delmarva Peninsula (Brumbaugh 1996), coastal Georgia (Li 2013), and Louisiana (Li et al. 2009) demonstrated that wind impacts within such systems can have a stronger influence on controlling flow than tidal forcing. These locations are analogous to our study sites, having multiple inlets to the lagoons. A numerical experiment was used (Li 2013) to determine the impact of wind in such a system. It is shown that for along-shore winds, the outward flow usually occurs through the downwind inlet with inward flow through the upwind inlet. For cross shore winds, the wind-driven flow is usually in the downwind direction through the shallower inlet(s) but against the wind in the deepest inlet, given that these inlets have comparable widths.

Arctic lagoons in northern Alaska are similar to those in lower latitudes, being characterized as very shallow (~ 1–10 m) and bounded by barrier islands with multiple openings to the coastal ocean (Kjerfve and Magill 1989; Kjerfve 1994). They are affected by tides and more so by winds (Li 2013). The similarity, however, stops quickly when other factors, such as ecosystem characteristics and human habitation conditions, are considered. These lagoons are critical for supporting Arctic fisheries production, subsistence activities and regional coastal ecology (Logerwell et al. accepted). As climate change and associated warming of the Arctic and sea-level rise become frequent topics of discussion, the need for an understanding of these generally under-studied systems increases. The work presented here is aimed at an understanding of the response of water to wind in the Elson Lagoon (Figure 3.1), the northern most lagoon of the U.S. located within the Arctic Circle.

In this area of the Arctic Alaska, the meso-scale atmospheric high pressure systems are frequent. In between these high pressure systems are low pressure centers or cyclones (Serreze 1997) or fronts separating different air masses, which can be associated with storms (Vavrus 2013). The movement of these systems over the Arctic coastal areas causes the local wind to shift between northeasterly and westerly or northwesterly. The importance of wind to the ocean circulation, exchange between the lagoons and coastal ocean, and biological responses has long been recognized by several studies. For instance, Okkonen (2008) studied the water exchange between the Elson Lagoon and the Beaufort Sea continental shelf with bottom mounted current meters measuring the near bottom currents between August and September of 2006. This study found that the near bottom velocity is correlated with the east and west winds and the outflow produced fronts that aggregated zooplankton. The effect of wind is even associated with the bowhead whale feeding behavior (Okkonen et al. 2011). This study is built upon the Okkonen (2008) study aimed at determining the transport of water through Elson Lagoon Estuary under summer weather conditions. Our study examines the entire water column by using an acoustic Doppler

current profiler that measured the velocity profiles. We also examine the dominant contemporaneous weather systems and conduct a multi-variable regression to quantify the correlation with the wind that can be used to estimate/predict the transport of water through the major inlet of the Elson Lagoon under various wind conditions.

3.2 Study Area and Instrumentation

Elson Lagoon (Figure 3.1) is the northern most coastal lagoon of the United States bounded roughly by $156^{\circ} 36' W$, $155^{\circ} 54' W$, $71^{\circ} 12' N$, and $71^{\circ} 23' N$. It is approximately a rectangle of $\sim 8 \text{ km} \times 25 \text{ km}$, with shallow water of 2–3 m in the interior with deeper channels at the passes connecting to the coastal ocean and Beaufort Sea. The deepest location is at the western-most channel, the Eluitkak Pass, with a water depth of $\sim 10\text{--}16 \text{ m}$. Since the bottom of the Eluitkak Pass is coarse sandy sediment, the strong winds and waves are constantly changing the topography and coastline, and thus the channel depths at the passes are expected to vary over time. The Elson Lagoon is oriented in the northwest – southeast direction. The axis of the lagoon is estimated to have a $\sim 31^{\circ}$ angle from the true west-east direction (Figure 3.1).

Aimed at determining the response of the flow of water in and out of the lagoon to winds generated by passing meso-scale cyclonic and anti-cyclonic weather systems, we deployed an RD Instrument 1200 KHz Broadband Workhorse acoustic Doppler current profiler (ADCP) at Plover Point within the Eluitkak Pass for approximately 4.9 days between 00:00 August 19 (day 231 from January 1) and 20:48 August 23 (day 235), 2013. This instrument was deployed at $71^{\circ} 21.560' N$, $156^{\circ} 21.152' W$, on a relatively flat bottom at 9.6 m depth, slightly east of the deepest water ($\sim 16 \text{ m}$) in the main channel. The ADCP was mounted on an aluminum cross comprised of four weighted legs. The ADCP was configured to record the three components of the velocity vector at 0.5 m vertical intervals every 60 seconds. Within each of the 60-second, the ADCP sampled 50 times and provided an average for the ensemble.

In addition, a HOBO U20 Titanium Water Level Logger was also deployed inside the North Salt Lagoon, which is an enclosed circular lagoon of $\sim 1.3 \text{ km}$ diameter connected to the Elson Lagoon at the south-western most corner of the latter (Figure 3.1, marked by H). The purpose of this pressure sensor was to record the water level variation and compare with that measured by the pressure sensor on the ADCP so that a pressure gradient can be obtained. The pressure gradient is expected to vary with the wind direction and magnitude. The true water level variation was resolved with an atmospheric reference logger (Bosch BMP085) approximately 2.5 km away, sampled at 0.5 Hz and had an equivalent resolution of height change of 0.25 m in the air at an averaged sea level condition, or 0.306 millimeter of water level change at $4^{\circ} C$. The HOBO U20 Titanium pressure sensor was deployed in the North Salt Lagoon between 23:33 August 19 and 13:25 August 23, 2013 UTC time. Therefore, the HOBO data were shorter than the ADCP data by more than a day ($\sim 30 \text{ hours}$).

3.3 Weather Conditions

Large-scale weather maps were obtained from NOAA (supplemental materials). The meteorological conditions during the ADCP deployment (00:00 August 19, 2013 UTC) were dominated by a low air pressure system (cyclone) located over the Bering Strait, with a linear stationary front connecting several low pressure centers across the entire Alaska into southwest Canada in a northwest-southeast orientation (supplemental materials). Coincident with this was another low air pressure system located over Ellesmere Island in northern Canada. A high

pressure (anti-cyclone) system was juxtaposed to the north of the study area, in between these major low air pressure systems, generating relatively strong northeasterly winds at Elson Lagoon (supplemental information). The northeasterly wind peaked before August 20 (day 232, Figure 3.2a). This condition lasted for approximately a day as the systems gradually moved to the south. As a result, the high pressure system moved over the study area. Concurrently, as the high-pressure system moved southeastward, the stationary atmospheric front developed into a couple of cold fronts occupying the Bering Strait and Eastern Alaska. At 03:00 UTC August 21 (day 233), the center of the high pressure moved over the Barrow area remaining there for less than 24 h (see supplemental materials) and was confirmed by the air pressure data recorded in Barrow (supplemental information). During this period, the measured wind intensity at the study area was weak (Figure 3.2a, day 233). As the low pressure originally centered over the Ellesmere Island area moved to the south on August 22 (day 234), pushing the high pressure system away, the study area was influenced by a persistent northwesterly wind. This variation in wind direction is typical for the area during the summer period with cyclones and anti-cyclones passing the region, resulting in variation in dominant wind directions (e.g., northeasterly to westerly or northwesterly).

3.4 Data Processing and Analysis

As mentioned above, the axis of Elson Lagoon is oriented at an angle of about -31° from the east-west direction (Figure 3.1). To examine the effect of the along lagoon (northwest – southeast directions) and cross lagoon (northeast – southwest directions) wind components, the wind vector was rotated by this magnitude ($= -31^\circ$, so that a positive along lagoon wind is toward the southeast) using the following transformation:

$$w_a = w_x \cos(\alpha) + w_y \sin(\alpha) \quad (1)$$

$$w_c = -w_x \sin(\alpha) + w_y \cos(\alpha) \quad (2)$$

in which w_a and w_c are the along-lagoon and cross-lagoon components of the wind, respectively. The time series of rotated wind components during the study period are shown in Figure 3.2a.

3.4.1 Correction of Water Level for Air Pressure Effect

The air pressure data measured on land, at 0.5 Hz were re-mapped to have the same time intervals of the HOBO U20 total pressure data (at 0.016 Hz, or 60 second intervals). For cross verification, we also used atmospheric air pressure data available from the nearby Barrow Airport. The air pressure our land station was subtracted from the total pressure from the HOBO sensor to calculate water level (m), which was then de-meanned to preserve the variation from the mean. The de-meanned time series was then low pass filtered with a 30-hour sixth order Butterworth Infinite Impulse Response (IIR) low-pass filter effectively removing tidal oscillations from the water level data. During the period of ADCP deployment (~ 4.9 days) we measured nearly 9 semidiurnal tidal cycles with an averaged tidal range of about 0.2 m (supplemental material). This is a typical micro tidal condition. This justifies the need to subtract the air pressure effect because of its relative significance due to the small variation of tides. The ADCP also recorded the water depth above the instrument. However, this water depth is converted from the pressure measured by ADCP which included the effect of atmospheric pressure. This data should therefore also be corrected by subtracting the air pressure. A similar procedure was applied to take out the air pressure effect on the depth measured from the ADCP,

i.e., the mean value of the water level over the entire study period (~4.9 days) was subtracted. After this, the surface elevation variation referenced to the mean water level measured by the ADCP (ζ_1) at the Plover Point within the Eluitkak Pass and that measured by HOBO at the North Salt Lagoon (ζ_2) were used to calculate the sea level difference ($\delta\zeta$).

3.4.2 Low Pass Filtering of the ADCP Velocity Data

The water velocity data from the ADCP indicated a stronger north component than east component. The maximum east velocity component was about 1/3 of that of the north component, however each component had detectable tidal signals. The velocity magnitude was generally larger near the water surface than near the substrate. The velocity at each level was low pass filtered by a 30 hour Butterworth low pass filter (Figure 3.2c). To avoid including contaminated data near surface due to the side lobe effect of the transducers, the analysis of the velocity profile was restricted below 9.36 m. The blue lines above the velocity contours in Figure 3.2c shows the surface elevation measured by the ADCP's pressure sensor excluding the air pressure effect. The low pass filtered north velocity component appears to have a variation very similar to that of the pressure difference ($\delta\zeta$) at all levels (Figure 3.2b), indicating a strong linear correlation. Since the HOBO U20 was deployed about 23 hours later and retrieved 7 hours earlier than the ADCP, the pressure difference comparison with the low pass filtered velocity (Figure 3.2b) was possible only during the time of the HOBO U20 deployment.

3.4.3 Regression Analysis

Figure 3.2b shows that the pressure difference between the North Salt Lagoon and Plover Point is correlated with the flow at the pass – a relatively higher (lower) water level in the North Salt Lagoon correlates to an outward (inward) low pass filtered flow at the Eluitkak Pass. Note that here outward refers to flow direction being from the lagoon to coastal ocean. A related assumption regarding the subtidal flow is that it is driven by a pressure gradient generated by the wind. The pressure gradient between North Salt Lagoon and Plover Point is therefore a result of wind forcing. To examine the correlation among these variables, i.e., wind velocity components, pressure gradient, and subtidal flow at the Plover Point, four different regressions were attempted. These regressions are expressed by the following equations:

$$u(t)=A W_a(t)+B W_c(t)+C \quad (t \in [T_{\text{HOBO1}}, T_{\text{HOBO2}}]) \quad (3)$$

$$u(t)=A \delta\zeta(t)+B W_a(t)+C W_c(t)+D \quad (t \in [T_{\text{HOBO1}}, T_{\text{HOBO2}}]) \quad (4)$$

$$u(t)=A W_a(t)+B W_c(t)+C \quad (t \in [T_{\text{ADCP1}}, T_{\text{ADCP2}}]) \quad (5)$$

$$u(t)=A W_a(t)+B W_a^2(t)+C W_c(t)+D W_c^2(t)+E \quad (t \in [T_{\text{ADCP1}}, T_{\text{ADCP2}}]) \quad (6)$$

in which $u(t)$, $W_a(t)$, $W_c(t)$, $\delta\zeta(t)$ are, respectively, the time series of outward component of the subtidal (low pass filtered) velocity (positive outward) at the Plover Point, the along-lagoon wind velocity component, the cross-lagoon wind velocity component, and the pressure difference between the North Salt Lagoon site and the Plover Point; t is time; A , B , C , D and E are the regression coefficients; while $[T_{\text{HOBO1}}, T_{\text{HOBO2}}]$ represents the time interval between the beginning time T_{HOBO1} and ending time T_{HOBO2} for the HOBO U20 and $[T_{\text{ADCP1}}, T_{\text{ADCP2}}]$ represents the time interval between the beginning time T_{ADCP1} and ending time T_{ADCP2} for the ADCP. As mentioned earlier, T_{HOBO1} was 23 hours later than T_{ADCP1} and T_{HOBO2} was 7 hours earlier than T_{ADCP2} , making $T_{\text{HOBO2}} - T_{\text{HOBO1}}$ to be ~30 hours shorter than $T_{\text{ADCP2}} - T_{\text{ADCP1}}$.

Therefore, even the regressions represented by equation (3) and (5) have the same format, the time intervals are different and the regression coefficients are different. The second regression represented by equation (4) includes the effect of pressure gradient. The last regression represented by equation (6) includes the quadratic wind velocity effect.

3.5 Results and Discussion

The results indicate that the subtidal velocity is correlated to and apparently largely determined by wind velocity. When the north-northeasterly wind was peaking, just prior to day 232 (August 20), the water velocity was at a maximum and moving out of the lagoon against the wind. When the wind switched to west and northwest on day 235 (August 23), velocity reversed direction. The first regression was made to compare with the second for the time period when the pressure gradient due to surface elevation difference was available. Without using the pressure gradient, the correlation (Table 3.1, supplemental materials) was relatively high (R^2 between 0.78 and 0.87). The coefficients A and B were all negative, indicating that a positive (negative) along-lagoon wind corresponds to inward (outward) subtidal flow, and a positive (negative) cross-lagoon wind also corresponds to an inward (outward) subtidal flow at the Eluitkak Pass at all depths. When the pressure gradient is taken into account for the same time period, the R^2 increased to 0.92 in the subsurface (Table 3.2, supplemental materials). The correlation of the subtidal flow with the along-lagoon and cross-lagoon winds are consistent with the first regression. Modification of the first regression to include the full time series from the ADCP yielded an increase in the correlation $R^2=$ to 0.92 on the surface, albeit the regression coefficient B changed sign (Table 3.3, supplemental materials). When comparing the data with the regression results (Figure 3.3c), a significant phase shift and mismatch between the regression model and the data were observable despite the high overall correlation ($R^2 > 0.8$). This suggests that the flow may be related to the wind in a nonlinear fashion which is verified by an improved regression model following equation (6). Indeed, the improved regression with a quadratic wind component reduced the mismatch of phase significantly (Figure 3.3d). As a result, the coefficients for the along-lagoon and cross-lagoon wind components are again consistent with the other regressions (both A and B are negative, Table 3.4, supplemental materials). The R^2 values increased further at all depth, up to 0.96.

The correlations among the subtidal velocity, wind, and pressure gradient caused by the surface slope of the water can be interpreted with the subtidal momentum equations, which emerge following low pass filtering, or a tidal-averaging of the shallow water equations. The tidal averaging will effectively take out the local acceleration and the major force balance would be the Coriolis force, pressure gradient force caused by the surface slope of water, wind stress, and bottom friction. The low pass filtering is similar to a tidal averaging over at least a tidal cycle and therefore to the lowest order of approximation it will effectively eliminate the local acceleration. If we consider the momentum equation that further ignores the advection, the following equations can be obtained:

$$u = (-g)/(\beta^2 - f^2) (\beta \partial \zeta / \partial x - f \partial \zeta / \partial y) + \alpha / (\beta^2 - f^2) (\beta W_x - f W_y) \quad (7)$$

$$v = g / (\beta^2 - f^2) (\beta \partial \zeta / \partial y - f \partial \zeta / \partial x) + \alpha / (\beta^2 - f^2) (f W_x - \beta W_y) \quad (8)$$

in which the variables include the velocity components (u, v), surface elevation of the water (ζ), horizontal coordinates (x, y), and the wind velocity components (W_x, W_y), respectively. All

variables used here are considered as low pass filtered, thus the local acceleration can be neglected. The coefficients for the wind stress and bottom stress α, β can themselves be functions of the wind velocity and bottom velocity, respectively. However, for the purpose of relating the momentum to the regression equations, they can be considered just as parameters as there is no derivative involved.

These equations are similar to the second regression Eq. (4) such that the wind velocity and pressure gradient are linearly related to the subtidal velocity. A major difference however is that in the regression, effectively, only one pressure gradient component is included. In addition, Eqns. (7) and (8) are not solutions of the problem in a general sense because the pressure gradient is rarely measured or given. It is often part of the solution, rather than a known quantity. The true dynamical solution needs to add the continuity equation and boundary conditions. Conceptually, the solution u and v should depend on the forcing W_x and W_y . It is therefore not surprising that the last regression Eq. (6) worked the best because wind stress is generally accepted as a quadratic function of wind velocity.

To better view the effect of wind, we also ran the Weather Research Forecast (WRF, supplemental materials) model that produced the wind field over the study area (Figure 3.4). The dashed arrows represent the wind vectors, the solid black arrows indicate the subtidal flows, while the gray arrows represent the plausible flows away from the mooring position. The reason that a northeasterly wind causes a northeasterly flow (out of the lagoon) can be explained by this: the wider opening at the eastern Elson Lagoon receives more forcing from the wind stress; while the much narrower opening at the northwestern end receives much less forcing from the wind stress. The barrier islands can effectively block the flow and therefore wind stress need not to be considered there for the purpose of water transport through the inlets. The large wind forcing on the eastern than the western side causes a “torque” similar to that discussed by Engelund (1973, 1986), Fischer (1976), Li (1996), and Li et al. (2008) which tends to push water into the lagoon from the wider opening, generating a higher water level on the eastern side, causing a pressure gradient induced flow to exit the lagoon through the western narrow inlet, the Eluitkak Pass.

3.6 Summary

In this paper, we analyzed flow data collected with a bottom mounted ADCP at the Eluitkak Pass / Plover Point of the Elson Lagoon in the Arctic between the Beaufort Sea and Chukchi Sea in the summer of 2013, and investigated the regression between the wind vector, low pass filtered subtidal velocity at various depths, and pressure gradient force, after taking out the effect of the atmospheric pressure changes over time. The multi-variable correlation has the basis in physics when the momentum equations are considered. The quadratic wind works the best for the regression with the R^2 value reaching up to 0.96. We noted that we observed a strong counter wind current at the Eluitkak Pass and provided an explanation considering the wind induced torque. In a sense, the whole lagoon with its multiple openings works as a system that can “amplify” the wind effect so that the pressure gradient established by the wind stress can be relieved through relatively strong flows in the narrow pass. As all the pressure gradient induced flow has to go through the narrow inlet, the flow has a strong signal correlating to the wind stress. More specifically, for example, when there is northeasterly wind, the subtidal (low pass filtered) current at the pass moves against the wind flowing out of the Elson Lagoon. This is caused by the pressure gradient due to a net input of water mass from the much wider openings of the lagoon on its eastern side. The significance of the strong correlation (high R^2) of the

regression can be seen considering the potential of using the regression coefficients to calculate wind induced currents from the Elson Lagoon to the coastal ocean, and vice versa, given the wind vector time series (whether from model prediction, hindcast, or direct measurements). The calculated currents can then be used for applications for various purposes such as larva transport or interpretation for fishery and ecological studies. Our study is a step further based on Okkonen (2008) and the velocity in the upper layer of the water column revealed much larger flow velocities than that at the bottom. The length of the data is relatively short. However, in the Arctic environment, the challenges of obtaining longer time series is substantially greater than that in lower latitude areas where it is mostly much easier to access and much less costly to conduct field work.

3.7 Acknowledgements

This project was funded by the North Pacific Research Board (NPRB, project #1229) to KM Boswell and C Li. Supports at all scales by and discussion with Kevin Boswell, Mark Barton, Johanna Vollenweider, Ron Heintz, Brenda Norcross, and others are highly appreciated. Without these collaborative activities, this work would not have been possible. Logistic support was provided by UMIAQ. Additional support was from North Slope Borough. Without a promise to technical support on the use of ADCP data (which should be directed to the manufacture), the flow data from this study is available from the lead author after publication of this paper.

3.8 References

- Aubrey DG and Giese GS (Eds.) 1993. Formation and Evolution of Multiple Tidal Inlets, Coastal and Estuarine Studies, 44, AGU, Washington, D. C.
- Brumbaugh RD. 1996. Recruitment of blue crab, *Callinectes sapidus*, postlarvae to the back-barrier lagoons of Virginia's eastern shore, PhD dissertation, Old Dominion Univ., 174 pp.
- Engelund F. 1973. Steady wind set-up in prismatic lakes, reprinted in Environmental Hydraulics: Stratified Flows (Lecture Notes on Coastal and Estuarine Studies, vol. 18) edited by F. B. Pedersen, Springer, 1986, 205–212.
- Engelund F. 1986. In: Pedersen, F.B. (Ed.), Steady wind set-up in prismatic lakes, in Environmental Hydraulics: Stratified Flows. Coastal Estuarine Stud. vol.18. Springer-Verlag, New York, pp. 205–212.
- Fischer HB. 1976. Mixing and dispersion in estuaries. Annu. Rev. Fluid Mech. 8: 107–133.
- Janzen CD, Wong K-C. 1998. On the low-frequency transport processes in a shallow coastal lagoon. Estuaries. 21: 754–766.
- Kjerfve B. 1994. Coastal Lagoon Processes, Elsevier Science Publishers, Amsterdam, xx + 577p.
- Kjerfve B, Magill KE. 1989. Geographic and hydrodynamic characteristics of shallow coastal lagoons. Mar. Geol. 88: 187–199.
- Li C. 1996. Tidally induced residual circulation in estuaries with cross channel bathymetry, Ph.D. dissertation, University of Connecticut, Storrs, Conn., 242p.
- Li C. 2013. Subtidal Water Flux through a Multi-inlet System: Observations Before and During a Cold Front Event and Numerical Experiments, J Geophys Res - Oceans, VOL. 118: 1–16, doi:10.1029/2012JC008109, 2013.
- Li C, Weeks E, Rego J. 2009. In situ measurements of saltwater flux through tidal passes of Lake Pontchartrain estuary by Hurricanes Gustav and Ike in September 2008, *Geophys. Res. Lett.*, 36, L19609, doi:10.1029/2009GL039802.

- Li C, Walker N, Hou A, Georgiou I, Roberts H, Laws E, McCorquodale JA, Weeks E, Li X, Crochet J. 2008. Circular Plumes in Lake Pontchartrain Estuary under Wind Straining. *Estuarine, Coastal and Shelf Sciences*. 80: 161–172.
- Logerwell E, Busby M, Carothers C, Cotton S, Duffy-Anderson J, Farley E, Goddard P, Heintz R, Holladay B, Horne J. (accepted), Fish communities across a spectrum of habitats in the western Beaufort Sea and Chukchi Sea, *Progress in Oceanography*.
- Pritchard DW. 1956. The dynamic structure of a coastal plain estuary, *J. Mar. Res.* 15: 33–42.
- Okkonen SR, Ashjian CJ, Campbell RG, Clarke JT, Moore SE, Taylor KD. 2011. Satellite observations of circulation features associated with a bowhead whale feeding ‘hotspot’ near Barrow, Alaska. *Remote Sensing of Environment*. 115: 2168–2174.
- Okkonen SR. 2008. Exchange Between Elson Lagoon and the Nearshore Beaufort Sea and Its Role in the Aggregation of Zooplankton, MMS Report OCS Study MMS 2008-010, 18p.
- Pacheco A, Ferreira A, Williams JJ, Garel E, Vila-Concejo A, Dias JA. 2010. Hydrodynamics and equilibrium of a multiple-inlet system. *Mar. Geol.* 274(1–4): 32–42. doi:10.1016/j.margeo.2010.03.003
- Serreze MC, Carse F, Barry RG. 1997. Icelandic Low Cyclone Activity: Climatological Features, Linkages with the NAO, and Relationships with Recent Changes in the Northern Hemisphere Circulation. *J of Climate*. 10: 453–464.
- van de Kreeke, J. 1984. Stability of multiple inlets, *Proc. 10th Coastal Eng. Conf.*, 1360–1370.
- van de Kreeke, J. 1985. Stability of tidal inlets—Pass Cavallo, Texas. *Estuarine Coastal Shelf Sci.* 21: 33–34.
- van de Kreeke, J. 1990. Can multiple inlets be stable? *Estuarine Coastal Shelf Sci.* 30: 261–273.
- Vavrus SJ. 2013. Extreme Arctic cyclones in CMIP5 historical simulations. *Geophysical Research Letters*. 40(23): 6208. doi:10.1002/2013GL058161

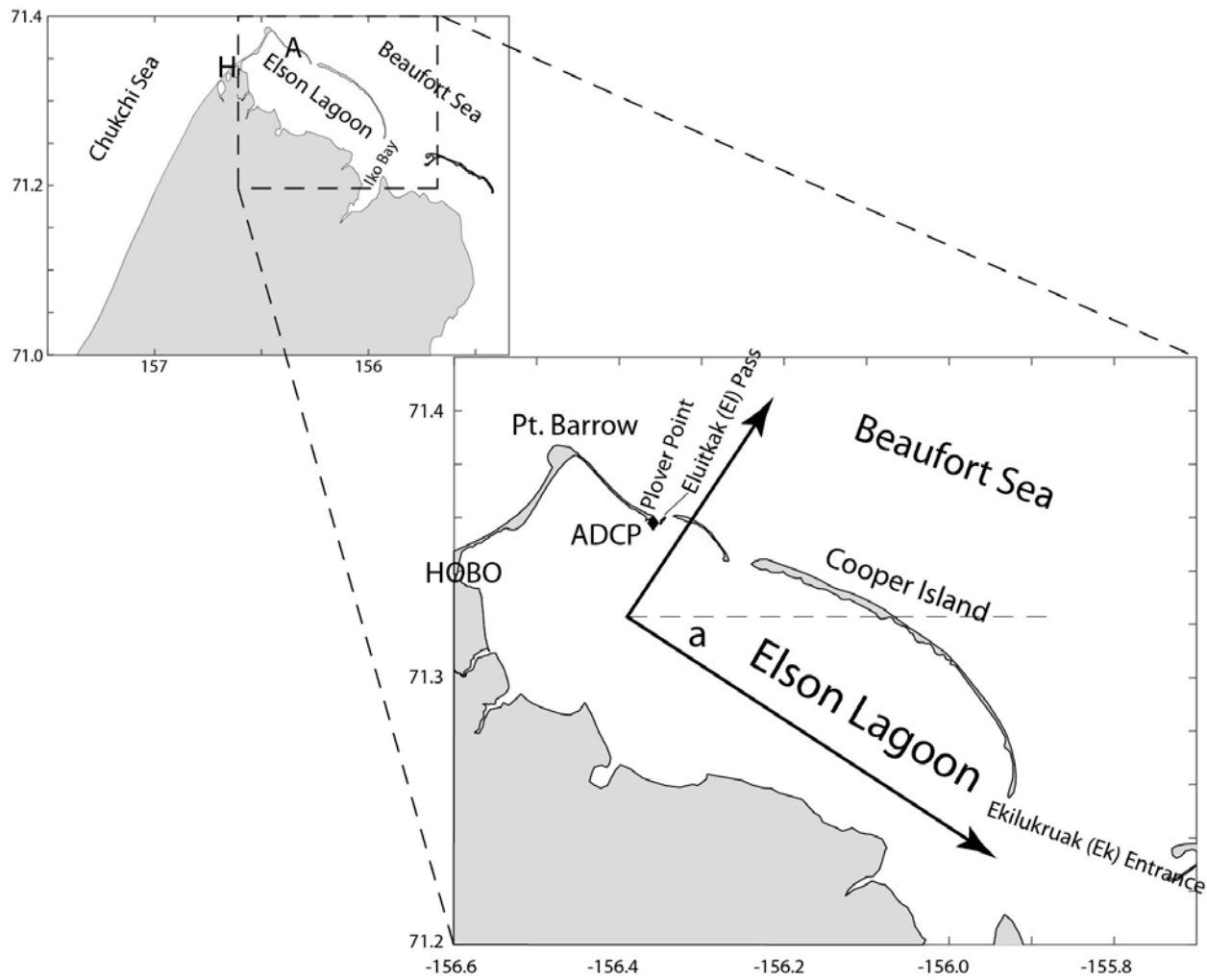


Figure 3.1 Study area. The inset shows the position of the Elson Lagoon being at the corner of the Beaufort Sea and Chukchi Sea. The Elson Lagoon main axis is about -31 degree off the east-west direction. H on the inset marks the location of North Salt Lagoon. The North Salt Lagoon deployment site is also shown as HOB0 in the zoomed in map (without showing the lagoon because it is at the edge of the map).

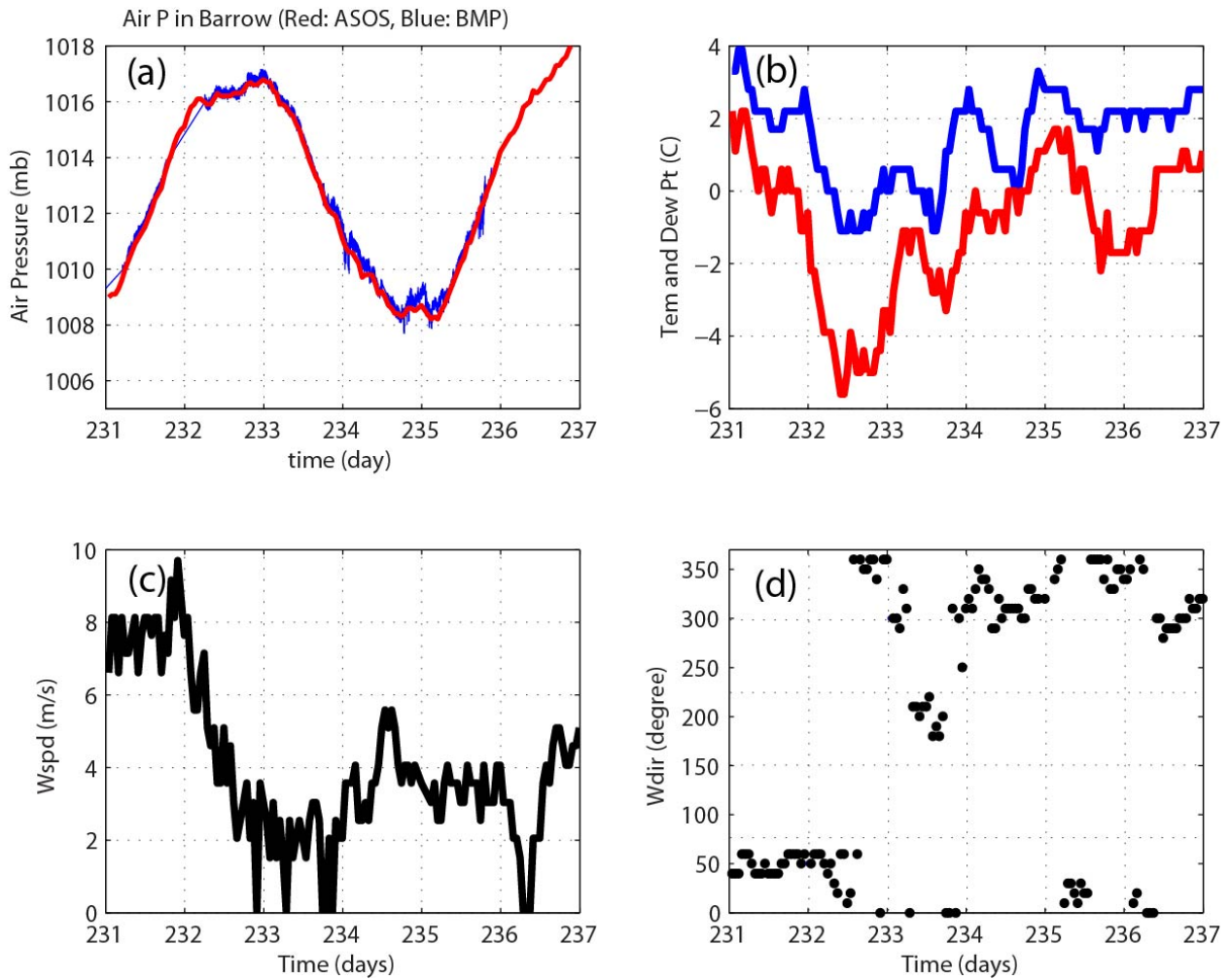


Figure 3.2 Time series of rotated wind components during the study period. (a) wind velocity components along the lagoon (blue) and across (red); (b) comparison of subtidal flow at various depths and the pressure difference between ADCP and HOBO sites; (c) subtidal velocity profile time series.

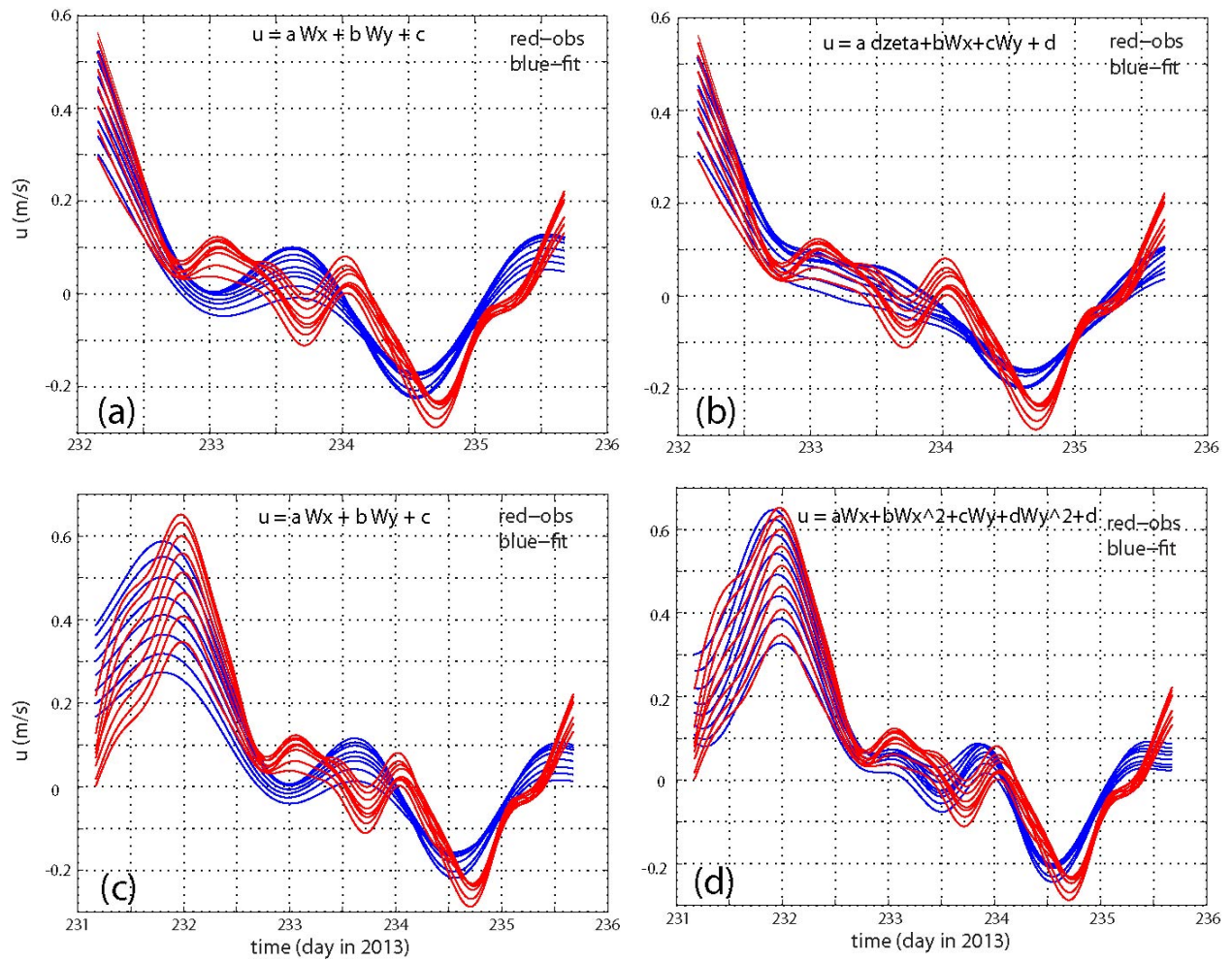


Figure 3.3 Comparison of observed and regression model produced subtidal flows in and out of the lagoon (positive out of the lagoon onto the shelf). Red lines are from observations and blue lines are from the regression: (a), (b), (c), and (d) are for the four regression models, respectively.

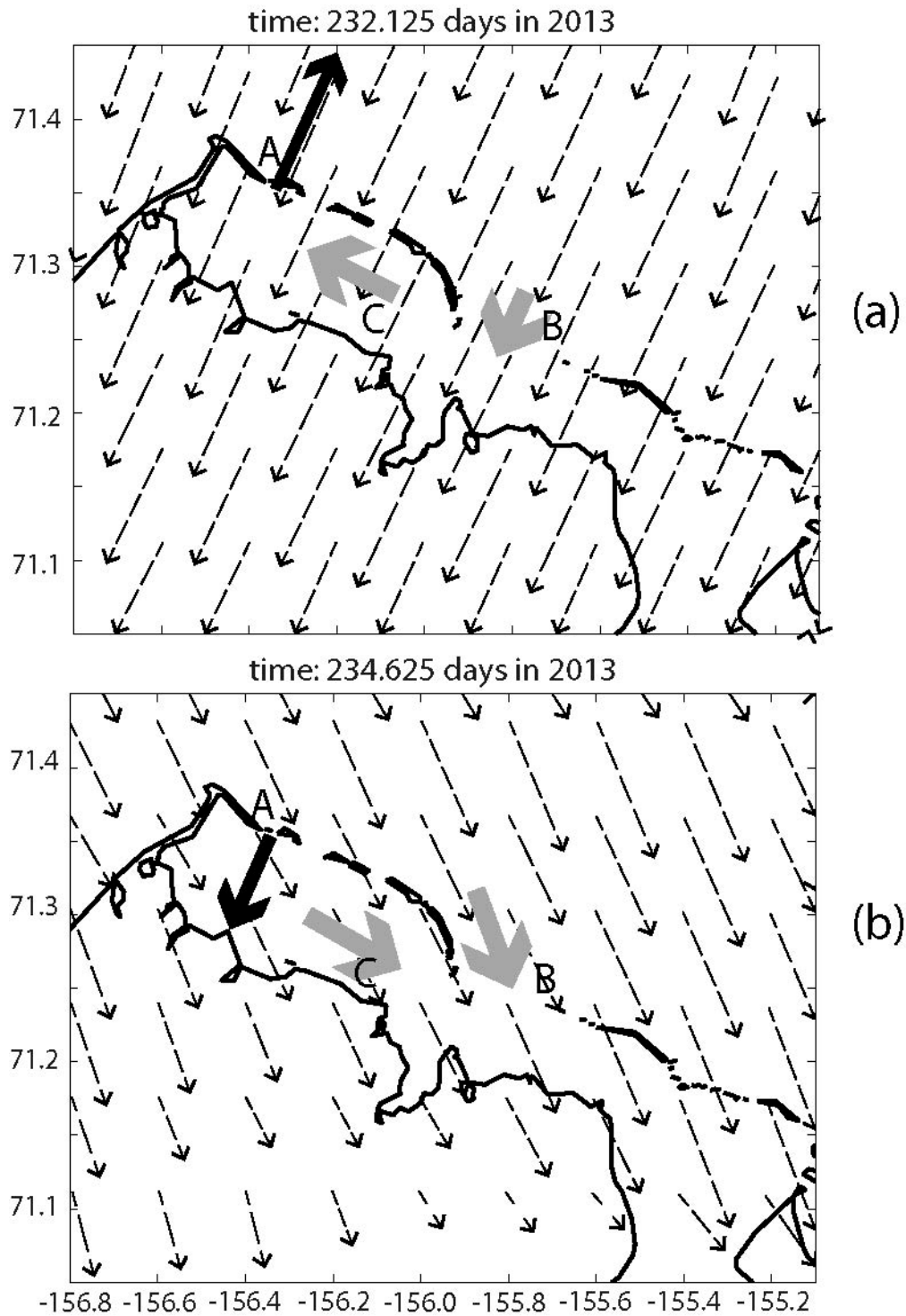


Figure 3.4 Schematic snapshots of the wind vectors based on the WRF model results showing the two wind conditions resulting in two different flow conditions (a) northeasterly wind condition producing outward flow at the Eluitkak Pass; (b) northwesterly wind condition producing the inward flow at the Eluitkak Pass.

A3.0 Chapter 3 Appendix. Supporting Information for “Mesoscale Weather System Induced Flushing of a Multi-inlet Arctic Lagoon in Summer”

A3.1 Introduction

In this supplemental information file, we provide the weather maps from NOAA, our raw data from the acoustic Doppler current profiler (ADCP), the regression tables with the ADCP data, the weather station time series data, and the Weather Research Forecast (WRF) model description and relevant references. The weather maps were obtained from <http://www.wpc.ncep.noaa.gov/>. The ADCP data can be obtained from the lead author through email (cli@lsu.edu) after publication of the article. The ADCP data processing was similar to many published studies (e.g. Li 2013).

A3.2 Weather Station Time Series Data

Weather station data from Barrow Airport (including air pressure, air temperature and dew point temperature, wind speed, and wind direction (Figure A1).

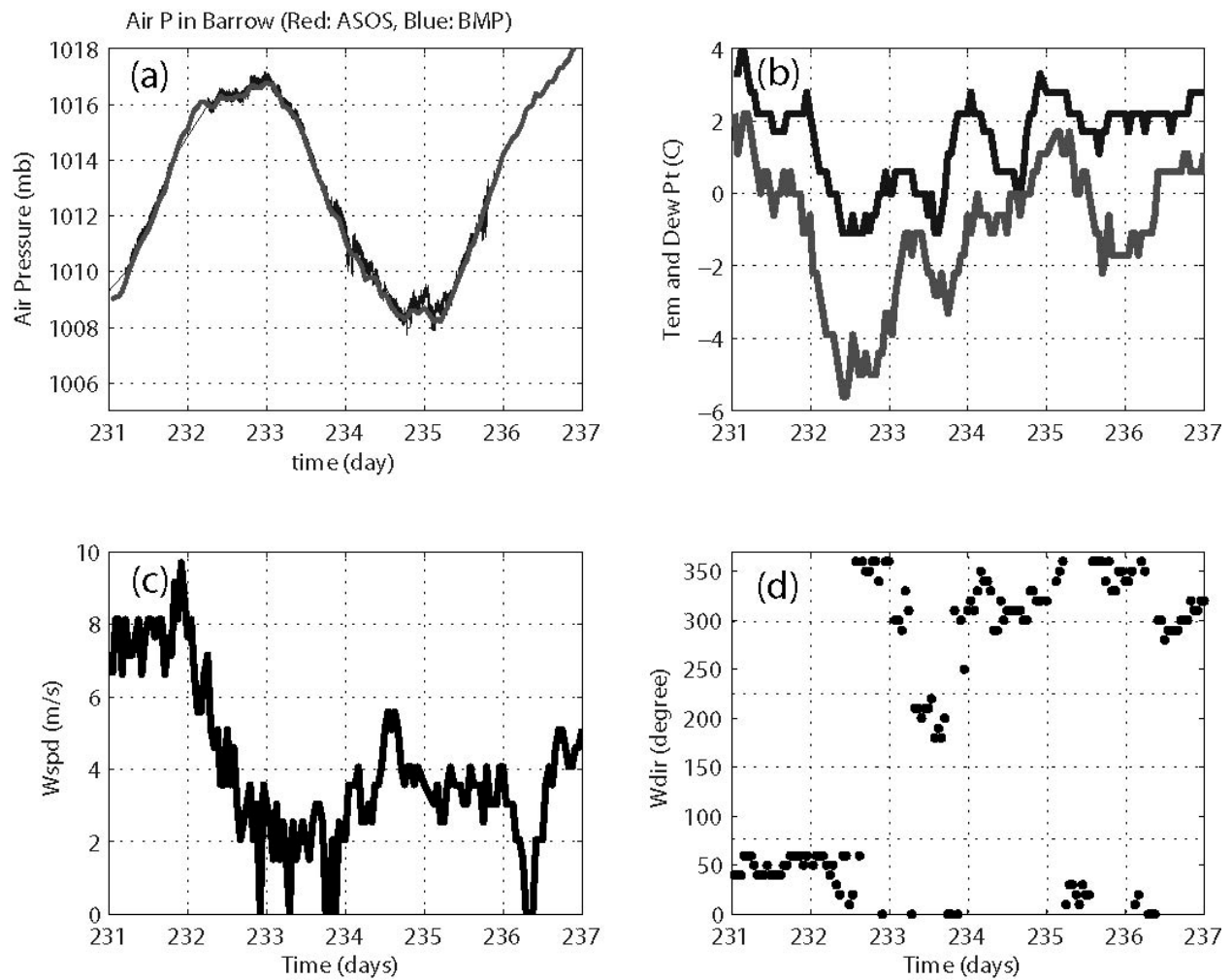


Figure A1. Weather data. (a) air pressure (dashed line was from Barrow airport); (b) air temperature (think line) and dew point temperature (dashed line); (c) wind speed; (d) wind direction.

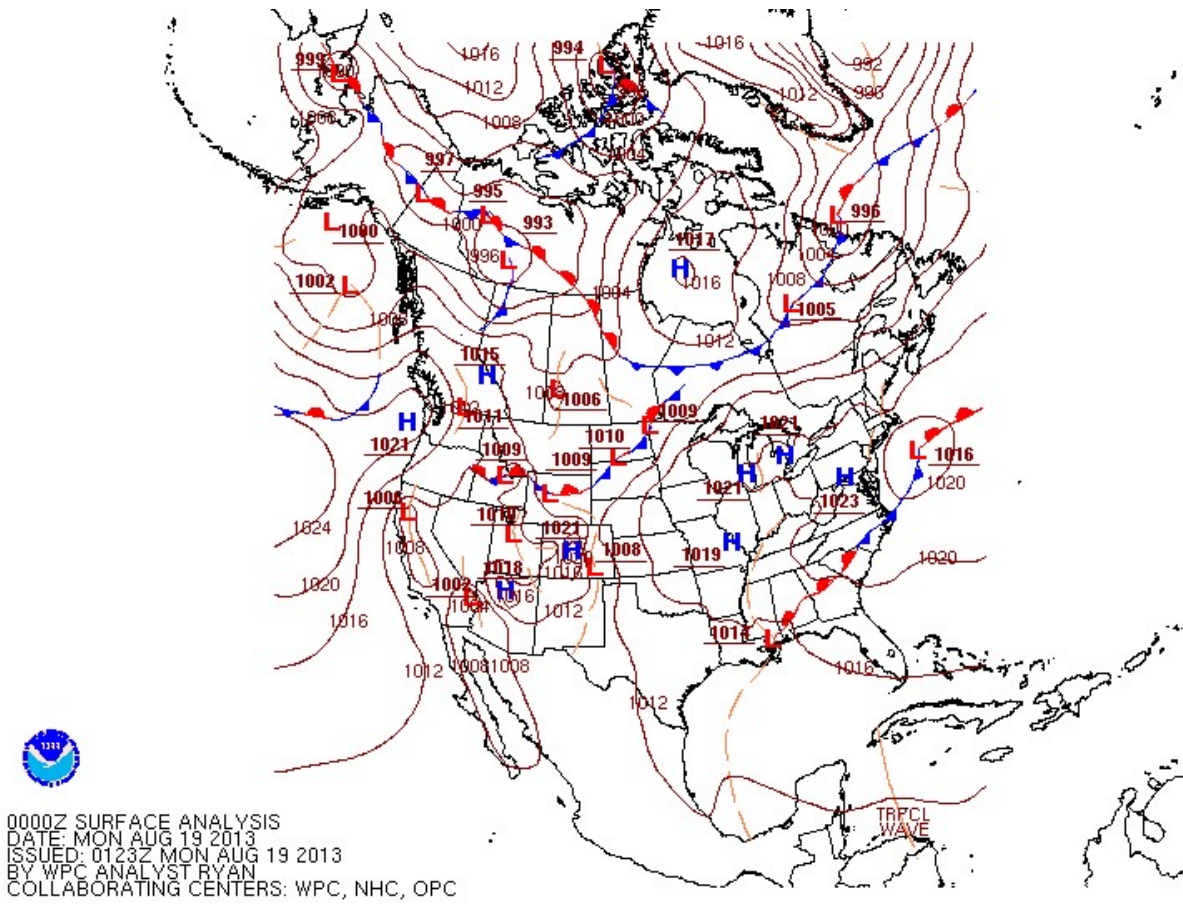


Figure A2. Weather map 1 at 0000Z, Aug. 19, 2013.

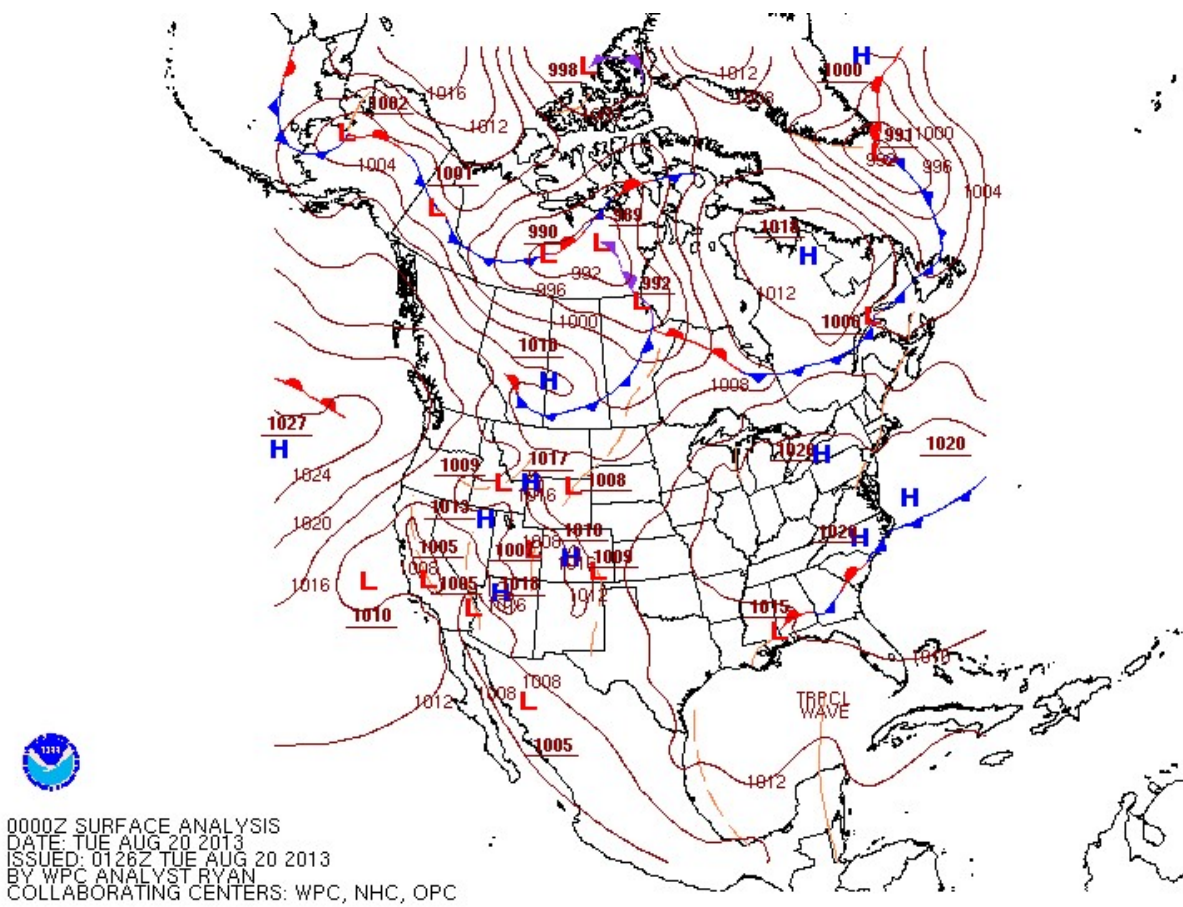


Figure A3. Weather map 2 at 0000Z, Aug. 20, 2013.

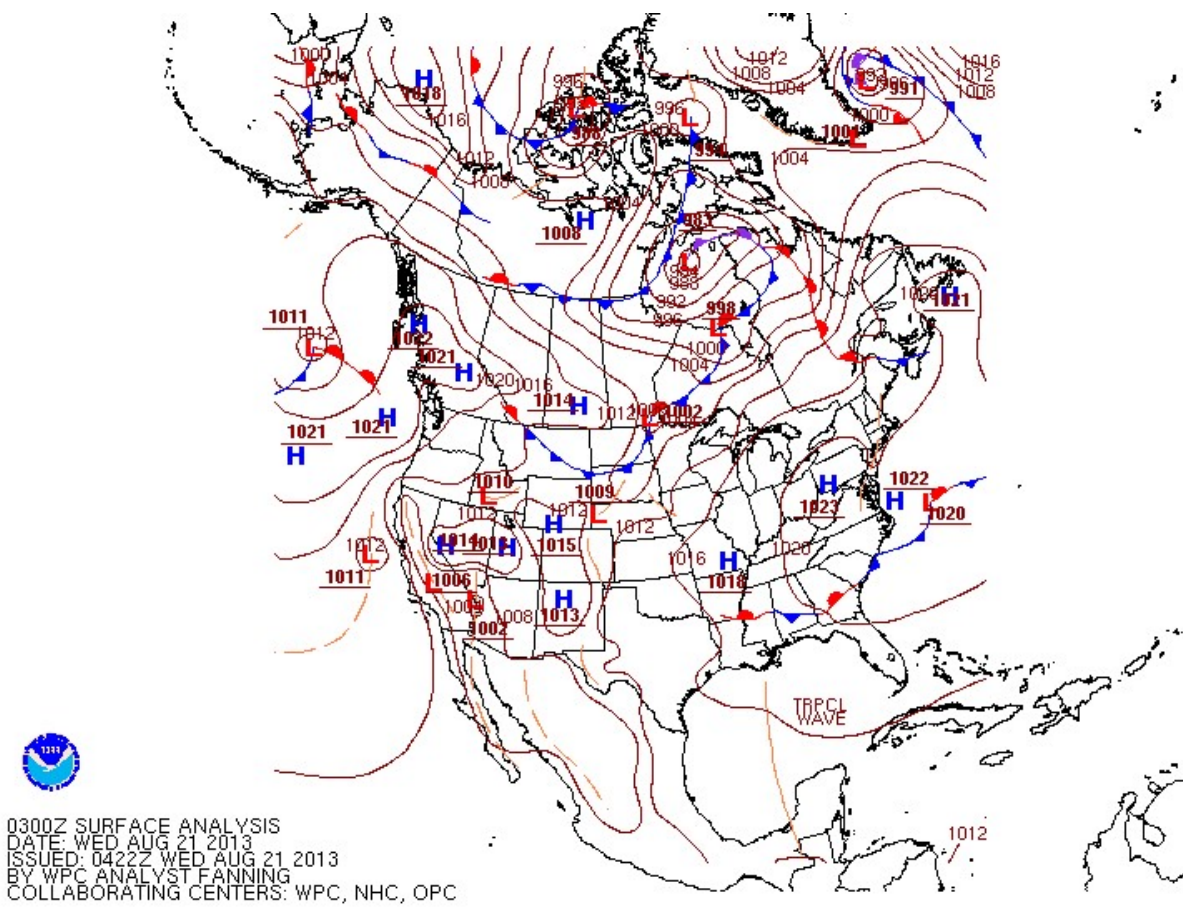


Figure A4. Weather map 3 at 0300Z, Aug. 21, 2013.

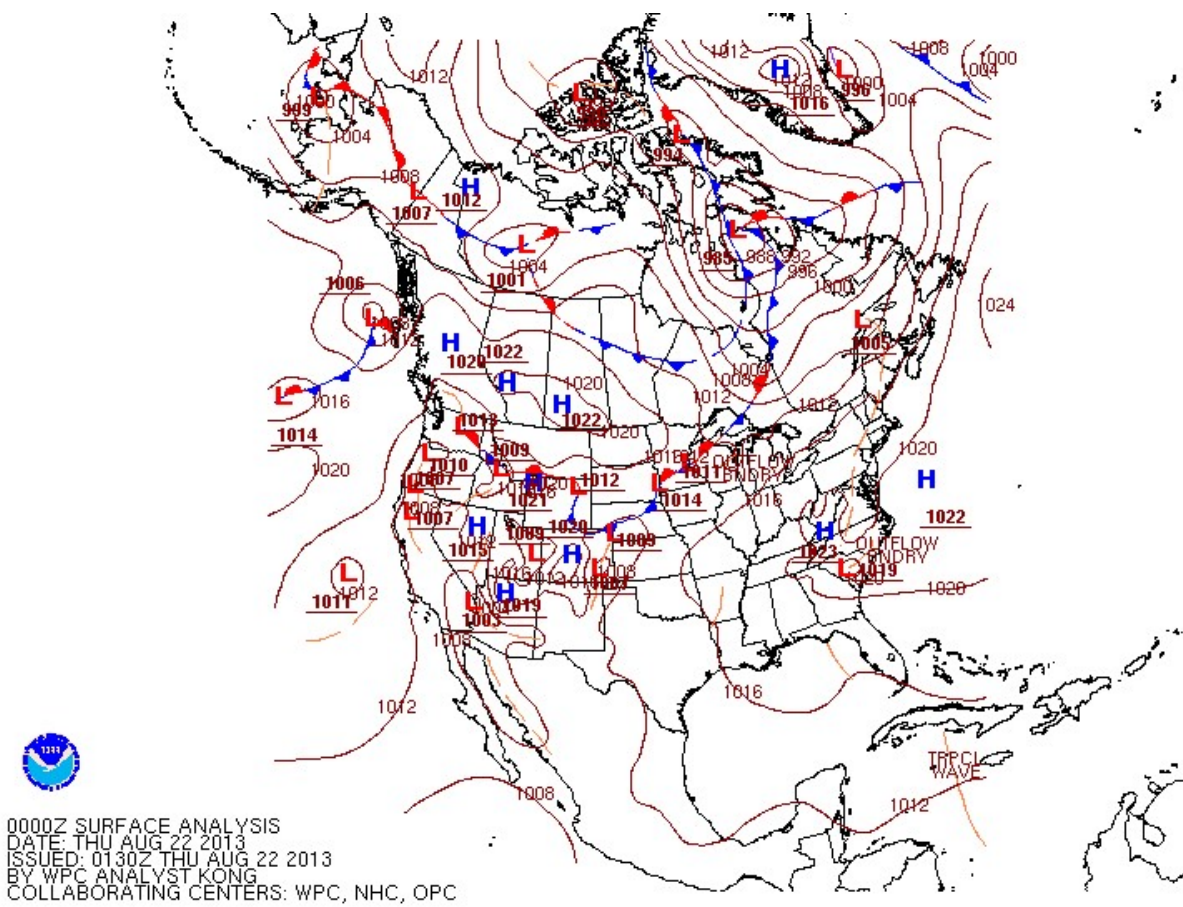


Figure A5. Weather map 4 at 0000Z, Aug. 22, 2013.

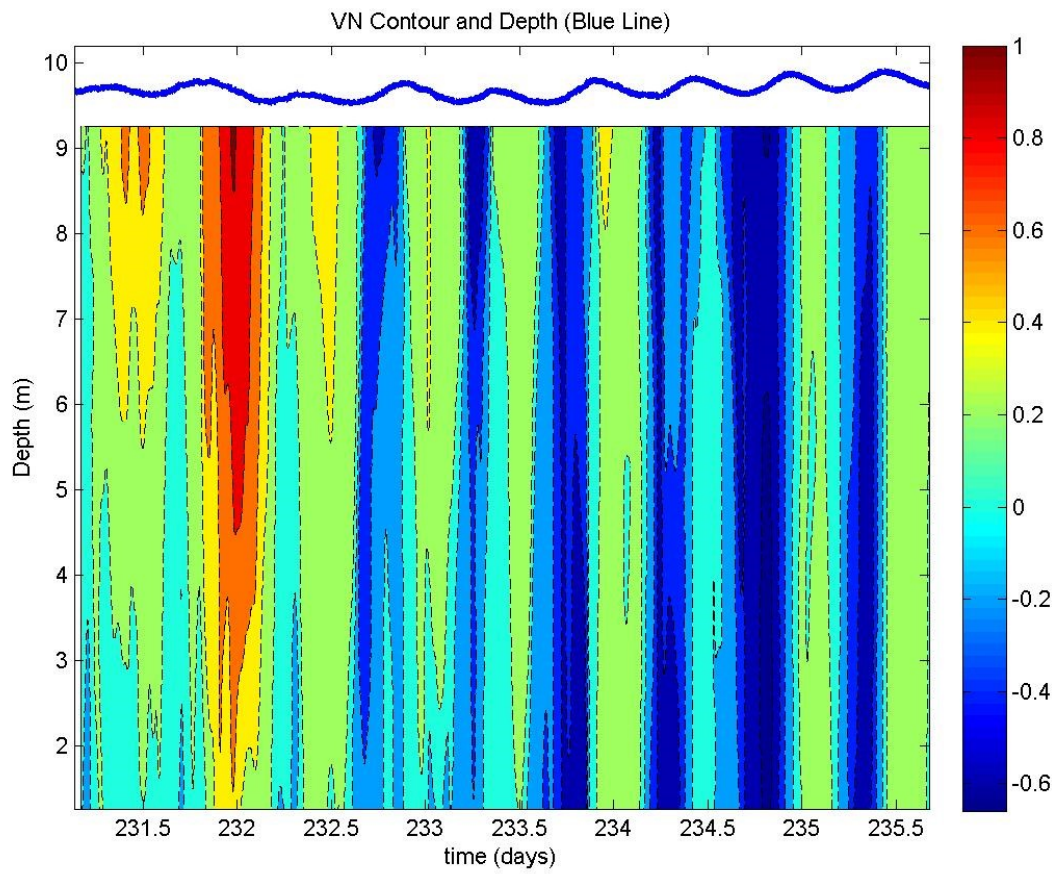


Figure A6. The velocity profiles time series from the ADCP (positive outward): raw data.

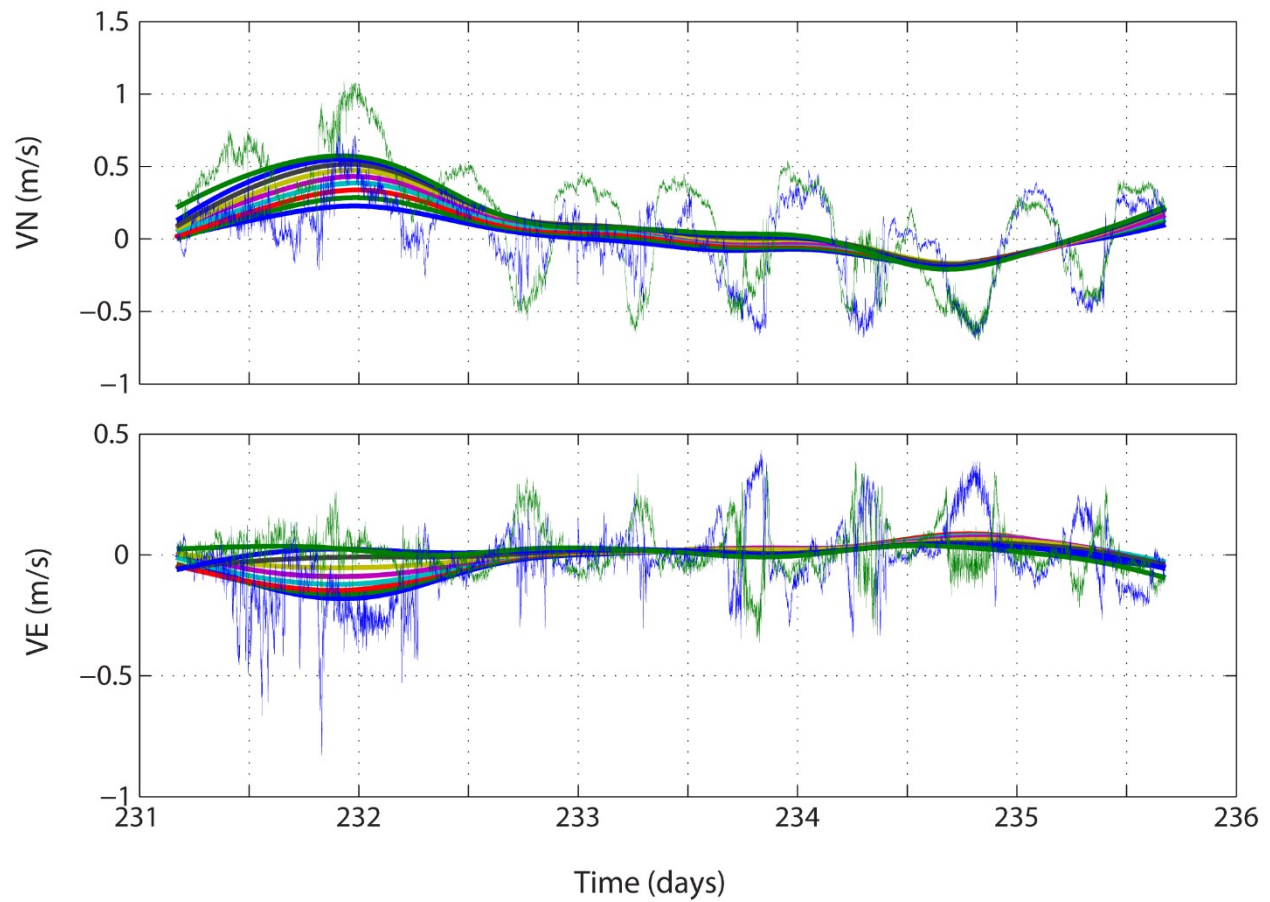


Figure A7. The velocity time series from the ADCP (showing both the north and east components). Raw data (thin lines) and 30-hr low pass filtered data (thick lines): different lines are from different depths. Generally, the closer to the bottom, the smaller the flow is (true for both raw and filtered data).

Table A1. Regression of subtidal velocity with wind components for the time period when the southern station using HOBO was measuring water level.

H (mab)	Regression Coefficient ($U=A W_a + B W_c + C$) A, B, C	95% Confidence Interval C		R ²
9.36	-0.0863 -0.0333 0.1290	-0.0874 -0.0342 0.1260	-0.0852 -0.0323 0.1319	0.8676
8.36	-0.0803 -0.0343 0.1170	-0.0814 -0.0352 0.1141	-0.0792 -0.0333 0.1199	0.8618
7.36	-0.0726 -0.0334 0.1063	-0.0738 -0.0344 0.1033	-0.0715 -0.0324 0.1094	0.8251
6.36	-0.0660 -0.0333 0.0909	-0.0672 -0.0343 0.0877	-0.0648 -0.0322 0.0942	0.7875
5.36	-0.0633 -0.0309 0.0781	-0.0645 -0.0319 0.0749	-0.0621 -0.0299 0.0812	0.7834
4.36	-0.0604 -0.0287 0.0655	-0.0615 -0.0296 0.0627	-0.0594 -0.0278 0.0683	0.8011
3.36	-0.0551 -0.0284 0.0464	-0.0560 -0.0292 0.0438	-0.0541 -0.0276 0.0489	0.8131
2.36	-0.0489 -0.0284 0.0216	-0.0498 -0.0292 0.0193	-0.0481 -0.0277 0.0239	0.8119

Table A2. Regression of subtidal velocity with pressure difference and wind components for the time period when the southern station using HOBO was measuring water level.

H (mab)	Regression Coefficient ($U=A \delta\zeta + B W_a + C W_c + D$) A, B, C, D	95% Confidence Interval C		R ²
9.36	1.4317 -0.0555 -0.0213 0.0608	1.3756 -0.0570 -0.0222 0.1020	1.4879 -0.0540 -0.0204 0.1072	0.9113
8.36	1.5807 -0.0464 -0.0211 0.0901	1.5298 -0.0478 -0.0219 0.0877	1.6316 -0.0450 -0.0203 0.0925	0.9202
7.36	1.8635 -0.0326 -0.0179 0.0747	1.8145 -0.0339 -0.0187 0.0724	1.9125 -0.0313 -0.0171 0.0770	0.9166
6.36	2.0545 -0.0219 -0.0161 0.0560	2.0058 -0.0232 -0.0169 0.0537	2.1032 -0.0206 -0.0154 0.0583	0.9096
5.36	2.0487 -0.0193 -0.0138 0.0432	2.0044 -0.0205 -0.0145 0.0412	2.0931 -0.0181 -0.0131 0.0453	0.9172
4.36	1.7447 -0.0229 -0.0142 0.0359	1.7017 -0.0241 -0.0149 0.0339	1.7877 -0.0218 -0.0135 0.0379	0.9116
3.36	1.4038 -0.0249 -0.0167 0.0225	1.3607 -0.0261 -0.0174 0.0205	1.4469 -0.0238 -0.0160 0.0245	0.8964
2.36	1.2137 -0.0229 -0.0183 0.0010	1.1717 -0.0240 -0.0190 -0.0010	1.2556 -0.0217 -0.0176 0.0029	0.8849

Table A3. Regression of subtidal velocity with wind velocity components for the entire time period when the ADCP was measuring velocity.

H (mab)	Regression Coefficient ($U=A W_a + B W_c + C$) A, B, C	95% Confidence Interval C		R ²
9.36	-0.0382 0.0101 0.1345	-0.0385 0.0096 0.1314	-0.0379 0.0106 0.1377	0.9275
8.36	-0.0357 0.0092 0.1244	-0.0360 0.0086 0.1210	-0.0353 0.0097 0.1278	0.9060
7.36	-0.0323 0.0082 0.1151	-0.0327 0.0076 0.1114	-0.0320 0.0088 0.1187	0.8719
6.36	-0.0292 0.0070 0.0997	-0.0296 0.0064 0.0959	-0.0289 0.0076 0.1035	0.8358
5.36	-0.0274 0.0072 0.0857	-0.0277 0.0066 0.0820	-0.0270 0.0078 0.0894	0.8278
4.36	-0.0253 0.0074 0.0724	-0.0256 0.0069 0.0689	-0.0250 0.0080 0.0759	0.8171
3.36	-0.0228 0.0063 0.0521	-0.0231 0.0058 0.0489	-0.0224 0.0069 0.0554	0.8044
2.36	-0.0203 0.0046 0.0257	-0.0205 0.0041 0.0227	-0.0200 0.0051 0.0287	0.8006

Table A4. Regression of subtidal velocity with wind velocity components and their squares for the entire time period when the ADCP was measuring velocity.

H (mab)	Regression Coefficient ($U=A W_a + B W_a^2 + C W_c + D W_c^2 + E$) A, B, C, D, E	95% Confidence Interval C		R ²
9.36	-0.0458 0.0004 -0.0125 -0.0038 0.1702	-0.0462 0.0004 -0.0132 -0.0039 0.1677	-0.0454 0.0004 -0.0118 -0.0037 0.1726	0.9628
8.36	-0.0443 0.0005 -0.0169 -0.0045 0.1652	-0.0446 0.0005 -0.0176 -0.0046 0.1628	-0.0439 0.0005 -0.0162 -0.0044 0.1677	0.9591
7.36	-0.0416 0.0006 -0.0204 -0.0049 0.1595	-0.0420 0.0005 -0.0211 -0.0050 0.1570	-0.0412 0.0006 -0.0197 -0.0048 0.1621	0.9470
6.36	-0.0395 0.0005 -0.0233 -0.0052 0.1476	-0.0399 0.0005 -0.0241 -0.0053 0.1448	-0.0391 0.0006 -0.0226 -0.0051 0.1503	0.9324
5.36	-0.0376 0.0004 -0.0220 -0.0049 0.1325	-0.0380 0.0004 -0.0227 -0.0050 0.1299	-0.0373 0.0005 -0.0213 -0.0048 0.1351	0.9282
4.36	-0.0360 0.0003 -0.0214 -0.0048 0.1196	-0.0363 0.0003 -0.0220 -0.0049 0.1172	-0.0356 0.0003 -0.0208 -0.0047 0.1219	0.9313
3.36	-0.0339 0.0002 -0.0219 -0.0046 0.0995	-0.0342 0.0001 -0.0224 -0.0047 0.0975	-0.0336 0.0002 -0.0213 -0.0045 0.1016	0.9349
2.36	-0.0313 -0.0000 -0.0215 -0.0041 0.0710	-0.0316 -0.0000 -0.0221 -0.0042 0.0692	-0.0311 0.0000 -0.0210 -0.0041 0.0729	0.9376

A3.3 The WRF Model

The Weather Research Forecast (WRF) model simulates the atmospheric circulation, providing weather forecast or hindcast. Our simulation period is from Aug. 19 to Aug. 23, 2013. The Global Forecast System (GFS) data produced by the National Centers for Environmental Prediction (NCEP) were used as input, with a spatial resolution of 0.5°. These data are calculated four times per day every 6 hours. We use three nested domains for the simulation. The center of the 1st domain is at 71.36° N and 156.35° W. The resolution for the 1st domain is 16 km, while the resolution for the 3rd domain is approximately 1.78 km (Figure A7). The model outputs results at hourly intervals for analysis. For the microphysics (mp_physics), we choose the New Thompson scheme (Thompson et al. 2008), which is a new scheme with ice, snow and graupel processes suitable for high-resolution simulations. We use the rapid and accurate radiative transfer model (RRTM) (Mlawer et al. 1997) for the longwave radiation and shortwave radiation. RRTM parameterizes longwave processes containing the effect of water vapor, ozone, CO₂, and trace gases. Furthermore, it has been found that during clear-sky conditions, the RRTM scheme is more applicable than other longwave radiation schemes for previous simulations of Arctic environments in the treatment of longwave energy (Inoue et al. 2006; Pinto et al. 1997; Ruffieux et al. 1995). The selection of another parameter icloud is set to 1 to enable the use of Xu-Randall method (Xu et al. 1996). For land surface, the Noah LSM with an Eta similarity surface layer and fractional sea ice are selected.

A3.4 References for the Supplemental Materials

- Inoue J, Liu J, Pinto JO, Curry J. 2006. Intercomparison of Arctic regional climate models: Modeling clouds and radiation for SHEBA in May 1998. *J Clim.* 19: 4167–4178. doi:10.1175/JCLI3854.1
- Li C. 2013. Subtidal water flux through a multi-inlet system: Observations before and during a cold front event and numerical experiments. *J Geophys Res. – Oceans.* 118: 1–16. doi:10.1029/2012JC008109
- Mlawer EJ, Taubman SJ, Brown PD, Iacono MJ, Clough A. 1997. Radiative transfer for inhomogenous atmosphere: RRTM, a validated correlated-k model for the longwave. *J Geophys Res.* 102(D14): 16663–16682. doi:10.1029/97JD00237
- Pinto JO, Curry JA, Fairall CW. 1997. Radiative characteristics of the Arctic atmosphere during spring as inferred from ground-based measurements. *J Geophys Res.* 102(D6): 6941–6952. doi:10.1029/96JD03348
- Ruffieux D, Persson POG, Fairall CW, Wolfe DE. 1995. Ice pack and lead surface energy budgets during LEADDEX 92. *J Geophys Res.* 100(C3): 4593–4612. doi:10.1029/94JC02485
- Thompson G, Field PR, Rasmussen RM, Hall WD. 2008. Explicit forecasts of winter precipitation using an improved bulk microphysics scheme. Part II: Implementation of a new snow parameterization. *Monthly Weather Review.* 136: 5095–5115. doi:10.1175/2008MWR2387.1
- Xu K-M, Randall DA. 1996. A semiempirical cloudiness parameterization for use in climate models. *J. Atmos. Sci.* 53: 3084–3102.

4.0 Patterns in Arctic Nearshore Communities Across Multiple Spatial and Temporal Scales

M. Barton, J. Vollenweider, R. Heintz

4.1 Introduction

The Arctic nearshore is a habitat expected to be impacted differently from offshore, pelagic regions from the effects of changing sea ice conditions, coastal erosion, increased ship traffic and related infrastructure, and oil development. Much work has been done to inventory fish communities in the coastal region where fish and their predators are known to be important resources for subsistence users (e.g., Craig et al. 1982, Schmidt et al. 1983, Craig 1984, Thorsteinson et al. 1991, Jarvela and Thorsteinson 1999, Majewski et al. 2009, Johnson et al. 2012, Thedinga et al. 2013). The environmental conditions structuring seasonal and annual variation in nearshore fish community composition is less understood but critical in understanding and predicting future scenarios (Roux et al. 2016). Over the course of three summers (2013-2015) we characterized nearshore fish communities in three converging waterbodies in the area adjacent to Point Barrow, Alaska, including the Chukchi and Beaufort Seas, and Elson Lagoon. We determined the sampling frequency to accurately describe seasonal changes throughout the summer ice-free season.

4.2 Methods

4.2.1 Study Area

Point Barrow, AK is a unique area where multiple Arctic nearshore habitat types are found in close proximity to each other. Furthermore, Point Barrow is bordered on the West by the relatively narrow shelf of the Chukchi Sea (CHS) and to the East by the broad shelf of the Beaufort Sea (BFS), with the large estuarine Elson Lagoon (ESL) opening into the Beaufort Sea just 5 km Southeast of Point Barrow (Figure 1.1). These distinct water bodies have distinct conditions that are likely to support different species assemblages (See chapter 2). Furthermore, this dynamic area undergoes a great change as it shifts from ice-covered winter to open water summer, and these changes are expected to drive changes in community composition as the seasons progress.

4.2.2 Sample Collection

Fish were sampled using beach seines at 12 sites on a weekly basis throughout the summer, ice-free season from July – August in three years, 2013-2015. Fish communities were sampled using a beach seine at 12 stations (5 CHS, 3 BFS, and 4 ESL) at weekly intervals from July 14 – September 4. Sampling weeks were designated as calendar weeks for this time period (weeks 28 – 34). The beach seine was 37 m long with variable mesh sizes: 10 m of 32 mm outer panels, 4 m of 6 mm middle panels, and 9 m of 3.2 mm blunt panel. Each set was round-haul style, paid out of a 3 m inflatable zodiac following methods used by Johnson et al. (2010). All collections occurred during daylight hours irrespective of tide as tidal cycles in Barrow are small. The entire catch was put in a Ziploc bag and placed on ice to be processed in the lab. In the case of very large catches (> 1000 fish), fish larger than 40 mm were set aside, the remainder of the catch was weighed in the field, and a 1 liter subsample was placed in a Ziploc bag to be processed in the lab. Once in the lab, all fish were sorted and enumerated to the lowest practical taxon. For cottids, larval sculpin were classified as “sculpin unidentified”. In the case of a subsample, the

subsample was counted and weighed by each species and the ratios of counts to weights were applied to the total weight from the field to estimate species abundances. Fish were frozen after processing to be used in multiple analyses that are detailed in other chapters. Oceanographic and atmospheric parameters were measured concurrently with fish catches and are presented in Chapter 2. Impacts of these parameters on community composition are discussed in Chapter 5.

In addition to on-shore beach seine collections, fish samples were collected from small vessels (~15 m long) offshore of beach seine sites to water depths to 175 m. In 2013 the R/V Launch 1273 incurred engine problems and the vessel survey was canceled. In 2014, acoustic trawl surveys were conducted aboard the R/V Launch 1273 on July 25-28 and August 21-22. Severe wind storms limited the July sampling period and vessel complications cut the August sampling period short. In 2015, acoustic trawl surveys were conducted aboard the R/V Annika Marie during August 6-15 and aboard the R/V Ukpik during September 10-15 with the support of North Slope Borough Funding. In all three years, benthic fish were sampled using a 3 m plumb staff beam trawl with 7 mm mesh in the body of the net and 4 mm mesh in the codend liner following methods described by Norcross et al. (2013). In 2015, pelagic schools of fish were identified with SIMRAD ER60 hydroacoustics and sampled using an Aluette mid-water trawl with a mouth opening of 5 m wide by 3.5 m deep and decreasing mesh sizes from 20 to 12 mm with a 4 mm codend liner. Vessel-based fish catches from 2013 and 2014 (funded under BOEM and NPRB) are not consistent and are simply enumerated in this report. 2015 vessel survey data will be further explored in a final report to the NSB.

4.2.3 Determination of Sampling Frequency

Though Johnson and Thedinga (2012) presented valuable information about annual species abundance in the Chukchi nearshore, seasonal changes throughout the ice-free season remain a datagap. To determine the appropriate temporal scale for sampling these nearshore fish populations, we used similarity percentage analysis (SIMPER) in Primer v. 6.0. Analyses were conducted on catch compositions at scales of sequential days, weeks, and years.

4.2.4 Analytical Approach

Data are presented as summaries of catch and frequency of occurrence. Raw catch data for select species are provided on maps to evaluate spatial patterns. Comparisons of catch between various sampling strata (i.e. years, weeks, water bodies) rely on measures of CPUE which is equivalent to the number of fish per haul for beach seine data. Very few sets were conducted on trawl vessels and those data are not described here in detail. In other cases, the contribution of a species to total catch is estimated as the percentage of that species of the summed catches of all species. Frequency of occurrence is presented as the percentage of hauls in which the species was present in order to facilitate comparisons across strata.

Data summaries are presented across a range of spatial and temporal scales. Data are presented on the broadest scales, year or water bodies and then on progressively finer scales (e.g. weeks in a water body during a given year). Species richness, the number of species encountered, is plotted as a function of sampling week for each year and water body. Non-parametric Multidimensional Scaling (NMDS) ordinations were used to identify visual patterns in community composition of beach seine catches. Models were constructed on Bray Curtis similarity matrices after logarithmically transforming CPUE.

4.4 Results and Discussion

Over the course of three 6-week summer sampling seasons (2013–15) we pulled 172 beach seines yielding a total catch of 37,112 fish with an average of 216 fish per seine haul (CPUE). A total of 51 species of fish were caught from 14 families. Cottids were by far the most speciose family. A total of 39 species from 12 families were caught in both the beach seines and bottom trawls. Fewer fish were caught in pelagic habitats, only 13 species of fish from 7 families were caught in midwater trawls (Table 4.1)

4.4.1 Spatial Variation in Catch

Overall, catches were greatest in the Chukchi Sea, on average, catches there were fourfold those of the Beaufort Sea and sixfold those in Elson Lagoon (Table 4.2). Annual variation in catch was similar in the marine water bodies but not Elson Lagoon. In both the Chukchi and Beaufort Seas, catch was approximately 5 times greater in 2013 than 2014 when catch was lowest. Similarly, catches in these marine habitats in 2014 were about one third those in 2015. In Elson Lagoon, catch varied 3-fold between 2014, the year of greatest abundance, and 2015, the year of least abundance.

Community structure varied most between the marine habitats and Elson Lagoon. Rainbow Smelt (*Osmerus mordax*), and Whitefishes (*Coregonus spp.*) were exclusive to the Elson Lagoon (Table 4.3, Figures) while Snailfish (*Liparis sp.*) and Fourhorn Sculpin (*Cottis quadricornis*) were most frequently encountered there (Table 4.3, Figures 4.3, 4.8 and 4.13). In contrast, species found predominately in the Beaufort Sea and Chukchi Sea could also be found in the Elson Lagoon. However, catches of many of these species were more abundant in marine waters. This is evident in the mapped abundance data for Arctic Cod (*Boreogadus saida*), Capelin (*Mallotus villosus*), Pacific Sand Lance (*Ammodytes hexapterus*) and Saffron Cod (*Eleginus gracilis*) are shown in (Figures 4.1-4.15).

The differences in community composition between catches in Elson Lagoon and the marine locations is evident in the 2-dimensional non-parametric multidimensional scaling (NMDS) plot (Figure 4.16). Though much overlap exists between communities in Elson Lagoon and those of the Beaufort and Chukchi Sea, the spread of points along the first axis indicates separation between an “Elson” type catch and a “marine” type catch. The vertical spread of points in the positive direction is largely due to Capelin dominated catches versus Sand Lance dominated catches in the negative direction. The relative abundance of species between water bodies (Figure 4.17) supports this idea. The majority of catches in the Elson Lagoon consisted of fourhorn sculpin (*Myoxocephalus quadricornis*) and unidentified larval sculpin. In the nearshore Chukchi and Beaufort, Fourhorn Sculpin are in negligible abundance as are larval sculpin, but there are large contributions from Capelin and Sand Lance (*Ammodytes hexapterus*) in these water bodies.

4.4.2 Temporal variation in catch

Catch was quite variable across the three summers. The overall abundance of fish was greatest in 2013 when CPUE averaged 328 fish per haul (Table 4.2). In contrast, abundance dropped to about a third of that level in 2014 and increased again in 2015. These catches followed the general pattern for sea surface temperatures. The warmest year being 2013 and the coldest year being 2014. See Chapter 1 for details on environmental variables.

The CPUEs observed in the two warmest years (2013, 2015) were largely driven by relatively large catches of Capelin. In 2013 the catch was dominated by Pacific Sand lance, Capelin, Slender Eelblenny and larval Sculpin (Figure 4.18). The community in 2015 was similar with the exception that Saffron Cod were more abundant than Pacific Sand lance. In contrast, there were few Capelin caught in the 2014 and the catch composition was dominated by larval Sculpin and Pacific Sand lance.

A consistent pattern of increasing species richness with time was apparent across all years. As the summer season progressed, the species richness increased consistently across water bodies and years 5 to 6 weeks before declining (Figure 4.16). Catch compositions further demonstrate this phenomenon (Figure 4.20). In the early weeks of the surveys catches are dominated by larval Sculpin, but after week 31 the diversity of the catches increases in all locations.

Breaking down the catch composition by year suggests communities in the three water bodies are independent. In 2013 species diversity was highest in the Chukchi Sea, but it was highest in Elson Lagoon in the latter years (Tables 4.5 – 4.7). Diversity in the Beaufort Sea was always lower than the other water bodies (Tables 4.5 – 4.13). In some years gradients could be detected between sites in the Chukchi Sea and Elson Lagoon. For example in 2014, the contribution of larval Sculpin to total catch increases progressively from the Chukchi Sea to the Beaufort Sea and finally to Elson Lagoon (Figure 4.21). Similarly, the contribution of Pacific Sand lance decreases progressively from the Chukchi Sea, to the Beaufort Sea and Elson Lagoon. However, no such pattern exists in 2013 even though the catch in all three water bodies is dominated by Pacific Sand lance, larval Sculpin and Capelin. While there is evidence of a progressive decline in the catch of Capelin between the Chukchi Sea and Elson Lagoon in 2015 there is no evidence of a pattern with other dominant species.

4.4.3 Scales of fish community dynamics

To determine the appropriate time scale to sample nearshore fish communities, we compared beach seine catches on annual, monthly, weekly, and daily periodicity. Weekly variation in nearshore fish communities was as great as annual variation, as shown by a similar magnitude of dissimilarity between annual (78.3 ± 14.4) and weekly intervals (2013: 83.09 ± 15.9 ; 2014: 75.5 ± 19.8). Daily dissimilarity (42.8 ± 15.9) in community composition was much lower than dissimilarity between weeks and years. This indicates that variation between weeks in a given year can be as great as variation between years for the same week. Consequently, weekly sampling is required to adequately characterize the community structure over a given year. In contrast, daily samples are more auto-correlated indicating that less frequent sampling will adequately characterize community structure.

4.5 Acknowledgements

We would like to thank the multiple funding sources that payed for fish collections, including the Bureau of Ocean Energy Management (BOEM), the North Pacific Research Board (NPRB), and the North Slope Borough (NSB). The NSB also provided invaluable logistical help that made many of these fish collections possible, in particular Leandra Sousa, Todd Sformo, Craig George, Brian Person, Billy Adams, Robert Suydam and Taqulik Hepa. We also thank the scientists and vessel crew, in particular Kevin Boswell, Brenda Norcross, and Alexei Pinchuk. Additional key field personnel include Ann Robertson and Sam George who spent several summers in Barrow, AK running the beach seining effort, as well as Eric Wood, Alyssa Frothingham, Stella Moser, and Wyatt Fournier. Matt Callahan provided extensive database and mapping support for this project and Courtney Weiss was instrumental in tabulating data and creating figure and tables.

4.6 References

- Bluhm B, Gradinger R. 2008. Regional Variability in Food Availability For Arctic Marine Mammals. *Ecol Appl*. 18: S77–S96. doi: <http://dx.doi.org/10.1890/06-0562.1>
- Craig P. 1984. Fish use of coastal waters of the Alaskan Beaufort Sea: a review. *Trans Am Fish Soc*. 113: 37–41.
- Craig PC, Griffiths B, Haldorson L, McElderry H. 1982. Ecological Studies of Arctic Cod (*Boreogndus saida*) in Beaufort Sea Coastal Waters, Alaska. *Can Bull Fish Aquat Sci* 39: 395–406. doi: 10.1139/f82-057
- Craig P, Haldorson L. 1986. Pacific salmon in the North American Arctic. *Arctic*. 39(1): 2-7.
- Drinkwater KF. 2011. The influence of climate variability and change on the ecosystems of the Barents Sea and adjacent waters: Review and synthesis of recent studies from the NESSAS Project. *Prog Oceanogr*. 90: 47–61. doi: 10.1016/j.pocean.2011.02.006
- Dunton KH, Schonberg S V, Cooper LW. 2012. Food Web Structure of the Alaskan Nearshore Shelf and Estuarine Lagoons of the Beaufort Sea. *Estuaries and Coasts*. 35: 416–435. doi: 10.1007/s12237-012-9475-1
- Dunton KH, Weingartner T, Carmack EC. 2006. The nearshore western Beaufort Sea ecosystem: Circulation and importance of terrestrial carbon in arctic coastal food webs. *Prog Oceanogr*. 71: 362–378. doi: 10.1016/j.pocean.2006.09.011
- Gradinger R. 2009. Sea-ice algae: Major contributors to primary production and algal biomass in the Chukchi and Beaufort Seas during May/June 2002. *Deep Res Part II Top Stud Oceanogr*. 56: 1201–1212. doi: 10.1016/j.dsr2.2008.10.016
- Huntington HP, Nelson M, Quakenbush LT. 2012. Traditional Knowledge Regarding Walrus near Point Lay and Wainwright, Alaska. December: 1-9.
- Iverson SJ, Frost KJ, Lang SLC. 2002. Fat content and fatty acid composition of forage fish and invertebrates in Prince William Sound, Alaska: factors contributing to among and within species variability. *Mar Ecol Prog Ser*. 241: 161–181.
- Johnson SW, Thedinga JF, Neff AD, Hoffman CA. 2010. Fish Fauna in Nearshore Waters of a Barrier Island in the Western Beaufort Sea, Alaska. July: 1-29.
- Majewski, AR, Reist JD, Park BJ, Sareault JE, Lowdon MK. 2009. Fish catch data from offshore sites in the Mackenzie River estuary and Beaufort Sea during the open water season, July and August, 2005, aboard the CCGS Nahidik. Canadian Data Report of Fisheries and Aquatic Sciences 1204, Fisheries and Oceans, Canada.

- Michaud J, Fortier L, Rowe P, Ramseier R. 1996. Feeding success and survivorship of Arctic cod larvae, *Boreogadus saida*, in the northeast Water polynya (Greenland Sea). *Fish Oceanogr.* 5: 120–135.
- Norcross BL, Raborn SW, Holladay BA, Gallaway BJ, Crawford ST, Priest JT, Edenfield LE, Meyer R. 2013. Northeastern Chukchi Sea demersal fishes and associated environmental characteristics, 2001-2010. *Continental Shelf Research.* 67:77-95.
- Rass TS. 1968. Spawning and development of polar cod. *Rapp Proces-Verbeaux Reun du Cons Int pour l'Exploration la Mer.* 158: 135–137.
- Roux MJ, Harwood LA, Zhu X, Sparling P. 2016. Early summer near-shore fish assemblage and environmental correlates in an Arctic estuary. *Journal of Great Lakes Research.* 42:256-266.
- Schmidt DR, McMillan RO, Gallaway BJ. 1983. Nearshore fish survey in the Western Beaufort Sea Harrison Bay to Elson Lagoon. Outer Continental Shelf Environmental Assessment Program, Final Report, 491-552.
- Thedinga J, Johnson S, Neff A, Hoffman CA, Maselko JM. 2013. Nearshore Fish Assemblages of the Northeastern Chukchi Sea, Alaska. *Juneau, AK. Arctic.* 66(3): 257–268.
- Thorsteinson LK, Jarvela LE, Hale DA. 1991. Arctic fish habitat use investigations: nearshore studies in the Alaskan Beaufort Sea, summer 1990. Annual Report. OCS Study MMS 92-0011. 78 p.
- Watanabe E, Kishi MJ, Ishida A, Aita MN. 2012. Western Arctic primary productivity regulated by shelf-break warm eddies. *J Oceanogr.* 68: 703–718. doi: 10.1007/s10872-012-0128-6
- Wilson M, Jump C, Duffy-Anderson J. 2006. Comparative analysis of the feeding ecology of two pelagic forage fishes: capelin *Mallotus villosus* and walleye pollock *Theragra chalcogramma*. *Mar Ecol Prog Ser.* 317: 245–258. doi: 10.3354/meps317245

2013 Arctic cod catch

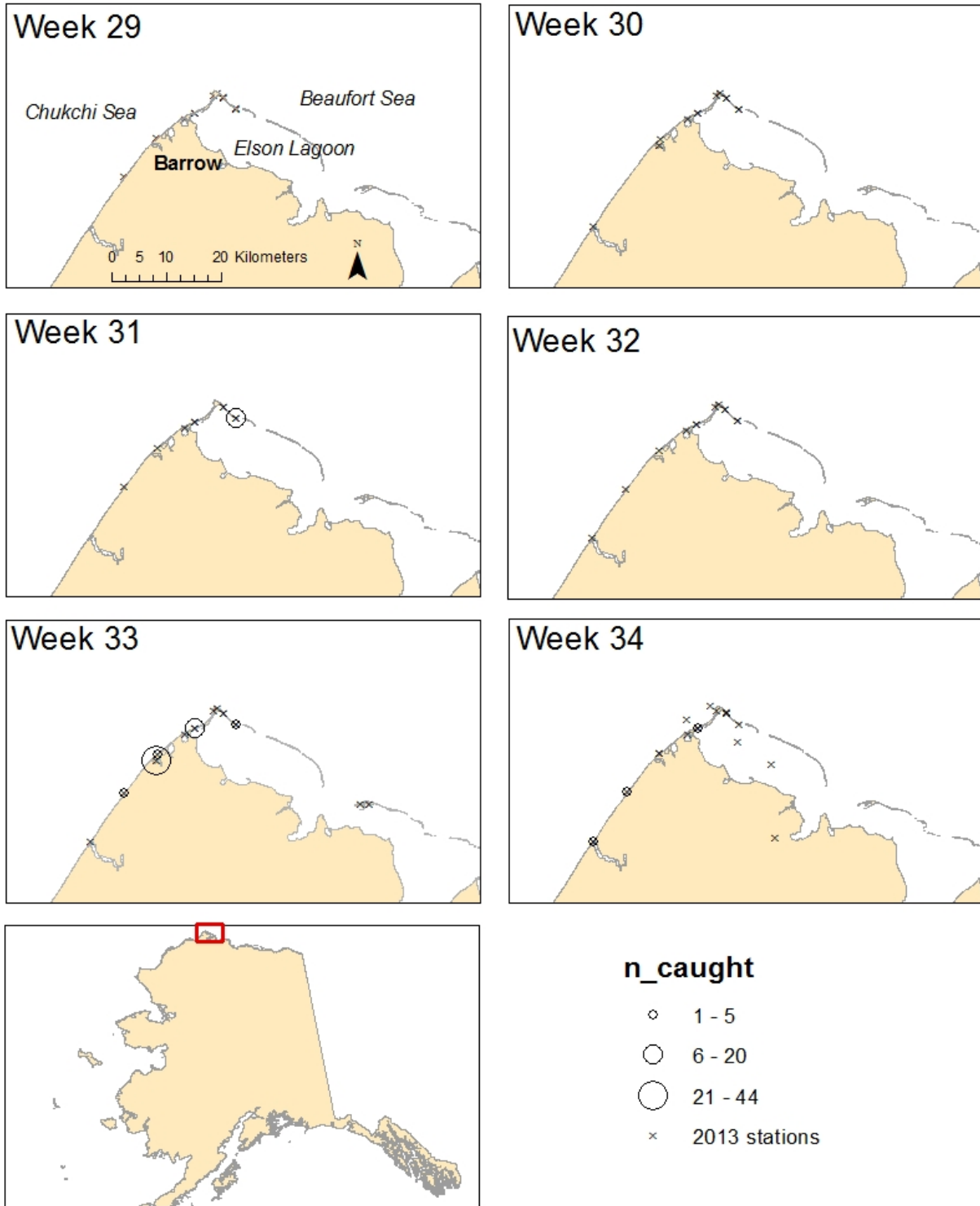


Figure 4.1 2013 Arctic cod catch by week. The red box depicted on the map of Alaska is the area that is expanded upon in the weekly catch maps.

2013 Capelin catch

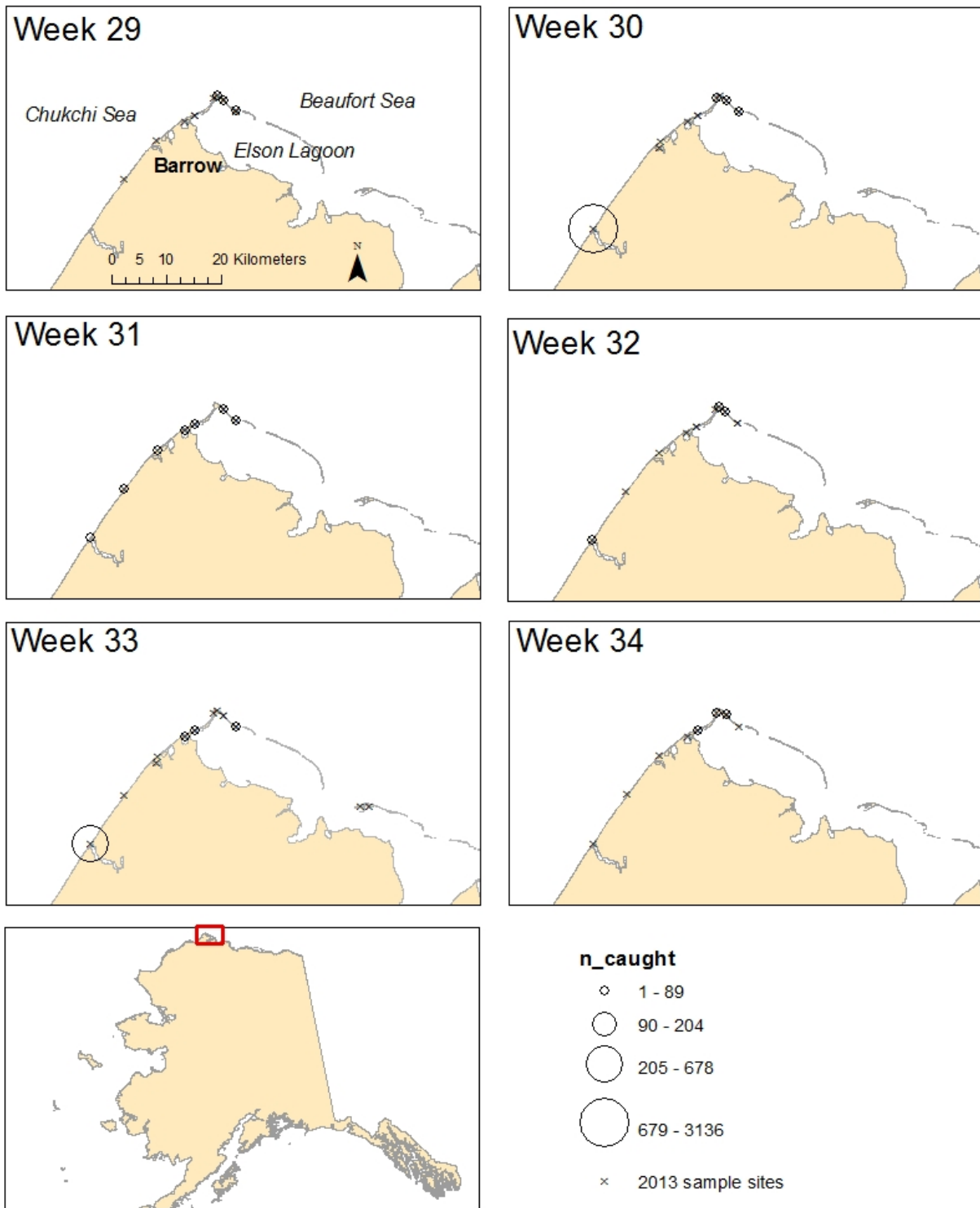


Figure 4.2 2013 capelin catch by week. The red box depicted on the map of Alaska is the area that is expanded upon in the weekly catch maps.

2013 Fourhorn sculpin catch

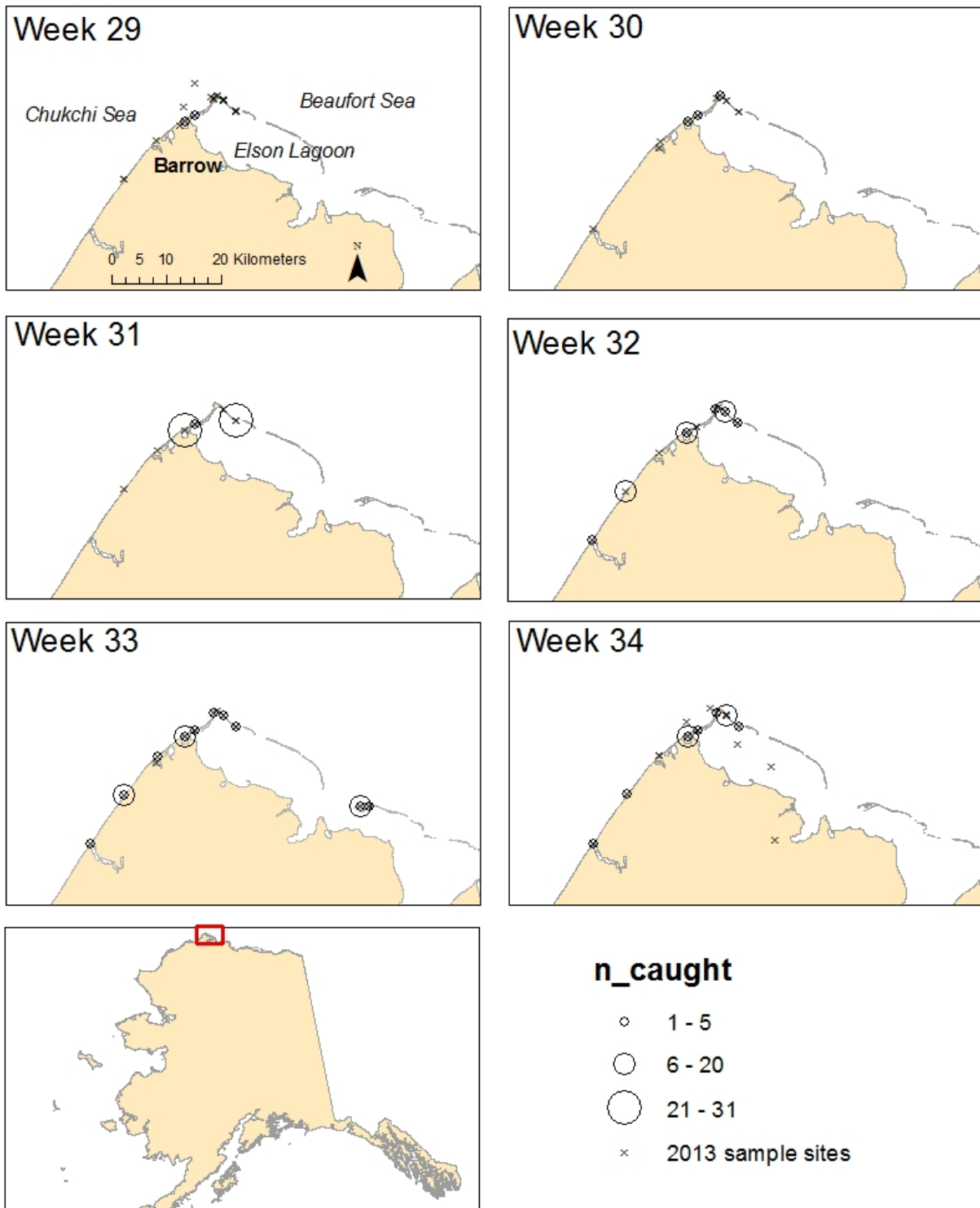


Figure 4.3 2013 fourhorn sculpin catch by week. The red box depicted on the map of Alaska is the area that is expanded upon in the weekly catch maps.

2013 Pacific sand lance catch

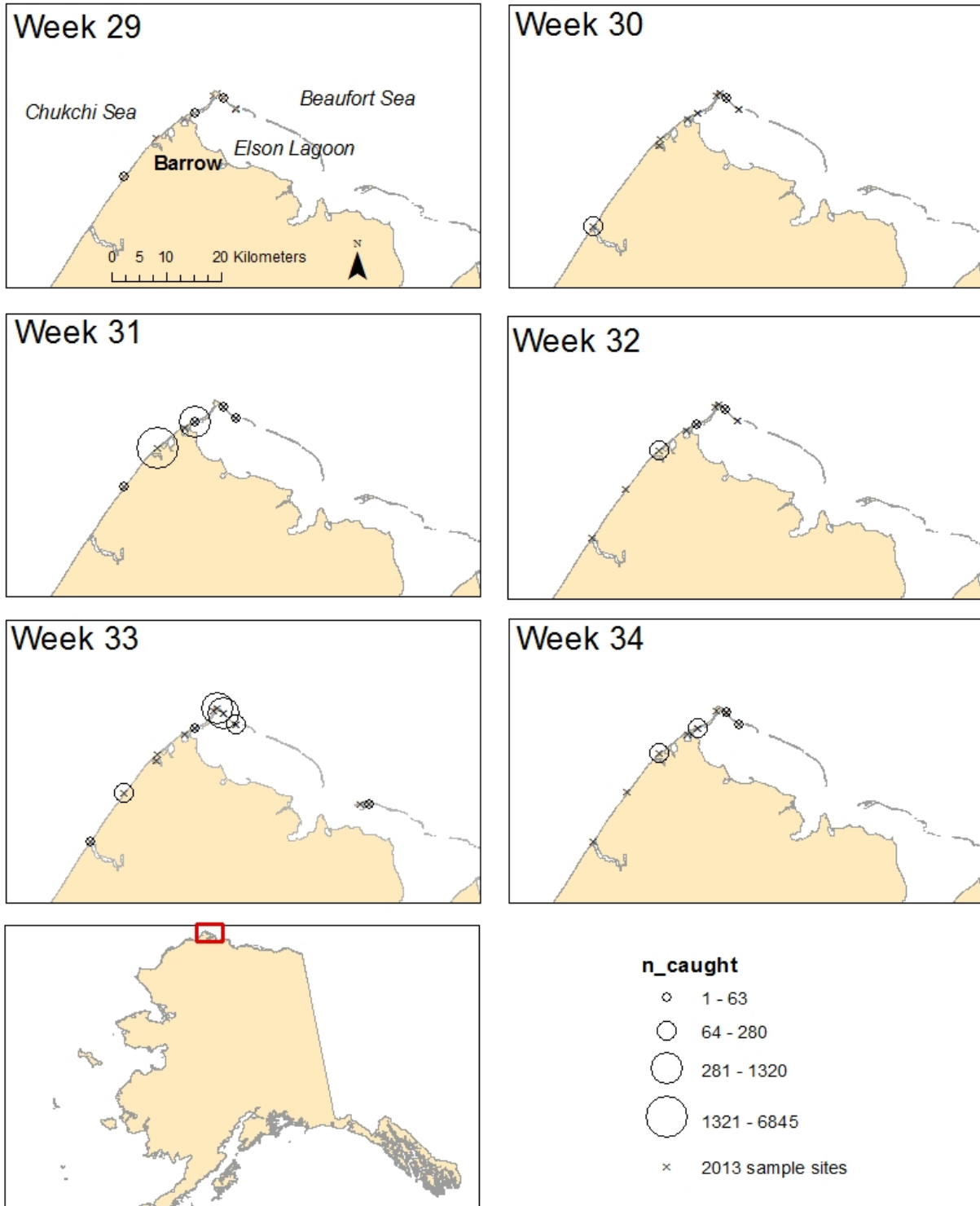


Figure 4.4 2013 Pacific sand lance catch by week. The red box depicted on the map of Alaska is the area that is expanded upon in the weekly catch maps.

2013 Saffron cod catch

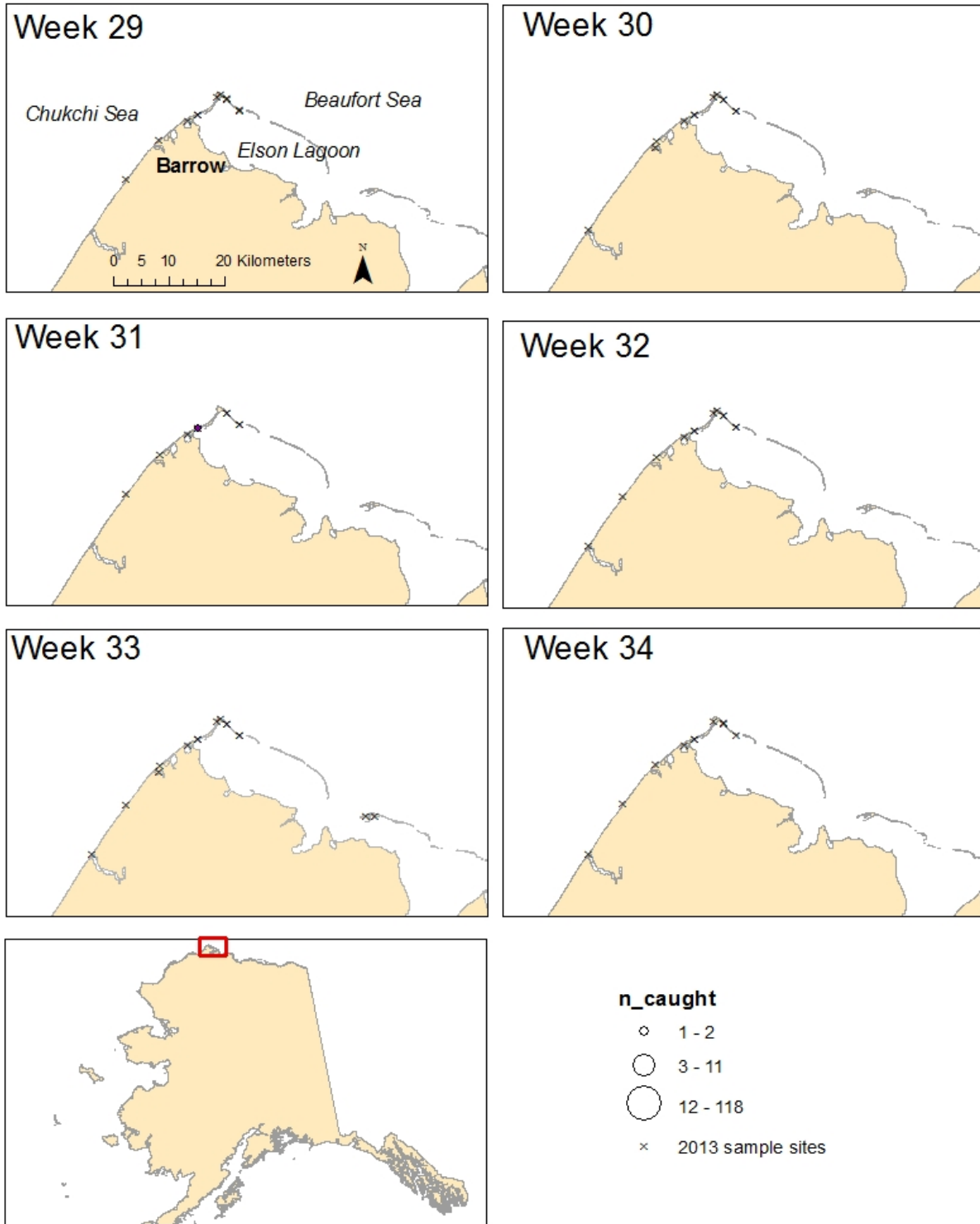


Figure 4.5 2013 saffron cod catch by week. The red box depicted on the map of Alaska is the area that is expanded upon in the weekly catch maps.

2014 Arctic cod catch

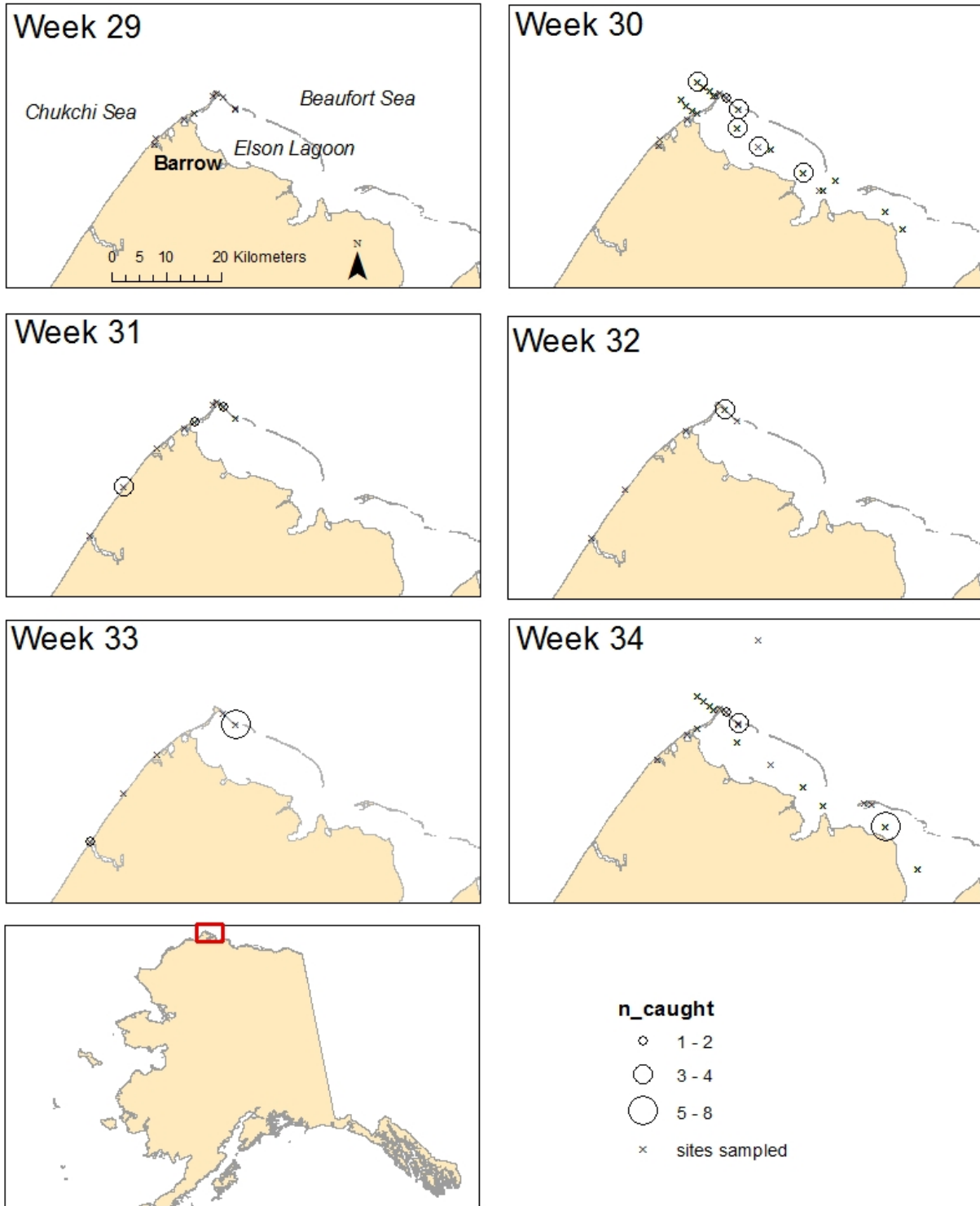


Figure 4.6 2014 Arctic cod catch by week. The red box depicted on the map of Alaska is the area that is expanded upon in the weekly catch maps.

2014 Capelin catch

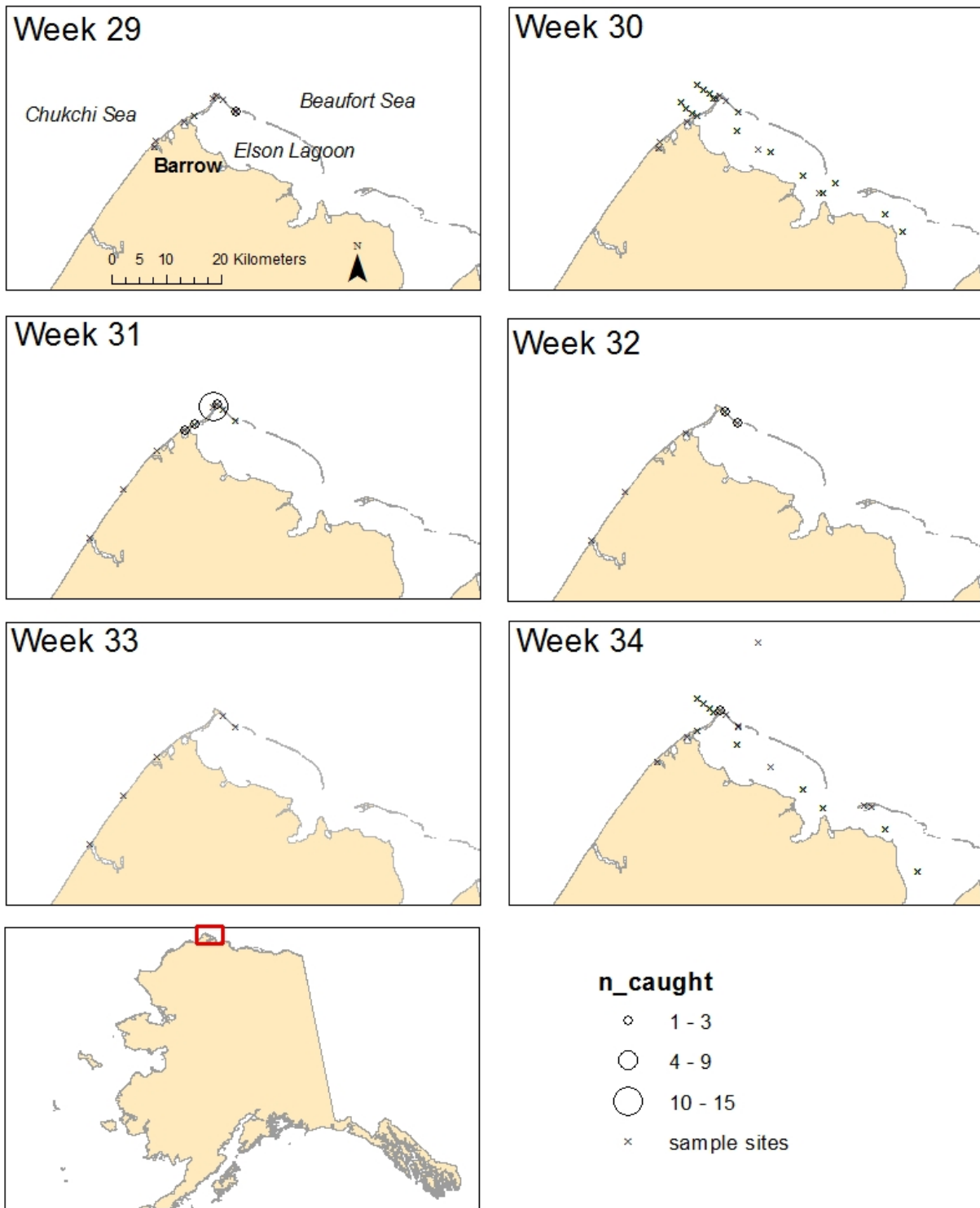


Figure 4.7 2014 capelin catch by week. The red box depicted on the map of Alaska is the area that is expanded upon in the weekly catch maps.

2014 Fourhorn sculpin catch

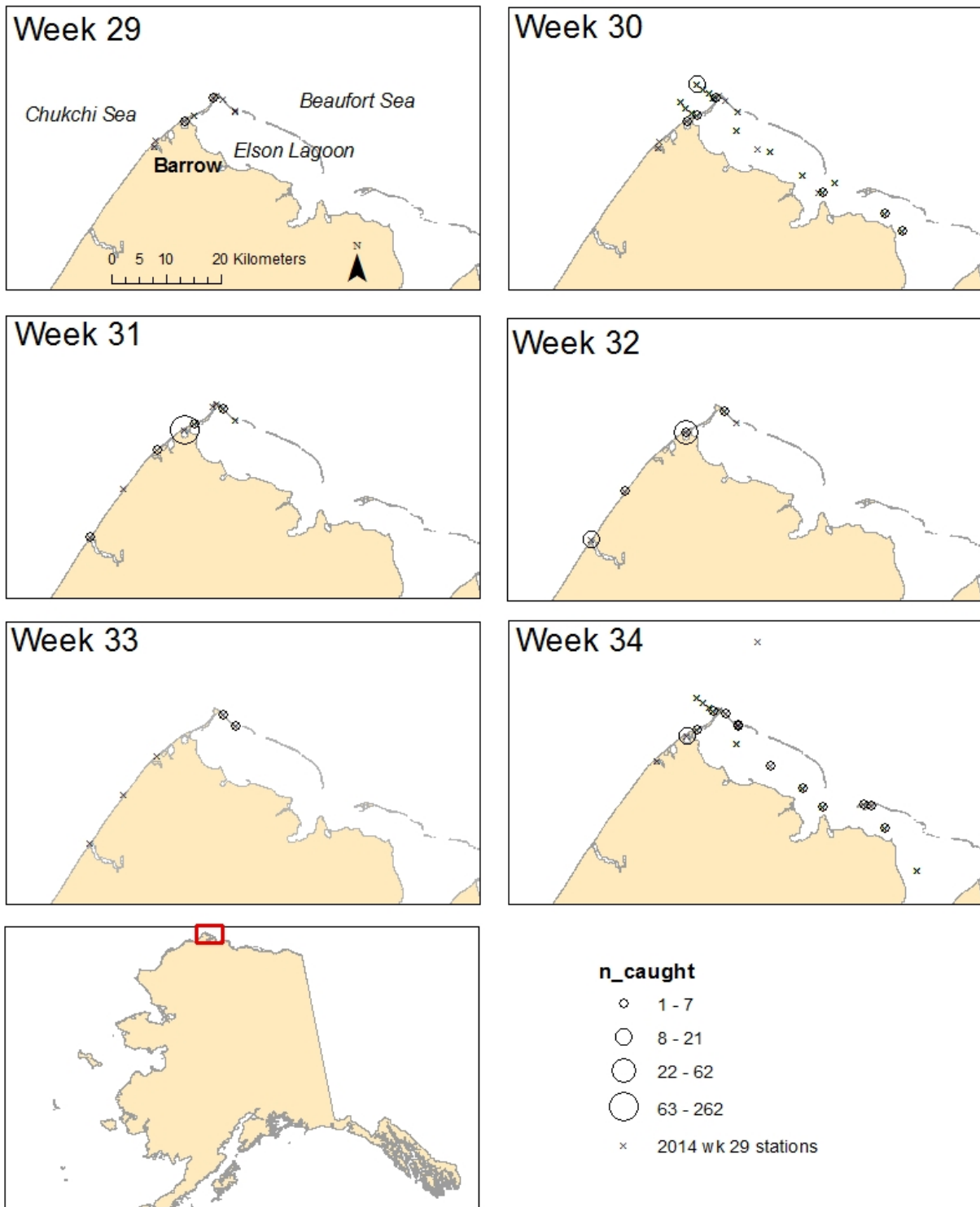


Figure 4.8 2014 fourhorn sculpin catch by week. The red box depicted on the map of Alaska is the area that is expanded upon in the weekly catch maps.

2014 Pacific sand lance catch

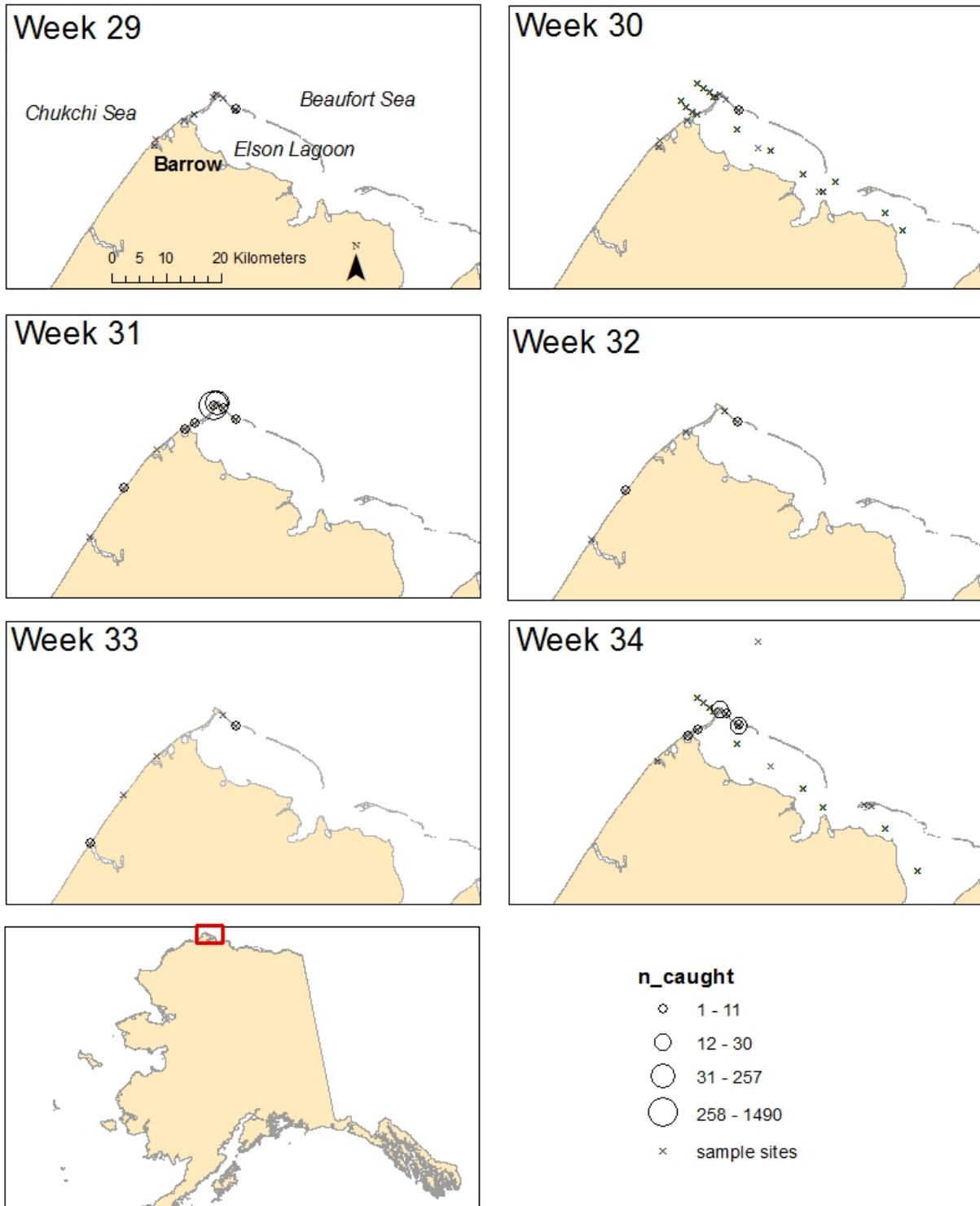


Figure 4.9 2014 Pacific sand lance catch by week. The red box depicted on the map of Alaska is the area that is expanded upon in the weekly catch maps.

2014 Saffron cod catch

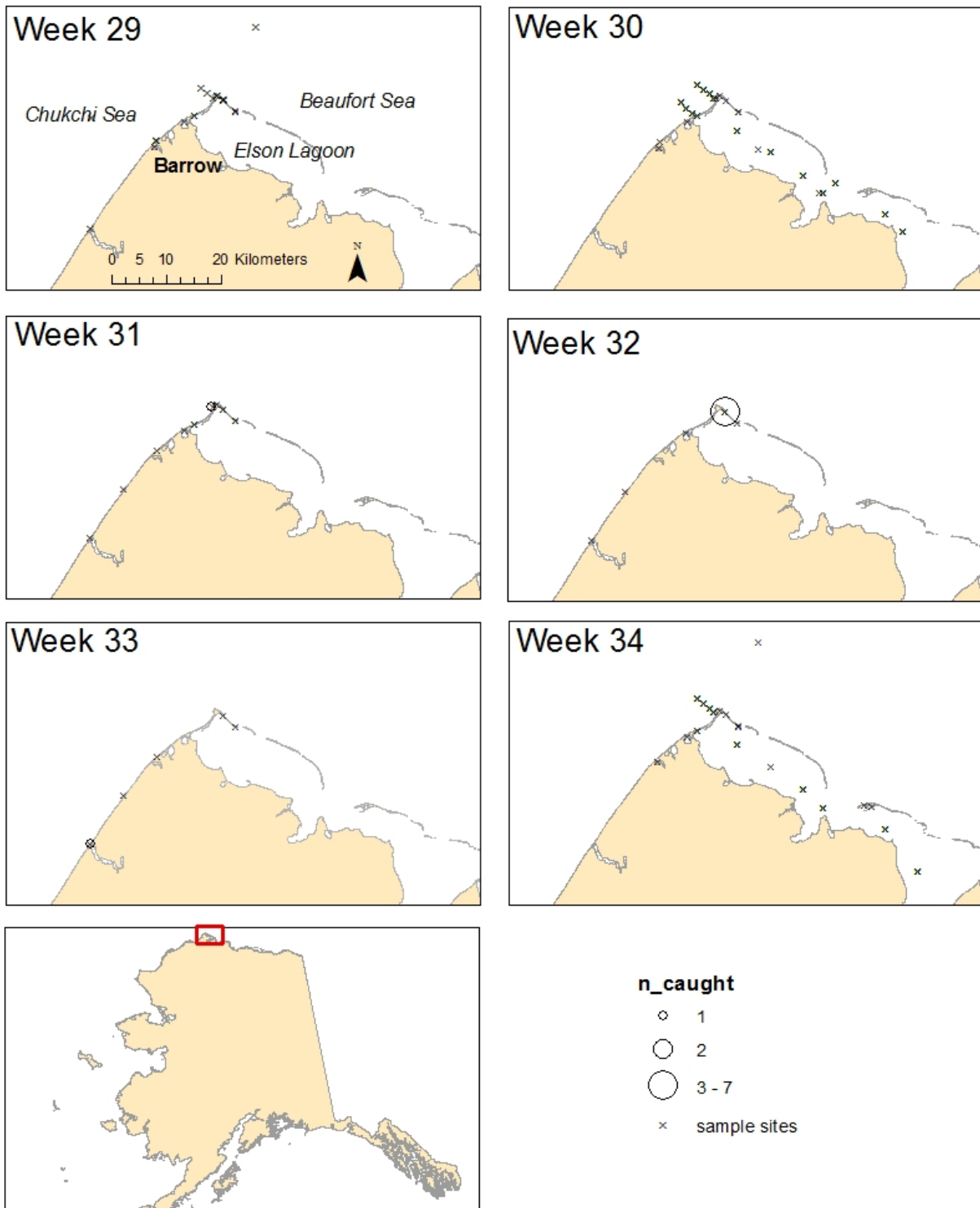


Figure 4.10 2014 saffron cod catch by week. The red box depicted on the map of Alaska is the area that is expanded upon in the weekly catch maps.

2015 Arctic cod catch

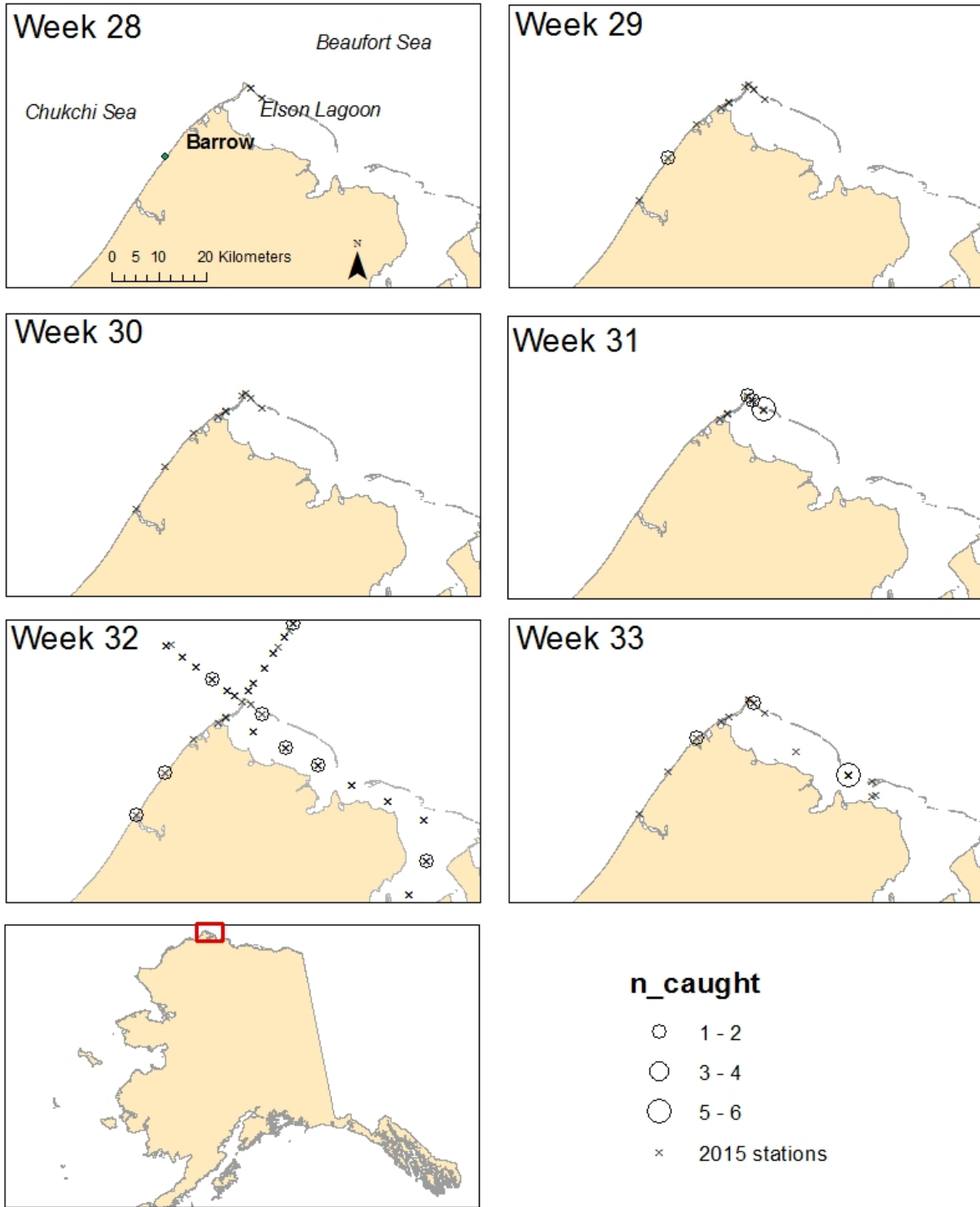


Figure 4.11 2015 Arctic cod catch by week. The red box depicted on the map of Alaska is the area that is expanded upon in the weekly catch maps.

2015 Capelin catch

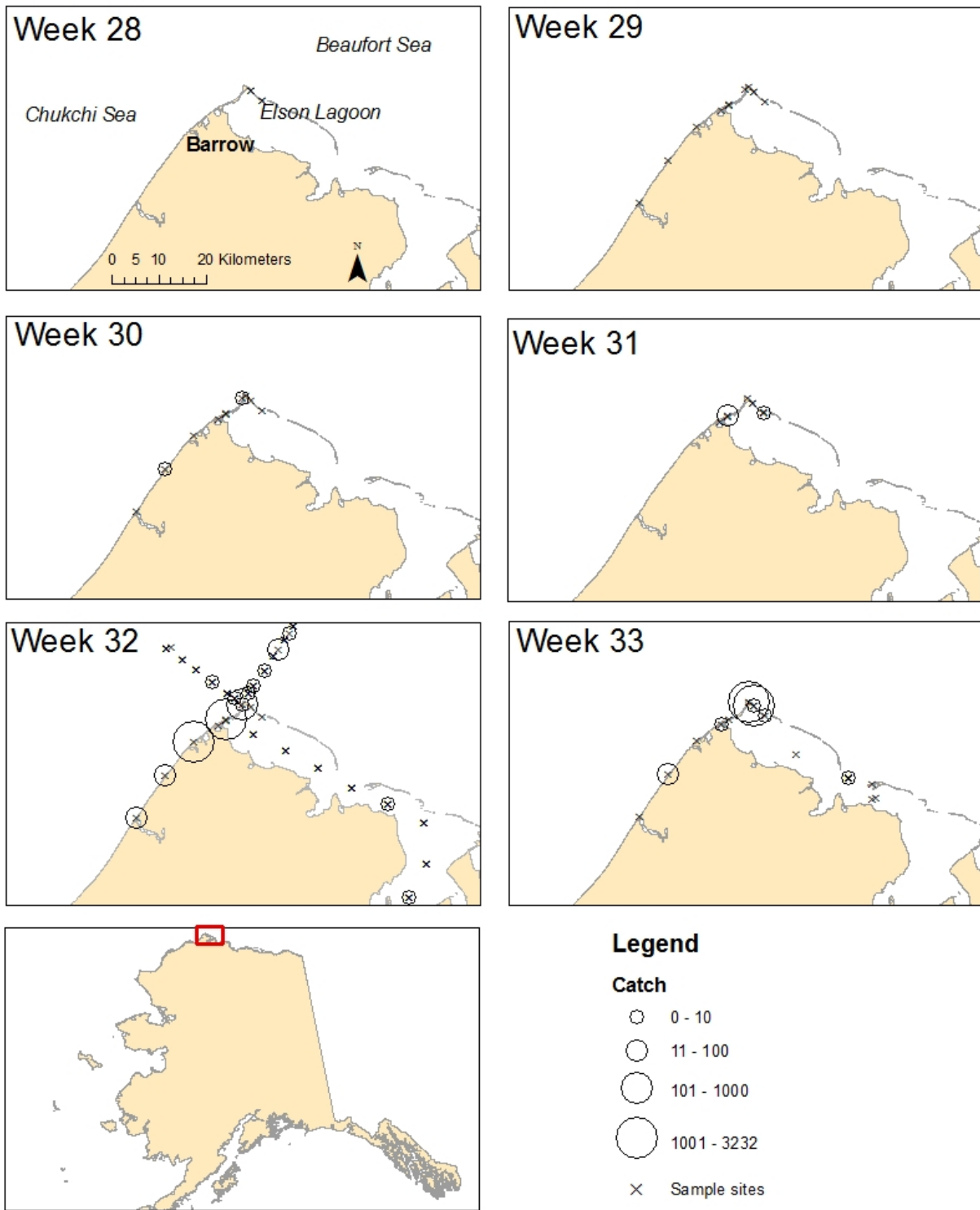


Figure 4.12 2015 capelin catch by week. The red box depicted on the map of Alaska is the area that is expanded upon in the weekly catch maps.

2015 Fourhorn sculpin catch

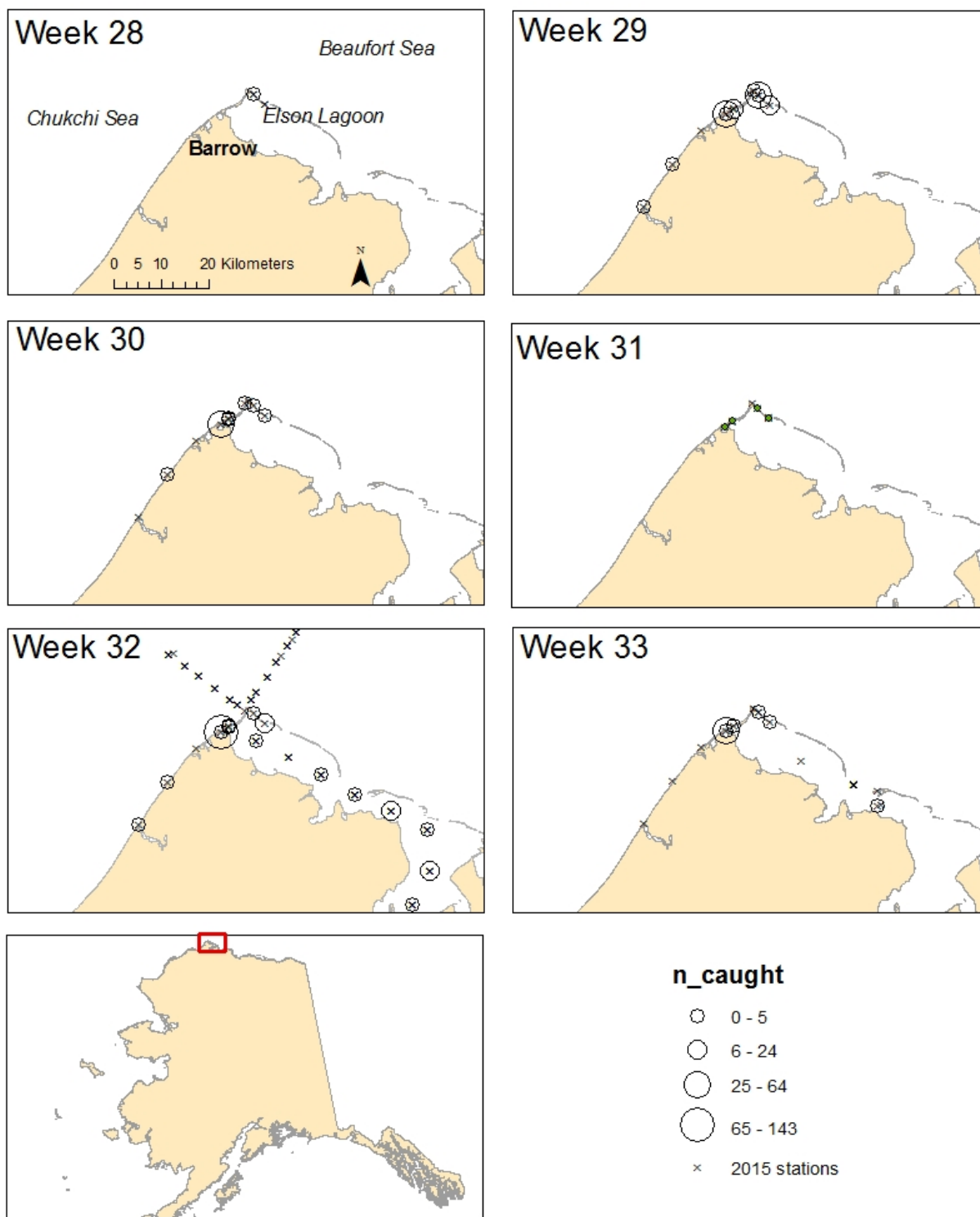


Figure 4.13 2015 fourhorn sculpin catch by week. The red box depicted on the map of Alaska is the area that is expanded upon in the weekly catch maps.

2015 Pacific sand lance catch

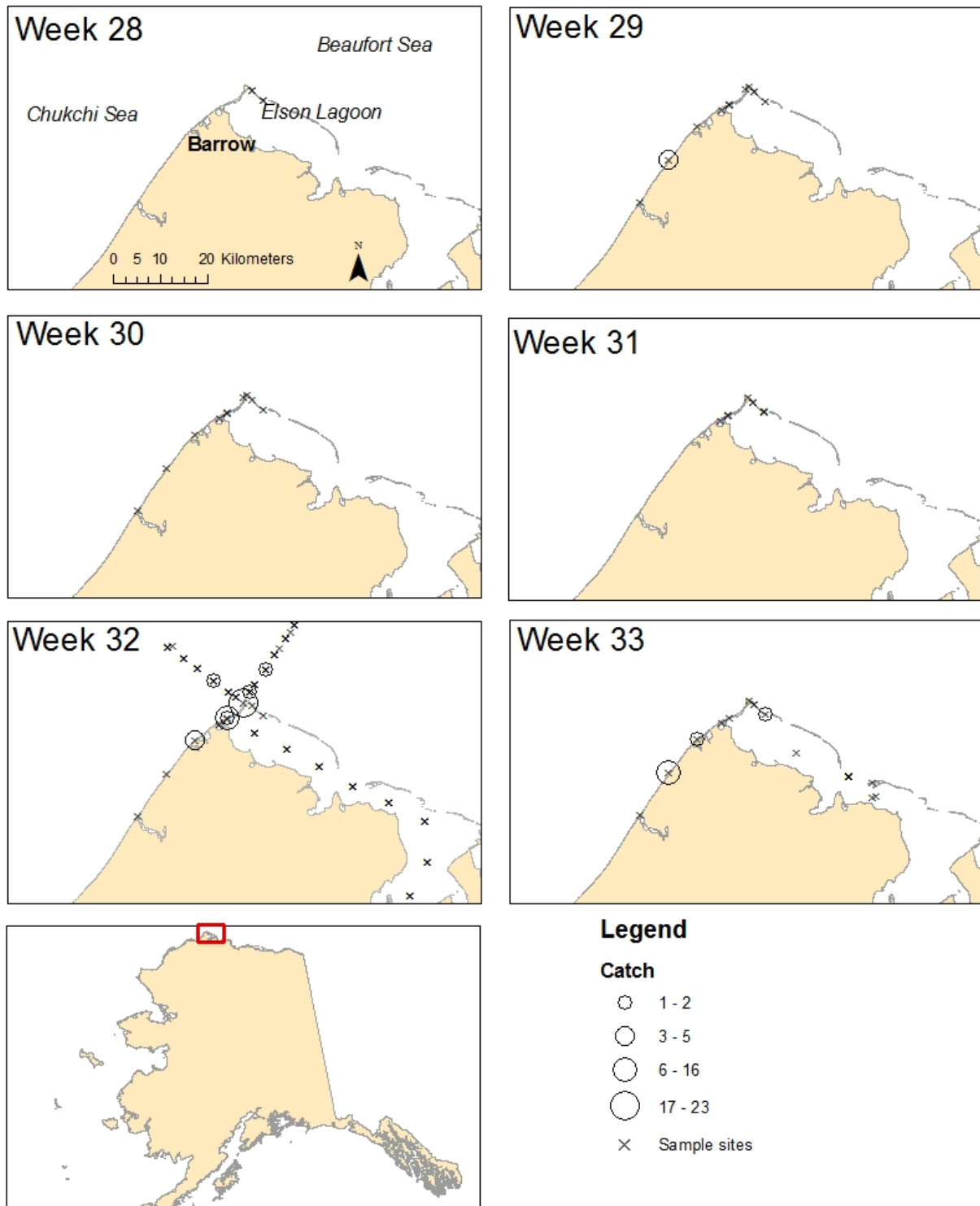


Figure 4.14 2015 Pacific sand lance catch by week. The red box depicted on the map of Alaska is the area that is expanded upon in the weekly catch maps.

2015 Saffron cod

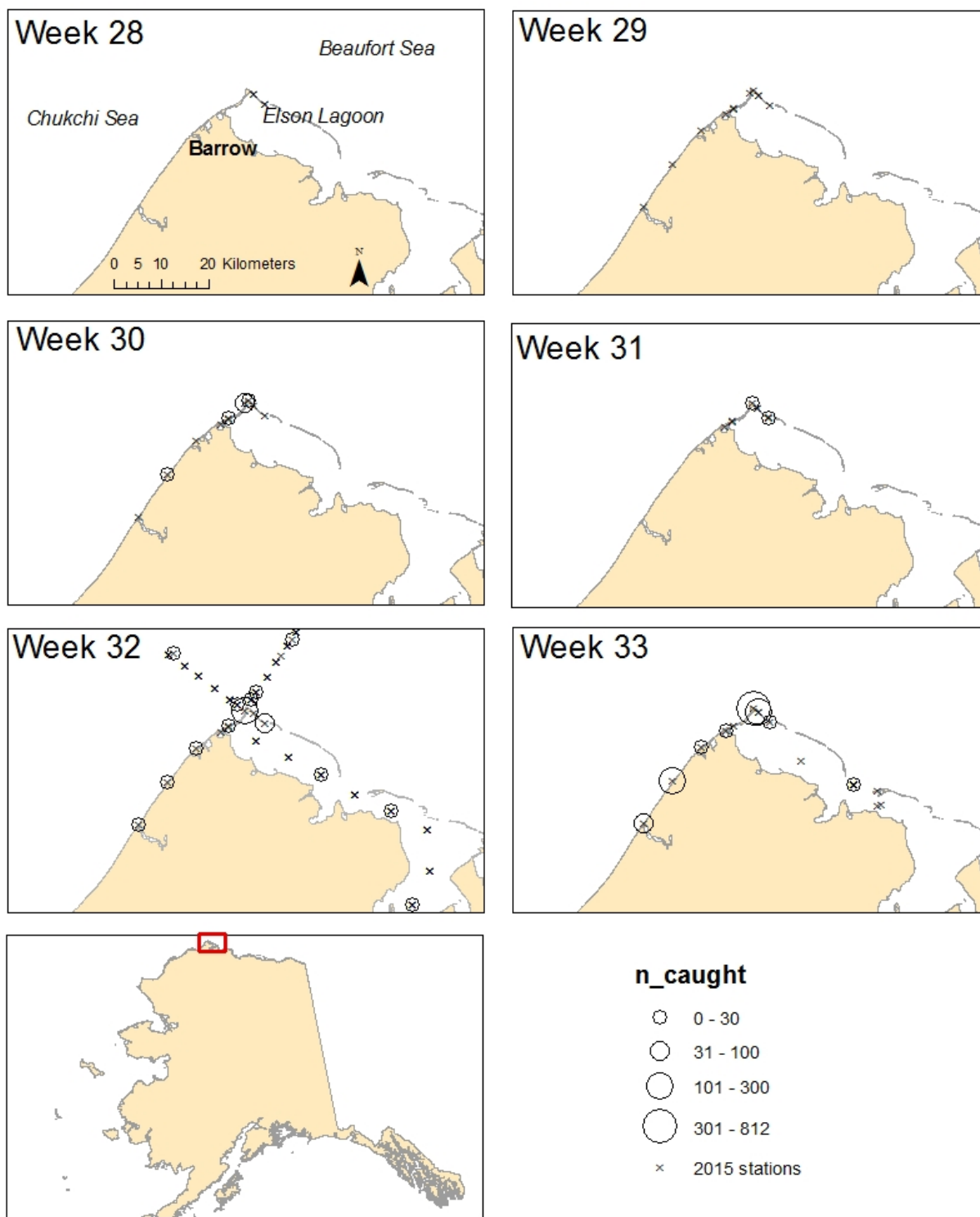


Figure 4.15 2015 saffron cod catch by week. The red box depicted on the map of Alaska is the area that is expanded upon in the weekly catch maps.

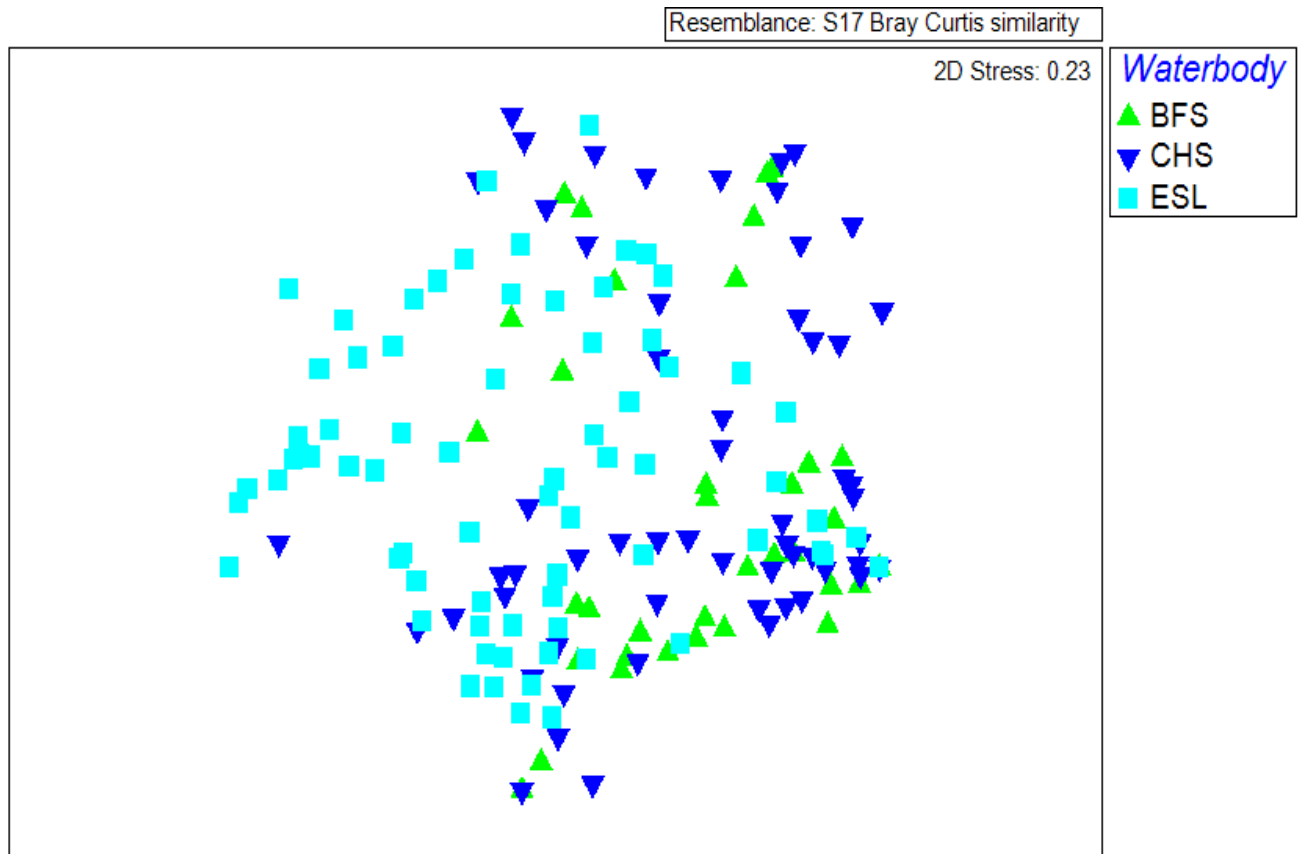


Figure 4.16 A Non-parametric Dimensional Scaling model representing Bray-Curtis dissimilarity in a two dimensional space. Each point represents the catch composition of a single beach seine haul, and are color coded by water body. Abbreviations: Beaufort Sea – BFS, Chukchi Sea – CHS, Elson Lagoon - ESL

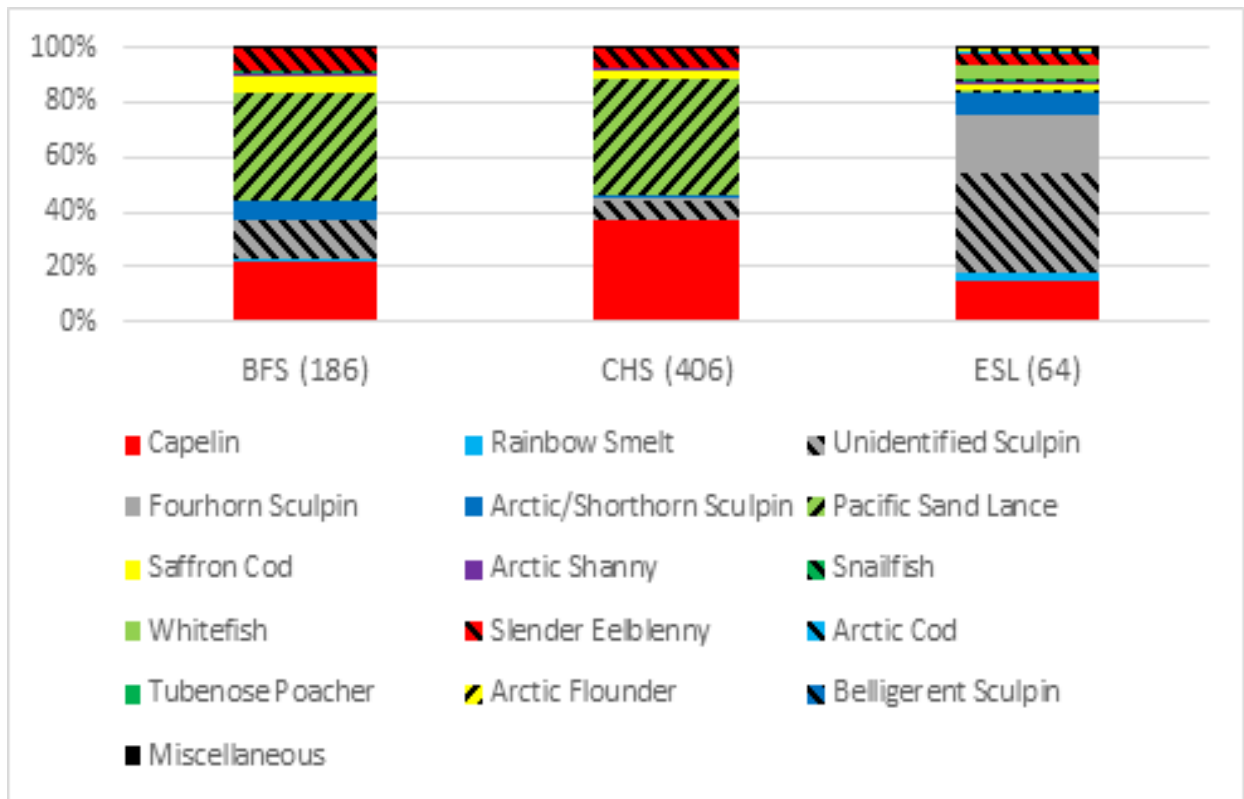


Figure 4.17 Community composition of all beach seine samples broken down by water body (x-axis) represented by relative abundance of all species caught. The numbers in parentheses under each bar represent the average CPUE for each water body. The “Miscellaneous” portion represents all species that were encountered in less than 5% of the beach seine hauls (9 hauls out of 178), and includes: nine-spined stickleback (*Pungitius pungitius*), three-spined stickleback (*Gasterosteus aculeatus*), gunnels (*Pholidae spp.*), Arctic poacher (*Aspidophoroides olrikii*), longhead dab (*Limanda proboscidea*), stout eelblenny (*Anisarchus medius*), pink salmon (*Onchorhynchus gorbuscha*), Alaska plaice (*Pleuronectes quadrituberculatus*), and unidentified larvae. Note, unidentified sculpin were larvae. Abbreviations: Beaufort Sea – BFS, Chukchi Sea – CHS, Elson Lagoon - ESL

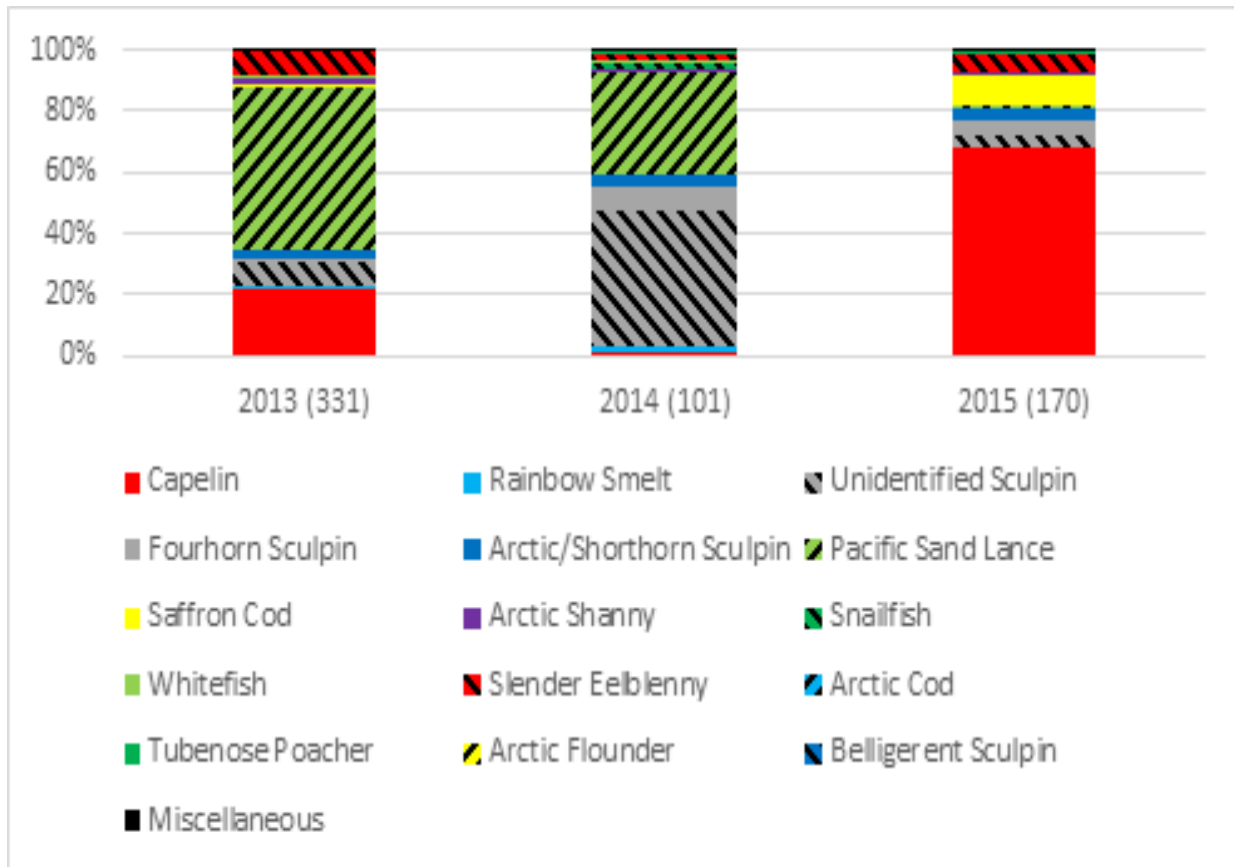


Figure 4.18 Community composition of all beach seine samples broken down by year (x-axis) represented by relative abundance of all species caught. The numbers in parentheses under each bar represent the average CPUE for each year. The “Miscellaneous” portion represents all species that were encountered in less than 5% of the beach seine hauls (9 hauls out of 178), and includes: nine-spined stickleback (*Pungitius pungitius*), three-spined stickleback (*Gasterosteus aculeatus*), gunnels (*Pholidae spp.*), Arctic poacher (*Aspidophoroides olrikii*), longhead dab (*Limanda proboscidea*), stout eelblenny (*Anisarchus medius*), pink salmon (*Onchorhynchus gorbuscha*), Alaska plaice (*Pleuronectes quadrituberculatus*), and unidentified larvae. Note larval Sculpin are shown as unidentified Sculpin. Abbreviations: Beaufort Sea – BFS, Chukchi Sea – CHS, Elson Lagoon - ESL

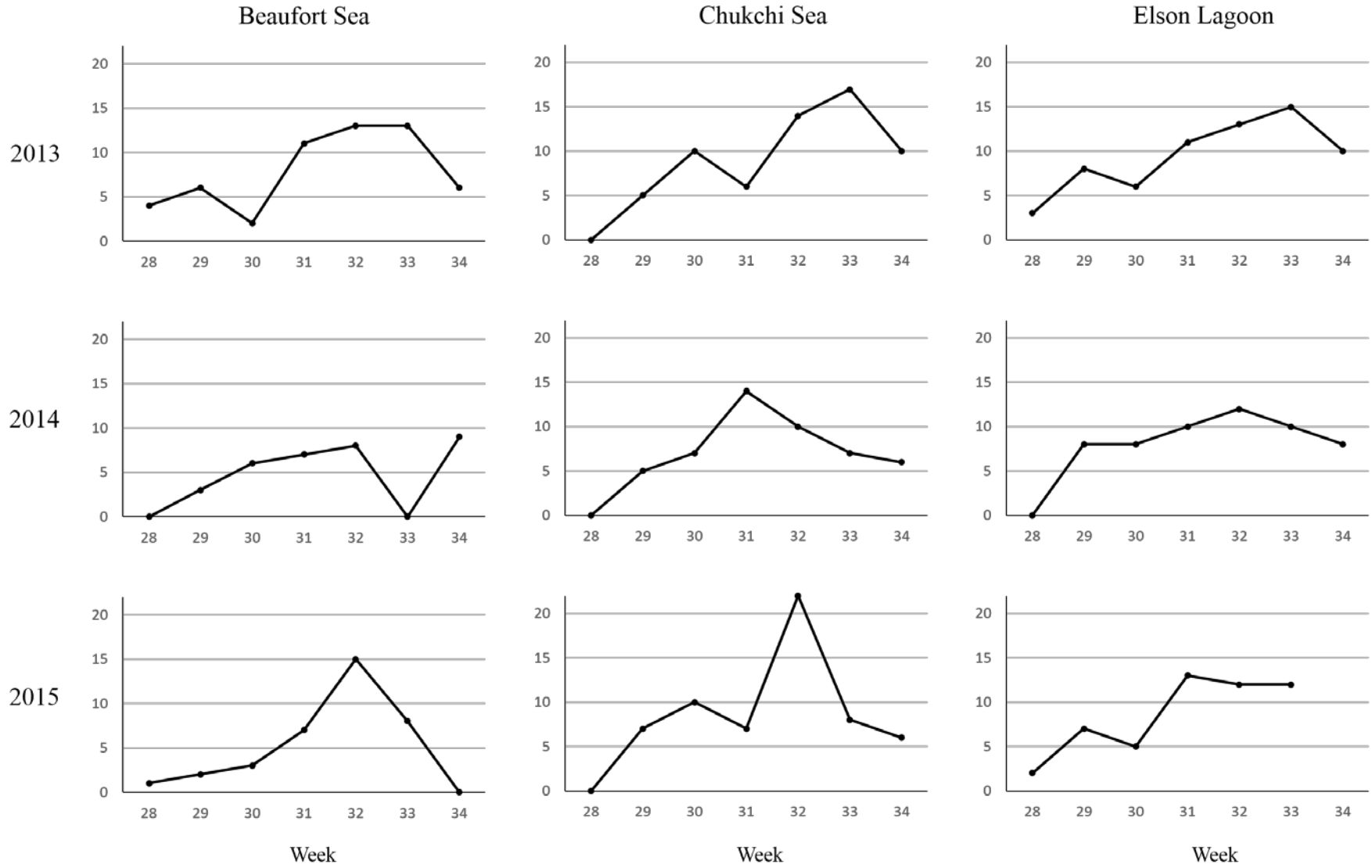


Figure 4.19 Weekly species richness of beach seine catches by year and water body. Weeks are expressed as calendar week.

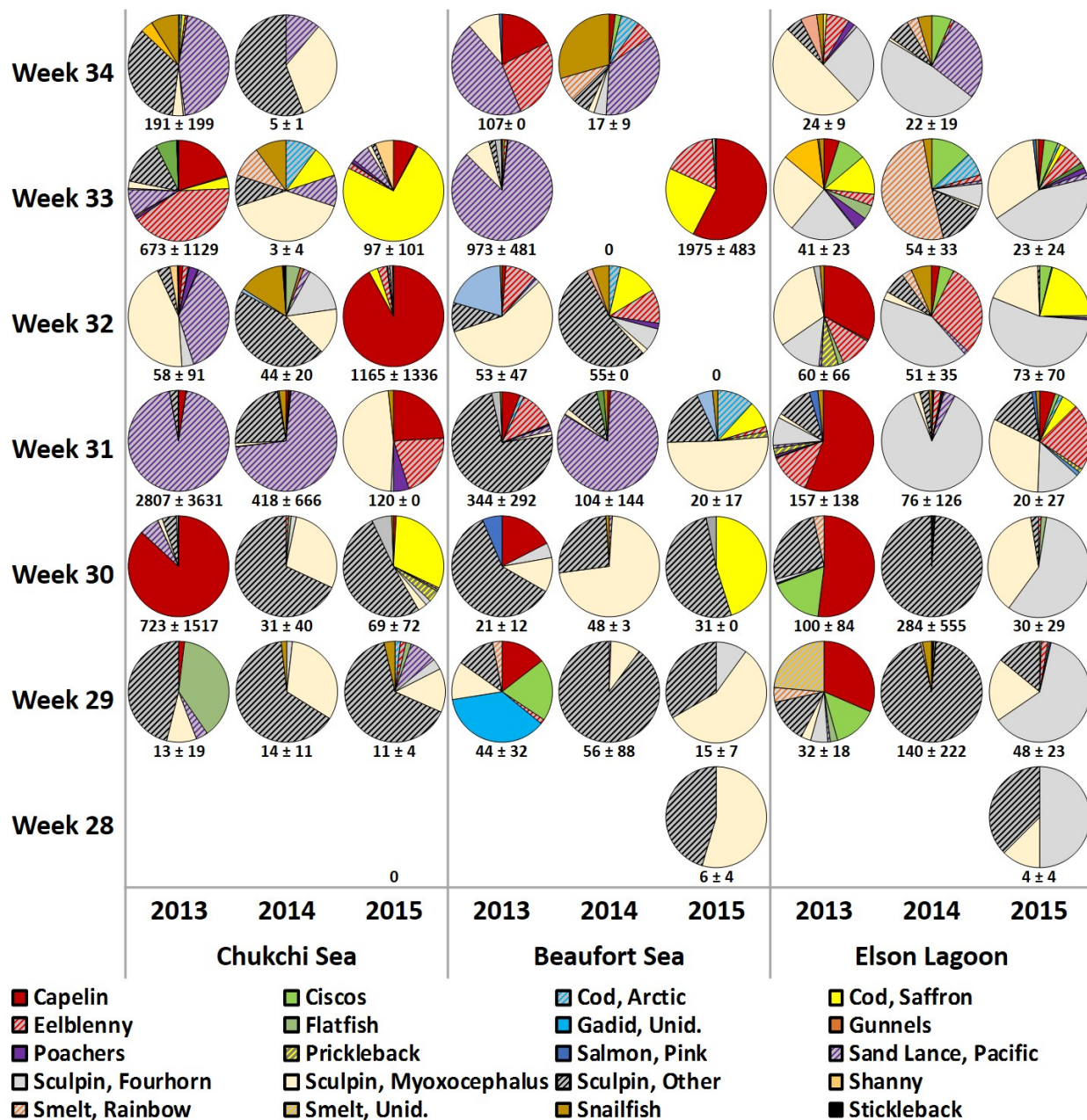


Figure 4.20 Pie charts of community composition of all beach seine samples broken down by water body and year (x-axis) and week (y-axis) represented by relative abundance of all species caught. The numbers under each pie chart represent the average CPUE for each water body/year/week combination. Blank spaces indicate that no beach seines were pulled for that water body/year/week. . Note larval Sculpin are shown as unidentified Sculpin, Sculpin, Myoxocephalus depicts juveniles Abbreviations: Beaufort Sea – BFS, Chukchi Sea – CHS, Elson Lagoon - ESL

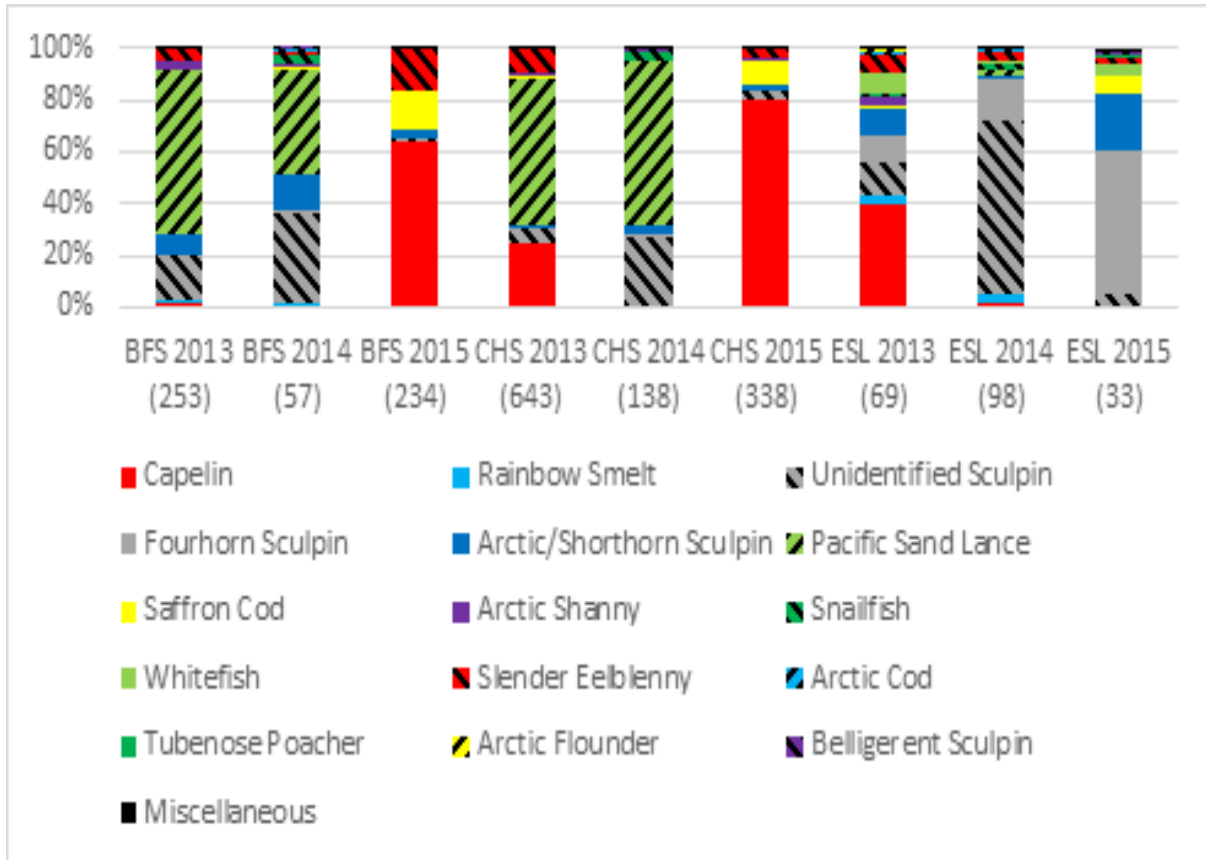


Figure 4.21 Community composition of all beach seine samples broken down by water body and year (x-axis) represented by relative abundance of all species caught. The numbers in parentheses under each bar represent the average CPUE for each water body and year combination. The “Miscellaneous” portion represents all species that were encountered in less than 5% of the beach seine hauls (9 hauls out of 178), and includes: nine-spined stickleback (*Pungitius pungitius*), three-spined stickleback (*Gasterosteus aculeatus*), gunnels (*Pholidae spp.*), Arctic poacher (*Aspidophoroides olrikii*), longhead dab (*Limanda proboscidea*), stout eelblenny (*Anisarchus medius*), pink salmon (*Onchorhynchus gorbuscha*), Alaska plaice (*Pleuronectes quadrituberculatus*), and unidentified larvae. . Note larval Sculpin are shown as unidentified Sculpin. Abbreviations: Beaufort Sea – BFS, Chukchi Sea – CHS, Elson Lagoon - ESL

Table 4.1 Fish caught by sampling method.

Common Name	Scientific Name	Family	Beach Seine	Bottom Trawl	Midwater Trawl
Alligatorfish	<i>Aspidophoroides monopterygius</i>	Agonidae	X	X	X
Alligatorfish, Arctic	<i>Aspidophoroides olrikii</i>	Agonidae	X	X	
Capelin	<i>Mallotus villosus</i>	Osmeridae	X	X	X
Cisco, Arctic	<i>Coregonus autumnalis</i>	Salmonidae	X		
Cisco, Bering	<i>Coregonus laurettae</i>	Salmonidae	X		
Cisco, Least	<i>Coregonus sardinella</i>	Salmonidae	X	X	
Cisco, Unid.	<i>Coregonus spp.</i>	Salmonidae	X		
Cod, Arctic	<i>Boreogadus saida</i>	Gadidae	X	X	X
Cod, Saffron	<i>Eleginus gracilis</i>	Gadidae	X	X	X
Dab, Longhead	<i>Limanda proboscidea</i>	Pleuronectidae	X	X	
Doctor, Fish	<i>Gymnelus viridis</i>	Zoarcidae		X	
Eelblenny, Slender	<i>Lumpenus fabricii</i>	Stichaeidae	X	X	X
Eelblenny, Stout	<i>Anisarchus medius</i>	Stichaeidae	X	X	
Eelblenny, Unid.		Stichaeidae	X	X	X
Eelpout, Canadian	<i>Lycodes polaris</i>	Zoarcidae		X	
Eelpout, Longear	<i>Lycodes seminudus</i>	Zoarcidae		X	
Eelpout, Marbled	<i>Lycodes raridens</i>	Zoarcidae		X	
Eelpout, Saddled	<i>Lycodes mucosus</i>	Zoarcidae		X	
Fish, Unid.			X		
Flatfish, Unid.		Pleuronectidae	X	X	
Flounder, Arctic	<i>Pleuronectes glacialis</i>	Pleuronectidae	X	X	
Flounder, Bering	<i>Hippoglossoides robustus</i>	Pleuronectidae		X	
Gadid, Unid.		Gadidae	X		
Gunnel, Banded	<i>Pholis fasciata</i>	Pholidae	X		
Gunnel, Unid.		Pholidae	X		
Herring, Pacific	<i>Clupea pallasii</i>	Clupeidae	X		
Poacher, Atlantic	<i>Leptagonus decagonus</i>	Agonidae	X		
Poacher, Tubenose	<i>Pallasina barbata</i>	Agonidae	X		
Poacher, Unid.		Agonidae	X		
Poacher, Veteran	<i>Podothecus veterinus</i>	Agonidae	X	X	
Pollock, Walleye	<i>Gadus chalcogrammus</i>	Gadidae			X
Pout, Unid.		Zoarcidae		X	
Prickleback, Blackline	<i>Acantholumpenus mackayi</i>	Stichaeidae		X	
Prickleback, Unid.		Stichaeidae	X	X	
Salmon, Pink	<i>Oncorhynchus gorbuscha</i>	Salmonidae	X		
Sand Lance, Pacific	<i>Ammodytes personatus</i>	Ammodytidae	X	X	X
Sculpin, Arctic	<i>Myoxocephalus scorpioides</i>	Cottidae			
Sculpin, Arctic Staghorn	<i>Gymnocanthus tricuspis</i>	Cottidae	X	X	X
Sculpin, Belligerent	<i>Megalocottus platycephalus</i>	Cottidae	X		
Sculpin, Buffalo	<i>Enophrys bison</i>	Cottidae	X		
Sculpin, Eyeshade	<i>Nautichthys pribilovius</i>	Hemitripteridae		X	
Sculpin, Fourhorn	<i>Myoxocephalus quadricornis</i>	Cottidae	X	X	
Sculpin, Hairhead	<i>Trichocottus brashnikovii</i>	Cottidae	X		
Sculpin, Hamecon	<i>Artediellus scaber</i>	Cottidae	X	X	
Sculpin, <i>Myoxocephalus</i>	<i>Myoxocephalus sp.</i>	Cottidae	X	X	
Sculpin, Pacific Staghorn	<i>Leptocottus armatus</i>	Cottidae		X	
Sculpin, Ribbed	<i>Triglops pingelii</i>	Cottidae	X	X	X

Sculpin, Shorthorn	<i>Myoxocephalus scorpius</i>	Cottidae			
Sculpin, Spatulate	<i>Icelus spatula</i>	Cottidae	X	X	
Sculpin, Unid.		Cottidae	X	X	X
Sculpin, Warty	<i>Myoxocephalus verrucosus</i>	Cottidae		X	
Shanny, Arctic	<i>Stichaeus punctatus</i>	Stichaeidae	X	X	
Shanny, Daubed	<i>Leptoclinus maculatus</i>	Gasterosteidae	X	X	
Smelt, Rainbow	<i>Osmerus mordax</i>	Osmeridae	X	X	
Smelt, Unid.		Osmeridae	X		
Snailfish, Festive	<i>Liparis marmoratus</i>	Liparidae		X	X
Snailfish, Gelatinous	<i>Liparis fabricii</i>	Liparidae		X	X
Snailfish, Kelp	<i>Liparis tunicatus</i>	Liparidae	X	X	X
Snailfish, <i>Liparis</i>	<i>Liparis sp.</i>	Liparidae	X	X	X
Snailfish, Variegated	<i>Liparis gibbus</i>	Liparidae	X	X	
Snakeblenny, Fourline	<i>Eumesogrammus praecisus</i>	Stichaeidae	X	X	
Sole, Yellowfin	<i>Limanda aspera</i>	Pleuronectidae	X	X	
Stickleback, Ninespine	<i>Pungitius pungitius</i>	Gasterosteidae	X	X	
Stickleback, Threespine	<i>Gasterosteus aculeatus</i>	Gasterosteidae	X		

Table 4.2 Productivity in the three water bodies and three years from beach seine sampling. The average number of fish per haul (CPUE) is listed in the top of each cell, with # of beach seine hauls in the middle, and total number of fish caught on the bottom of the cell.

Year	Chukchi Sea	Beaufort Sea	Elson Lagoon	Overall
2013	600	271	67	328
	28	15	26	69
	16,811	4,072	1,744	22,627
2014	113	57	106	100
	21	12	21	53
	2,375	680	2,231	5,286
2015	349	196	36	184
	19	9	22	50
	6,634	1,764	801	9,199
Overall	380	181	69	216
	68	36	69	172
	25,820	6,516	4,776	37,112

Table 4.3 Frequency of occurrence (%) of fish in beach seine catches throughout 2013-2015 field seasons. Overall frequency of occurrence by water body, sampling year, and sampling week.

	<u>Water Body</u>			<u>Sampling Year</u>			<u>Sampling Week</u>						
	Chukchi Sea	Beaufort Sea	Elson Lagoon	2013	2014	2015	28	29	30	31	32	33	34
Alligatorfish	15	5	9	12	9	10	0	3	0	24	22	10	5
Alligatorfish, Arctic	3	3	1	3	0	4	0	0	0	0	4	7	5
Capelin	30	32	26	41	15	27	0	19	22	45	37	34	20
Cisco, Arctic	0	3	1	0	2	2	0	0	0	0	4	0	5
Cisco, Bering	0	0	3	0	2	2	0	0	0	0	4	3	0
Cisco, Least	0	3	27	10	15	10	0	13	3	3	22	17	15
Cisco, Unid.	2	0	10	7	6	0	0	6	13	0	0	7	0
Cod, Arctic	20	22	10	12	19	19	0	3	6	24	15	28	30
Cod, Saffron	29	22	11	19	6	37	0	0	13	14	26	55	20
Dab, Longhead	11	0	1	0	4	12	0	3	9	3	7	0	5
Eelblenny, Slender	27	32	33	35	21	35	0	16	13	41	33	48	45
Eelblenny, Stout	0	0	1	0	2	0	0	0	0	0	4	0	0
Eelblenny, Unid.	2	0	1	0	0	4	0	0	0	0	0	3	5
Flatfish, Unid.	2	0	3	1	2	2	0	3	3	0	4	0	0
Flounder, Arctic	5	0	16	12	6	6	0	13	13	7	7	7	0
Gadid, Unid.	2	3	1	4	0	0	0	3	0	3	4	0	0
Gunnel, Banded	2	0	0	0	2	0	0	0	0	0	4	0	0
Gunnel, Unid.	0	3	0	1	0	0	0	0	0	3	0	0	0
Herring, Pacific	0	0	3	0	0	4	0	0	0	0	0	7	0
Poacher, Atlantic	0	0	1	1	0	0	0	0	0	0	0	3	0
Poacher, Tubenose	14	11	7	16	0	13	0	0	0	14	15	31	5
Poacher, Unid.	0	3	0	1	0	0	0	0	0	0	0	3	0
Prickleback, Unid.	2	3	3	1	0	6	0	0	3	10	0	0	0
Salmon, Pink	2	0	1	0	0	4	0	0	0	3	4	0	0
Sand Lance, Pacific	36	32	24	40	36	13	0	16	9	52	30	38	55
Sculpin, Arctic Staghorn	5	0	7	0	9	6	0	3	3	3	15	3	0
Sculpin, Belligerent	20	5	6	7	19	8	0	19	9	17	11	3	5
Sculpin, Buffalo	0	3	0	0	2	0	0	0	0	3	0	0	0
Sculpin, Fourhorn	41	22	76	49	45	60	25	38	44	45	67	55	70
Sculpin, Hairhead	2	5	3	6	0	2	0	0	0	3	7	0	10
Sculpin, Hamecon	0	3	0	1	0	0	0	0	0	0	4	0	0
Sculpin, <i>Myoxocephalus</i>	68	81	49	71	57	60	75	69	47	62	74	69	55
Sculpin, Ribbed	0	0	4	0	4	2	0	0	0	3	4	3	0
Sculpin, Spatulate	2	3	0	3	0	0	0	0	0	0	4	3	0
Sculpin, Unid.	77	81	46	63	75	58	75	88	84	76	44	41	45
Shanny, Arctic	36	41	20	51	11	23	0	0	22	38	44	55	35
Shanny, Daubed	2	0	0	1	0	0	0	0	0	0	0	0	5
Smelt, Rainbow	8	8	14	7	21	4	0	9	9	3	15	10	20
Smelt, Unid.	5	0	4	9	0	0	0	6	0	3	0	7	5
Snailfish, Kelp	2	0	0	1	0	0	0	0	0	0	0	0	5
Snailfish, <i>Liparis</i> Unid.	21	30	23	22	38	12	0	9	13	41	22	31	35
Snailfish, Variegated	0	5	0	0	2	2	0	0	0	3	0	0	5
Snakeblenny, Fourline	3	0	7	9	2	0	0	0	0	7	15	3	0
Sole, Yellowfin	2	0	0	1	0	0	0	3	0	0	0	0	0
Stickleback, Ninespine	5	3	0	4	2	0	0	0	0	0	4	10	0
Stickleback, Threespine	3	0	0	3	0	0	0	0	3	0	4	0	0

Table 4.5 2013 average catch per unit effort (CPUE) of the Chukchi Sea by sampling week. * indicates estimated CPUE.

	2013 Chukchi Sea						Year AVG CPUE ± SD
	29	30	31	32	33	34	
Alligatorfish	0	0	3 ± 0	3 ± 1	1 ± 0	0	1 ± 1
Alligatorfish, Arctic	0	0	0	0	0	0	0
Capelin	1 ± 0	1569 ± 2217	103 ± 136	2 ± 1	* 678 ± 0	2 ± 1	392 ± 634
Cisco, Arctic	0	0	0	0	0	0	0
Cisco, Bering	0	0	0	0	0	0	0
Cisco, Least	0	0	0	0	0	0	0
Cisco, Unid.	0	1 ± 0	0	0	0	0	0
Cod, Arctic	0	0	0	0	4 ± 4	2 ± 2	1 ± 2
Cod, Saffron	0	0	4 ± 0	0	* 43 ± 65	5 ± 6	9 ± 17
Dab, Longhead	0	0	0	0	0	0	0
Eelblenny, Slender	0	1 ± 0	0	3 ± 2	* 462 ± 741	2 ± 2	78 ± 188
Eelblenny, Stout	0	0	0	0	0	0	0
Eelblenny, Unid.	0	0	0	0	0	0	0
Flatfish, Unid.	0	0	0	0	0	0	0
Flounder, Arctic	10	1 ± 0	0	0	1 ± 0	0	2 ± 4
Gadid, Unid.	0	0	0	1 ± 0	0	0	0
Gunnel, Banded	0	0	0	0	0	0	0
Gunnel, Unid.	0	0	0	0	0	0	0
Herring, Pacific	0	0	0	0	0	0	0
Poacher, Atlantic	0	0	0	0	0	0	0
Poacher, Tubenose	0	0	0	1 ± 0	* 9 ± 6	1 ± 0	2 ± 4
Poacher, Unid.	0	0	0	0	0	0	0
Prickleback, Unid.	0	0	0	0	0	0	0
Salmon, Pink	0	0	0	0	0	0	0
Sand Lance, Pacific	1 ± 0	228 ± 0	2654 ± 3663	111 ± 0	95 ± 160	215 ± 53	551 ± 1034
Sculpin, Arctic Staghorn	0	0	0	0	0	0	0
Sculpin, Belligerent	2 ± 0	0	0	0	1 ± 0	0	1 ± 1
Sculpin, Buffalo	0	0	0	0	0	0	0
Sculpin, Fourhorn	0	3 ± 0	0	4 ± 3	3 ± 2	2 ± 1	2 ± 2
Sculpin, Hairhead	0	0	0	2 ± 0	0	0	0 ± 1
Sculpin, Hamecon	0	0	0	0	0	0	0
Sculpin, <i>Myoxocephalus</i>	2 ± 1	18 ± 27	1 ± 0	14 ± 27	* 7 ± 4	6 ± 8	8 ± 7
Sculpin, Ribbed	0	0	0	0	0	0	0
Sculpin, Spatulate	0	0	0	0	2 ± 0	0	0 ± 1
Sculpin, Unid.	6 ± 7	24 ± 23	78 ± 56	5 ± 3	97 ± 203	84 ± 164	49 ± 42
Shanny, Arctic	0	21 ± 0	6 ± 6	2 ± 1	* 45 ± 68	2 ± 2	13 ± 18
Shanny, Daubed	0	0	0	0	0	31 ± 0	5 ± 13
Smelt, Rainbow	0	3 ± 0	0	0	0	0	1 ± 1
Smelt, Unid.	0	0	1 ± 0	0	1 ± 0	1 ± 0	1 ± 1
Snailfish, Kelp	0	0	0	0	0	84 ± 0	14 ± 34
Snailfish, <i>Liparis</i> Unid.	0	0	0	0	2 ± 1	1 ± 0	1 ± 1
Snailfish, Variegated	0	0	0	0	0	0	0
Snakeblenny, Fourline	0	0	0	1 ± 0	14 ± 0	0	3 ± 6
Sole, Yellowfin	10	0	0	0	0	0	2 ± 4
Stickleback, Ninespine	0	0	0	0	9 ± 1	0	1 ± 3
Stickleback, Threespine	0	1 ± 0	0	1 ± 0	0	0	0 ± 1
Number of beach seines	4	5	3	5	5	5	27
Average Weekly CPUE ± SD	13 ± 19	723 ± 1517	2807 ± 3631	58 ± 91	* 673 ± 1129	191 ± 199	618 ± 1056

Table 4.6 2013 average catch per unit effort (CPUE) of the Beaufort Sea by sampling week.

	<u>2013 Beaufort Sea</u>						Year AVG
	29	30	31	32	33	34	CPUE ± SD
Alligatorfish	0	0	0	1±0	0	0	0
Alligatorfish, Arctic	0	0	0	0	1±0	0	0
Capelin	10±8	11±0	40	1±0	2±1	19±0	14±14
Cisco, Arctic	0	0	0	0	0	0	0
Cisco, Bering	0	0	0	0	0	0	0
Cisco, Least	26±0	0	0	0	0	0	4±11
Cisco, Unid.	0	0	0	0	0	0	0
Cod, Arctic	0	0	9±0	0	1±0	0	2±4
Cod, Saffron	0	0	0	0	6±5	0	1±2
Dab, Longhead	0	0	0	0	0	0	0
Eelblenny, Slender	2±0	0	41±49	16±0	14±16	28±0	17±16
Eelblenny, Stout	0	0	0	0	0	0	0
Eelblenny, Unid.	0	0	0	0	0	0	0
Flatfish, Unid.	0	0	0	0	0	0	0
Flounder, Arctic	0	0	0	0	0	0	0
Gadid, Unid.	48±0	0	0	0	0	0	8±20
Gunnel, Banded	0	0	0	0	0	0	0
Gunnel, Unid.	0	0	1±0	0	0	0	0
Herring, Pacific	0	0	0	0	0	0	0
Poacher, Atlantic	0	0	0	0	0	0	0
Poacher, Tubenose	0	0	3±0	0	6±0	0	2±3
Poacher, Unid.	0	0	0	0	1±0	0	0
Prickleback, Unid.	0	0	0	0	0	0	0
Salmon, Pink	0	0	0	0	0	0	0
Sand Lance, Pacific	0	0	6±7	0	832±612	48±0	148±336
Sculpin, Arctic Staghorn	0	0	0	0	0	0	0
Sculpin, Belligerent	3±0	1±0	0	0	0	0	1±1
Sculpin, Buffalo	0	0	0	0	0	0	0
Sculpin, Fourhorn	0	3±0	0	2±0	0	0	1±1
Sculpin, Hairhead	0	0	0	5±0	0	0	1±2
Sculpin, Hamecon	0	0	0	1±0	0	0	0
Sculpin, <i>Myoxocephalus</i>	3±2	4±2	5±5	18±18	48±82	6±1	14±18
Sculpin, Ribbed	0	0	0	0	0	0	0
Sculpin, Spatulate	0	0	0	2±0	0	0	0±1
Sculpin, Unid.	7±2	9±6	169±207	4±4	15±10	0	34±67
Shanny, Arctic	0	4±0	10±2	16±20	19±18	1±0	8±8
Shanny, Daubed	0	0	0	0	0	0	0
Smelt, Rainbow	4±0	0	0	0	0	0	1±2
Smelt, Unid.	0	0	0	0	0	0	0
Snailfish, Kelp	0	0	0	0	0	0	0
Snailfish, <i>Liparis</i> Unid.	0	0	4±0	1±0	2±2	0	1±2
Snailfish, Variegated	0	0	0	0	0	0	0
Snakeblenny, Fourline	0	0	0	0	0	0	0
Sole, Yellowfin	0	0	0	0	0	0	0
Stickleback, Ninespine	0	0	0	0	1±0	0	0
Stickleback, Threespine	0	0	0	0	0	0	0
Number of beach seines	3	3	2	3	3	1	15
Average Weekly CPUE ± SD	44±32	21±12	344±292	53±47	973±481	107±0	271±370

Table 4.7 2013 average catch per unit effort (CPUE) of Elson Lagoon by sampling week.

	<u>2013 Elson Lagoon</u>						Year AVG
	29	30	31	32	33	34	CPUE ± SD
Alligatorfish	0	0	2 ± 0	0	6 ± 0	1 ± 0	2 ± 2
Alligatorfish, Arctic	0	0	0	0	0	1 ± 0	0
Capelin	20 ± 27	105 ± 141	88 ± 84	79 ± 0	6 ± 7	0	50 ± 46
Cisco, Arctic	0	0	0	0	0	0	0
Cisco, Bering	0	0	0	0	0	0	0
Cisco, Least	9 ± 0	68 ± 0	0	1 ± 0	7 ± 6	0	14 ± 27
Cisco, Unid.	5 ± 4	1 ± 0	0	0	1 ± 0	0	1 ± 2
Cod, Arctic	0	0	0	0	0	0	0
Cod, Saffron	0	0	0	0	10 ± 13	1 ± 0	2 ± 4
Dab, Longhead	0	0	0	0	0	0	0
Eelblenny, Slender	0	0	43 ± 11	25 ± 0	3 ± 3	4 ± 4	12 ± 18
Eelblenny, Stout	0	0	0	0	0	0	0
Eelblenny, Unid.	0	0	0	0	0	0	0
Flatfish, Unid.	1 ± 0	0	0	0	0	0	0
Flounder, Arctic	2 ± 0	1 ± 0	1 ± 0	2 ± 1	6 ± 4	0	2 ± 2
Gadid, Unid.	0	0	1 ± 0	0	0	0	0
Gunnel, Banded	0	0	0	0	0	0	0
Gunnel, Unid.	0	0	0	0	0	0	0
Herring, Pacific	0	0	0	0	0	0	0
Poacher, Atlantic	0	0	0	0	2 ± 0	0	0 ± 1
Poacher, Tubenose	0	0	2 ± 1	0	2 ± 0	0	1 ± 1
Poacher, Unid.	0	0	0	0	0	0	0
Prickleback, Unid.	0	0	1 ± 0	0	0	0	0
Salmon, Pink	0	0	0	0	0	0	0
Sand Lance, Pacific	1 ± 0	1 ± 0	2 ± 1	1 ± 0	1 ± 0	1 ± 0	1 ± 0
Sculpin, Arctic Staghorn	0	0	0	0	0	0	0
Sculpin, Belligerent	0	0	0	0	0	1 ± 0	0
Sculpin, Buffalo	0	0	0	0	0	0	0
Sculpin, Fourhorn	2 ± 2	1 ± 1	14 ± 15	8 ± 8	5 ± 4	4 ± 4	6 ± 5
Sculpin, Hairhead	0	0	0	0	0	2 ± 0	0 ± 1
Sculpin, Hamecon	0	0	0	0	0	0	0
Sculpin, <i>Myoxocephalus</i>	1 ± 1	0	5 ± 5	13 ± 16	8 ± 9	8 ± 6	6 ± 5
Sculpin, Ribbed	0	0	0	0	0	0	0
Sculpin, Spatulate	0	0	0	0	0	0	0
Sculpin, Unid.	4 ± 3	21 ± 41	18 ± 15	0	0	0	7 ± 10
Shanny, Arctic	0	0	9 ± 2	3 ± 2	7 ± 9	2 ± 1	3 ± 4
Shanny, Daubed	0	0	0	0	0	0	0
Smelt, Rainbow	6 ± 0	7 ± 8	0	0	0	0	2 ± 3
Smelt, Unid.	15 ± 20	0	0	0	1 ± 0	0	3 ± 6
Snailfish, Kelp	0	0	0	0	0	0	0
Snailfish, <i>Liparis</i> Unid.	0	0	6 ± 2	2 ± 1	4 ± 0	1 ± 0	2 ± 2
Snailfish, Variegated	0	0	0	0	0	0	0
Snakeblenny, Fourline	0	0	12 ± 0	4 ± 5	0	0	3 ± 5
Sole, Yellowfin	0	0	0	0	0	0	0
Stickleback, Ninespine	0	0	0	0	0	0	0
Stickleback, Threespine	0	0	0	0	0	0	0
Number of beach seines	4	4	4	4	6	4	26
Average Weekly CPUE ± SD	32 ± 18	100 ± 84	157 ± 138	60 ± 66	41 ± 23	24 ± 9	67 ± 51

Table 4.8 2014 average catch per unit effort (CPUE) of the Chukchi Sea by sampling week.

	<u>2014 Chukchi Sea</u>						Year AVG
	29	30	31	32	33	34	CPUE ± SD
Alligatorfish	0	0	1 ± 1	0	0	0	0 ± 1
Alligatorfish, Arctic	0	0	0	0	0	0	0
Capelin	0	0	8 ± 10	0	0	0	1 ± 3
Cisco, Arctic	0	0	0	0	0	0	0
Cisco, Bering	0	0	0	0	0	0	0
Cisco, Least	0	0	0	0	0	0	0
Cisco, Unid.	0	0	0	0	0	0	0
Cod, Arctic	0	0	2 ± 1	0	1 ± 0	0	0 ± 1
Cod, Saffron	0	0	2 ± 0	0	1 ± 0	0	1 ± 1
Dab, Longhead	0	0	2 ± 0	4 ± 0	0	0	1 ± 2
Eelblenny, Slender	0	1 ± 0	7 ± 0	0	0	0	1 ± 3
Eelblenny, Stout	0	0	0	0	0	0	0
Eelblenny, Unid.	0	0	0	0	0	0	0
Flatfish, Unid.	0	1 ± 0	0	0	0	0	0
Flounder, Arctic	0	0	0	0	0	0	0
Gadid, Unid.	0	0	0	0	0	0	0
Gunnel, Banded	0	0	0	1 ± 0	0	0	0
Gunnel, Unid.	0	0	0	0	0	0	0
Herring, Pacific	0	0	0	0	0	0	0
Poacher, Atlantic	0	0	0	0	0	0	0
Poacher, Tubenose	0	0	0	0	0	0	0
Poacher, Unid.	0	0	0	0	0	0	0
Prickleback, Unid.	0	0	0	0	0	0	0
Salmon, Pink	0	0	0	0	0	0	0
Sand Lance, Pacific	0	0	373 ± 745	2 ± 0	1 ± 0	1 ± 0	63 ± 152
Sculpin, Arctic Staghorn	1 ± 0	0	0	1 ± 0	0	0	0 ± 1
Sculpin, Belligerent	3 ± 1	2 ± 0	3 ± 2	5 ± 4	0	0	2 ± 2
Sculpin, Buffalo	0	0	0	0	0	0	0
Sculpin, Fourhorn	1 ± 0	2 ± 0	1 ± 0	7 ± 5	0	0	2 ± 2
Sculpin, Hairhead	0	0	0	0	0	0	0
Sculpin, Hamecon	0	0	0	0	0	0	0
Sculpin, <i>Myoxocephalus</i>	5 ± 4	6 ± 6	4 ± 4	7 ± 4	1 ± 1	3 ± 0	4 ± 2
Sculpin, Ribbed	0	0	0	0	0	0	0
Sculpin, Spatulate	0	0	0	0	0	0	0
Sculpin, Unid.	10 ± 10	27 ± 45	52 ± 78	15 ± 4	1 ± 0	2 ± 1	18 ± 19
Shanny, Arctic	0	0	9 ± 0	1 ± 0	0	0	2 ± 4
Shanny, Daubed	0	0	0	0	0	0	0
Smelt, Rainbow	0	0	1 ± 0	0	1 ± 0	0	0 ± 1
Smelt, Unid.	0	0	0	0	0	0	0
Snailfish, Kelp	0	0	0	0	0	0	0
Snailfish, <i>Liparis</i> Unid.	1 ± 0	0	12 ± 8	13 ± 0	1 ± 0	0	4 ± 6
Snailfish, Variegated	0	0	0	0	0	0	0
Snakeblenny, Fourline	0	0	0	0	0	0	0
Sole, Yellowfin	0	0	0	0	0	0	0
Stickleback, Ninespine	0	0	0	1 ± 0	0	0	0
Stickleback, Threespine	0	0	0	0	0	0	0
Number of beach seines	4	4	5	2	3	2	20
Average Weekly CPUE ± SD	14 ± 11	31 ± 40	418 ± 666	44 ± 20	3 ± 4	5 ± 1	119 ± 164

Table 4.9 2014 average catch per unit effort (CPUE) of the Beaufort Sea by sampling week.

	2014 Beaufort Sea						Year AVG
	29	30	31	32	33	34	CPUE \pm SD
Alligatorfish	0	0	0	1 \pm 0	0	0	0
Alligatorfish, Arctic	0	0	0	0	0	0	0
Capelin	0	0	2 \pm 1	0	0	1 \pm 0	1 \pm 1
Cisco, Arctic	0	0	0	0	0	1 \pm 0	0
Cisco, Bering	0	0	0	0	0	0	0
Cisco, Least	0	0	0	0	0	0	0
Cisco, Unid.	0	0	0	0	0	0	0
Cod, Arctic	0	0	0	2 \pm 0	0	2 \pm 1	1 \pm 1
Cod, Saffron	0	0	0	7 \pm 0	0	0	1 \pm 3
Dab, Longhead	0	0	0	0	0	0	0
Eelblenny, Slender	0	0	0	6 \pm 0	0	3 \pm 0	2 \pm 3
Eelblenny, Stout	0	0	0	0	0	0	0
Eelblenny, Unid.	0	0	0	0	0	0	0
Flatfish, Unid.	0	0	0	0	0	0	0
Flounder, Arctic	0	0	0	0	0	0	0
Gadid, Unid.	0	0	0	0	0	0	0
Gunnel, Banded	0	0	0	0	0	0	0
Gunnel, Unid.	0	0	0	0	0	0	0
Herring, Pacific	0	0	0	0	0	0	0
Poacher, Atlantic	0	0	0	0	0	0	0
Poacher, Tubenose	0	0	0	0	0	0	0
Poacher, Unid.	0	0	0	0	0	0	0
Prickleback, Unid.	0	0	0	0	0	0	0
Salmon, Pink	0	0	0	0	0	0	0
Sand Lance, Pacific	1 \pm 0	1 \pm 0	257 \pm 0	0	0	6 \pm 9	53 \pm 114
Sculpin, Arctic Staghorn	0	0	0	0	0	0	0
Sculpin, Belligerent	0	0	0	0	0	0	0
Sculpin, Buffalo	0	0	1 \pm 0	0	0	0	0
Sculpin, Fourhorn	0	0	1 \pm 0	4 \pm 0	0	1 \pm 0	1 \pm 2
Sculpin, Hairhead	0	0	0	0	0	0	0
Sculpin, Hamecon	0	0	0	0	0	0	0
Sculpin, <i>Myoxocephalus</i>	3 \pm 2	12 \pm 16	2 \pm 1	1 \pm 0	0	1 \pm 0	4 \pm 5
Sculpin, Ribbed	0	0	0	0	0	0	0
Sculpin, Spatulate	0	0	0	0	0	0	0
Sculpin, Unid.	50 \pm 84	25 \pm 0	11 \pm 14	30	0	2 \pm 1	23 \pm 19
Shanny, Arctic	0	0	4 \pm 2	1 \pm 0	0	0	1 \pm 2
Shanny, Daubed	0	0	0	0	0	0	0
Smelt, Rainbow	0	0	0	0	0	2 \pm 0	0 \pm 1
Smelt, Unid.	0	0	0	0	0	0	0
Snailfish, Kelp	0	0	0	0	0	0	0
Snailfish, <i>Liparis</i> Unid.	0	1 \pm 0	4 \pm 0	3 \pm 0	0	4 \pm 4	2 \pm 2
Snailfish, Variegated	0	0	0	0	0	2 \pm 0	0 \pm 1
Snakeblenny, Fourline	0	0	0	0	0	0	0
Sole, Yellowfin	0	0	0	0	0	0	0
Stickleback, Ninespine	0	0	0	0	0	0	0
Stickleback, Threespine	0	0	0	0	0	0	0
Number of beach seines	3	2	3	1	0	3	12
Average Weekly CPUE \pm SD	56 \pm 88	48 \pm 3	104 \pm 144	55 \pm 0	0	17 \pm 9	57 \pm 31

Table 4.10 2014 average catch per unit effort (CPUE) of Elson Lagoon by sampling week.

	<u>2014 Elson Lagoon</u>						Year AVG
	29	30	31	32	33	34	CPUE ± SD
Alligatorfish	0	0	1±0	0	0	0	0
Alligatorfish, Arctic	0	0	0	0	0	0	0
Capelin	1±0	0	1±0	2±1	0	0	1±1
Cisco, Arctic	0	0	0	0	0	0	0
Cisco, Bering	0	0	0	1±0	0	0	0
Cisco, Least	1±0	0	0	2±1	13±0	2±1	3±5
Cisco, Unid.	0	1±0	0	0	1±0	0	0±1
Cod, Arctic	0	2±1	1±0	0	8±0	0	2±3
Cod, Saffron	0	0	0	0	0	0	0
Dab, Longhead	0	0	0	0	0	0	0
Eelblenny, Slender	1±0	0	4±1	23±29	2±0	1±0	5±9
Eelblenny, Stout	0	0	0	1±0	0	0	0
Eelblenny, Unid.	0	0	0	0	0	0	0
Flatfish, Unid.	0	0	0	0	0	0	0
Flounder, Arctic	2±0	3±0	1±0	0	0	0	1±1
Gadid, Unid.	0	0	0	0	0	0	0
Gunnel, Banded	0	0	0	0	0	0	0
Gunnel, Unid.	0	0	0	0	0	0	0
Herring, Pacific	0	0	0	0	0	0	0
Poacher, Atlantic	0	0	0	0	0	0	0
Poacher, Tubenose	0	0	0	0	0	0	0
Poacher, Unid.	0	0	0	0	0	0	0
Prickleback, Unid.	0	0	0	0	0	0	0
Salmon, Pink	0	0	0	0	0	0	0
Sand Lance, Pacific	0	0	4±5	2±0	1±0	16±21	4±6
Sculpin, Arctic Staghorn	0	0	0	1±0	1±0	0	0±1
Sculpin, Belligerent	1±0	0	0	0	0	0	0
Sculpin, Buffalo	0	0	0	0	0	0	0
Sculpin, Fourhorn	1±0	1±0	132±185	32±42	3±3	7±8	29±52
Sculpin, Hairhead	0	0	0	0	0	0	0
Sculpin, Hamecon	0	0	0	0	0	0	0
Sculpin, <i>Myoxocephalus</i>	0	2±0	6±0	4±0	1±0	1±0	2±2
Sculpin, Ribbed	0	0	0	6±0	9±0	0	3±4
Sculpin, Spatulate	0	0	0	0	0	0	0
Sculpin, Unid.	132±222	281±554	5±1	2±1	6±0	4±3	72±114
Shanny, Arctic	0	1±0	0	0	0	0	0
Shanny, Daubed	0	0	0	0	0	0	0
Smelt, Rainbow	3±0	0	0	3±2	14±11	2±0	4±5
Smelt, Unid.	0	0	0	0	0	0	0
Snailfish, Kelp	0	0	0	0	0	0	0
Snailfish, <i>Liparis</i> Unid.	12±0	2±0	2±1	10	3±0	5±0	6±4
Snailfish, Variegated	0	0	0	0	0	0	0
Snakeblenny, Fourline	0	0	1±0	0	0	0	0
Sole, Yellowfin	0	0	0	0	0	0	0
Stickleback, Ninespine	0	0	0	0	0	0	0
Stickleback, Threespine	0	0	0	0	0	0	0
Number of beach seines	3	4	4	3	2	5	21
Average Weekly CPUE ± SD	140±222	284±555	76±126	51±35	54±33	22±19	106±97

Table 4.11 2015 average catch per unit effort (CPUE) of the Chukchi Sea by sampling week.

	2015 Chukchi Sea						Year AVG
	28	29	30	31	32	33	CPUE ± SD
Alligatorfish	0	0	0	1±0	2±1	0	1±1
Alligatorfish, Arctic	0	0	0	0	2±0	1±0	1±1
Capelin	0	0	2±1	29±0	893±1310	22±0	189±393
Cisco, Arctic	0	0	0	0	0	0	0
Cisco, Bering	0	0	0	0	0	0	0
Cisco, Least	0	0	0	0	0	0	0
Cisco, Unid.	0	0	0	0	0	0	0
Cod, Arctic	0	1±0	0	0	2±1	1±0	1±1
Cod, Saffron	0	0	36±37	0	33±44	72±75	28±30
Dab, Longhead	0	1±0	1±0	0	3±1	1±0	1±1
Eelblenny, Slender	0	1±0	2±0	25±0	87±52	2±0	23±37
Eelblenny, Stout	0	0	0	0	0	0	0
Eelblenny, Unid.	0	0	0	0	0	1±0	0
Flatfish, Unid.	0	0	0	0	0	0	0
Flounder, Arctic	0	0	0	0	0	0	0
Gadid, Unid.	0	0	0	0	0	0	0
Gunnel, Banded	0	0	0	0	0	0	0
Gunnel, Unid.	0	0	0	0	0	0	0
Herring, Pacific	0	0	0	0	0	0	0
Poacher, Atlantic	0	0	0	0	0	0	0
Poacher, Tubenose	0	0	0	5±0	5±0	2±0	2±3
Poacher, Unid.	0	0	0	0	0	0	0
Prickleback, Unid.	0	0	13±0	0	0	0	3±6
Salmon, Pink	0	0	0	0	1±0	0	0
Sand Lance, Pacific	0	5±0	0	0	10±10	9±11	5±5
Sculpin, Arctic Staghorn	0	0	0	0	0	0	0
Sculpin, Belligerent	0	0	1±0	0	1±0	0	0±1
Sculpin, Buffalo	0	0	0	0	0	0	0
Sculpin, Fourhorn	0	1±0	2±2	1±0	1±1	0	1±1
Sculpin, Hairhead	0	0	0	0	0	0	0
Sculpin, Hamecon	0	0	0	0	0	0	0
Sculpin, <i>Myoxocephalus</i>	0	3±3	5±6	29±39	22±17	2±1	12±12
Sculpin, Ribbed	0	0	0	0	0	0	0
Sculpin, Spatulate	0	0	0	0	0	0	0
Sculpin, Unid.	0	7±5	35±50	0	3±1	4±0	10±14
Shanny, Arctic	0	0	7±8	0	5±6	9±5	4±4
Shanny, Daubed	0	0	0	0	0	0	0
Smelt, Rainbow	0	0	0	0	1±0	0	0
Smelt, Unid.	0	0	0	0	0	0	0
Snailfish, Kelp	0	0	0	0	0	0	0
Snailfish, <i>Liparis</i> Unid.	0	2±0	1±0	2±0	0	0	1±1
Snailfish, Variegated	0	0	0	0	0	0	0
Snakeblenny, Fourline	0	0	0	0	0	0	0
Sole, Yellowfin	0	0	0	0	0	0	0
Stickleback, Ninespine	0	0	0	0	0	0	0
Stickleback, Threespine	0	0	0	0	0	0	0
Number of beach seines	0	5	5	1	5	3	19
Average Weekly CPUE ± SD	0	11±4	69±72	120	1165±1336	97±101	349±489

Table 4.12 2015 average catch per unit effort (CPUE) of the Beaufort Sea by sampling week.

	2015 Beaufort Sea						Year AVG
	28	29	30	31	32	33	CPUE \pm SD
Alligatorfish	0	0	0	0	0	0	0
Alligatorfish, Arctic	0	0	0	0	0	0	0
Capelin	0	0	0	0	0	758 \pm 661	152 \pm 339
Cisco, Arctic	0	0	0	0	0	0	0
Cisco, Bering	0	0	0	0	0	0	0
Cisco, Least	0	0	0	0	0	0	0
Cisco, Unid.	0	0	0	0	0	0	0
Cod, Arctic	0	0	0	4 \pm 4	0	1 \pm 0	1 \pm 2
Cod, Saffron	0	0	14 \pm 0	5 \pm 0	0	476 \pm 475	99 \pm 211
Dab, Longhead	0	0	0	0	0	0	0
Eelblenny, Slender	0	0	0	1 \pm 0	0	336 \pm 108	67 \pm 150
Eelblenny, Stout	0	0	0	0	0	0	0
Eelblenny, Unid.	0	0	0	0	0	0	0
Flatfish, Unid.	0	0	0	0	0	0	0
Flounder, Arctic	0	0	0	0	0	0	0
Gadid, Unid.	0	0	0	0	0	0	0
Gunnel, Banded	0	0	0	0	0	0	0
Gunnel, Unid.	0	0	0	0	0	0	0
Herring, Pacific	0	0	0	0	0	0	0
Poacher, Atlantic	0	0	0	0	0	0	0
Poacher, Tubenose	0	0	0	0	0	3 \pm 2	1 \pm 1
Poacher, Unid.	0	0	0	0	0	0	0
Prickleback, Unid.	0	0	0	1 \pm 0	0	0	0
Salmon, Pink	0	0	0	0	0	0	0
Sand Lance, Pacific	0	0	0	0	0	0	0
Sculpin, Arctic Staghorn	0	0	0	0	0	0	0
Sculpin, Belligerent	0	0	0	0	0	0	0
Sculpin, Buffalo	0	0	0	0	0	0	0
Sculpin, Fourhorn	0	2 \pm 1	0	0	0	0	0 \pm 1
Sculpin, Hairhead	0	0	0	4 \pm 0	0	0	1 \pm 2
Sculpin, Hamecon	0	0	0	0	0	0	0
Sculpin, <i>Myoxocephalus</i>	3 \pm 0	9 \pm 5	0	10 \pm 13	0	14 \pm 8	7 \pm 6
Sculpin, Ribbed	0	0	0	0	0	0	0
Sculpin, Spatulate	0	0	0	0	0	0	0
Sculpin, Unid.	5 \pm 0	5 \pm 3	16 \pm 0	2 \pm 1	0	3 \pm 1	6 \pm 6
Shanny, Arctic	0	0	1 \pm 0	3 \pm 0	0	12 \pm 0	3 \pm 5
Shanny, Daubed	0	0	0	0	0	0	0
Smelt, Rainbow	0	0	0	0	0	0	0
Smelt, Unid.	0	0	0	0	0	0	0
Snailfish, Kelp	0	0	0	0	0	0	0
Snailfish, <i>Liparis</i> Unid.	0	0	0	0	0	0	0
Snailfish, Variegated	0	0	0	1 \pm 0	0	0	0
Snakeblenny, Fourline	0	0	0	0	0	0	0
Sole, Yellowfin	0	0	0	0	0	0	0
Stickleback, Ninespine	0	0	0	0	0	0	0
Stickleback, Threespine	0	0	0	0	0	0	0
Number of beach seines	2	2	1	3	0	2	10
Average Weekly CPUE \pm SD	6 \pm 4	15 \pm 7	31 \pm 0	20 \pm 17	0	1975 \pm 483	408 \pm 875

Table 4.13 2015 average catch per unit effort (CPUE) of Elson Lagoon by sampling week.

	<u>2015 Elson Lagoon</u>						Year AVG
	28	29	30	31	32	33	CPUE ± SD
Alligatorfish	0	1±0	0	0	0	1±0	0±1
Alligatorfish, Arctic	0	0	0	0	0	0	0
Capelin	0	0	0	2±0	0	1±0	1±1
Cisco, Arctic	0	0	0	0	8±0	0	1±3
Cisco, Bering	0	0	0	0	0	2±0	0±1
Cisco, Least	0	1±0	0	1±0	2±1	3±0	1±1
Cisco, Unid.	0	0	0	0	0	0	0
Cod, Arctic	0	0	0	1±0	1±0	1±0	1±1
Cod, Saffron	0	0	0	4±0	60	1±0	11±24
Dab, Longhead	0	0	1±0	0	0	0	0
Eelblenny, Slender	0	2±0	1±0	9±11	0	3±2	2±3
Eelblenny, Stout	0	0	0	0	0	0	0
Eelblenny, Unid.	0	0	0	0	0	3±0	1±1
Flatfish, Unid.	0	0	0	0	1±0	0	0
Flounder, Arctic	0	1±0	1±0	0	1±0	0	1±1
Gadid, Unid.	0	0	0	0	0	0	0
Gunnel, Banded	0	0	0	0	0	0	0
Gunnel, Unid.	0	0	0	0	0	0	0
Herring, Pacific	0	0	0	0	0	1±0	0
Poacher, Atlantic	0	0	0	0	0	0	0
Poacher, Tubenose	0	0	0	0	2±0	1±0	1±1
Poacher, Unid.	0	0	0	0	0	0	0
Prickleback, Unid.	0	0	0	1±0	0	0	0
Salmon, Pink	0	0	0	1±0	0	0	0
Sand Lance, Pacific	0	0	0	0	0	2±0	0±1
Sculpin, Arctic Staghorn	0	0	1±0	3±0	2±0	0	1±1
Sculpin, Belligerent	0	1±0	0	3±0	0	0	1±1
Sculpin, Buffalo	0	0	0	0	0	0	0
Sculpin, Fourhorn	4±0	24±21	23±36	4±4	23±52	8±17	14±10
Sculpin, Hairhead	0	0	0	0	0	0	0
Sculpin, Hamecon	0	0	0	0	0	0	0
Sculpin, <i>Myoxocephalus</i>	1±0	20±19	23±15	8±7	18±25	19±22	15±8
Sculpin, Ribbed	0	0	0	1±0	0	0	0
Sculpin, Spatulate	0	0	0	0	0	0	0
Sculpin, Unid.	2±1	9±7	1±0	5±0	0	0	3±3
Shanny, Arctic	0	0	0	1±0	0	1±0	0±1
Shanny, Daubed	0	0	0	0	0	0	0
Smelt, Rainbow	0	0	0	0	0	0	0
Smelt, Unid.	0	0	0	0	0	0	0
Snailfish, Kelp	0	0	0	0	0	0	0
Snailfish, <i>Liparis</i> Unid.	0	0	0	1±0	0	1±0	0±1
Snailfish, Variegated	0	0	0	0	0	0	0
Snakeblenny, Fourline	0	0	0	0	0	0	0
Sole, Yellowfin	0	0	0	0	0	0	0
Stickleback, Ninespine	0	0	0	0	0	0	0
Stickleback, Threespine	0	0	0	0	0	0	0
Number of beach seines	2	4	4	4	4	5	23
Average Weekly CPUE ± SD	4±4	48±23	30±29	20±27	73±70	23±24	35±24

5.0 Variance Partitioning for Environmental, Spatial, and Temporal Drivers of Community Structure

M. Barton

5.1 Introduction

The discovery of global climate change has drawn the attention of many environmental scientists to polar regions where its effects occur most rapidly (Johannesson et al. 2004). In addition to environmental changes, decreasing sea ice cover is providing opportunities for oil and gas exploration, tourism, and the shipping industry (Berkman and Young 2009). In response to these imminent threats, a considerable amount of research has been focused on understanding Arctic marine systems and establishing baselines from which we can assess the severity of these effects. However, to date, most of this effort has overlooked the lagoons and barrier island chains that span much of the Arctic Ocean's coastlines. Analogous estuarine habitats play vital roles as nurseries and foraging grounds for many important species in well-studied lower latitude systems (Elliott et al. 1990; Dunton et al. 2006); and we presume that their Arctic counterparts are of similar importance. Furthermore, these habitats are home to several endangered and protected marine mammals and seabirds, and provide an important resource for subsistence fisherman and hunters in local villages. We need a better understanding of these nearshore ecosystems and the communities that inhabit them in order to predict how they will fair in the face of climate change and imminent anthropogenic impacts.

Spatio-temporal changes in community composition may be the best indicator of ecosystem changes. The Arctic nearshore is subject to extreme environmental fluctuations that can range from interannual to seasonal scales (ie. transitioning between ice covered winters and open water summers) to hourly scales (ie. highly unpredictable weather patterns). Consequently, inhabiting communities can have complex responses to environmental variables that generate heterogeneity in species distributions in space and time (beta diversity) (Legendre et al. 2005; Logue et al. 2011), and it is important to understand these responses under normal conditions so that we may interpret how communities change in the future. The best approach is to first identify the most important factors that drive changes in community composition. This not only provides crucial information to understand beta diversity, but also streamlines future monitoring efforts so that no effort is wasted on irrelevant data collection. Given that these communities consist of multiple species with varying life histories, we expect that community composition will be driven by multiple environmental factors, therefore a multivariate approach that incorporates multiple independent variables as well as multiple response variables is needed (Legendre and Gauthier 2014) (Dray et al. 2012; Legendre and Gauthier 2014).

Environmental explanatory variables are important tools to understand spatiotemporal beta diversity, but these variables are often confounded by the space and time between sampling events. In order to truly understand the response of communities to environmental factors, we must also understand their response to spatial and temporal factors. Anderson and Gribble (1998) used twelve different combinations of explanatory variable matrices in Canonical Correspondence Analysis (CCA) to partition the variance in community composition explained by environmental, spatial and temporal variables to identify the most explanatory variables in

beta diversity changes. We use this same method to identify important drivers of beta diversity in Arctic nearshore fish communities at lagoon, barrier island, and beach habitats in the Chukchi and Beaufort Sea near Point Barrow, Alaska.

5.2 Methods

5.2.1 Study Area

Point Barrow, Alaska is a unique area where multiple Arctic nearshore habitat types are found in close proximity to each other. Furthermore, Point Barrow is bordered on the West by the Chukchi Sea (CHS), and to the East by the Beaufort Sea (BFS), with the large estuarine Elson Lagoon (ESL) opening into the Beaufort Sea just 5 km Southeast of Point Barrow (Figure 1.1). These distinct water bodies that have shorelines facing several directions face a variety of conditions that are likely to drive beta diversity in various ways; therefore offers an excellent opportunity to study how nearshore fish communities change through time and space.

5.2.2 Sample Collection

The communities were sampled using a beach seine at 12 stations (5 CHS, 3 BFS, and 4 ESL) at weekly intervals from July 14th – August 25th for three consecutive years (2013–15). The seine was 37 m long with variable mesh sizes (10 m of 32 mm outer panels, 4 m of 6 mm middle panels, and 9 m of 3.2 mm blunt panel). Each set was round-haul style, paid out of a 3 m inflatable zodiac following methods used by Johnson et al. (2010). All collections occurred during daylight hours. The entire catch was put in a Ziploc bag and placed on ice to be processed in the lab. In the case of very large catches (> 1000 fish), fish larger than 40 mm were set aside, the remainder of the catch was weighed in the field, and a 1 liter subsample was placed in a Ziploc bag to be processed in the lab. Once in the lab, all fish were sorted by species and enumerated. In the case of a subsample, the subsample was counted and weighed by each species and the ratios of counts to weights were applied to the total weight from the field to estimate species abundances. Fish were frozen after processing to be used in multiple analyses that are not discussed further in this article. Temperature, salinity, and Dissolved Oxygen (DO) were recorded using a YSI EXO2 data sonde at each sampling event. Wind speed, direction and air temperature were recorded using a handheld anemometer.

5.2.3 Canonical Correspondence Analysis

Several constrained ordination methods exist, with Canonical Correspondence Analysis (CCA) and Canonical Redundancy Analysis (RDA) being the most popular for abundance data, but CCA was selected for this analysis for two reasons: (1) CCA assumes that the response variables (community composition) have a unimodal distribution in relation to the explanatory variables, whereas RDA assumes a linear relationship between response and explanatory variables (Anderson and Gribble 1998). These linear functions are more appropriate when the gradient of explanatory variables is short, but given that environmental patterns in the Arctic are highly variable, a CCA seems more suitable. Furthermore, CCA also has a linear face and thus is also capable of handling short gradient variables (Palmer 1986). (2) Beach seines are notoriously susceptible to operator error, and thus the data collected from them should be used as relative abundance, not actual abundance. A CCA focuses on relative abundance but a RDA does not, and thus the CCA is the most appropriate model for our analysis (Palmer 1986).

5.2.4 Variance Partitioning

In order to partition the variance explained by environmental, spatial, and temporal variables, we used four fundamental matrices: Environmental variables (ENV), Spatial variables (SPT), temporal variables (TMP), and Response variables (ASP). For each of the twelve steps of variance partitioning outlined by Anderson and Gribble (1998), a combination of one or more of these three explanatory variable matrices was used to constrain the CCA analysis of ASP: ENV+SPT, ENV+TMP, SPT+TMP, ENV+SPT+TMP. The sum of eigenvalues generated by a CCA (constrained inertia) over the sum of all eigenvalues generated by an unconstrained correspondence analysis (CA; total inertia) yields the proportion of variability in the response matrix (ASP) explained by the constraining variables (ENV, SPT, TMP, etc.). Because the explanatory variables in ENV, SPT, and TMP often overlap with each other, we can include them as covariables so that the overlapping variance explained is partialled out of the analysis (partialled inertia). The remaining variability in ASP that is not explained is termed “unconstrained inertia”. Using this method we may identify the true proportion of variance explained by each matrix of variables, and thus the true total of variance explained by all of the variables.

Figure 5.1 shows a modified version of Anderson and Gribble’s (1998) diagrammatic representation of the variance in ASP and how much of it is explained by the explanatory variables. To find the variance explained by each of the variable types, we simply use one of the fundamental matrices in the CCA model ([1], [2], or [3]); but these models have redundant explanatory power (represented by the overlapping segments of the Venn Diagram) that need to be accounted for in order to find the true explanatory power of all variables. The variance explained by purely ENV or SPT or TMP can be found by partialling out the overlapping portions of each circle ([6] or [9] or [12], respectively). The last step is to calculate the variance explained by one fundamental matrix with only one of the overlapping sections partialled out ([4], [5], [7], [8], [10], or [11]). Once the values corresponding to all sections of the Venn diagram are known, the total variance explained by all variables can be calculated using one of three equations: [1] + [7] + [12], or [2] + [4] + [12], or [3] + [5] + [9]

5.2.5 Explanatory Model Variables

Several variables were included in the modeling process. The following is an account of all variables that were included in the forward selection process outlined by Blanchet et al. (2008). A summary of all variables can be found in Table 5.1.

5.2.5.1 Environmental Variables

As previously mentioned, temperature, salinity, DO were collected in situ at each seine event using a YSI EXO2 data sonde. Wind speed and wind direction were collected using a handheld anemometer, but due to technical difficulties, this data was not recorded for the entire sampling period. Instead, the field collected data was used to create a correction factor for wind data collected at the Wiley Post-Will Rogers Memorial Airport NOAA Weather Station in Barrow, AK. Because wind effects on water can take some time to manifest, we accounted for lag time by creating several variables with the average wind speed and direction from 0, 1, 3, 6, 12, 24, 72, and 168 hrs before the sampling event. Furthermore, a categorical wind direction was with 16 categories (N, NNE, NE, ENE, E etc.) because wind directions should not be weighted over each other.

Given that the nearshore is sheltered during an offshore wind and vulnerable during an onshore wind, our sampling stations that have different geographic orientations are likely to respond differently to wind conditions. To create a comparable measure for the effects of wind we corrected wind direction to beach orientation so that a direct onshore wind scored 90, an along shore wind scored 0, and a direct offshore wind scored -90; this variable was then transformed into radians to minimize the range of the variable (Figure 5.2). Furthermore, we also created a wind vector variable that incorporated the wind speed and corrected wind direction by multiplication. This variable is expected to represent wave impact, as a higher wind speed or more direct onshore angle should result in a more intense wave impact.

Other variables used from the NOAA weather station include Barometric pressure, Air temperature at 2m above sea level (asl), and humidity.

5.2.5.2 Spatial Variables

One of the benefits of CCA is that it is compatible with categorical or dummy variables as well as numeric variables (Ter Braak 1987). Spatial patterns can be represented by both Euclidean distance or as dummy variables. In this case, we chose to use both types of spatial variables as they may explain different spatial patterns. We used the dummy variables water body and sampling station; the station variable consisted of the 12 sampling stations, and sampling stations were separated into three groups for the water body variable (Chukchi Sea, Beaufort Sea, and Elson Lagoon; Figure 1.1, Introduction) to investigate the similarity or difference between water bodies. We recognize that these three water bodies are connected and that stations at the edge of adjacent water bodies may have similarities. For this reason we included variables generated by the Principle Components of Neighbor Matrices (PCNM) method, to represent the autocorrelation associated with Euclidean distance (Legendre et al. 2005; Dray et al. 2012; Legendre and Gauthier 2014). Because our water bodies are separated by a landmass we could not use Latitude and Longitude to create a spatial matrix, instead the distance between each station was measured and entered into a matrix manually. This results in a neighbor matrix that represents a map of sampling stations that appear to be in a straight line (Figure 1.1).

5.2.5.3 Temporal Variables

Similar to the spatial variables, temporal variables can be represented as both dummy variables and Euclidean distance variables, and both were used in this analysis. Dummy variables included year (2013–15) to account for interannual differences and week (1–6) to account for smaller temporal scales. A variable was created for days since ice break-up in the Elson lagoon. The Elson Lagoon is always the first to become ice free in the beginning of summer, therefore this variable was created to identify seasonal patterns such as the succession of emigration to newly available habitat after winter conditions subside. Another variable was created based on the number of days since a significant wind event, because sampling became impossible when a wind vector value of 6.061 was surpassed (calculated from a wind speed of 7.72 m/s at an angle of 45° or 0.79 radians). Any day in which this value was surpassed we would deem it a significant wind event, and focus our efforts on stations that were less affected by the wind. Days since a significant wind event was counted from the last day during which the threshold was surpassed, allowing us to account for the effects of strong winds on community composition without being able to sample during the wind event. Furthermore, PCNM was performed on a

Euclidean distance matrix to account for autocorrelation associated with time between sampling events.

5.3 Results

5.3.1 Forward Selection of Variables

5.3.1.1 Environmental Variables

The first step of the forward selection process was to determine which wind lag time explains the most variability in community composition in Arctic nearshore fish communities. This was done by creating multiple environmental variable matrices, each with a different wind lag time, and comparing the R² values to find the model that explained the most variance in ASP. The global model (including all environmental variables) with 12 hr lag wind variables had the highest R² (0.31). The other lag timed wind variables were removed from the global environmental variables matrix so it could be used in the forward selection process outlined by Blanchet et al. (2008). The following were selected as the most explanatory variables and made up the environmental variables matrix (ENV) for the variance partitioning portion of the analysis: Wind speed, Wind vector, Air Temperature and Salinity.

5.3.1.2 Spatial Variables

The PCNM method created 9 principal components representing positive spatial autocorrelation, and forward selection of these principal components selected Spatial Principal Components 1 and 3 (SPC1 and SPC3) based on p and R² values. The global model with SPC1, SPC3, water body and station had an R² of 0.30; SP1 and SP3 were selected as important explanatory variables and made up the spatial variables matrix (SPT) for the variance partitioning portion of the analysis.

5.3.1.3 Temporal Variables

The PCNM method created 8 principal components representing positive temporal autocorrelation, and forward selection of these principal components selected Temporal Principal Components 1 and 2 (TPC1 and TPC2) based on p and R² values. The global model with TPC1, TPC2, Year, Week, Days since Break-up, and Days since a significant wind event had an R² of 0.30. Year was the only selected explanatory variable, and made up the temporal variables matrix (TMP) for the variance partitioning portion of the analysis.

5.3.2 Variance Partitioning

The total inertia in the ASP matrix was 7.9394; CCA models created with each of the three fundamental explanatory matrices explained 23.32 % (ENV), 12.76 % (SPT), and 15.6 % (TMP) of the total inertia. The sum of these values would indicate that all variables combined can explain 52 % of the variability in ASP, however when the variance is partitioned and we remove the redundant explanatory power, we find that these variables only explain approximately 38 % of the variance (Fig. 4.3). The environmental variables have most explanatory power ([6] = 9.85 %), followed by the temporal variables ([12] = 8.14 %) and finally the spatial variables ([9] = 6.08 %). This sums to approximately 24 % of the variance, leaving 14 % explained by overlapping variance between the three fundamental explanatory matrices.

5.4 Discussion

When establishing monitoring efforts in relatively new study system, it is important to determine which variables drive changes in the communities that inhabit it. An important aspect of forward selection that is often overlooked is not only the selection of these important variables, but also the variables that are not selected and therefore are not as explanatory as others. Removing the need to record these less explanatory variables from a sampling plan can greatly streamline efforts and increase efficiency.

In these Arctic nearshore habitats, we found that only 7 of our 18 variables had significant explanatory power; 4 Environmental, 2 Spatial, and 1 Temporal. Unfortunately, this analysis does not identify the direct relationships between these variables and the species in the communities. However, we can consider the range of habitat conditions that could be related to each variable, and indicate the types of decisions that they may drive.

5.4.1 Environmental Variables

Given the extremely cold temperatures in the Arctic nearshore surrounding Barrow, it seems likely that these communities would be driven by changes in temperature. Air temperature was selected as a more explanatory variable over sea surface temperature, perhaps indicating that these fish communities react to weather patterns in anticipation of their effects on the water. During early summer in Barrow, the sea ice is usually within 100km from shore, when wind blows from the East (Beaufort Sea) or the West (Chukchi Sea) or North (both) it is cooled by the sea ice before reaching the nearshore. However, when the wind slows the air is able to be warmed by the sun, consequently allowing the sea surface temperature to increase also.[M1] 2013 was relatively warmer than 2014 and 2015 (average temperature: 6.23 °C, 3.63 °C, and 3.47 °C, respectively), which coincided with wind speed/air temperature relationship described above (average wind speed: 4.48 m/s, 6.17 m/s, and 5.05 m/s respectively).

Alternatively, warmer air temperatures could be related to a slow South wind, where the air is warmed over the land before reaching the nearshore, however, South winds are not common in Barrow, AK. These scenarios all indicate that cold air is accompanied by relatively high speed wind which is likely to be followed by stronger wave action and currents. Warmer air temperatures are likely to indicate that calm nearshore conditions are to follow, and species may respond to these precursors to take advantage of the impending conditions.

Wind Vector has the potential to be covariant with air temperature and wind speed, but these relationships are hard to predict given the nature of the Wind Vector variable. A High Wind Speed coupled with a low Beach Oriented Wind Direction (BOWD) would yield a low Wind Vector. Similarly, a low Wind Speed coupled with a high BOWD would yield a low Wind Vector. Due to this relationship, these three variables can be considered orthogonal and thus can explain different axes of variation in species abundances.

It is important to consider the conditions that are created when our measured variables fluctuate, and how these conditions may be beneficial to different types of species. Because fish are poikilotherms, their metabolisms are highly dependent on the temperature in their surroundings (Fonds et al. 1992), therefore an increased temperature would allow them to break down more food in less time. However, this is not advantageous if food is not in high abundance. The warmer conditions that may be associated with warm air temperature are likely to be

accompanied by reduced turbulence in the water because of less wave action. For benthic species, this may be beneficial as suspended foods will settle to the benthos. However, pelagic species may find these calm conditions to be unfavorable, and thus be more abundant when Wind Vector is higher. On the opposite extreme, highly turbulent water might create a higher pelagic food item encounter rate, but make it more difficult to capture (Dower et al. 1997).

Sea Surface Salinity was also an important variable, and this seems likely as there are major differences in salinity between the water bodies. This would lead to the presumption that salinity is largely structured by spatial variables. And though the variance partitioning ENV – SPT does reduce the explanatory power of the environmental variables from 23% to 17%, indicating that this portion of the environmental variance explained is spatially structured, it is not possible to identify which of the four ENV variables are most redundant with SPT.

5.4.2 Spatial Variables

In the case of the spatial variables, the categorical variables (Water body and Station) were not selected, but the distance based eigenvector variables (SP1 and SP3) were selected as important variables. This indicates that the spatial variability is relatively gradual or not highly heterogeneous. If changes in community composition through space were abrupt (highly heterogeneous), we would expect that there would be low autocorrelation, thus minimizing the variability explained by distance (Legendre et al. 2005; Blanchet et al. 2008). Though there is clearly a distance based pattern in the community compositions of nearshore Arctic communities, these variables only explain approximately 6 % of the variance after ENV and TMP are partialled out.

5.4.3 Temporal Variables

Though the explanatory power of the TMP variables is less than ENV (10 % and 8 % respectively), TMP is only made up one on variable (Year), whereas ENV is made up of four. By this logic, one could argue that the categorical variable Year is the most explanatory of all variables included in this analysis. The time based temporal variables were not selected, suggesting that this variance in time is not dependent on how much time has passed, but rather is dependent on different conditions during each summer sampling season. Wind speed and Air temperature averages differed between years, but these differences are partialled out, there must be variables that were not included in the analysis that differ between years to explain the variance.

It is possible that the spatiotemporal beta diversity is determined by succession of immigration to newly available habitat after landfast ice conditions associated with winter subside. Nearshore ice in the Arctic can reach 3 m thickness; given that most of the lagoons and nearshore waters we sampled are less than 3 m deep, it is likely to make these habitats inhabitable or at least extremely unforgiving during winter (Dunton et al. 2005; Dunton et al. 2006). After the ice breaks free and floats offshore, species are expected to migrate into these areas to take advantage of the high productivity associated with estuaries (Dunton et al. 2012). Perhaps the conditions at the start of a given summer dictate which species will settle first, and a competitive dynamic takes over to control species abundance for that given year.

With this concept in mind, we might expect larval recruitment to play a vital role in our catch composition; especially since the majority of our catches are larval and juvenile fish. In order to

approach this aspect of community ecology we would need to know mortality, survival, fecundity, maturation, etc. for numerous species in the Arctic (Gotelli 2001). Unfortunately, little is known about the life histories of Arctic nearshore species, but this is certainly a gap in knowledge that should be addressed in the future.

Another factor that differs annually and could affect the recruitment of species to the Arctic nearshore is the velocity of the Alaska Coastal Current (ACC). This current originates in the Gulf of Alaska, is largely driven by freshwater inputs from coastal habitats, and flows North along the Alaskan coast and around the tip of Point Barrow (Stabeno et al. 1995; Chan et al. 2011; Danielson et al. 2014). In the summer of 2013, the ACC was highly variable, and even temporarily reversed flow several times (Seth Danielson Unpublished Data). Given that the nearshore habitats in Point Barrow are all supplied by the ACC, its behavior prior to and during the summer can have a significant effect on recruitment of larval species that have been transported from lower latitudes. A future study of recruitment in this region would certainly benefit from the inclusion of larval settlement from the ACC.

Though there are clearly gaps in knowledge that can help elucidate patterns in community ecology in the Arctic nearshore, this analysis has identified a model consisting of 7 explanatory variables that explain approximately 38 % of the variance in community composition. Of this 38 % explained by the global model, 14 % is explained by overlap between ENV, SPT, and TMP. It is clear that the environmental drivers are a combination of wind speed, wind direction, and air temperature, as well as salinity. Salinity is heavily structured by spatial variables as one of the study areas was an estuary that was usually low in salinity. The remaining environmental variables are probably confounded by the temporal variables as air temperature differed between years. Perhaps the most interesting point of discussion is that Year was the single most explanatory variable, but only accounts for approximately 16 % of the variance in beta diversity. The remaining unexplained variance can be explained by a number of variables, but it is likely that community composition is affected by large spatial and temporal scaled variables that fell outside of the scope of this project. Much can be learned about the Arctic nearshore from age structured population models for dominant species as well as recruitment models involving the Alaska Coastal Current. In future work we will focus our efforts on understanding which species are most affected by the important variables that we identified in hopes that this will lead to more accurate models to predict and conserve the future of these Arctic nearshore communities.

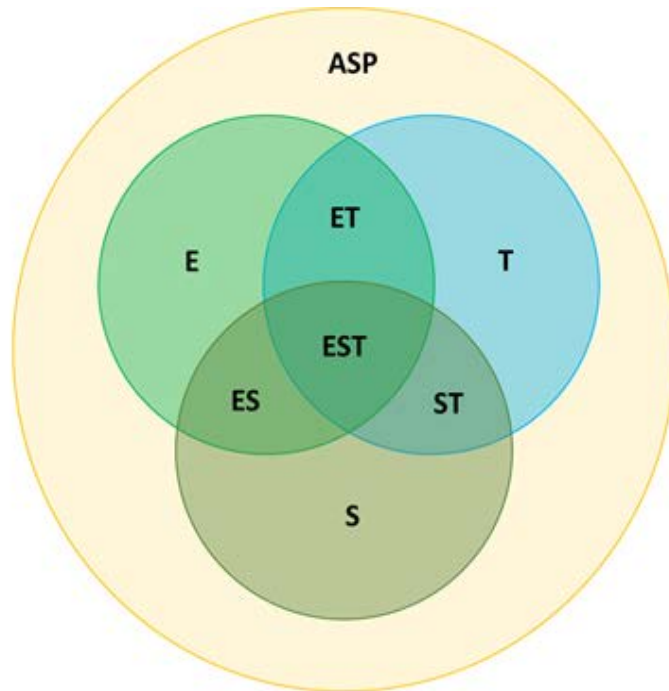
5.5 References

- Anderson M, Gribble N. 1998. Partitioning the variation among spatial, temporal and environmental components in a multivariate data set. *Austral J Ecol.* 23: 158–167.
- Berkman P, Young O. 2009. Governance and environmental change in the Arctic Ocean. *Science.* (80-324): 339–340.
- Blanchet F, Legendre P, Borcard D. 2008. Forward selection of explanatory variables. *Ecology.* 89: 2623–2632.
- Chan P, Halfar J, Williams B, et al. 2011. Freshening of the Alaska Coastal Current recorded by coralline algal Ba/Ca ratios. *J Geophys Res Biogeosciences.* 116: 1–8. doi: 10.1029/2010JG001548
- Danielson SL, Weingartner TJ, Hedstrom KS, et al. 2014. Coupled wind-forced controls of the Bering-Chukchi shelf circulation and the Bering Strait throughflow: Ekman transport,

- continental shelf waves, and variations of the Pacific-Arctic sea surface height gradient. *Prog Oceanogr* 125: 40–61. doi: 10.1016/j.pocean.2014.04.006
- Dower J, Miller T, Leggett W. 1997. The role of microscale turbulence in the feeding ecology of larval fish. *Adv Mar Biol.* 175–188.
- Dray S, Pelissier R, Couteron P, Fortin M, Legendre P, Peres-Neto P, Bellier E, Bivand R, Blanchet F, De Caceres M, et al. 2012. Community ecology in the age of multivariate multiscale spatial analysis. *Ecol Monogr.* 82: 257–275.
- Dunton KH, Goodall JL, Schonberg SV, Grebmeier JM, Maidment DR. 2005. Multi-decadal synthesis of benthic-pelagic coupling in the western arctic: Role of cross-shelf advective processes. *Deep Res Part II Top Stud Oceanogr.* 52: 3462–3477. doi: 10.1016/j.dsr2.2005.09.007
- Dunton KH, Schonberg S V, Cooper LW. 2012. Food web structure of the Alaskan nearshore shelf and estuarine lagoons of the Beaufort Sea. *Estuaries and Coasts.* 35: 416–435. doi: 10.1007/s12237-012-9475-1
- Dunton KH, Weingartner T, Carmack EC. 2006. The nearshore western Beaufort Sea ecosystem: Circulation and importance of terrestrial carbon in arctic coastal food webs. *Prog Oceanogr.* 71: 362–378. doi: 10.1016/j.pocean.2006.09.011
- Elliott M, O'Reilly MG, Taylor CJL. 1990. The forth estuary: a nursery and overwintering area for North Sea fishes. *Hydrobiologia.* 195: 89–103. doi: 10.1007/BF00026816
- Fonds M, Cronie R, Vethaak A, Puyl P. 1992. Metabolism, food consumption and growth of Plaice (*Pleuronectes platessa*) and Flounder (*Platichthys flesus*) in relation to fish size and temperature. *Netherlands J Sea Res.* 29: 127–143.
- Gotelli N. 2001. *A Primer of Ecology*, 3rd edn. Sinauer Associates Inc. Publishers, Sunderland, Massachusetts.
- Johannesson OM, Bengtsson L, Miles MW, Kuzmina S, Semenov V, Alekseev G, Nagurnyi A, Zakharov V, Bobylev L, Pettersson L, et al. 2004. Arctic climate change : observed and modelled temperature and sea-ice variability. *Tellus.* 56: 328–341.
- Johnson SW, Thedinga JF, Neff AD, Hoffman CA. 2010. Fish Fauna in Nearshore Waters of a Barrier Island in the Western Beaufort Sea, Alaska. *July:* 1–29.
- Legendre P, Borcard D, Peres-neto PR. 2005. Analyzing Beta Diversity: Partitioning the spatial variation of community composition data. *Ecol Monogr.* 75: 435–450.
- Legendre P, Gauthier O. 2014. Statistical methods for temporal and space – time analysis of community composition data. *Proc R Soc B.* 281: 20132728.
- Logue JB, Mouquet N, Peter H, Hillebrand H. 2011. Empirical approaches to metacommunities: A review and comparison with theory. *Trends Ecol Evol.* 26: 482–491. doi: 10.1016/j.tree.2011.04.009
- Palmer M. 1986. Pattern in Corticolous Bryophyte communities of the North Carolina Piedmont: Do mosses see the forest or the trees? *Bryologist.* 89: 59–65.
- Stabeno PJ, Reed RK, Schumacher JD. 1995. The Alaska coastal current: Continuity of transport and forcing. *J Geophys Res.* 100: 2477–2485.
- Ter Braak C. 1987. The analysis of vegetation-environment relationships by canonical correspondence analysis. *Vegetation.* 69: 69–77.

Table 5.1 A summary of the variables that were entered into the forward selection process. The last column indicates whether or not the variable was selected and thus used in the variance partitioning portion of the analysis.

Variable	Type	Selection
Sea Surface Temperature	Environmental	No
Sea Surface Salinity	Environmental	Yes
Dissolved Oxygen	Environmental	No
12-Hour Lag Wind Speed	Environmental	Yes
12-Hour Lag Wind Direction Category	Environmental	No
12-Hour Beach Orientation Corrected Wind Speed	Environmental	No
12-Hour Wind Vector	Environmental	Yes
Barometric Pressure	Environmental	No
Air Temperature at 2 m above sea level	Environmental	Yes
Humidity	Environmental	No
Waterbody	Spatial	No
Sampling Station	Spatial	No
Spatial Principle Component 1	Spatial	Yes
Spatial Principle Component 3	Spatial	Yes
Year	Temporal	Yes
Week	Temporal	No
Days Since Ice Break-up in Elson Lagoon	Temporal	No
Days Since Significant Wind Event	Temporal	No



Parti on #	Diagrammatical Area(s)	Constraining Variables	Partialled Variables	Model Equation
[1]	E + ES + ET + EST	ENV		E
[2]	S + ES + ST + EST	SPT		S
[3]	T + ST + ET + EST	TMP		T
[4]	E + ET	ENV	SPT	E – S
[5]	E + ES	ENV	TMP	E – T
[6]	E	ENV	SPT + TMP	E – (S+T)
[7]	S + ST	SPT	ENV	S – E
[8]	S + ES	SPT	TMP	S – T
[9]	S	SPT	ENV + TMP	S – (E+T)
[10]	T + ST	TMP	ENV	T – E
[11]	T + ET	TMP	SPT	T – S
[12]	T	TMP	ENV + SPT	T – (E+S)

Figure 5.1 A theoretical representation of variance partitioning among three explanatory variable matrices (Environmental, Spatial, and Temporal). The green circle represents the variance explained by ENV matrix, gray is SPT, and blue is TMP. The orange circle represents the total variance in the Abundances of Species (ASP) matrix. ET, ES, ST, and EST, represent the overlapping explained variance between the variable matrices. In the supporting table, the twelve steps of variance partitioning outlines by Anderson and Gribble (1998). “Diagrammatical Area” refers to the areas of variance. “Constraining Variables” and “Partialled Variables” refers to the explanatory matrices used for each step. “Model equation” is a shorthand describing the variables used in each model; in this column, ENV, SPT, and TMP are shortened to E, S, and T, respectively.

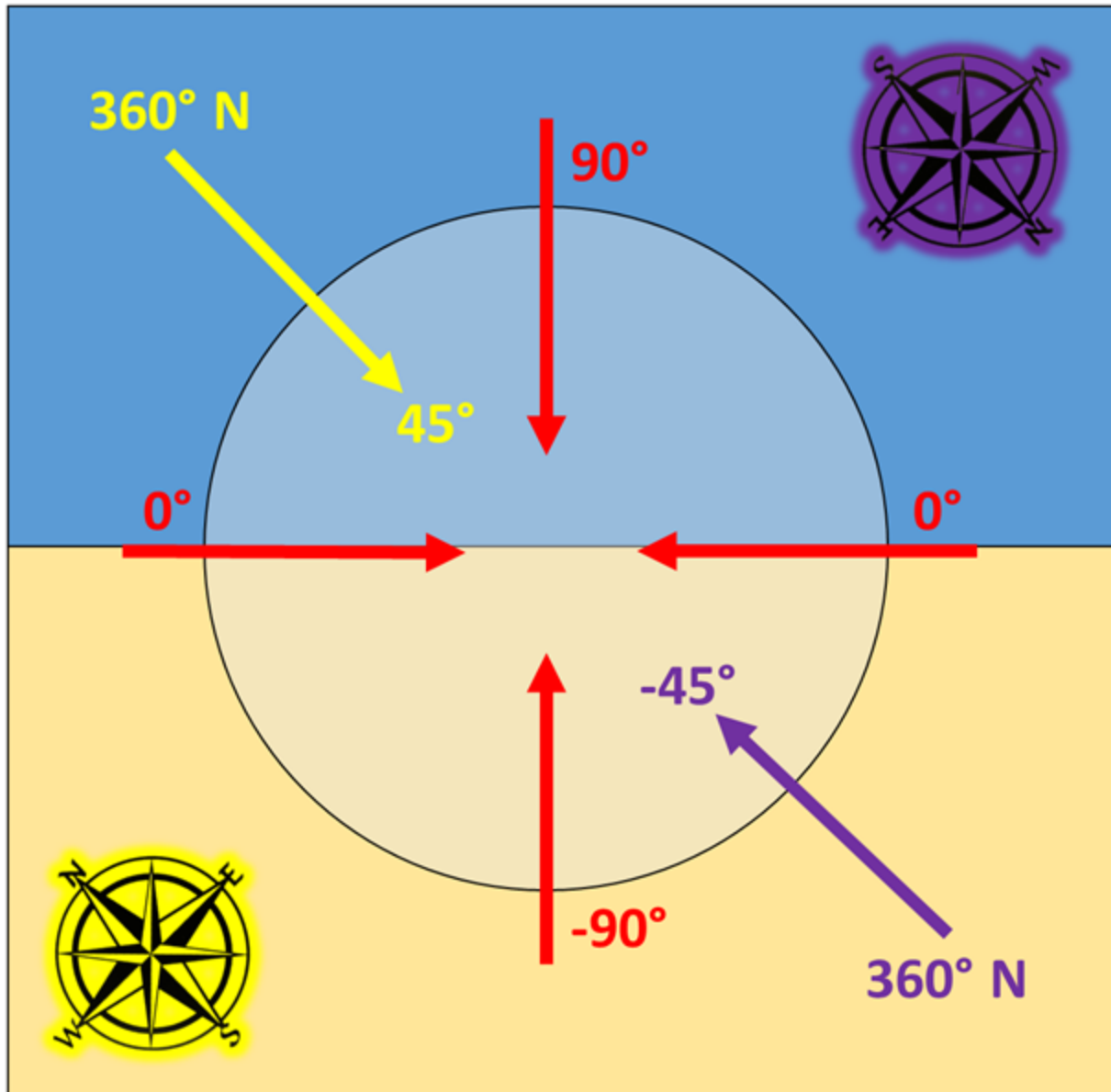
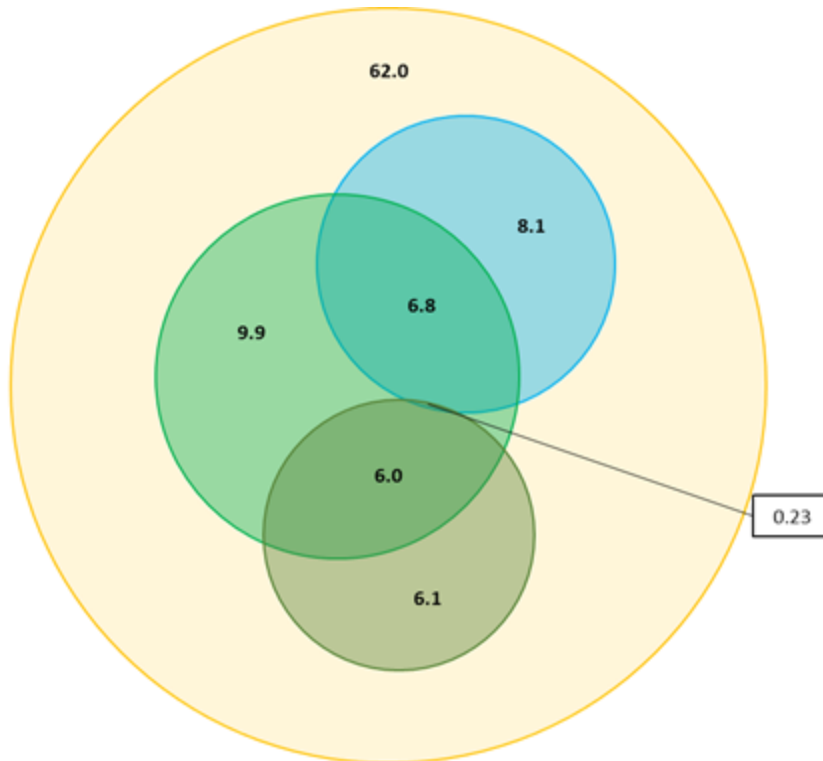


Figure 5.2 A diagrammatical representation of Beach Oriented Wind Direction (BOWD). The red arrow represent the structure of the BOWD variable. During an onshore wind the beach is exposed to waves and thus these winds are scored higher (up to 90°), an offshore wind renders the beach sheltered and thus this has the lower scores (down to -90°), and a longshore wind is ranked neutrally at 0° . To put the importance of this variable into perspective, two examples are given. In Yellow, the compass indicates that the beach is oriented in a Northeasterly direction, such as our Beaufort Sea station. In this case, a North wind (360°) would result in an onshore wind at a 45° angle to the beach. However, if we move to a Southwesterly facing beach such as the Elson stations EPP or ET2 (represented in purple), this same North wind would result in an offshore wind at 45° . This exemplifies the importance of accounting for beach orientation when considering wind direction.



CCA	Model Equation	Constrained Inertia	Unconstrained Inertia	Percent Explained (%)	P value
[1]	E	1.8518	6.0877	23.32	0.001
[2]	S	1.0133	6.9261	12.76	0.007
[3]	T	1.2386	6.7008	15.6	0.001
[4]	E-S	1.3561	5.5701	17.08	0.001
[5]	E-T	1.2946	5.4063	16.31	0.001
[6]	E-(S+T)	1.6647	4.0412	9.85	0.001
[7]	S-E	0.5176	5.5701	6.52	0.002
[8]	S-T	0.9949	5.7059	12.53	0.001
[9]	S-(E+T)	0.4827	4.9236	6.08	0.001
[10]	T-E	0.6814	5.4063	8.58	0.001
[11]	T-S	1.2202	5.7059	15.37	0.001
[12]	T-(E+S)	0.6465	4.9236	8.14	0.001
Total Variance Explained:		[1]+[7]+[12]	0.3798	Unexplained Variance: 0.6201	
		[2]+[4]+[12]	0.3798		
		[3]+[5]+[9]	0.3799	Total Inertia: 7.9394	

Figure 5.3. A proportional representation of partitioned variance explained by ENV (green), SPT (grey) and TMP (blue) of the total variance in the community composition matrix (ASP, orange). Numbers on the diagram represent the % of variance in ASP explained by each portion of the Venn diagram. More than half of the variance explained by ENV is also explained by SPT and TMP. However, SPT and TMP have almost no overlap (0.23 %). In the supporting table, results of variance partitioning. Variance is represented by the sum of eigenvalues in constrained models (inertia). The total inertia in the ASP matrix was 7.9394. In the rows where the sum of constrained and unconstrained inertia does not equal 7.9394, the difference is what has been partialled out. The proportion of variance explained by each model is given in percents.

6.0 Fish Life History Characteristics: Age, Length, Weight

B. Norcross, K. Walker, A. Frothingham

6.1 Introduction

Weight, length and age are important indicators of fish population status. Obtaining a better understanding of the differences in some aspects of life history of Arctic fishes from different habitats are important because juveniles and adults have been found in habitats with wide temperatures and salinity ranges that can greatly affect one particularly important aspect of life history (Craig et al. 1982, Falk-Petersen et al. 1986). Research dedicated to understanding basic life history, such as length at age with the use of otolith analysis in the Arctic is a new tool. Identifying basic life history of an Arctic species through otolith analysis may be useful when in situ observations are nearly impossible due to the Arctic's isolated nature and severe environmental conditions. By using length-at-age information from the Beaufort Sea, Chukchi Sea, and Elson Lagoon, we can better identify prime growth habitat for Arctic fish habitat. Lengths were examined for 14 species and one fish genus from nine families collected in the ACES study area and ages were estimated for ten species.

Length-weight relationships are useful in determining if a fish has a more allometric or isometric growth pattern. These relationships are calculated using the standard fisheries growth equation of $W = aL^b$, where W = weight of the fish, a = y-intercept (weight of the fish when initial length is zero), L = fish length and b = growth coefficient or slope (Ricker 1975, Froese 2006). These relationships relate to body type and growth patterns of fish species (Froese 2006). An isometric growth pattern is displayed when a fish increases in length and weight at the same rate and has a growth coefficient or slope (b) close to 3. Positive allometric growth ($b > 3$) indicates fish weight is increasing faster than length, i.e., body shape is short and stout. Negative allometric growth ($b < 3$) indicates that fish length is increasing faster than fish weight, i.e., body shape is long and thin. In this study, length-weight relationships were compared among study regions (Beaufort Sea, Chukchi Sea and Elson Lagoon) for fourteen species and one genus from nine families (Table 6.1) to determine if there were any differences in growth within species in the sampling area.

6.2 Methods

Fishes captured by beach seine from the Chukchi Sea, Beaufort Sea and Elson Lagoon (see Chapter 3) were processed at the University of Alaska Fisheries Oceanography Laboratory. Though not every fish that was captured was processed in Fairbanks as some were used for other purposes (see Chapters 6, 7, 8, 9), samples of all species represented the length range of those collected. Species were selected based on their relative abundance and importance to the Arctic food web. A total of 11,065 fishes were measured (*C. sardinella* = 192, *M. villosus* = 971, *O. mordax* = 178, *P. pungitius* = 41, *B. saida* = 4040, *E. gracilis* = 230, *M. platycephalus* = 52, *Myoxocephalus* spp. = 1587, *A. monopterygius* = 26, *Lumpenus fabricii* = 826, *S. punctatus* = 429, *A. hexapterus* = 2421, *Limanda aspera* = 10, *Limanda proboscidea* = 27, *Liopsetta glacialis* = 35; Table 6.1). Of the 11,065, 7,060 were collected from the Chukchi Sea, 1,751 were collected from the Beaufort Sea, 2,013 were collected from Elson Lagoon, and 242 did not have corresponding station information available. Nearly 64% of the fish measured were *B. saida*.

Each fish was thawed and blotted dry. Total length (TL) was measured to the nearest mm, and wet weight was measured to the nearest 0.1 g for larger fish and 0.0001 g for smaller fish. Sagittal otoliths were removed, cleaned, and stored dry in a centrifuge vial. Otoliths were prepared for aging from a subset of the weighed fish in each of the three ecological/geographical areas (Chukchi Sea, Beaufort Sea and Elson Lagoon). Fish species were chosen for processing based on the number of individuals available; ages were estimated from nine fish species and one fish genus. Specimens were selected for aging using a size-based process. The target quantity of specimens from each species was 20 individuals chosen at random from each 10 mm length increment; however, in many cases an insufficient number of fish was available to reach this target. In particular, there was a shortage of Capelin otoliths available for processing; Capelin otoliths are unusually brittle and transparent, making them difficult to find and successfully extract from the fish. Additionally, the Fisheries Oceanography Lab at UAF processed a small fraction of the total of Arctic Cod captured for this project because a small percentage of fish were received in our lab prior to the time of processing. Confidence intervals calculated for other research conducted in the Western Beaufort Sea indicated age-0 Arctic Cod length at age ranged up to 52 mm (Norcross et al. 2016). This multi-year project (ACES 2013-2014) concluded that all Arctic Cod with a length 50 mm or less can be definitively assigned age-0 without further processing for age, i.e., no otolith extraction and reading is necessary.

Because many of the sculpins were <50 mm there were problems identifying precisely to species. This affected the genus *Myoxocephalus*. Therefore for this analysis all weight, length and age analysis combines all *Myoxocephalus* species together, including Arctic Sculpin (*M. scorpiodes*), Fourhorn Sculpin (*M. quadricornis*), Plain Sculpin (*M. jaok*), and Shorthorn Sculpin (*M. scorpius*). Sculpins from other genera could accurately be identified.

One sagittal otolith was mounted to the center of a 1 x 3 inch glass slide using Crystalbond™ thermoplastic glue. The otolith was polished (transversely sectioned) using a Buehler rotating wheel with 1200 grit sandpaper while water was continuously sprayed on the sandpaper to lubricate the paper and remove waste. The otolith was polished down to the center and flipped onto its flattened edge and polished to the proper thickness for aging (200–300 μ). Using a compound microscope at 100 x magnification, the otolith was checked throughout the polishing process to ensure over-polishing did not occur. If over-polishing or other damage caused the first otolith to be unreadable, the second otolith was processed for aging.

Transverse cross sections of otoliths were photographed under transmitted light using a digital camera mounted on a Leica DM1000 dissecting microscope at 5x magnification. Otoliths were aged initially by two independent readers using the photographed image of each otolith. Ages were assigned by counting each full year of growth on the otolith. One full year or annual mark consists of one opaque zone of faster summer growth and one translucent zone of slower winter growth (Matta and Kimura 2012). Otolith ages for which the readers disagreed were reread collaboratively by the same readers and assigned an agreed-upon age. Otolith ages were used for constructing plots for data visualization and quality control. Because of time and available labor (and funding) constraints, only one reader aged *Liopsetta glacialis* (n=16), *Limanda aspera* (n=5), *Megalocottus platycephalus* (n=12), and *Myoxocephalus* spp. (n=122) for a total of 155 fish.

Statistical and graphical analyses were performed using SigmaPlot 12.5 software (Systat 2013). To exert control over the quality of data, for each species an initial length-weight relationship was estimated by polynomial linear regression using the standard fisheries allometric equation: $W = aL^b$, where W = total weight (g), L = total length (mm), a = the y-intercept, and b = the slope (Ricker 1975). The fishes were generally small and lengths were measured in mm, with the resulting a parameter expressed as 10^{-5} .

A length-frequency histogram was plotted as the percentage of individuals in length classes, and where applicable age-at-length data were plotted on the same x-axis. Frequencies were based on lengths of all fish measured in the lab. Specimens with a small length range were plotted by one mm length increments and those with large length ranges were plotted by 10 mm length bins (e.g., 41–50 mm). Age estimates at length were plotted on the same graph using a second y-axis.

6.3 Results and Discussion

6.3.1 Length-Weight Relationships

There were 14 species and one genus for which sufficient numbers of fish were captured in 2013–2014 so that length-weight relationships could be established (Table 6.2). The species were from nine families: Salmonidae – Least Cisco *Coregonus sardinella*, Osmeridae – Capelin *Mallotus villosus* and Rainbow Smelt *Osmerus mordax*, Gasterosteidae – Ninespine Stickleback *Pungitius pungitius*, Gadidae – Arctic Cod *Boreogadus saida* and Saffron Cod *Eleginus gracilis*, Cottidae – Belligerent Sculpin *Megalocottus platycephalus* and Sculpin of the genus *Myoxocephalus*, Agonidae – Alligatorfish *Aspidophoroides monopterygius*, Stichaeidae – Slender Eelblenny *Lumpenus fabricii* and Arctic Shanny *Sticheus punctatus*, Ammodytidae – Pacific Sand Lance *Ammodytes hexapterus* and Pleuronectidae – Yellowfin Sole *Limanda aspera*, Longhead Dab *Limanda proboscidea* and Arctic Flounder *Liopsetta glacialis*. The number of specimens per species ranged from 637 for *A. hexapterus* to seven for *Limanda proboscidea*, and was dependent on the quantity of specimens captured. When possible, species were separated and analyzed by region (Beaufort Sea, Chukchi Sea and Elson Lagoon). The minimum lengths for all species across all regions varied greatly (12–217 mm). The maximum size captured across all regions ranged from 24 to 313 mm and 0.02 to 309.28 g (Table 6.1). The minimum weights for all species from all regions ranged from 0.01 to 75.89 g.

For three species, weight-at-length regressions were not as precise as for the other 12 species. *O. mordax* in Elson Lagoon had an $r^2=0.68$, which is reasonable considering there were only six fish contributing to the relationship (Table 6.2). *S. punctatus* in the Chukchi Sea has the poorest relationship ($r^2=0.25$), which, despite very good fits in the other two regions, caused the combined-regions relationship to also be low ($r^2=0.45$). It is difficult to attribute the poor fit to a small sample size as there were 86 specimens measured in the Chukchi Sea. Furthermore, there was not wide range in sample lengths, as *S. punctatus* specimens were small (15–37 mm) in all regions. However, the weight range, while small (0.01–0.73 g), is 3.5 times greater in the Chukchi Sea than in the Beaufort Sea or Elson Lagoon.

Nine species collected over all sampling regions had enough specimens to analyze the Beaufort Sea samples separately (Table 6.2). Maximum lengths and weights ranged from 33 mm to 285 mm and from 0.19 g to 172.54 g. Minimum lengths and weights ranged from 14 mm to 217 mm and 0.01 g to 75.89 g. Slopes (b) ranged from 2.58 to 4.69. Seven of the species collected from

the Beaufort Sea displayed positive allometric growth (*C. sardinella*, *M. villosus*, *O. mordax*, *B. saida*, *Lumpenus fabricii*, *S. punctatus* and *A. hexapterus*). The *Myoxocephalus* genus and *E. gracilis* displayed negative allometric growth.

Nine species and the *Myoxocephalus* genus were analyzed separately by the Chukchi Sea region (Table 6.1). Maximum lengths and weights ranged from 37 mm to 115 mm and 0.73 g to 10.47 g. Minimum lengths and weights ranged from 15 mm to 50 mm and 0.01 g to 1.29 g. Slopes (b) ranged from 2.73 to 4.47. Six of the ten species displayed positive allometric growth (*M. villosus*, *E. gracilis*, *Megalocottus platycephalus*, *Lumpenus fabricii*, *S. punctatus* and *A. hexapterus*). Three species and *Myoxocephalus* spp. displayed negative allometric growth (*P. pungitius*, *B. saida*, *Myoxocephalus* spp. and *Limanda proboscidea*).

Nine species and the *Myoxocephalus* genus had enough specimens available to analyze by the Elson Lagoon study region (Table 6.2). Maximum lengths and weights ranged from 34 mm to 313 mm and 0.18 g to 309.28 g. Minimum lengths and weights ranged from 12 mm to 159 mm and 0.01 g to 25.44 g. Slopes (b) ranged from 2.36 to 4.01. Five species displayed positive allometric growth (*C. sardinella*, *M. villosus*, *Lumpenus fabricii*, *S. punctatus* and *A. hexapterus*). Three species and *Myoxocephalus* spp. displayed negative allometric growth (*O. mordax*, *E. gracilis*, *Megalocottus platycephalus* and *Myoxocephalus* spp.). *B. saida* was the only species that displayed isometric growth.

Several species display positive allometric growth in one location and negative growth in another; Analyzing across all three areas combined evened out the growth patterns. A b value close to 3.0 indicates isometric growth, i.e., growth of all body parts occurs at the same rate (Andreu-Soler et al. 2005, Froese 2006). The b value also indicates body shape; negative allometric growth indicates decrease and positive allometric growth indicates increase in body thickness with increasing fish length (Froese 2006). Over all of the regions, the range of growth coefficients (b) for the 15 taxa was 2.25–4.69 (Table 6.2). Three species (*B. saida*, *O. mordax* and *Liopsetta glacialis*) exhibited isometric growth with b values of 3.0 ± 0.10 . *B. saida* had positive growth in the Beaufort Sea, negative in the Chukchi Sea, and isometric in Elson Lagoon. *O. mordax* had positive growth in the Beaufort Sea and negative in Elson Lagoon. Six species exhibited positive allometric growth (*C. sardinella*, *M. villosus*, *E. gracilis*, *Lumpenus fabricii*, *S. punctatus* and *A. hexapterus*). Five of the species with positive growth displayed that pattern in each region. Only *E. gracilis* changed from positive isometric growth in the Chukchi Sea to negative growth in the Beaufort Sea and Elson Lagoon. Six species and one genus had b values less than 3.0, i.e., negative allometric growth (*P. pungitius*, *Megalocottus platycephalus*, *Myoxocephalus* spp., *A. monopterygius*, *Limanda aspera* and *Limanda proboscidea*). Most of these species did not have enough samples to compare among regions, though the two sculpin groups did. The *Myoxocephalus* genus had negative growth in all three areas. However, the sculpin species *Megalocottus platycephalus* changed from positive in the Chukchi Sea to negative in Elson Lagoon.

Changes in growth patterns within a single species across different regions indicate differences in environmental conditions that affect growth in fishes. These changes in growth patterns seem to be species specific. For example, some species displayed negative allometric growth in the Chukchi Sea (*B. saida*) whereas some displayed positive allometric growth there (*E. gracilis*,

Megalocottus platycephalus). One of the main environmental factors influencing fish growth is food availability. Fishes found in Elson Lagoon (with high enough numbers to separate from the other regions for analysis) more often displayed negative or isometric growth patterns (*B. saida*, *O. mordax*, *E. gracilis*, *Megalocottus platycephalus*) than those in the Beaufort and the Chukchi Sea. This finding indicates that there is perhaps a difference, i.e., quantity or quality, in food availability in Elson Lagoon than the Beaufort and Chukchi Seas (see Chapter 8). Currents are likely to have an effect on food availability, perhaps explaining why species display different growth patterns in different regions. Life history strategies could be influencing how each species is displaying growth. Young fish are known to display more positive growth patterns than mature adult fish (Froese 2006). More specimens are needed for further analysis, such as examining each species by age group in each sampling region. That additional analysis could reveal how growth patterns are changing within a species over the span of its life history.

Length-weight relationships have not been established for many marine Arctic fishes in Alaskan waters. This work establishes relationships that will be useful in future Arctic studies, especially those determining how the effects of climate change are affecting local fish populations. A previous study in the Beaufort Sea (Norcross et al. 2016) established length-weight relationships for several of the same species analyzed in this study (*B. saida*, *E. gracilis* and *Lumpenus fabricii*). The relationships for these species characterized in the Beaufort Sea differed in their growth coefficients and had vastly larger sample sizes. *Lumpenus fabricii* had the largest differences in sample size, growth coefficient (b) and length range. *B. saida* and *E. gracilis* did not differ as greatly in sample size, growth coefficient (b) or length range between the Transboundary project and the ACES project. During this project, only 75 *Lumpenus fabricii* were captured whereas during the Transboundary project (Norcross et al. 2016) 347 fish were caught. *Lumpenus fabricii* in the Beaufort Sea during the ACES study had a growth coefficient of 3.34, indicating positive allometric growth. *Lumpenus fabricii* captured during the Transboundary project in Beaufort Sea displayed negative allometric growth ($b = 2.75$). These differences could be attributed to the differences in sizes of specimens sampled. The length range of *Lumpenus fabricii* captured during the ACES project ranged from 22 – 47 mm, whereas the length range of fishes captured during the Transboundary project ranged from 45 – 173 mm. Younger, smaller fishes often display different growth patterns than adult fishes of the same species (Froese 2006). These findings indicate that length-weight relationships will likely differ when there are samples sizes are not equal and should not be applied to other specimens from future projects.

6.3.2 Length-Age

Length-frequency and age-at-length plots were examined for fishes collected from the Chukchi and Beaufort Seas and Elson Lagoon. Histograms show frequencies of total lengths for 14 species and one genus from nine families and varied greatly by species. A total of 309 fishes from nine different families were estimated for age (*C. sardinella* = 36, *M. villosus* = 13, *B. saida* = 30, *E. gracilis* = 46, *M. platycephalus* = 12, *Myoxocephalus* spp. = 142, *Limanda aspera* = 5, *L. proboscidea* = 5, *Liopsetta glacialis* = 20; Table 6.3).

The salmonid species *Coreogonus sardinella*, (Least Cisco), had an overall length range of 135 mm to 346 mm with median (13%) in the 180 mm range. Age estimations of *C. sardinella* from all regions combined ranged from 3 to 11 years (Figure 6.1). The modal size in the Beaufort Sea, where few fish were collected, was 235 mm (Figure 6.2); whereas in Elson Lagoon where

two orders of magnitude greater were collected, the modal size was 220 mm (Figure 6.3), the size at which Least Cisco typically reach maturity (Mann and McCart 1980). With so few *C. sardinella* estimated for age in the Beaufort Sea (n=7; Table 6.3) the age range was predictably limited and ranged from 4 to 6 years. While *C. sardinella* in Elson Lagoon ranged from 3 to 11 years, the mode was age-3. Juvenile stages for *C. sardinella* were noticeably absent from all regions and no samples were available to measure/age from the Chukchi Sea.

The two Osmerid species, *Mallotus villosus* (Capelin) and *Osmerus mordax* (Rainbow Smelt) displayed different patterns; *M. villosus* had more samples measured, but its maximum length was over 100 mm less than that of *O. mordax*. *M. villosus* had a length range of 19 mm to 152 mm (Figure 6.4), with similar length ranges in the Chukchi Sea (Figure 6.5), Beaufort Sea (Figure 6.6), and Elson Lagoon (Figure 6.7). However, the median length of *M. villosus* in the Chukchi and Beaufort Seas was 35 mm, whereas in Elson Lagoon, where there were more *M. villosus* collected, the mode was 45 mm (Figure 6.7). Ages (n=13; Table 6.3) of *M. villosus* were estimated for those collected in the Chukchi and Beaufort Sea with age ranges of 1 to 3 years and 0 to 1 year respectively. Because ages were only estimated to be as old as 3 years, *M. villosus* were likely juvenile or just reaching maturity (Winters 1982). *O. mordax* were captured as small as 24 mm, and had the same mode size (35 mm) as *M. villosus*; however, *O. mordax* as large as 263 mm were captured (Figure 6.8). *O. mordax* were smaller and less common in the Chukchi Sea (Figure 6.9) and Beaufort Sea (Figure 6.10). In Elson Lagoon, *O. mordax* were more abundant and much larger though the mode was still 35 mm (Figure 6.11). Both Osmerid species were collected in each of the three regions (Table 6.1), yet the modal size remained comparable. A modal size of 35 mm for all Osmerids indicate majority were juveniles.

One species of the Gasterosteidae family was included; the Ninespine Stickleback (*Pungitius pungitius*) had a length range of 26 mm to 55 mm, mode 35 mm (Figure 6.12), most of which were in the Chukchi Sea collections (Figure 5.13).

There were two Gadid (cod) species, *Boreogadus saida* (Arctic Cod) and *Eleginus gracilis* (Saffron Cod); the abundance of *B. saida* was an order of magnitude greater than that of *E. gracilis*. *B. saida* had a length range of 12 mm to 221 mm (Figure 6.14) as a result of the large collection in the Chukchi Sea where the mode was 105 mm (Figure 6.15). Additionally, of the Arctic Cod measured, over 50% Arctic Cod were between 90 mm to 130 mm indicating they may be in the adult stage (Nahrgang et al. 2016). *B. saida* was two orders of magnitude less abundant as well as smaller in the Beaufort Sea (14 to 79 mm; Figure 6.16) and Elson Lagoon (12 to 127 mm; Figure 6.17). A small number of *B. saida* were estimated for age (n=30; Table 6.3). Age estimations ranged from 0 to 2 years for *B. saida* (Figure 6.14). Male *B. saida* in the Beaufort Sea have been documented to mature at age-2, while females have been documented to mature at age-3 (Craig et al. 1982). The work previously done in the Beaufort Sea indicates mature *B. saida* were likely present in these regions for this study. *B. saida* age-at-length for age-0 and age-1 in this study were similar to average length at age from previous work in this region (Norcross et al. 2016). For example, age-1 *B. saida* on average were 103 mm in length in the present study, comparable to age-1 *B. saida* from the Beaufort Sea collected from 2012-2014 with an average of 105 mm in length. Research completed nearly thirty years ago suggest *B. saida* were smaller at each age. For example, previous age-1 *B. saida* from the Beaufort Sea averaged 84 mm in length (Craig et al. 1982). *E. gracilis* had a much larger size range (16 mm to 410 mm), though the majority (62%) was less than 40 mm (Figure 6.18). The majority of Saffron

Cod (71%) was collected in the Chukchi Sea, though they were all less than 70 mm, mode 25 mm (Figure 6.19). In the Beaufort Sea, *E. gracilis* were quite small (≤ 35 mm, mode 29 mm; Figure 6.20). The majority were small (mode 24 mm) in Elson lagoon, but there were only two individuals >250 mm (Figure 6.21). Age ranged from 0 to 7 years for *E. gracilis*, though most were ≤ 2 (Figure 6.18).

Two genera were measured from the Cottidae family. *Megalacottus platycephalus* (Belligerent Sculpin) had a length range of 35 mm to 142 mm, though only one fish was >90 mm (Figure 6.22). Most of the samples were collected from the Chukchi Sea (83%) and represented the total length range and had a mode of 55 mm (Figure 6.23). Very few *M. platycephalus* were caught in Elson Lagoon (Figure 6.24). All the *Myoxocephalus* spp. were grouped together from all regions. The length range for all *Myoxocephalus* spp. was 13 mm to 240 mm, with over 83% of the samples less than 50 mm (Figure 6.25). *Myoxocephalus* spp. captured in the Chukchi Sea (Figure 6.26) and Elson Lagoon (Figure 6.28) had the same length range, whereas in the Beaufort Sea (Figure 6.27) all *Myoxocephalus* spp. were <80 mm. The modal size of *Myoxocephalus* spp. in all three locations was 15 mm. Similar to the Gadidae family, the majority of the measured fish from the Cottidae family were collected from the Chukchi Sea. Nearly identical length ranges of *Myoxocephalus* spp. from Elson Lagoon and the Chukchi Sea may suggest food sources are of similar quality, or may be the result of grouping all *Myoxocephalus* spp., i.e., perhaps there was a large species that was not collected in the Beaufort Sea. For *M. platycephalus*, age estimates ranged from 1 to 3 years (Figure 6.22), while *Myoxocephalus* spp. age ranged from 0 to 5 years (Figure 6.25).

Unlike the sculpins, there were very few *Aspidophoroides monopterygius*, (Alligatorfish), from the family Agonidae captured. Overall, they had a very small length range, from 15 mm to 35 mm, with a mode of 20 mm (Figure 6.29). With so few measured *A. monopterygius*, (n= 26) few inferences can be made.

The two species from the Stichaeidae family were collected in all three regions (Chukchi Sea, Beaufort Sea, and Elson Lagoon). *Lumpenus fabricii* (Slender Eelblenny) had an overall length range from 15 mm to 167 mm (Figure 6.30), of which the upper end was from fish collected in the Chukchi Sea, though the mode was only 25 mm (Figure 6.31). *L. fabricii* were smaller in the Beaufort Sea, but the modal size was still 25 mm (Figure 6.32) and Elson Lagoon, mode 35 mm (Figure 6.33). *Stichaeus punctatus* (Arctic Shanny) had a much smaller length range, from 15 mm to 43 mm, though many samples were measured (n= 429, Figure 6.34). The modal length of *S. punctatus* in the Chukchi Sea was 25 mm (Figure 6.35). In the Beaufort Sea the length distribution of *S. punctatus* was bimodal, 25 and 30 mm (Figure 6.36), whereas in Elson Lagoon (Figure 6.37) the single mode was 28 mm.

Of the one species collected from the Ammodytidae family, *Ammodytes hexapterus* (Pacific Sand Lance), over half of the samples were collected from the Chukchi Sea (n=1,440). Overall, the length range of *A. hexapterus* was 24 mm to 115 mm (Figure 6.38), which was similar in the three regions: Chukchi Sea (Figure 6.39), Beaufort Sea (Figure 6.40) and Elson Lagoon (Figure 6.41). Likewise, the modal size of 55 or 65 mm was similar in all areas. The majority of *Ammodytes hexapterus* diet consists of calanoid and cyclopoid copepods (Chapter 7, this report, Field 1988). While the Chukchi Sea is nutrient rich, the shallow nature of the region produces

high benthic abundance (Grebmeier et al. 1988). Comparatively, the Beaufort Sea's extensive ice coverage, narrow shelf, and currents limit primary production, and is more of a pelagic system (Grebmeier and Barry, 1991) conducive for calanoid and cyclopoid copepods. Despite the disparity in sample collection among regions, similar length ranges for *Ammodytes hexapterus* from all regions suggest prey availability and habitat quality may be comparable in the Chukchi Sea and Elson Lagoon when compared to the Beaufort Sea.

Three species from the Pleuronectidae family were measured. *Limanda aspera* (Yellowfin Sole) had the smallest length range from 35 mm to 42 mm (Figure 6.42) and the smallest number of fish measured (n=10). Similarly, few *L. aspera* ages were estimated (n=5) and all were age-1 (Figure 6.42). The 35 *Liopsetta glacialis* (Arctic Flounder) measured had the largest range in length from 31 mm to 209 mm (Figure 6.43). *L. glacialis* captured in the Chukchi Sea were much smaller (<70 mm, mode 39 mm; Figure 6.44) than those in Elson Lagoon that encompassed the whole length range 31–209 mm and had no definitive mode (Figure 6.45). Ages of *L. glacialis* ranged from 0 to 7 years, older than the two fish species from the Pleuronectidae family. *Limanda proboscidea* (Longhead Dab) measured (n=28) had a length range from 35 mm to 104 mm with a modal size of 45 mm (Figure 6.46). *L. proboscidea* had an age range from 1 to 3 years (Figure 6.46).

Overall, the results of this research add to the limited information about fish community and age at length of abundant fishes in the nearshore regions of the Chukchi and Beaufort Seas. Habitat can greatly affect aspects of life history and highlights the necessity to study Arctic fishes from diverse habitats. Length-frequency estimates of Osmerid species (*O. mordax* and *M. villosus*) indicate juveniles were present in large numbers in each of the three regions. Furthermore, the oldest age estimated for *M. villosus* was only age-3, the earliest age when transition to maturity begins (Chambers et al. 1989). Juveniles from the genus *Myoxocephalus* spp were also present in all three regions in large percentages. *Myoxocephalus* spp. estimated to be age-0 ranged in size from 19 mm to 44 mm. With a mode of 15 mm in all three regions, it is clear juvenile *Myoxocephalus* spp. have no preference in the three regions. Similar distributions of juveniles of both fishes in the Stichaeidae family occurred in all three regions. While age estimations were not done for the species *Stichaeus punctatus*, the maximum length of 43 mm indicates juveniles were abundant in all regions as juveniles have been documented as large as 50 mm (Farwell et al. 1976).

Early life stages of species such as *O. mordax*, *M. villosus*, *S. punctatus* did not demonstrate a preference for region, yet this was not the pattern for all species. For example, *C. sardinella* was not found in the Chukchi Sea. Additionally, the size range and age estimations (3 to 11 years) indicate adult *C. sardinella* utilize the Beaufort Sea, but more commonly are found in Elson Lagoon. Finding *C. sardinella* in Elson Lagoon is expected as this species is abundant in many nearshore estuarine and streams in the Arctic (Roux et al. 2016). Contrary to *C. sardinella*, the majority of *Eleginus gracilis* were juveniles (mode of 25 mm) and were found in the Chukchi Sea (71%). Both Saffron Cod and Arctic Cod were collected in greater numbers in the Chukchi Sea when compared to the other two regions. The Chukchi Sea is a shallow region supported with an abundance of nutrients transported from the Bering Sea (Weingartner 1997) increasing regional productivity. This may be indicative of a greater presence of prey for Gadids in the Chukchi Sea region that could support the abundance of larger Arctic Cod collected in this

region. In general, these results suggest the Chukchi Sea is a productive region for many abundant Arctic fishes including both species in the Gadidae and Cottidae family included in this study. Because three regions were sampled in the nearshore marine Arctic waters, we were able to provide more information on preferential habitat for life stages of different species.

Very few studies included a detailed look at age-at-length data of marine and estuarine fishes from a variety of Arctic marine habitats. A comparative length-at-age study that includes fishes from the Chukchi and Beaufort Seas and Elson Lagoon did not previously exist. Length-at-age of species present in this study have not been documented extensively. Previous research in the Beaufort Sea only include *Boreogadus saida* age-at-length data (Craig et al. 1982, Norcross et al. 2016,) to compare to this study. Other Arctic fishes included in this study have been documented in the region, but do not have detailed age-at-length information for multiple habitats in the Arctic. By examining age-at-length and overall length frequencies by region, we were able to contribute to limited understanding of nearshore habitat in the Arctic. Further research should replicate the sampling efforts of this project to document the effects of a changing environment to Arctic species.

6.4 References

- Andreu-Soler A., Oliva-Paterna FJ and Torralva M. 2005. A review of length-weight relationships of fish from the Segura River basin (Siberian Peninsula). *J Appl Ichthyol.* 22: 295–296.
- Craig P, Griffiths W, Haldorson L and McElderry H. 1982. Ecological studies of Arctic cod (*Boreogadus saida*) in Beaufort Sea coastal waters, Alaska. *Can J Fish Aqua Sci.* 39(3): 395–406.
- Chambers, RC, Leggett, WC, & Brown, JA. (1989). Egg size, female effects, and the correlations between early life history traits of capelin, *Mallotus villosus*: An appraisal at the individual level. *Fishery Bulletin*, 87(3), 515-523.
- Falk-Petersen I-B, Frivoll V, Gulliksen B and Haug T. 1986. Occurrence and size/age relations of polar cod, *Boreogadus saida* (Lepechin), in Spitsbergen coastal waters. *Sarsia.* 71(3–4): 235–245.
- Farwell, M. K., Green, J. M., & Pepper, VA. (1976). Distribution and known life history of *Stichaeus punctatus* in the northwest Atlantic. *Copeia*, 1976(3), 598-602.
- Field, JL 1988. Pacific sand lance, *Ammodytes hexapterus*, with notes on related *Ammodytes* species. In: NJ Wilimovsky, LS Incze, and SJ Westrheim (eds.), *Species synopses: Life histories of selected fish and shellfish of the northeast Pacific and Bering Sea.* Washington Sea Grant Program and Fisheries Research Institute, University of Washington, Seattle. 111 pp.
- Froese R. 2006. Cube law, condition factor and weight-length relationships: history, meta-analysis and recommendations. *J Appl Ichthyol.* 22(4): 241–253.
- Grebmeier, JM, McRoy CP, and Feder H.M. 1988. Pelagic-benthic coupling on the shelf of the northern Bering and Chukchi seas. Food supply source and benthic biomass. *Marine ecology progress series.* Oldendorf 48.1: 57-67.
- Grebmeier, JM, and Barry JP. 1991. "The influence of oceanographic processes on pelagic-benthic coupling in polar regions: a benthic perspective." *Journal of Marine Systems* 2.3: 495-518.

- Mann GJ and McCart PJ. 1981. Comparison of sympatric dwarf and normal populations of least cisco (*Coregonus sardinella*) inhabiting Trout Lake, Yukon Territory. *Can J Fish Aqua Sci.* 38(2): 240–244.
- Matta ME, and Kimura DK. 2012. Age determination manual of the Alaska Fisheries Science Center Age and Growth Program: US Department of Commerce, National Oceanic and Atmospheric Administration, National Marine Fisheries Service, Scientific Publications Office.
- Nahrgang J, Storhaug E, Murzina SA, Delmas O, Nemova NN, Berge J. 2016. Aspects of reproductive biology of wild-caught polar cod (*Boreogadus saida*) from Svalbard waters. *Polar Biol.* 1–10.
- Norcross BL, Apsens SJ, Bell LE, Bluhm BA, Dissen JN, Edenfield LE, Frothingham A, Gray BP, Hardy SM, Holladay BA, Hopcroft RR, Iken KB, Smoot CA, Walker KL, Wood ED. 2016. US-Canada Transboundary Fish and Lower Trophic Communities: Abundance, Distribution, Habitat and Community Analysis. Draft Final Report v.2 for BOEM Agreement Number M12AC00011. University of Alaska Fairbanks. 447 pp + appendices.
- Ricker WE. 1975. Computation and interpretation of biological statistics of fish populations. *Bulletin of the Fisheries Research Board of Canada*, 191, 1–382.
- Roux, MJ, Harwood, LA, Zhu, X., & Sparling, P. (2016). Early summer near-shore fish assemblage and environmental correlates in an Arctic estuary. *Journal of Great Lakes Research*, 42(2), 256-266.
- Winters, G.H., 1982. Life history and geographical patterns of growth in capelin, *Mallotus villosus*, of the Labrador and Newfoundland areas. *Journal of Northwest Atlantic Fishery Science*, 3(2), pp.105-114.
- Weingartner, TJ. 1997. A review of the physical oceanography of the northeastern Chukchi Sea. *Fish ecology in Arctic North America. American Fisheries Society Symposium.*

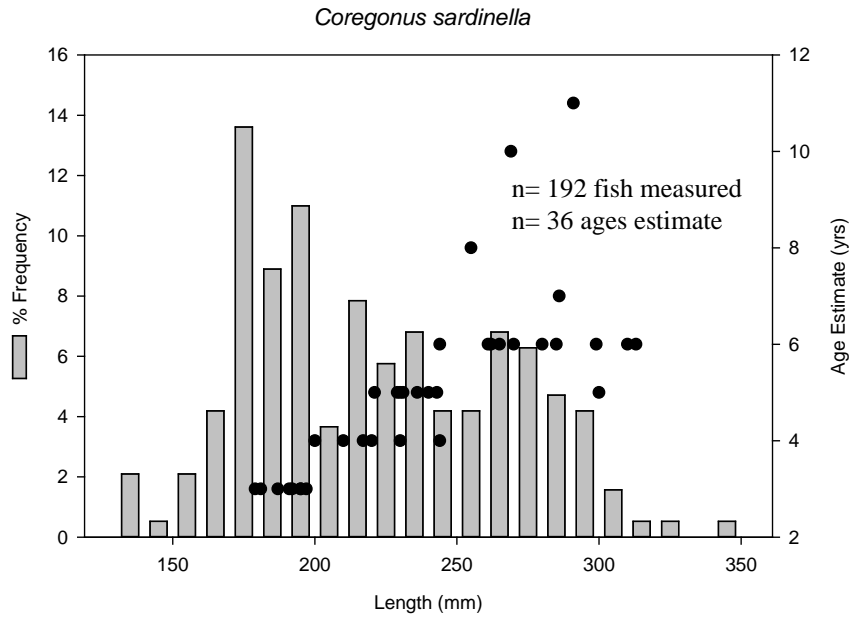


Figure 6.1 Salmonidae: *Coregonus sardinella* (Least Cisco). Length frequency and age frequency estimates with all collection areas included from ACES 2013-2014.

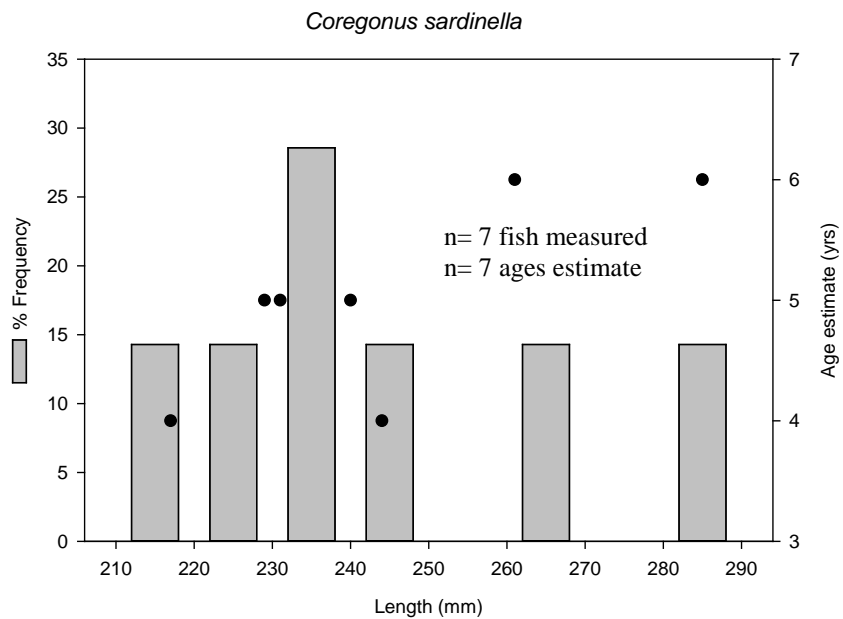


Figure 6.2 Salmonidae: *Coregonus sardinella* (Least Cisco). Length frequency and age frequency estimates, only Beaufort Sea collection areas included from ACES 2013-2014.

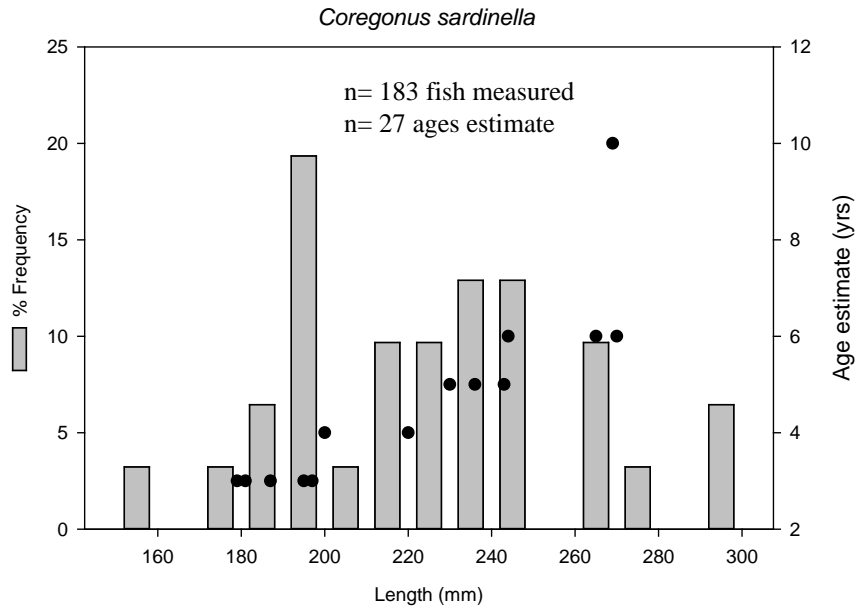


Figure 6.3 Salmonidae: *Coregonus sardinella* (Least Cisco). Length frequency and age frequency estimates, only Elson Lagoon collection areas included from ACES 2013-2014.

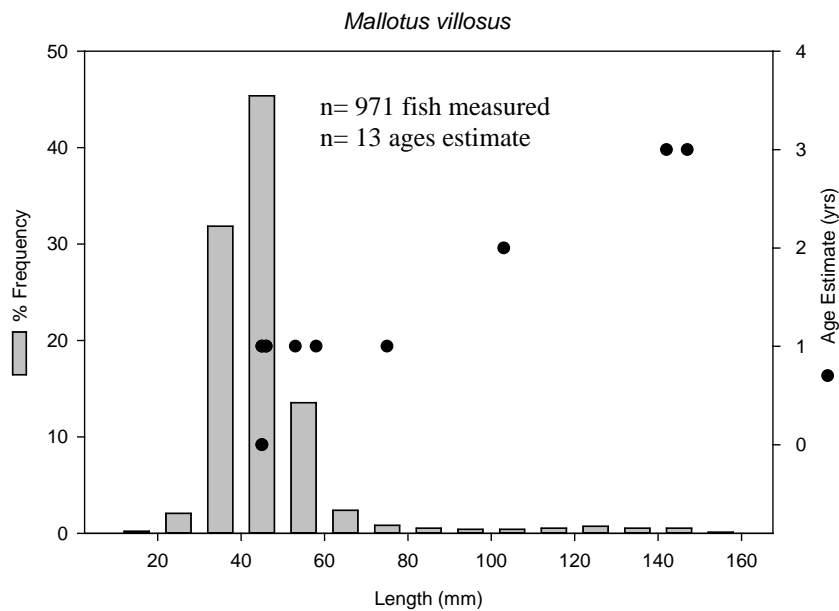


Figure 6.4 Osmeridae: *Mallotus villosus* (Capelin). Length frequency and age frequency estimates with all collection areas included from ACES 2013-2014.

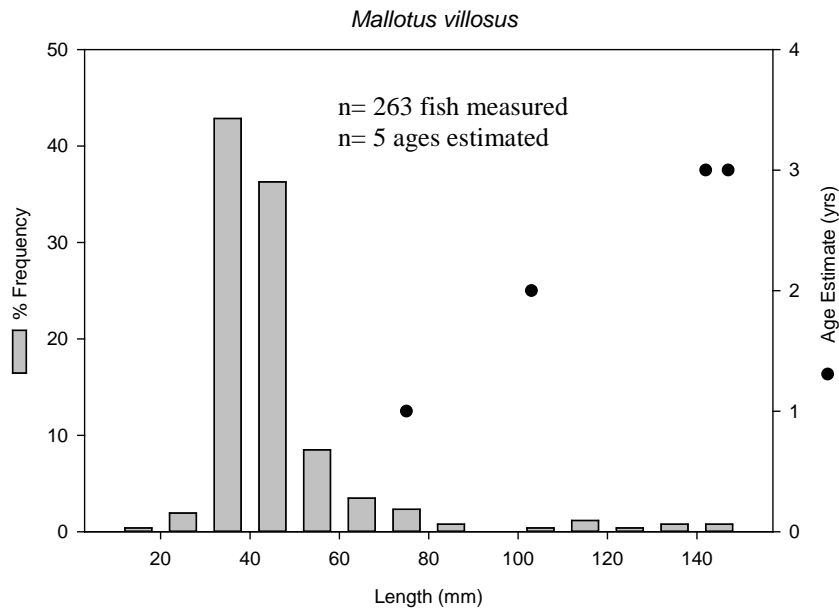


Figure 6.5 Osmeridae: *Mallotus villosus* (Capelin). Length frequency and age frequency estimates, only Chukchi Sea collection areas included from ACES 2013-2014.

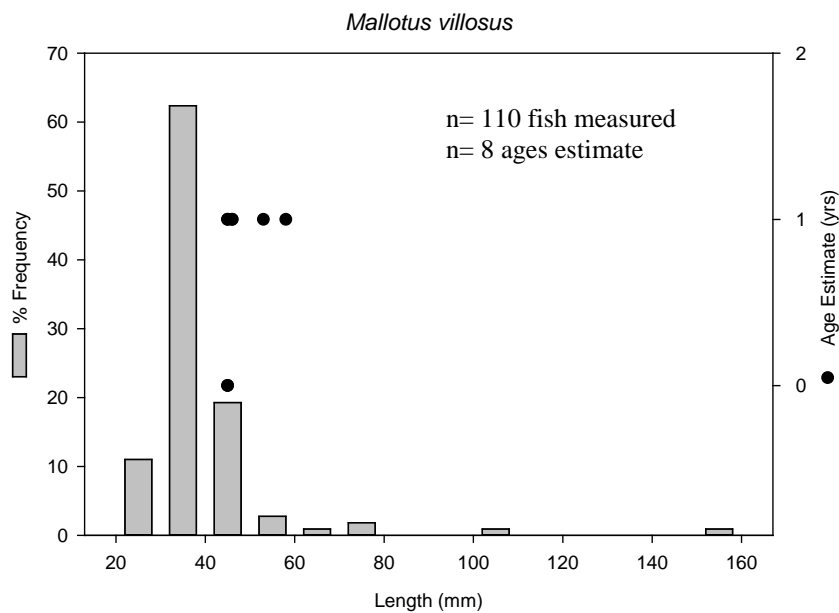


Figure 6.6 Osmeridae: *Mallotus villosus* (Capelin). Length frequency and age frequency estimates, only Beaufort Sea collection areas included from ACES 2013-2014.

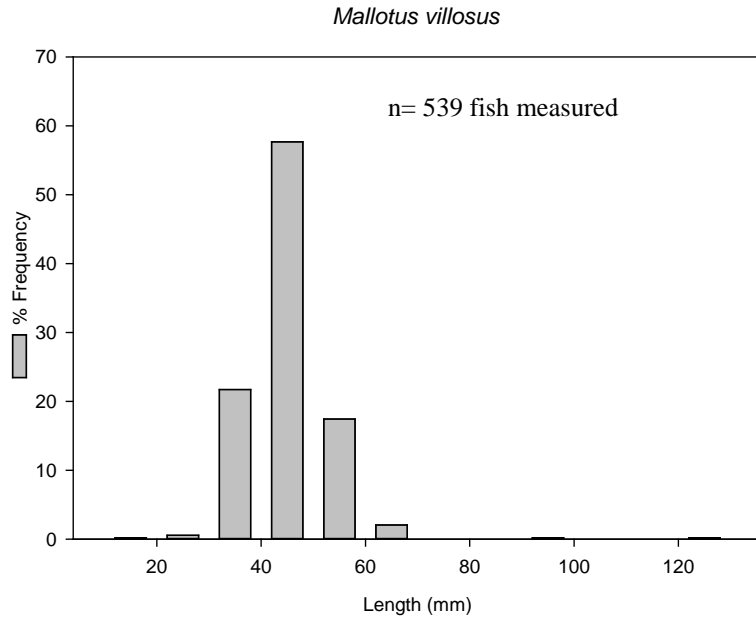


Figure 6.7 Osmeridae: *Mallotus villosus* (Capelin). Length frequency estimates, only Elson Lagoon collection areas included from ACES 2013-2014.

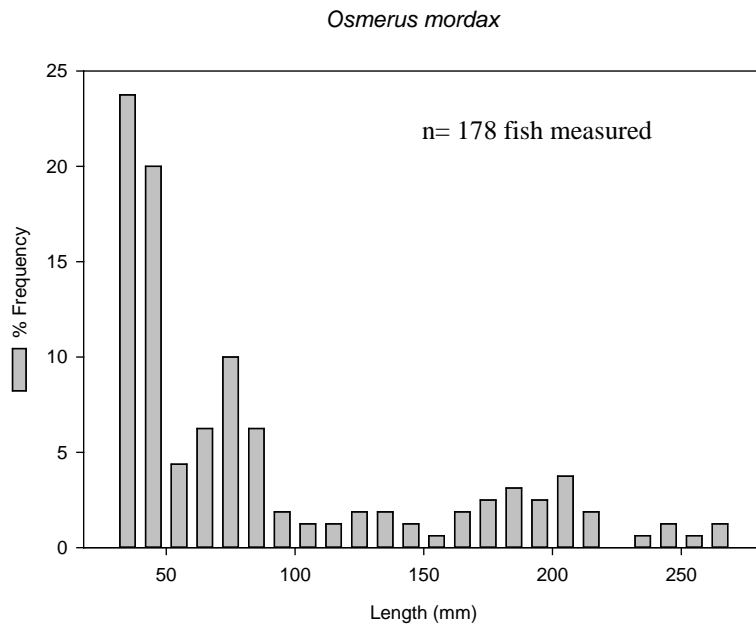


Figure 6.8 Osmeridae: *Osmerus mordax* (Rainbow Smelt). Length frequency estimates with all collection areas included from ACES 2013-2014.

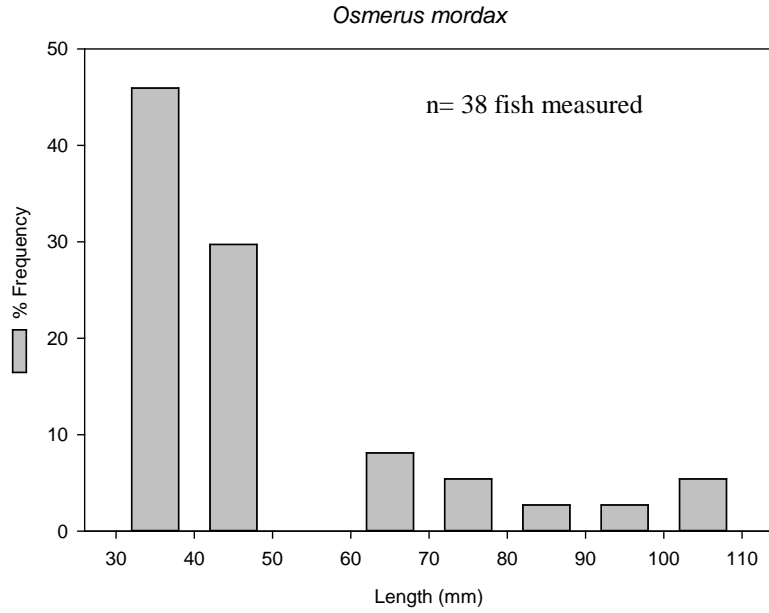


Figure 6.9 Osmeridae: *Osmerus mordax* (Rainbow Smelt). Length frequency estimates, only Chukchi Sea collection areas included from ACES 2013-2014.

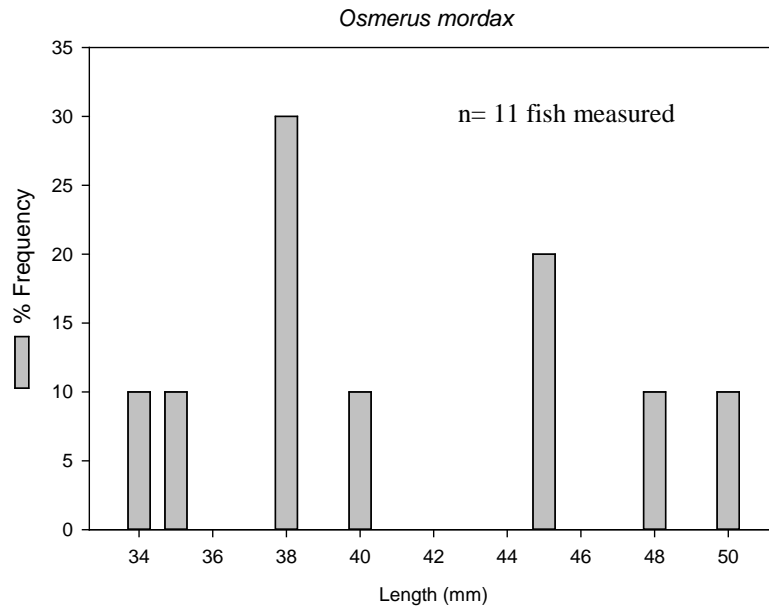


Figure 6.10 Osmeridae: *Osmerus mordax* (Rainbow Smelt). Length frequency estimates, only Beaufort Sea collection areas included from ACES 2013-2014.

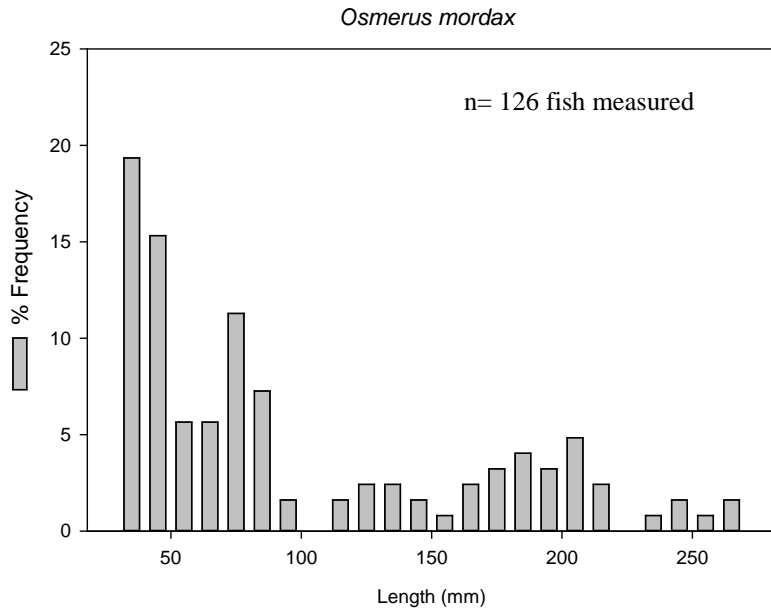


Figure 6.11 Osmeridae: *Osmerus mordax* (Rainbow Smelt). Length frequency estimates, only Elson Lagoon collection areas included from ACES 2013-2014.

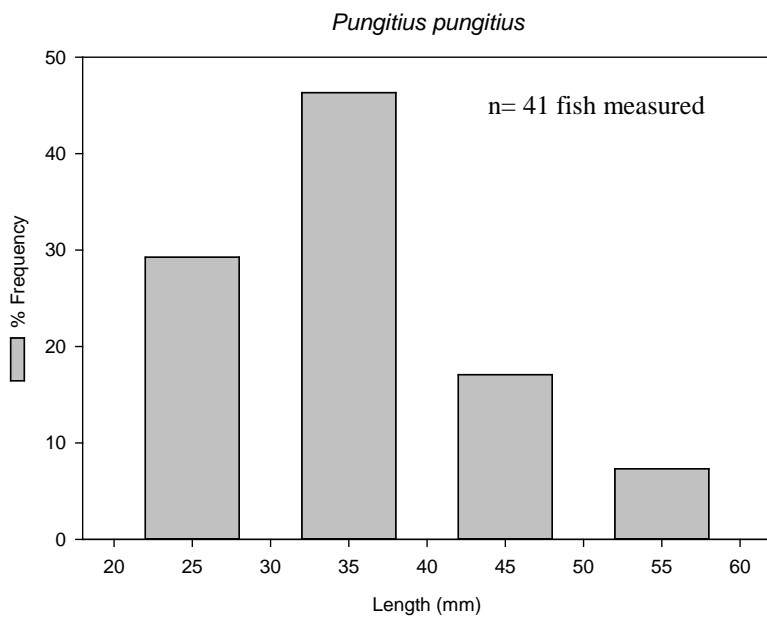


Figure 6.12 Gasterosteidae: *Pungitius pungitius* (Ninespine Stickleback). Length frequency estimates with all collection areas included from ACES 2013-2014.

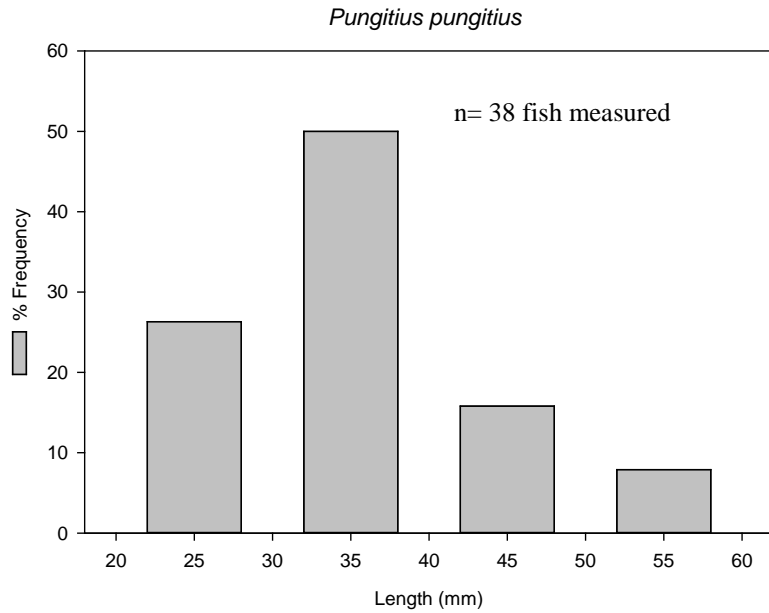


Figure 6.13 Gasterosteidae: *Pungitius pungitius* (Ninespine Stickleback). Length frequency estimates, only Chukchi Sea collection areas included from ACES 2013-2014.

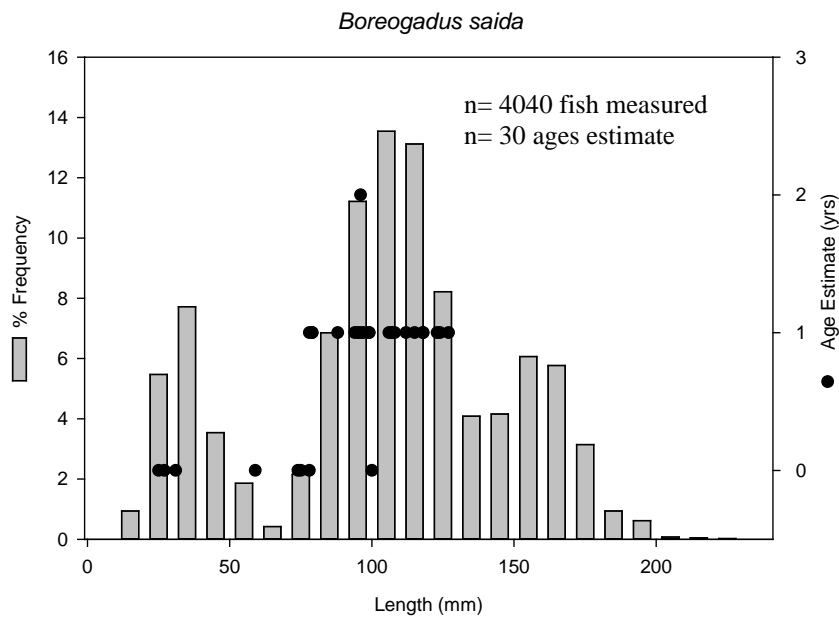


Figure 6.14 Gadidae: *Boreogadus saida* (Arctic Cod). Length frequency and age frequency estimates with all collection areas included from ACES 2013-2014 from ACES 2013-2014.

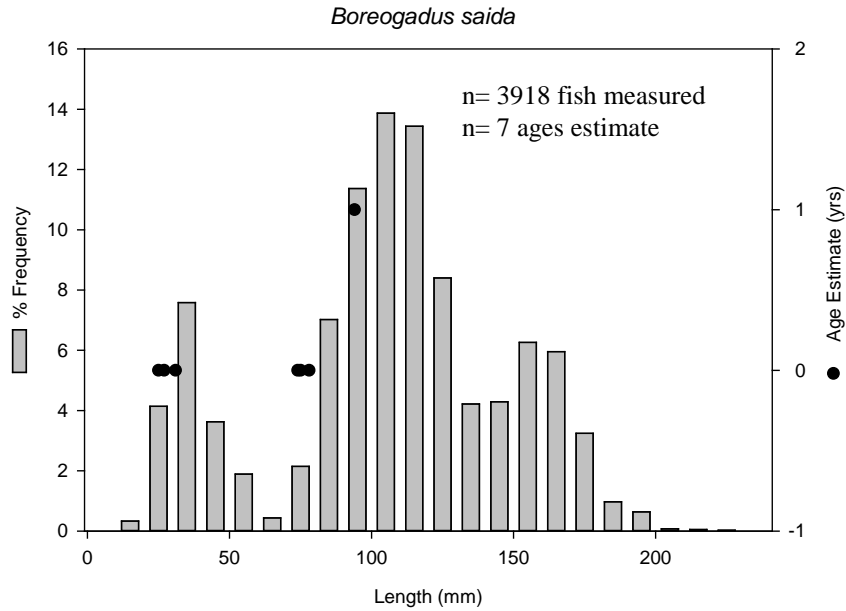


Figure 6.15 Gadidae: *Boreogadus saida* (Arctic Cod). Length frequency and age frequency estimates, only Chukchi Sea collection areas included from ACES 2013-2014.

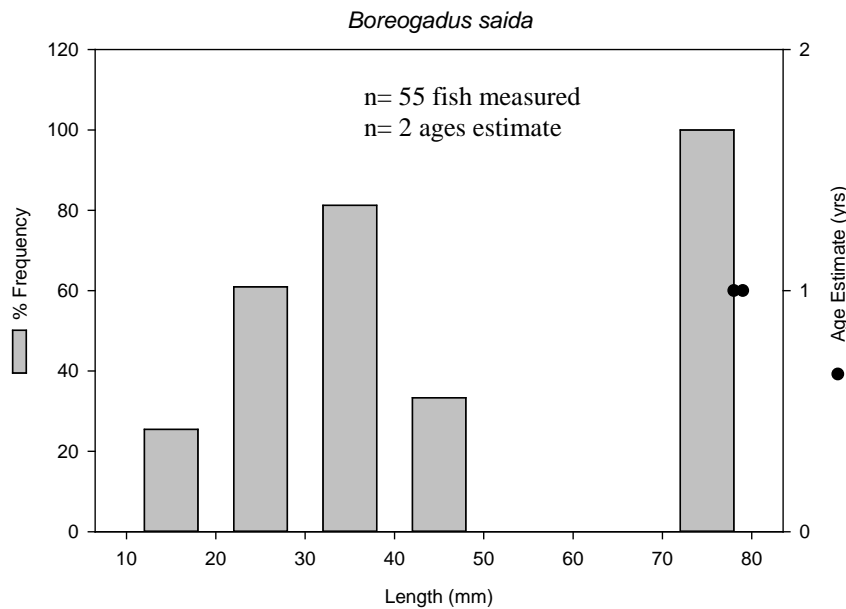


Figure 6.16 Gadidae: *Boreogadus saida* (Arctic Cod). Length frequency and age frequency estimates, only Beaufort Sea collection areas included from ACES 2013-2014.

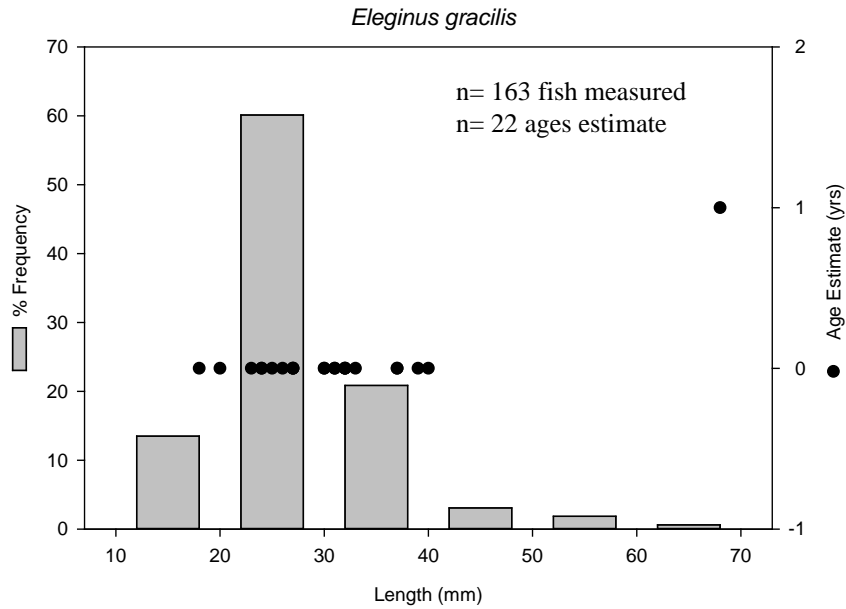


Figure 6.19 Gadidae: *Egleinus gracilis* (Saffron Cod). Length frequency and age frequency estimates, only Chukchi Sea collection areas included from ACES 2013-2014.

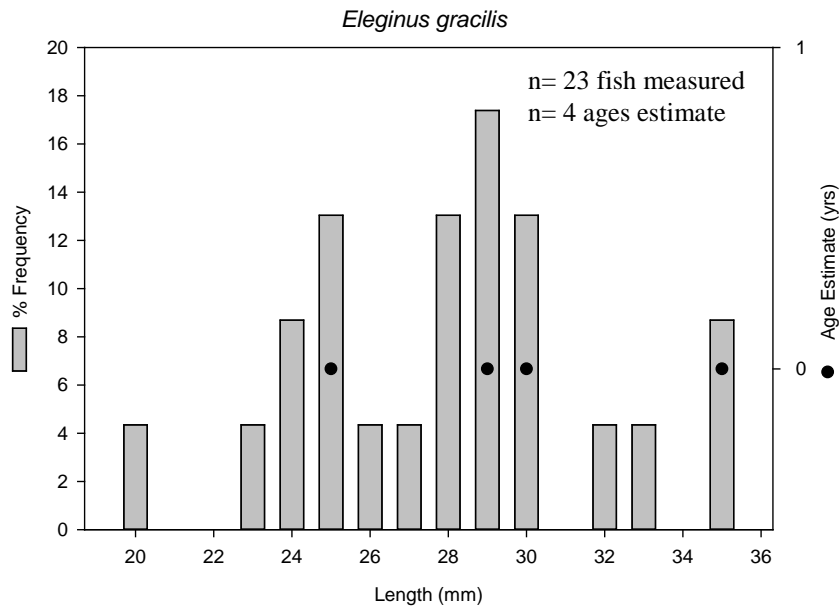


Figure 6.20 Gadidae: *Egleinus gracilis* (Saffron Cod). Length frequency and age frequency estimates, only Beaufort Sea collection areas included from ACES 2013-2014.

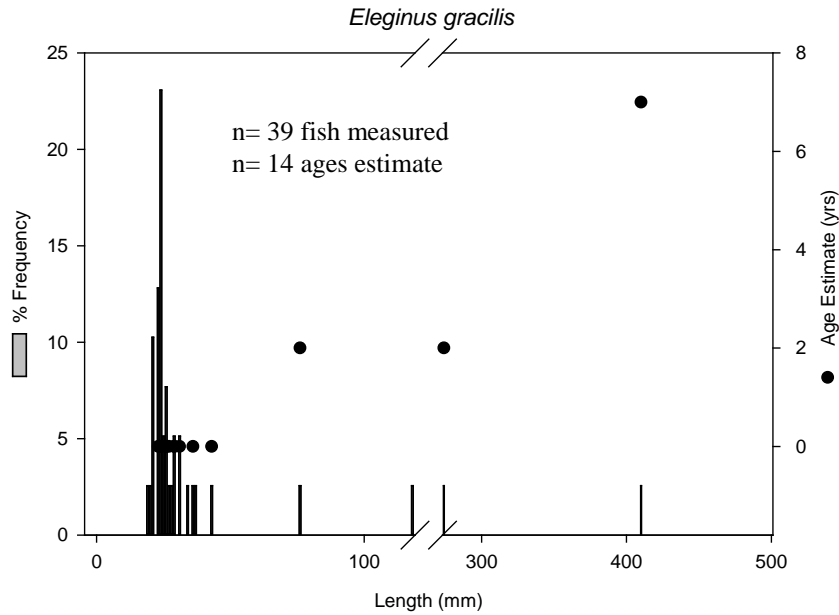


Figure 6.21 Gadidae *Eleginus gracilis* (Saffron Cod). Length frequency and age frequency estimates, only Elson Lagoon collection areas included ACES 2013-2014.

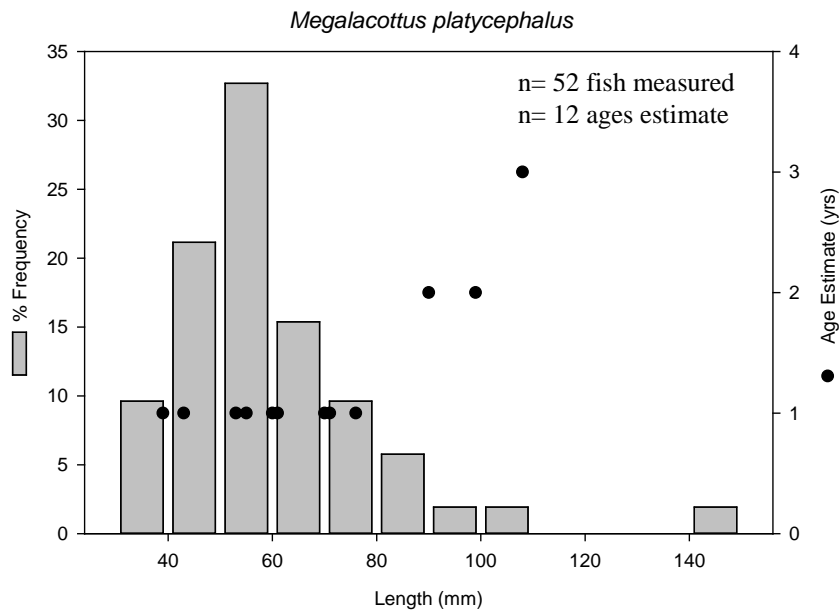


Figure 6.22 Cottidae: *Megalacottus platycephalus* (Belligerent sculpin). Length frequency and age frequency estimates with all collection areas included from ACES 2013-2014.

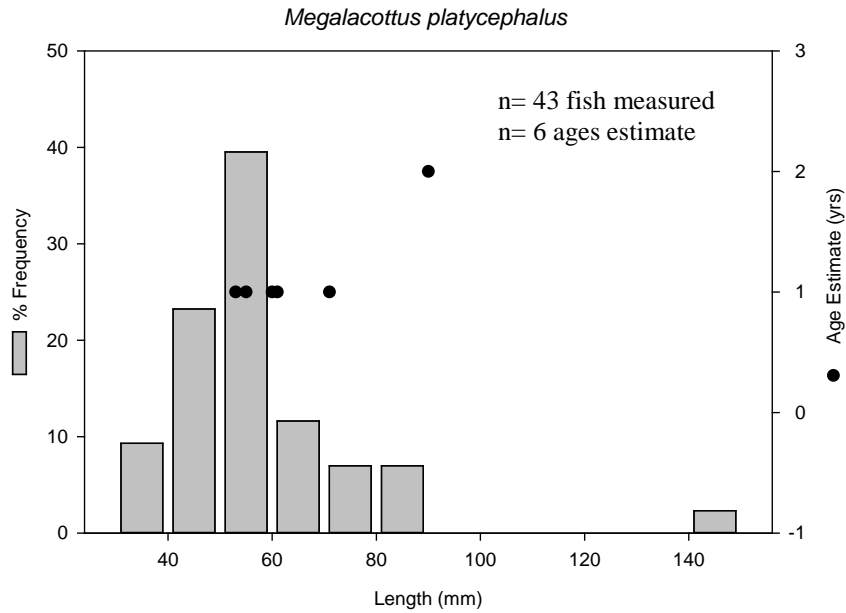


Figure 6.23 Cottidae: *Megalacottus platycephalus* (Belligerent sculpin). Length frequency and age frequency estimates, only Chukchi Sea collection areas included from ACES 2013-2014.

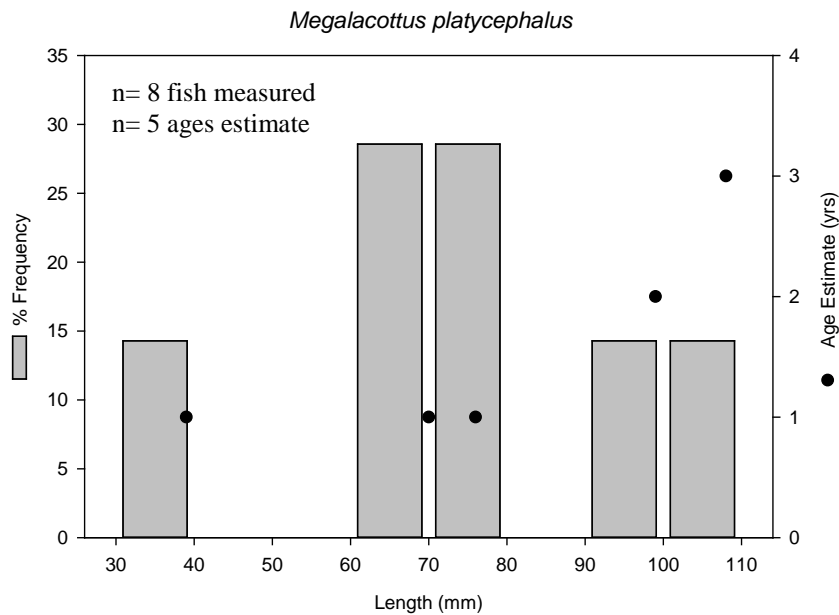


Figure 6.24 Cottidae: *Megalacottus platycephalus* (Belligerent sculpin). Length frequency and age frequency estimates, only Elson Lagoon collection areas included from ACES 2013-2014.

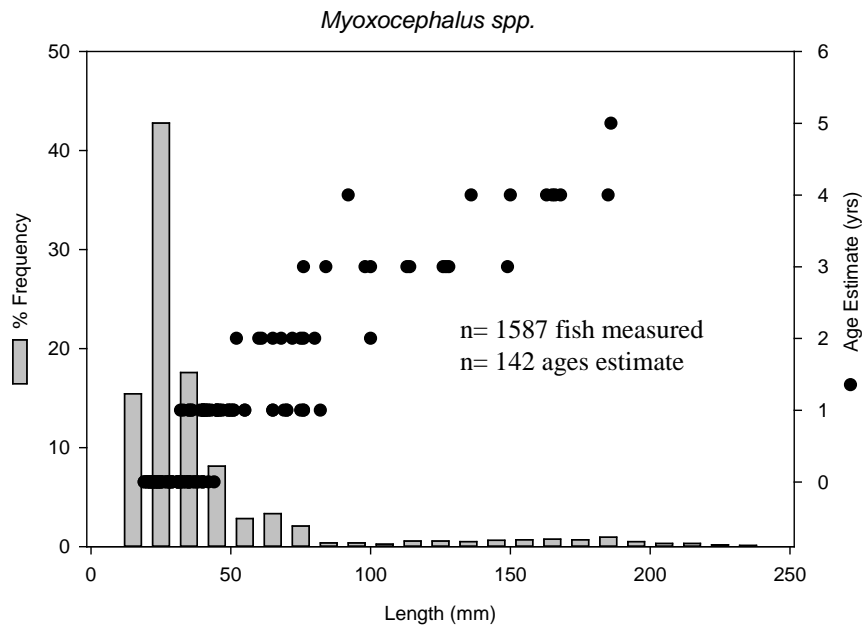


Figure 6.25 *Myoxocephalus spp.* (sculpin). Length frequency and age frequency estimates with all collection areas included from ACES 2013-2014.

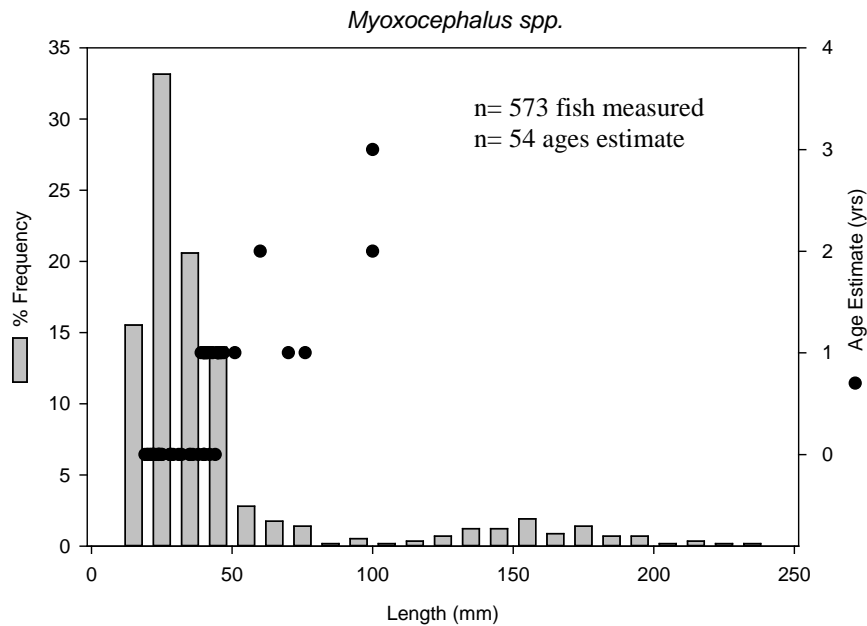


Figure 6.26 Cottidae: *Myoxocephalus spp.* (sculpin). Length frequency and age frequency estimates, only Chukchi Sea collection areas included from ACES 2013-2014.

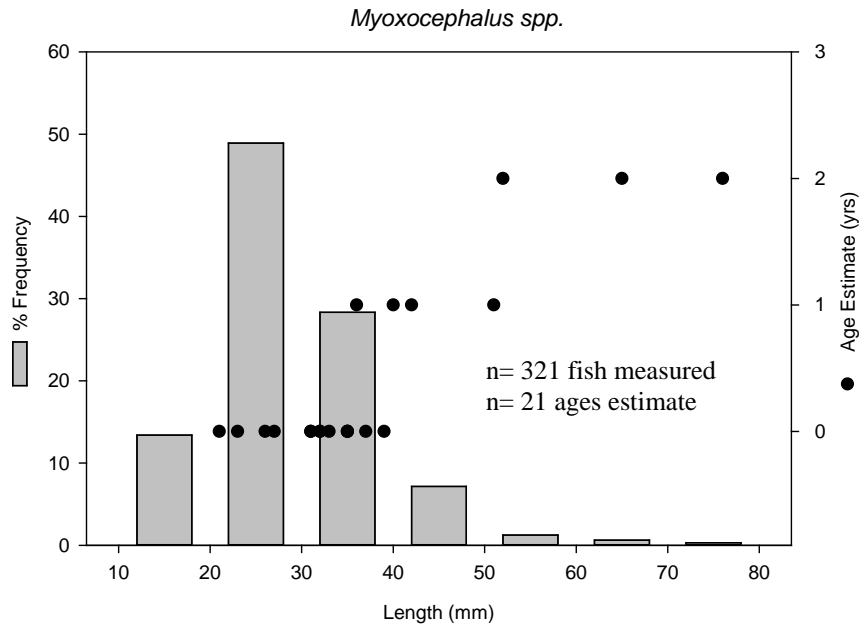


Figure 6.27 Cottidae: *Myoxocephalus* spp. (sculpin). Length frequency and age frequency estimates, only Beaufort Sea collection areas included from ACES 2013-2014.

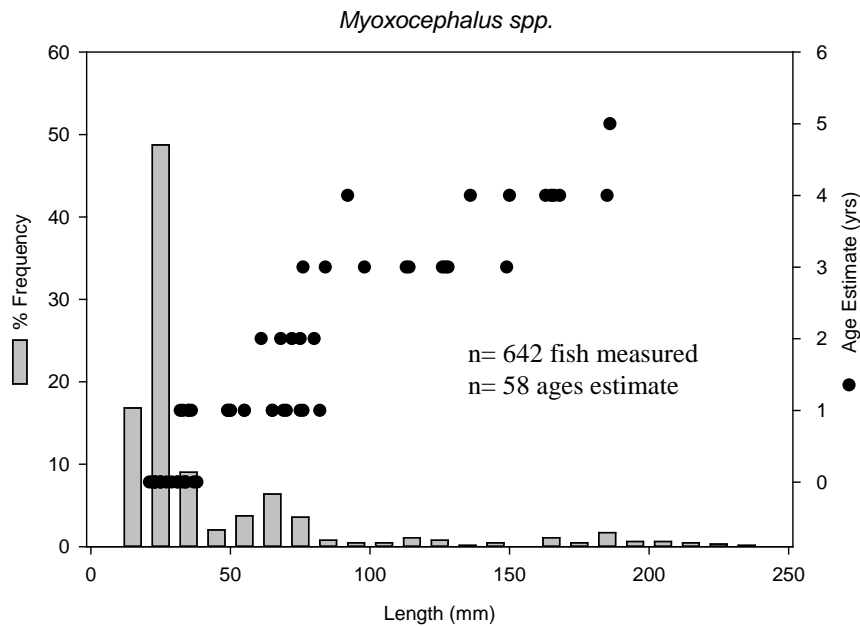


Figure 6.28 Cottidae: *Myoxocephalus* spp. (sculpin). Length frequency and age frequency estimates, only Elson Lagoon collection areas included from ACES 2013-2014.

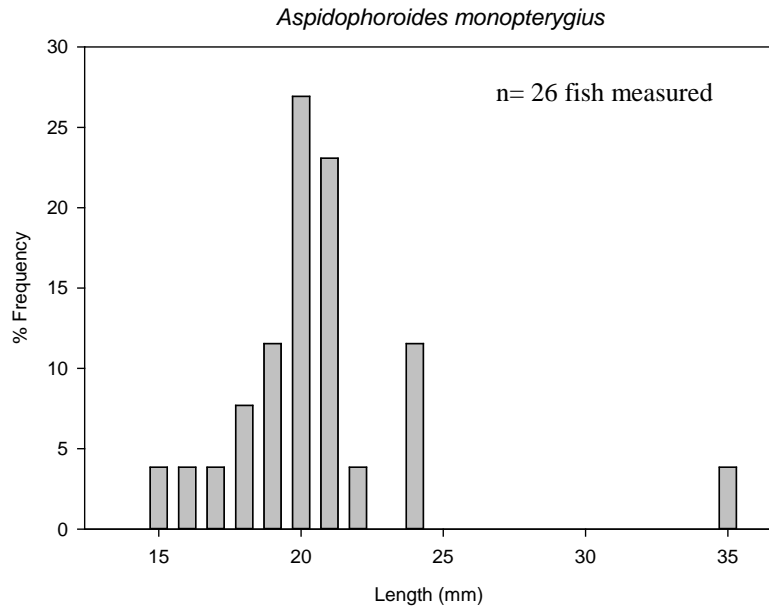


Figure 6.29 Agonidae: *Aspidothoroides monopterygius* (Alligatorfish). Length frequency estimates with all collection areas included from ACES 2013-2014.

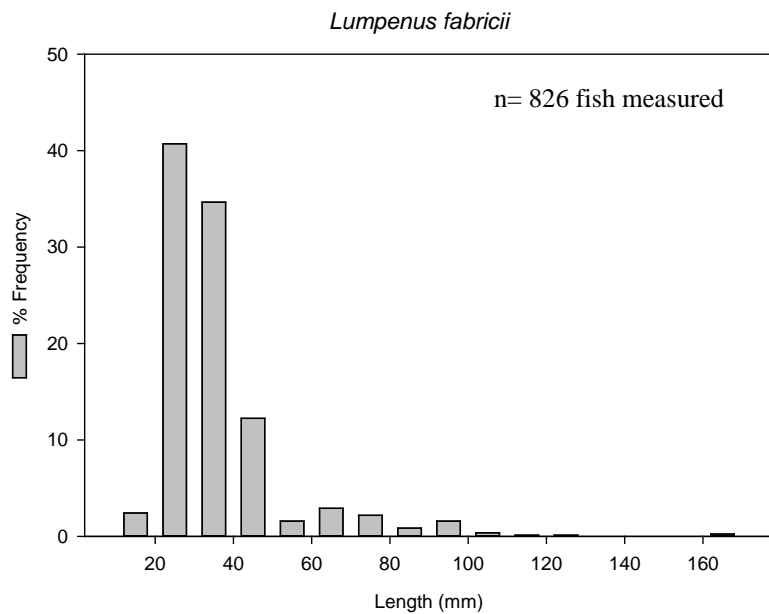


Figure 6.30 Stichaeidae: *Lumpenus fabricii* (Slender eelblenny). Length frequency estimates with all collection areas included from ACES 2013-2014.

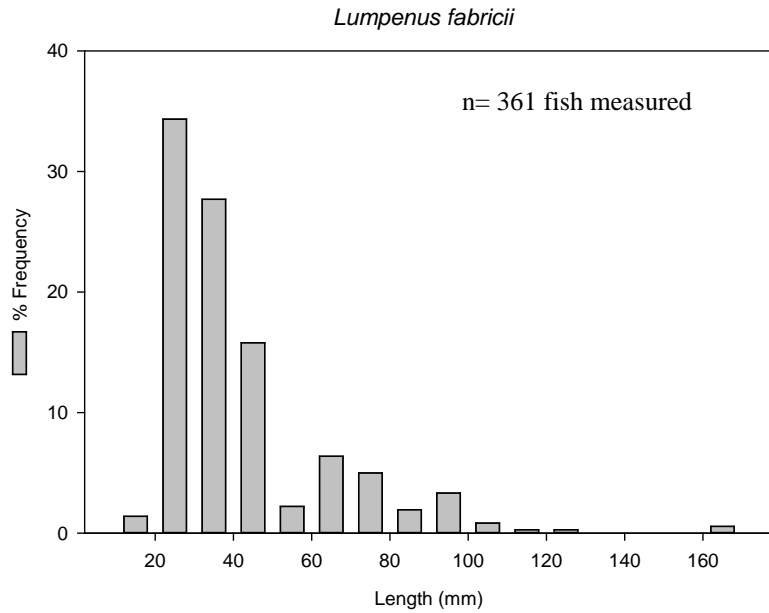


Figure 6.31 Stichaеidae: *Lumpenus fabricii* (Slender eelblenny). Length frequency estimates, only Chukchi Sea collection areas included from ACES 2013-2014.

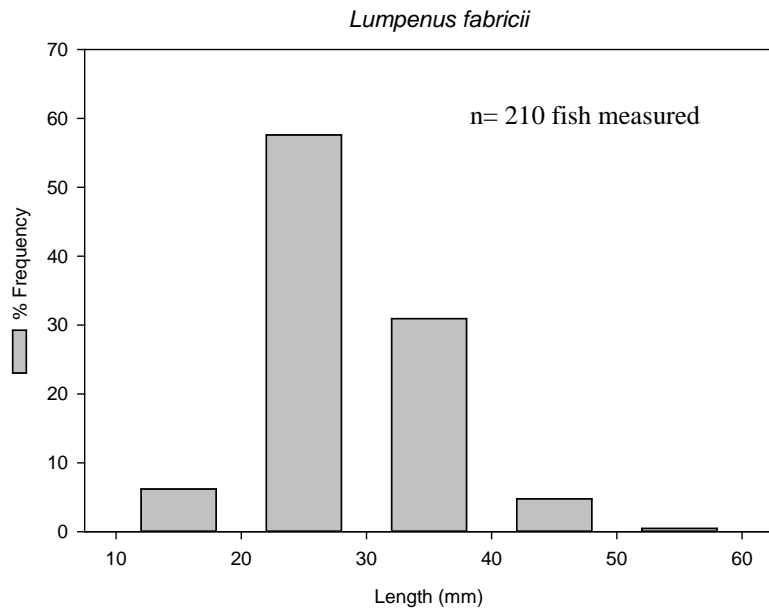


Figure 6.32 Stichaеidae: *Lumpenus fabricii* (Slender eelblenny). Length frequency estimates, only Beaufort Sea collection areas included from ACES 2013-2014.

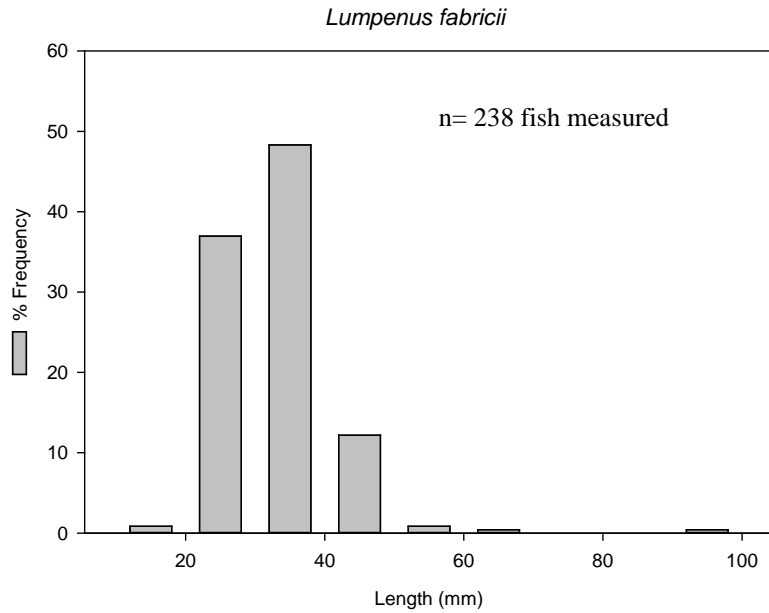


Figure 6.33 Stichaеidae: *Lumpenus fabricii* (Slender eelblenny). Length frequency estimates, only Elson Lagoon collection areas included from ACES 2013-2014.

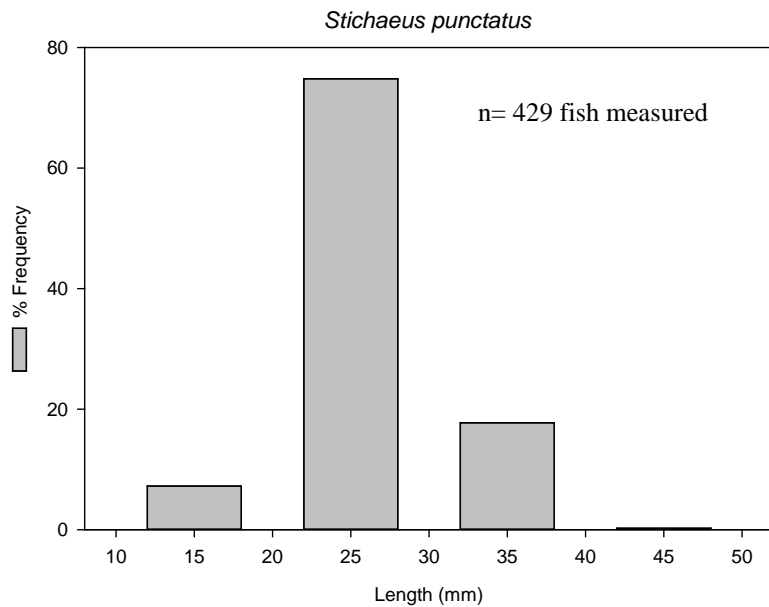


Figure 6.34 Stichaеidae: *Stichaeus punctatus* (Arctic Shanny). Length frequency estimates with all collection areas included from ACES 2013-2014.

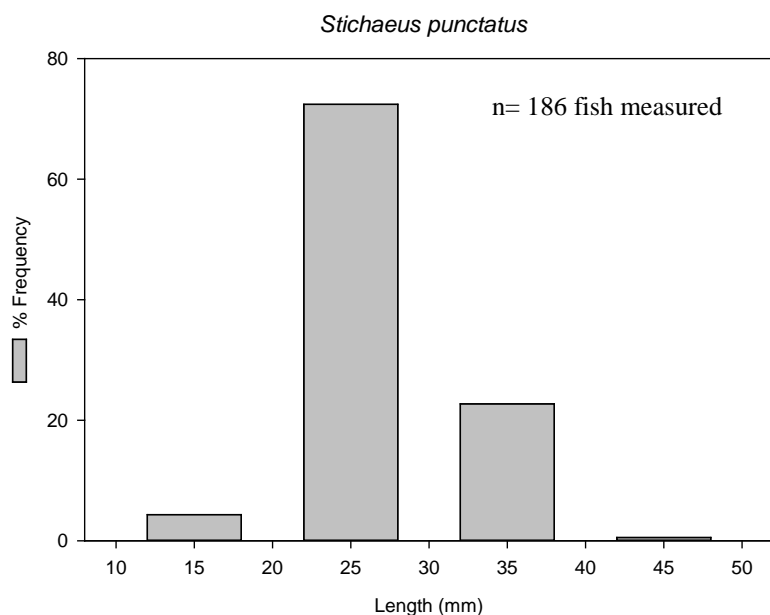


Figure 6.35 Stichaeidae: *Stichaeus punctatus* (Arctic Shanny). Length frequency estimates, only Chukchi Sea collection areas included from ACES 2013-2014.

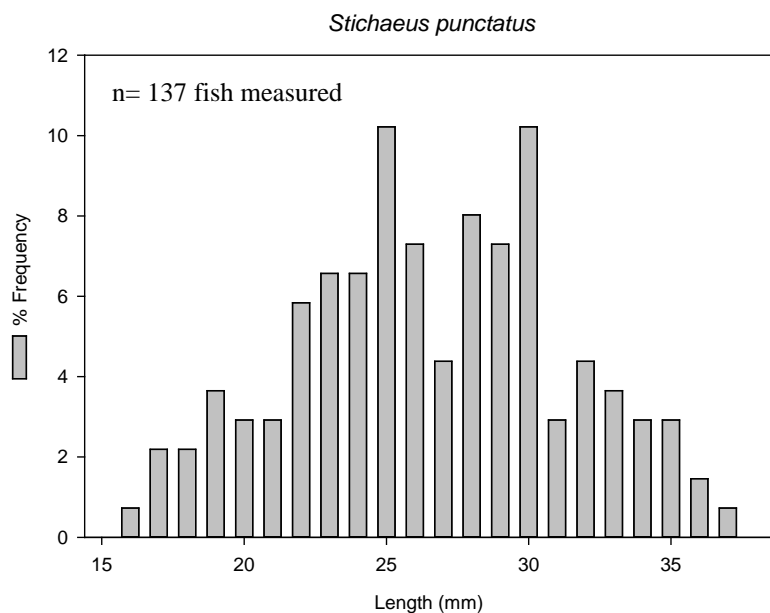


Figure 6.36 Stichaeidae: *Stichaeus punctatus* (Arctic Shanny). Length frequency estimates, only Beaufort Sea collection areas included from ACES 2013-2014.

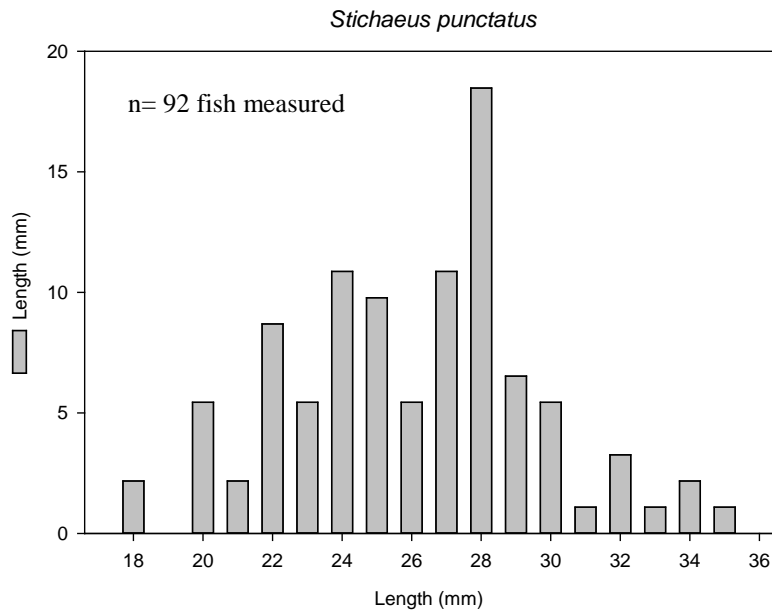


Figure 6.37 Stichaeidae: *Stichaeus punctatus* (Arctic Shanny). Length frequency estimates, only Elson Lagoon collection areas included from ACES 2013-2014.

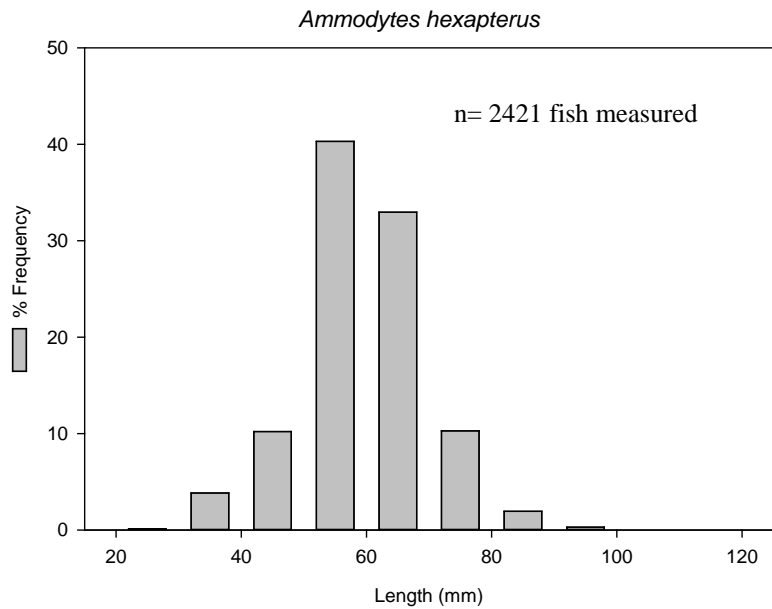


Figure 6.38 Ammodytidae: *Ammodytes hexapterus* (Pacific Sand Lance). Length frequency estimates with all collection areas included from ACES 2013-2014.

Ammodytes hexapterus

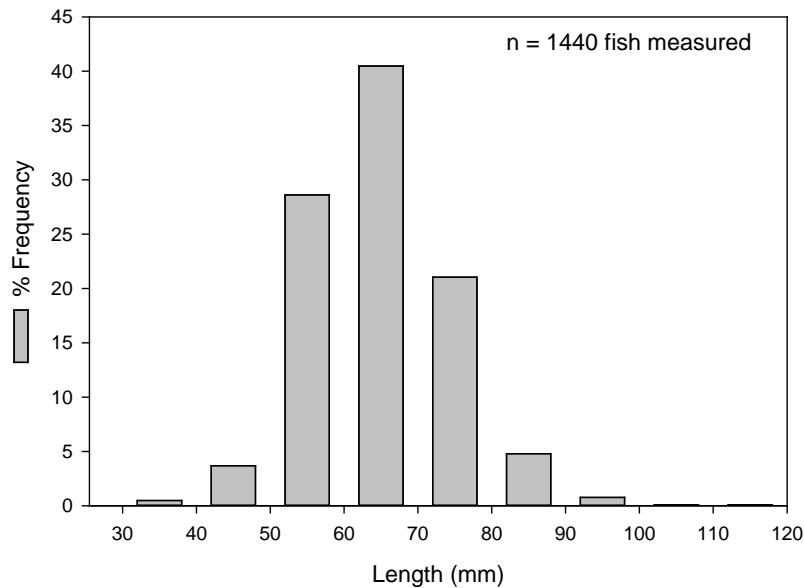


Figure 6.39 Ammodytidae: *Ammodytes hexapterus* (Pacific Sand Lance). Length frequency estimates, only Chukchi Sea collection areas included from ACES 2013-2014.

Ammodytes hexapterus

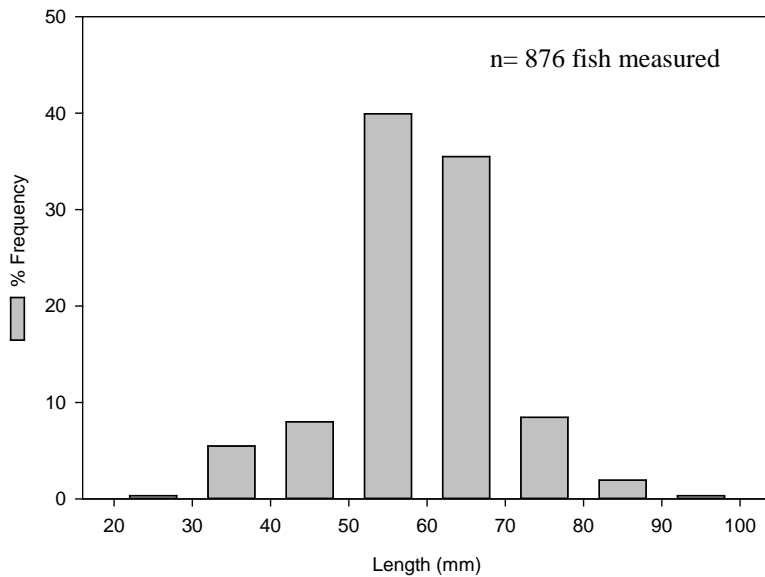


Figure 6.40 Ammodytidae: *Ammodytes hexapterus* (Pacific Sand Lance). Length frequency estimates, only Beaufort Sea collection areas included from ACES 2013-2014.

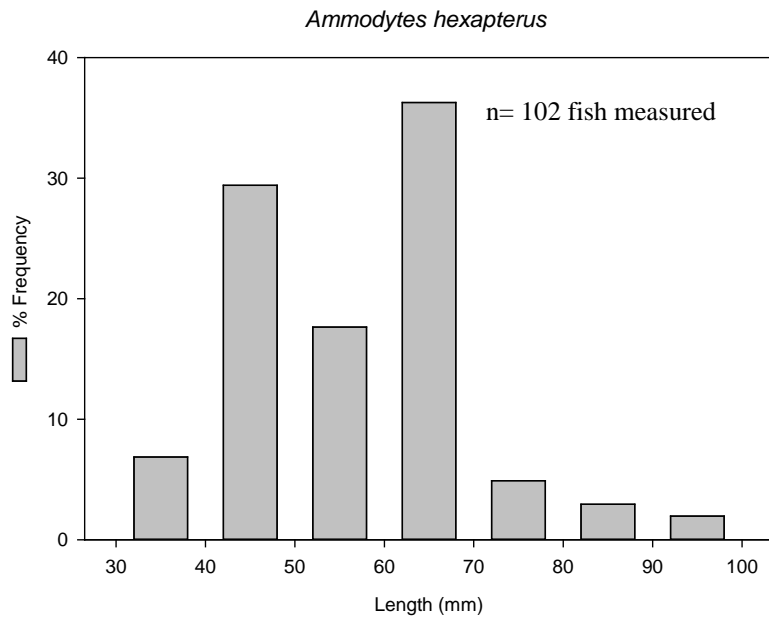


Figure 6.41 Ammodytidae: *Ammodytes hexapterus* (Pacific Sand Lance). Length frequency estimates only Elson Lagoon collection areas included from ACES 2013-2014.

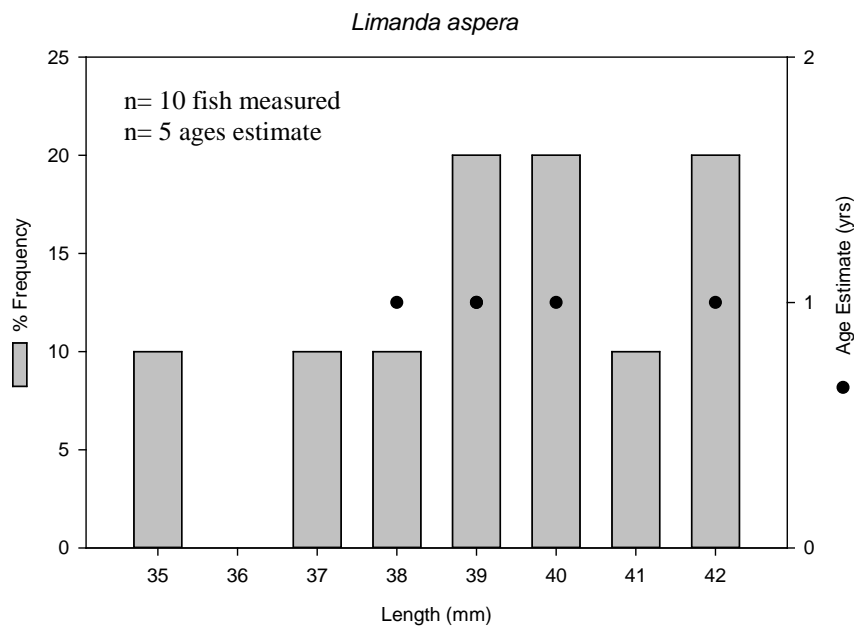


Figure 6.42 Pleuronectidae: *Limanda aspera* (Yellowfin sole). Length frequency and age frequency estimates with all collection areas included from ACES 2013-2014.

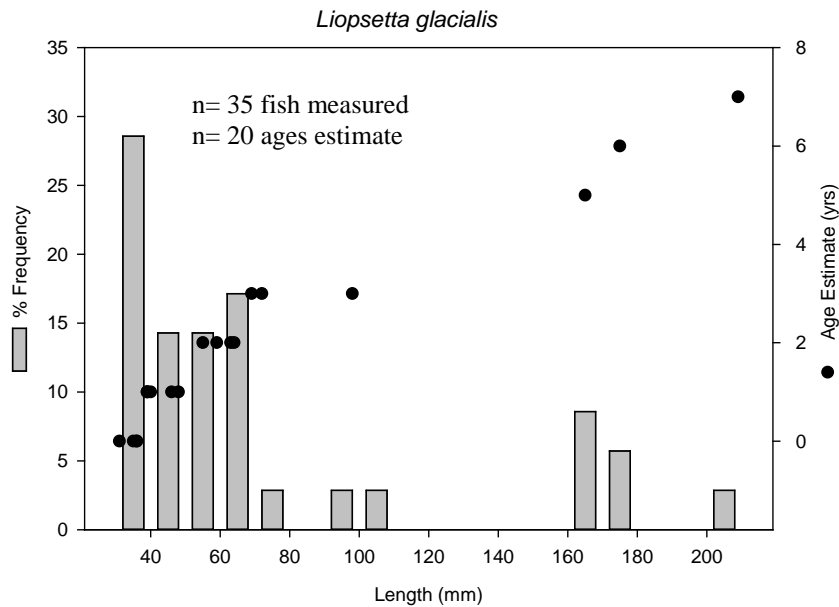


Figure 6.43 Pleuronectidae: *Liopsetta glacialis* (Arctic Flounder). Length frequency and age frequency estimates with all collection areas included from ACES 2013-2014.

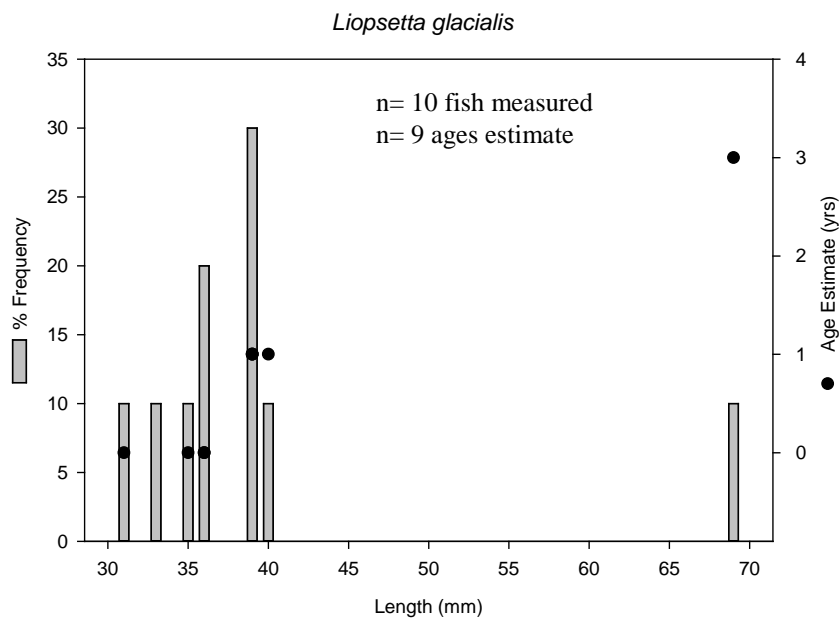


Figure 6.44 Pleuronectidae: *Liopsetta glacialis* (Arctic Flounder). Length frequency and age frequency estimates, only Chukchi Sea collection areas included from ACES 2013-2014.

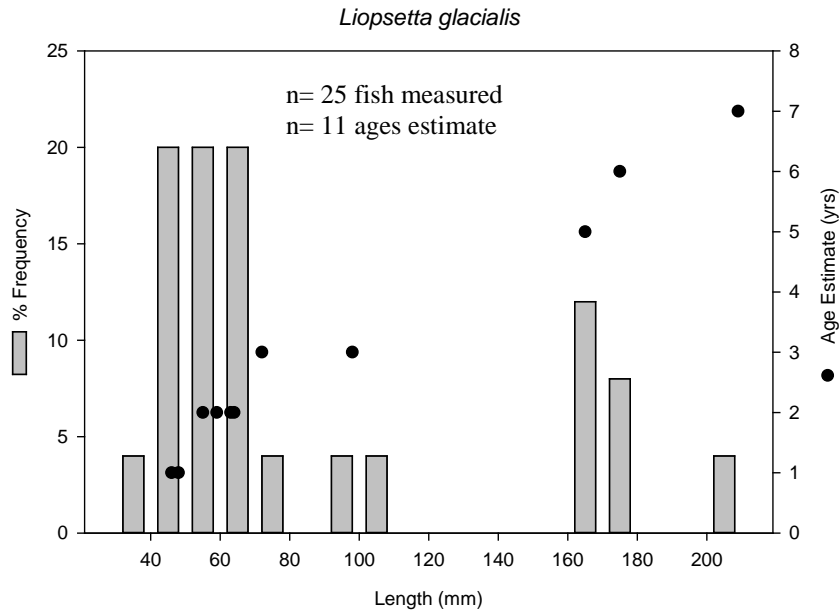


Figure 6.45 Pleuronectidae: *Liopsetta glacialis* (Arctic Flounder). Length frequency and age frequency estimates, only Elson Lagoon collection areas included from ACES 2013-2014.

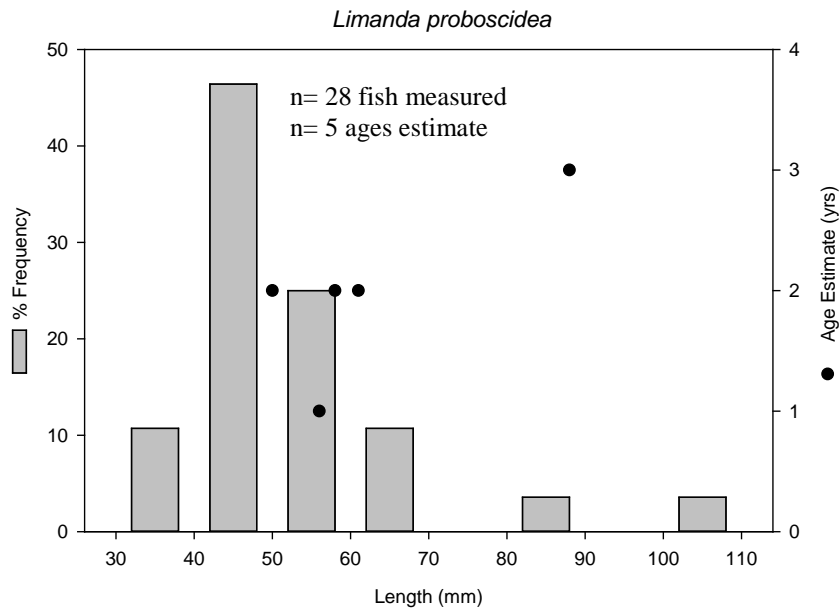


Figure 6.46 Pleuronectidae: *Limanda proboscidea* (Longhead dab). Length frequency and age frequency estimates with all collection areas included from ACES 2013-2014.

Table 6.1 Number of species or genera measured in the laboratory by region (Chukchi Sea, Beaufort Sea, Elson Lagoon) or without a known station location for ACES 2013-2014. Fish species are listed in phylogenetic order.

Species	All	Chukchi	Beaufort	Elson	Missing Station ID
<i>Coregonus sardinella</i>	192	0	7	183	2
<i>Mallotus villosus</i>	971	263	110	539	59
<i>Osmerus mordax</i>	178	38	11	126	3
<i>Pungitius pungitius</i>	41	38	0	0	3
<i>Boreogadus saida</i>	4040	3918	55	27	40
<i>Eleginus gracilis</i>	230	163	23	39	5
<i>Megalocottus platycephalus</i>	52	43	0	0	9
<i>Myoxocephalus spp.</i>	1587	573	321	642	51
<i>Aspidophoroides monopterygius</i>	26	0	0	0	26
<i>Lumpenus fabricii</i>	826	361	210	238	17
<i>Stichaeus punctatus</i>	429	186	137	92	14
<i>Ammodytes hexapterus</i>	2421	1440	876	102	3
<i>Limanda aspera</i>	10	0	0	0	10
<i>Limanda proboscidea</i>	27	27	0	0	0
<i>Liopsetta glacialis</i>	35	10	0	25	0
Total	11065	7060	1750	2013	242

Table 6.2 Length-weight relationships for 14 species and one genus. The total includes those individuals measured but for which the collection region was unknown in addition to the three regions. Columns indicate number of fish weight (n), weight range, length range, the length-weight growth equation ($W = a L^{-b}$). Fish species are listed in phylogenetic order.

Species	n	Weight range (g)	Length range (mm)	$a * 10^{-5}$	b	r ²
Salmonidae						
<i>Coregonus sardinella</i>	47	75.89 - 309.28	159 - 313	0.021	3.67	0.93
Beaufort	7	75.89 - 172.54	217 - 285	0.125	3.33	0.86
Elson Lagoon	38	25.44 - 309.28	159 - 313	0.033	3.58	0.94
Osmeridae						
<i>Mallotus villosus</i>	314	0.04 - 11.58	28 - 125	0.009	3.86	0.97
Beaufort	18	0.07 - 6.10	31 - 102	0.006	3.98	0.99
Chukchi	72	0.09 - 3.21	37 - 81	0.001	4.47	0.95
Elson Lagoon	218	0.04 - 11.58	28 - 125	0.005	3.96	0.98
<i>Osmerus mordax</i>	111	0.06 - 115.54	24 - 262	1.024	2.90	0.96
Beaufort	6	0.09 - 0.22	34 - 40	0.001	4.69	0.68
Elson Lagoon	98	0.06 - 115.54	31 - 262	1.033	2.90	0.96
Gasterosteidae						
<i>Pungitius pungitius</i>	19	0.09 - 0.95	27 - 53	0.900	2.86	0.84
Chukchi	18	0.11 - 0.95	27 - 53	1.018	2.83	0.83
Gadidae						
<i>Boreogadus saida</i>	139	0.01 - 12.57	12 - 127	0.707	2.95	0.99
Beaufort	45	0.02 - 3.34	14 - 79	0.116	3.40	0.99
Chukchi	29	0.02 - 4.63	17 - 94	1.797	2.75	0.99
Elson Lagoon	26	0.01 - 12.57	12 - 127	0.517	3.02	0.99
<i>Eleginus gracilis</i>	101	0.01 - 181.97	18 - 274	0.081	3.43	1.00
Beaufort	6	0.04 - 0.27	20 - 33	2.417	2.59	0.66
Chukchi	59	0.02 - 2.01	18 - 68	0.055	3.58	0.99
Elson Lagoon	32	0.01 - 181.97	19 - 274	1.129	2.95	1.00
Cottidae						
<i>Megalocottus platycephalus</i>	34	0.71 - 10.47	39 - 108	0.0003	2.25	0.88
Chukchi	27	1.03 - 10.47	44 - 90	0.928	3.09	0.97
Elson Lagoon	6	0.86 - 9.83	39 - 108	0.0002	2.36	0.96
<i>Myoxocephalus</i> spp.	416	0.01 - 84.87	15 - 230	2.311	2.80	0.97
Beaufort	46	0.04 - 1.81	19 - 60	4.872	2.58	0.91
Chukchi	172	0.01 - 9.69	15 - 100	1.800	2.85	0.96
Elson Lagoon	147	0.04 - 84.87	18 - 230	2.393	2.79	0.97
Agonidae						
<i>Aspidophoroides monopterygius</i>	10	0.01 - 0.02	15 - 24	0.818	2.48	0.69

Stichaeidae						
<i>Lumpenus fabricii</i>	252	0.01 - 0.91	20 - 91	0.024	3.53	0.98
Beaufort	75	0.01 - 0.19	22 - 47	0.046	3.34	0.92
Chukchi	86	0.01 - 1.06	20 - 75	0.012	3.71	0.98
Elson Lagoon	75	0.02 - 1.92	26 - 91	0.029	3.48	0.99
<i>Stichaeus punctatus</i>	202	0.01 - 0.73	15 - 37	0.025	3.83	0.45
Beaufort	64	0.01 - 0.21	17 - 35	0.009	4.23	0.87
Chukchi	86	0.01 - 0.73	15 - 37	0.212	3.22	0.25
Elson Lagoon	37	0.02 - 0.18	20 - 34	0.012	4.01	0.90
Ammodytidae						
<i>Ammodytes hexapterus</i>	1599	0.02 - 4.36	24 - 115	0.084	3.28	0.94
Beaufort	606	0.22 - 2.69	24 - 100	0.102	3.23	0.92
Chukchi	926	0.05 - 4.36	33 - 115	0.076	3.30	0.95
Elson Lagoon	64	0.07 - 2.01	36 - 91	0.046	3.39	0.97
Pleuronectidae						
<i>Limanda aspera</i>	10	0.32 - 0.61	35 - 42	7.259	2.41	0.73
<i>Limanda proboscidea</i>	7	1.29 - 6.08	50 - 88	2.947	2.73	0.99
Chukchi	6	1.29 - 6.08	50 - 88	2.918	2.73	0.99
<i>Liopsetta glacialis</i>	9	1.19 - 129.69	48 - 209	0.944	3.08	0.99

Table 6.3 Number of species or genus (denoted with *) estimated for age in the laboratory by region (Chukchi Sea, Beaufort Sea, Elson Lagoon) or without a known station location for ACES 2013-2014. Fish species are listed in phylogenetic order.

Species	Aged	Chukchi	Beaufort	Elson	Missing Station ID
<i>Coregonus sardinella</i>	36	0	7	27	2
<i>Mallotus villosus</i>	13	5	8	0	0
<i>Osmerus mordax</i>	0	0	0	0	0
<i>Pungitius pungitius</i>	0	0	0	0	0
<i>Boreogadus saida</i>	30	7	2	17	4
<i>Eleginus gracilis</i>	46	22	4	14	6
<i>Megalocottus platycephalus</i>	12	6	0	5	1
* <i>Myoxocephalus spp.</i>	142	54	21	58	9
<i>Aspidophoroides monopterygius</i>	0	0	0	0	0
<i>Lumpenus fabricii</i>	0	0	0	0	0
<i>Stichaeus punctatus</i>	0	0	0	0	0
<i>Ammodytes hexapterus</i>	0	0	0	0	0
<i>Limanda aspera</i>	5	0	0	0	5
<i>Limanda proboscidea</i>	5	4	0	0	1
<i>Liopsetta glacialis</i>	20	9	0	11	0
Total	309	107	42	132	28

7.0 Fish Diets

B. Gray, B. Norcross

7.1 Introduction

We examined the diets of eight fish species and one fish genus captured in the ACES study area: Least Cisco (*Coregonus sardinella*), Capelin (*Mallotus villosus*), Rainbow Smelt (*Osmerus mordax*), Arctic Cod (*Boreogadus saida*), Saffron Cod (*Eleginus gracilis*), Sculpins (*Myoxocephalus* spp.), Slender Eelblenny (*Lumpenus fabricii*), Arctic Shanny (*Stichaeus punctatus*), and Pacific Sand Lance (*Ammodytes hexapterus*). All are documented as important links between lower trophic level prey, such as pelagic zooplankton, benthic crustaceans, and insects (Table 7.1), and higher trophic level predators such as marine mammals, seabirds, and other fishes (Table 7.2). Each species' diet within the ACES study area is expected to vary from descriptions in Table 7.1 somewhat, given that their diets likely vary across spatial gradients. Note that because there are difficulties identifying some sculpins to species, all diets of *Myoxocephalus* sculpins were analyzed as together.

The goals of this research are to examine both inter- and intraspecific diet variability among these nine fish species within the ACES study area. This is accomplished through 1) a complete characterization of each species' diet, 2) an interspecific diet comparison using permutational multivariate analysis of variance (PERMANOVA) and nonmetric multidimensional scaling (nMDS), and 3) an intraspecific diet comparison using PERMANOVA. Interspecific diet variability is expected because there are documented differences in species' diets (Table 7.1). Intraspecific diet variability could arise in a multitude of ways; here we consider biological and spatial factors. Change in fish length is a biological example. As fishes grow larger, their diets typically change (Werner and Hall 1974; Labropoulou and Eleftheriou 1997). Differences among the three study regions (i.e., Beaufort Sea, Chukchi Sea, and Elson Lagoon) are examples of spatial processes that likely influence the distribution of these fishes' prey. Examining both inter- and intraspecific sources of diet variability offers a comprehensive account of these fishes' food habits and advances knowledge of lesser-known fishes in Arctic food webs.

7.2 Methods

7.2.1 Laboratory methods

All fishes were measured to the nearest 1 mm and stomachs (i.e., esophagus to pyloric valve) were removed, placed in petri dishes, and frozen in fresh water until examined. All recognizable prey items were identified to the lowest possible taxon. Once identified, prey were counted and the blotted wet weight of each prey item was recorded to the nearest 0.0001 g.

Fish diets were diverse (Table 7.3), therefore, all identifiable prey were aggregated into ten functional groups (based on phylum, order, class, or subclass level) for statistical comparisons. These groups included: harpacticoid copepods, calanoid copepods, other copepods (including cyclopoid and unidentified copepods), barnacle cyprids, amphipods (including benthic and hyperiid amphipods), crabs, euphausiids, mysids, diptera, and "other prey" (Table 7.3). "Other prey" included rare prey types (e.g., chaetognaths, cumaceans, and isopods) that did not contribute $\geq 5\%$ by biomass to at least one fish species' diet. Unidentifiable prey remains, such as unidentifiable animal tissues or crustacean fragments, were not included as a functional group in

statistical analyses because the remains lack ecological interpretability and because including such prey decreases the ability to distinguish predator's food habits by increasing dietary overlap (Garrison and Link 2000).

7.2.2 Descriptive diet analyses

Fish diets were characterized and compared using prey count and biomass data. Prey count data were used to summarize the amount of individual prey types consumed per prey category. Prey biomass data were used in percent mean weight (%MW) calculations. The results of the %MW calculations were used in both descriptive and multivariate analyses. Percent mean weight for fish species i was calculated as:

$$\%MW_i = 1/P \times \sum_{j=1}^P \left(W_{ij} / \sum_{i=1}^Q W_{ij} \right) \times 100$$

where %MW $_i$ is the percent mean weight of prey type i eaten by fish species, W_{ij} is the weight of prey i in a single fish stomach j , and $\sum W_{ij}$ is the sum of the weights of all Q prey types present in a fish stomach j . For each prey item, the sum of this calculation over all j stomachs was then divided by the number of non-empty stomachs, P . We ultimately chose %MW for statistical comparisons as it represented prey energetic importance and was a useful metric for comparing fish diet compositions.

Percent mean weight-based statistical analyses took into account only identifiable prey in each fish's diet, which meant that individuals that had empty stomachs, or only consumed unidentifiable prey, were not included. To ensure that all fishes were considered by this study, we included the %MW of unidentifiable prey and counts of empty stomachs in descriptive tables and figures.

Cumulative prey curves were generated at both fine and coarse taxonomic levels to determine how adequately the fishes' diets were described by our sample sizes and to visualize overall differences in diet diversity between species. This method plotted the occurrence of novel prey taxa or prey groups against a running total of examined stomachs (Chipps and Garvey 2007). When the curve was close to reaching an asymptote, fish diet diversity was said to be adequately described. Cumulative prey curves were constructed using the species-accumulation plot function in PRIMER v7 multivariate statistics package. Following the methods outlined in Hallett and Daley (2011), we randomized species-specific stomach contents data across 999 permutations using a bootstrap method. This removed biases associated with plotting the accumulation of prey types by sample order and allowed for a visualization of any major trends in prey use.

7.2.3 Statistical methods

Interspecific diet comparisons were conducted using permutational multivariate analysis of variance (PERMANOVA), along with nonmetric multidimensional scaling (nMDS). Only fishes that were definitively collected within one of three regions (Beaufort Sea, Chukchi Sea, or Elson Lagoon) over 2013 and 2014 were included in statistical analyses. Unidentified prey and stomach parasites were not included in the PERMANOVA or nMDS analyses. The PERMANOVA model included diet compositions of the nine species over three regions. Species and regions were included as fixed factors in a two-way analysis. Both PERMANOVA and

nMDS were conducted using the multivariate statistics package, PRIMER v7 with PERMANOVA. Prior to PERMANOVA and nMDS analyses, stomach contents data were 4th root transformed to assure both abundant and less-abundant prey groups contributed to the analyses. We have found that when diet data are not 4th root transformed, highly abundant prey groups tend to mask the contribution of less-abundant prey groups to differences between fish diet compositions. After transformation, pairwise Bray-Curtis distances were computed to quantify dissimilarities in diet composition among samples. PERMANOVA was performed on diet compositions of individual fish stomachs, whereas nMDS was performed on diet compositions aggregated by species. All PERMANOVA results were evaluated at a significance level of $\alpha=0.05$. Because an interaction between the main effects was significant, separate PERMANOVA models and PERMANOVA-based multiple comparisons were developed to evaluate the two-way interaction of species and regions. Analyzing this two-way interaction was of primary interest because it detailed the differences in diet compositions of fishes across the three regions. The nMDS ordination was generated to illustrate differences in fish diet compositions in multivariate space. Prey group vectors, based on Pearson correlations, were overlain to show the specific prey groups most closely associated with differences between the fishes' diets. The goodness of fit of the nMDS ordination was evaluated by a stress statistic, with a stress of <0.2 considered a good fit (Clarke 1993).

Within-species, intraspecific diet comparisons across regions and body sizes were also evaluated using PERMANOVA. The analysis of similar fish species' diets across regions included all available stomachs containing identifiable prey without accounting for the effect of fish size. This was done because size information was not available for all specimens. Intraspecific differences in diets related to body size were calculated by pooling all specimens by species and including fish length as a covariate in PERMANOVA. This allowed for more stomachs, per species, accompanied by length data, to be included in the size-based analysis.

7.3 Results and Discussion

Overall, a total of 414 fish stomachs (*C. sardinella* = 34, *M. villosus* = 41, *O. mordax* = 48, *B. saida* = 33, *E. gracilis* = 55, *Myoxocephalus* spp. = 60, *L. fabricii* = 20, *S. punctatus* = 48, *A. hexapterus* = 75) were included in the descriptive and multivariate analyses. An additional 51 stomachs were analyzed, but empty (*C. sardinella* = 0, *M. villosus* = 14, *O. mordax* = 12, *B. saida* = 1, *E. gracilis* = 1, *Myoxocephalus* spp. = 1, *L. fabricii* = 3, *S. punctatus* = 15, *A. hexapterus* = 4; Table 7.3). The causes of the relatively greater amount of empty stomachs found for *M. villosus*, *O. mordax*, and *S. punctatus* are unclear. Some possible reasons for the observed differences include: variability in species-specific feeding styles, prey availability in the nearby capture area, time of sampling, and species-specific physical responses to capture (e.g., prey regurgitation due to netting).

Sample sizes used per analysis varied depending upon region analyzed and whether or not the analysis took into account fish length, identifiable prey, combinations of identifiable and unidentifiable prey, or empty stomachs. For all species' diets combined, 26,236 prey items were counted; *C. sardinella* consumed the most prey in terms of counts (14,510 items), followed by *A. hexapterus* (5,085), *E. gracilis* (3,874), *L. fabricii* (988), *M. villosus* (506), *B. saida* (487), *O. mordax* (405), *Myoxocephalus* spp. (225), and *S. punctatus* (156; Table 7.4). The combination of calanoid, harpacticoid, and other copepods numerically dominated the diets of *C. sardinella* (count=13,003; 89% of diet by counts), *M. villosus* (430; 98%), *B. saida* (444; 94%), *E. gracilis*

(3,693; 95%), *L. fabricii* (981; 99%), *S. punctatus* (108; 92%), and *A. hexapterus* (5,003; 99%). *O. mordax* and *Myoxocephalus* spp. consumed fewer copepods, with mysids (*O. mordax*; 165; 43%) and amphipods (*Myoxocephalus* spp.; 117; 59%) composing large proportions of these species' diets (Table 7.4). Prey biomass, as measured by percent mean weight (%MW), followed similar patterns with the combination of copepods composing the bulk of identifiable prey biomass in the diets of *M. villosus*, *B. saida*, *E. gracilis*, *L. fabricii*, *S. punctatus*, and *A. hexapterus* (Table 7.3; Figure 7.1). Copepods composed less of identifiable prey biomass in *C. sardinella*, *O. mordax*, and *Myoxocephalus* spp. diets. The bulk of %MW for *C. sardinella* was composed of euphausiids, diptera (Elson Lagoon only), and amphipods, while mysids, and other prey combined to compose a high proportion of *O. mordax* diet (Table 7.3; Figure 7.1). *Myoxocephalus* spp. diet was dominated by a high %MW of amphipods (Table 7.3; Figure 7.1).

Each species consumed a diverse array of prey taxa and consequently, when prey were analyzed to the lowest possible taxon, cumulative prey curves did not attain an asymptote (i.e., more stomachs were needed to describe each species' diet; Figure 7.2). At our level of prey identification, the lowest taxonomic prey curves indicated that *C. sardinella* consumed the most diverse diet with over 25 unique prey taxa consumed, followed in decreasing order of diet diversity by *E. gracilis*, *A. hexapterus*, *O. mordax*, *B. saida*, *Myoxocephalus* spp., *S. punctatus*, *M. villosus*, and *L. fabricii* (Figure 7.2). Fish diets were generally better described when prey taxa were aggregated into the 10 coarse taxonomic groups. At this level of identification, cumulative prey curves for *C. sardinella*, *O. mordax*, and *L. fabricii* appeared to attain asymptotes at about 15 to 20 stomachs, *A. hexapterus* at about 40 stomachs, while curves for *M. villosus*, *B. saida*, *E. gracilis*, *Myoxocephalus* spp., and *S. punctatus* did not fully reach an asymptote (Figure 7.2). Although *M. villosus*, *E. gracilis*, *Myoxocephalus* spp., and *S. punctatus* cumulative prey curves did not reach an asymptote, we considered their diets as sufficiently described given most prey groups were accounted for in stomachs containing identifiable prey. *B. saida* diet was not as well described, but kept in analyses, where appropriate, because little information exists regarding their food habits within the ACES study region.

PERMANOVA found diet compositions of the nine fish species to significantly differ among each other across all regions combined (df=8, F=14.329, p=0.001) and among regions all species combined (df=2, F=2.558, p=0.017). Also, the interaction between species and region was significant (df=15, F=2.448, p=0.001) (Table 7.5). The three PERMANOVA models, developed to compare fish species' diets interspecifically within regions, determined that diet compositions differed among species within all regions: Beaufort Sea (df=8, F=7.400, p=0.001), Chukchi Sea (df=7, F=12.751, p=0.001), and Elson Lagoon (df=8, F=5.330, p=0.001) (Table 7.6).

Within the Beaufort Sea, *C. sardinella* and *B. saida* accounted for significant differences in diet compositions with all other eight species, including themselves. Additionally, *Myoxocephalus* spp. accounted for significant diet differences with seven other species, *A. hexapterus* (four other species), *S. punctatus* (4), *E. gracilis* (3), *L. fabricii* (3), *O. mordax* (3), and *M. villosus* (2) (Table 7.6). Relative to all other fish species, the major separation within the Beaufort Sea created by *C. sardinella*, *B. saida*, and *Myoxocephalus* spp. can be explained by a high %MW of euphausiids in *C. sardinella* diet, a lack of harpacticoid copepods and a high %MW of calanoid copepods in *B. saida* diet, and a greater %MW of amphipods and harpacticoid copepods in *Myoxocephalus* spp. diet (Table 7.7; Figures 7.3 and 7.4). Differences in %MW of harpacticoid

copepods, calanoid copepods, other copepods, crabs, and barnacle cyprids drove all other observed differences (Table 7.7; Figures 7.3 and 7.4).

Within the Chukchi Sea, *Myoxocephalus* spp. accounted for significant differences with all other seven species (*C. sardinella* not collected), *S. punctatus* (four other species), *B. saida* (3), *E. gracilis* (2), *M. villosus* (2), *O. mordax* (1), and *L. fabricii* (1) (Table 7.6). The separation between *Myoxocephalus* spp. and all other fish species was mostly due to a large proportion of amphipods in sculpin diets and the general lack of amphipods in all other fish diets (Table 7.8; Figures 7.5 and 7.6). Differences in %MW of harpacticoid copepods, calanoid copepods, other copepods, barnacle cyprids, crabs, euphausiids, and mysids drove all other observed differences (Table 7.8; Figures 7.5 and 7.6).

Diet variability was highest within Elson Lagoon: *O. mordax*, *Myoxocephalus* spp., and *L. fabricii* accounted for significant differences with all other seven species, including themselves (Table 7.6). Additionally, *C. sardinella* accounted for significant differences with six other species, *S. punctatus* (5 other species), *E. gracilis* (5), and *A. hexapterus* (4). The separation between *O. mordax* and other species was mostly due to large proportions of mysids in its diet (Table 7.9; Figures 7.7 and 7.8). Relative to all other species, *Myoxocephalus* spp. consumed the highest proportions of amphipods, *L. fabricii* consumed the greatest proportions of harpacticoid and other copepods, *C. sardinella* was the only species to consume diptera, *S. punctatus* consumed the greatest proportions of crabs and barnacle cyprids, *E. gracilis* consumed the greatest proportions of calanoid copepods, and the only identifiable prey consumed by *A. hexapterus* were copepods (Table 7.9; Figures 7.7 and 7.8).

Between regions, significant intraspecific differences in fish diet compositions, as determined by PERMANOVA, were found for *C. sardinella*, *O. mordax*, *B. saida*, *S. punctatus*, and *A. hexapterus* (Table 7.10). For *C. sardinella*, the Beaufort Sea population consumed high proportions of euphausiids whereas the Elson Lagoon population consumed a more varied diet consisting of high proportions of diptera, with amphipods also being an important contributor (Figures 7.3 and 7.7). *O. mordax* diet in Elson Lagoon was significantly different from conspecifics in both the Beaufort and Chukchi Seas, but not significantly different between the Beaufort and Chukchi Seas (Table 7.10), most likely due to high amounts of mysids in the diets of Elson Lagoon individuals, and greater proportions of copepods in diets of Beaufort and Chukchi Sea fish (Figures 7.3, 7.5, and 7.7). *B. saida* diet differed between the Beaufort and Chukchi Seas due to greater calanoid copepod, amphipod, and mysid consumption by Beaufort Sea conspecifics, with fish in the Chukchi Sea consuming higher proportions of crabs and barnacle cyprids in addition to calanoid copepods (Figures 7.3 and 7.5). *S. punctatus* diets in the Chukchi Sea were significantly different from conspecifics in both the Beaufort Sea and Elson Lagoon regions, most likely due to Chukchi Sea individuals consuming mostly copepods and those in the Beaufort Sea consuming some amphipods, crabs, and other prey, and conspecifics in Elson Lagoon consuming greater proportions of crabs, along with some barnacle cyprids (Figures 7.3, 7.5, and 7.7). *A. hexapterus* diets differed between the Beaufort and Chukchi Seas most likely due to greater proportions of copepods in Chukchi Sea diet and a more varied diet in the Beaufort Sea, including crabs and euphausiids (Figures 7.3 and 7.5).

The intraspecific, body-sized based analysis indicated that the diet compositions of *M. villosus*, *O. mordax*, *B. saida*, *Myoxocephalus* spp., and *A. hexapterus* were significantly influenced by changes in body size (Table 7.11). The general trend highlighted by this analysis was that smaller fish of each species consumed larger proportions of smaller prey, such as copepods, while larger individuals consumed larger prey in addition to copepods. *M. villosus* <80 mm consumed primarily copepods, whereas larger individuals consumed mysids and amphipods (Figure 7.9). *O. mordax* <70 mm consumed mostly copepods, with mysids becoming an important prey item in larger specimens' diets (Figure 7.10). *B. saida* <70 mm consumed smaller copepods, barnacle cyprids, and amphipods, whereas larger individuals consumed larger crabs, euphausiids, and mysids (Figure 7.11). *Myoxocephalus* spp. consumed a diet primarily composed of amphipods regardless of body size; however, copepods were important for ≤ 50 mm fish, while fish prey (listed as other prey) was consumed in high proportions by individuals >101 mm (Figure 7.12). *A. hexapterus* diet was characterized by a gradual decrease in the proportions of copepods consumed from 31–80 mm, with individuals >70 mm consuming a more diverse diet including higher proportions of amphipods, crabs, euphausiids, and mysids (Figure 7.13).

The PERMANOVA and nMDS analyses were successful in highlighting patterns in both inter- and intraspecific diet variability for all species. Within regions, each species' diet differed significantly from at least one other species, a pattern expected considering historical accounts of each species' diet (Table 7.1). This documents how different species partition prey within similar regions. Most diet similarities were due to large %MW proportions of copepods in diets; therefore, species such as *C. sardinella* and *Myoxocephalus* spp., which consumed less copepods by %MW, were consistently different from nearly all other species. In future interspecific research, exploring whether feeding guilds exist for these nine species could be useful. A guild analysis would allow one to determine if these fishes exploit different prey groups in similar ways (Root 1967; Garrison and Link 2000). This would offer a clearer view of interspecific processes in each region.

The intraspecific differences highlighted by these analyses show within-species diet variability among regions, which can give insight into how prey availability differs within each region. Gray et al. (2016a) demonstrated that *B. saida* diets differ across large, longitudinal gradients in the Beaufort and Chukchi Seas. Similarly, spatially influenced diet differences were highlighted here for *C. sardinella*, *O. mordax*, *B. saida*, *S. punctatus*, and *A. hexapterus*; however, in this study, sampling locations within different regions were much closer spatially. This suggests perhaps dynamically different processes acting on prey availability within the three regions. A clear example of this is diptera only being consumed by *C. sardinella* in the less-saline Elson Lagoon waters. There, *C. sardinella* consumed a large amount of diptera by %MW and counts, whereas Beaufort Sea conspecifics consumed primarily euphausiids, a prey group less represented in the Elson Lagoon population's diet. It is worth noting the lack of intraspecific, regional diet differences between *M. villosus*, *E. gracilis*, *Myoxocephalus* spp. and *L. fabricii* (Table 7.10), which indicates little variability in prey exploitation by these species between regions. It is possible these fishes' diets are more conserved in Arctic regions; however, further study is needed to confirm the existence of this pattern on larger geographic scales.

Intraspecific differences in diet were also related to fish body size. Changes in diet with an increase in body size are common in fishes (Werner and Hall 1974; Labropoulou and Eleftheriou

1997); five of the nine species collected here exhibited such a pattern (Table 7.11; Figures 7.9–7.13). The other four species did not exhibit any size-related shifts in diet. While this could be due to a lack of ontogenetic shifts in these four species' diets, it is more likely that our sampling methods did not collect a wide enough size range to document size-related shifts in diets of *C. sardinella* (size range = 179–310 mm), *E. gracilis* (21–76 mm), *L. fabricii* (25–58 mm), and *S. punctatus* (19–34 mm).

Habitat characteristics unique to the Beaufort Sea, Chukchi Sea, and Elson Lagoon study areas are most likely acting on prey availability, thus influencing the regional diet compositions of these species. Differences in water salinity and temperature, among other factors, no doubt influence fish prey assemblages. To quantitatively relate habitat differences to these fishes' diets, regional invertebrate abundances should be documented and related to regional environmental variables.

By examining patterns in inter- and intraspecific diet variability, this study gives insight into the roles of fishes' in regional Arctic marine food webs. Fishes within the ACES study area exploited a wide variety of pelagic zooplankton and benthic macroinvertebrates. By ingesting different prey types, these fishes effectively link prey of differing qualities to upper trophic level predators (e.g., predators listed in Table 7.2). Such a scenario is likely considering documented prey lipid values. The highest quality prey taken by ACES fishes were most likely *Calanus* copepods (56–64 % lipid by dry weight), *Themisto* amphipods (14–32%), and *Thysanoessa* euphausiids (52 %), while some of the lower quality prey may have included various gammarid amphipods (7–25 %) (Lee 1975; Percy and Fife 1981). Less is known about the lipid values of other prey taken by ACES fishes. Future researchers should consider a comprehensive diet study that directly measures prey quality and abundance of endemic invertebrates. Such a study would greatly enhance our understanding of fishes as trophic links in Alaska coastal food webs.

7.4 References

- Atkinson EG, Percy JA. 1992. Diet comparison among demersal marine fish from the Canadian Arctic. *Polar Biology* 11: 567–573.
- Bain H, Sekerak AD. 1978. Aspects of biology of Arctic cod, *Boreogadus saida*, in the Central Canadian Arctic. LGL, Ltd., Toronto pp 104.
- Barrett RT. 1991. Shags (*Phalacrocorax aristotelis* L.) as potential samplers of juvenile saithe (*Pollachius virens* (L.)) stocks in northern Norway. *Sarsia* 76(3): 153–156.
- Bond WA, Erickson RN. 1993. Fisheries investigations in coastal waters of Liverpool Bay, Northwest Territories. Canadian Manuscript Reports of Fisheries and Aquatic Sciences 2204: vi + 51 p.
- Bowering WR, Lilly GR. 1992. Greenland halibut (*Reinhardtius hippoglossoides*) off southern Labrador and northeastern Newfoundland (northwest Atlantic) feed primarily on capelin (*Mallotus villosus*). *Netherlands Journal of Sea Research* 29(1/3): 211–222.
- Chippis SR, Garvey JE. 2007. Assessment of diets and feeding patterns. In: Guy C.S., and M.L. Brown (eds) *Analysis and Interpretation of Freshwater Fisheries Data*, American Fisheries Society, Bethesda, Maryland, pp 473–514.
- Clarke KR. 1993. Non-parametric multivariate analyses of changes in community structure. *Australian J Ecol* 18: 117–143.
- Coyle KO, Gillespie JA, Smith RL, Barber I. 1997. Food habits of four demersal Chukchi Sea fishes. *Am Fish Soc Symp* 19: 310–318.

- Craig PC, Griffiths WB, Haldorson L, McElderry H. 1982. Ecological studies of Arctic cod (*Boreogadus saida*) in Beaufort Sea coastal waters, Alaska. *Can J Fish Aqua Sci* 39(3): 395–406.
- Dehn L-A, Sheffield GG, Follmann EH, Duffy LK, Thomas DL, O'Hara TM. 2007. Feeding ecology of phocid seals and some walrus in the Alaska and Canadian Arctic as determined by stomach contents and stable isotope analysis. *Polar Biology* 30: 167–181.
- Garrison LP, Link JS. 2000. Dietary guild structure of the fish community in the Northeast United States continental shelf ecosystem. *Mar Ecol Prog Ser* 202: 231–240.
- Gray BP, Norcross BL, Blanchard AL, Beaudreau AH, Seitz AC. 2016a. Variability in the summer diets of polar cod (*Boreogadus saida*) in the northeastern Chukchi and western Beaufort Seas. *Polar Biology* 39: 1069–1080. doi:10.1007/s00300-015-1796-7.
- Gray BP, Norcross BL, Blanchard AL, Beaudreau AH, Seitz AC. 2016b. Food habits of Arctic staghorn sculpin (*Gymnocanthus tricuspis*) and shorthorn sculpin (*Myoxocephalus scorpius*) in the northeastern Chukchi and western Beaufort Seas. *Deep-Sea Research II- Topical Studies in Oceanography*. <http://dx.doi.org/10.1016/j.dsr2.2016.05.013>.
- Haldorson L, Craig P. 1984. Life history and ecology of a Pacific-Arctic population of Rainbow Smelt in coastal waters of the Beaufort Sea. *Trans Am Fish Soc* 113(1): 33–38.
- Hall AJ, Watkins J, Hammond PS. 1998. Seasonal variation in the diet of harbour seals in the south-western North Sea. *Mar Ecol Prog Ser* 170: 269–281.
- Hallett CS., Daley RK. 2011. Feeding ecology of the southern lanternshark (*Etmopterus baxteri*) and the brown lanternshark (*E. unicolor*) off southeastern Australia. *ICES Journal of Marine Science* 68: 157–165.
- Jewett SC. 1978. Summer food of the pacific cod, *Gadus macrocephalus*, near Kodiak Island, Alaska. *Fisheries Bulletin* 76(3): 700–706.
- Jewett SC, Feder HM. 1980. Autumn food of adult starry flounders, *Platichthys stellatus*, from the northeastern Bering Sea and the southeastern Chukchi Sea. *Journal du Conseil international pour l'Exploration de la Mer*. 39(1): 7–14.
- Keats DW, Steele DH, Green JM, Martel GM. 1993. Diet and population size structure of the Arctic shanny, *Stichaeus punctatus* (Pisces: Stichaeidae), at sites in eastern Newfoundland and the eastern Arctic. *Environmental Biology of Fishes* 37(2): 173–180.
- Khudya VN. 1993. Pacific sand lance. pp 100–104 in F.S. Terziev (ed). Project "The seas". Hydrometeorology and Hydrochemistry of the seas. Vol. 9. Sea of Okhotsk. Sankt-Peterburg, Gidrometeoizdat.
- Khudya VN, Fedotova NA, Mukhametov IN. 1996. Feeding of sand lance (*Ammodytes hexapterus*) in Sakhalin coastal waters. pp. 45–50 in Fisheries studies in the Sakhalin-Kuril region and adjacent waters. Vol. 1. Collected papers. Yuzhno-Sakhalinsk, Sakhalinskoye Oblastnoye Knizhnoye Izdatel'stvo.
- Kuznetsova NA. 1997. Feeding of some planktonophagous fishes in the Sea of Okhotsk during summer period. *Izv. TINRO* 122: 255–275.
- Labropoulou M, Eleftheriou A. 1997. The foraging ecology of two pairs of congeneric demersal fish species: importance of morphological characteristic in prey selection. *Journal of Fish Biology* 50: 324–340.
- Lee RF. 1975. Lipids of Arctic zooplankton. *Comparative Biochemistry and Physiology*. 51B: 263–266.
- Loseto LL, Stern GA, Connelly TL, Diebel D, Gemmill B, Prokopowicz A, Fortier L, Ferguson SH. 2009. Summer diet of beluga whales inferred by fatty acid analysis of the eastern

- Beaufort Sea food web. *Journal of Experimental Marine Biology and Ecology* 374(1): 12–18.
- Lowry LF, Frost KJ. 1981. Distribution, growth, and foods of Arctic Cod (*Boreogadus saida*) in the Bering, Chukchi, and Beaufort Seas. *Canadian Field Naturalist* 95: 186–191
- Mann GJ, McCart PJ. 1981. Comparison of sympatric dwarf and normal populations of least cisco (*Coregonus sardinella*) inhabiting Trout Lake, Yukon Territory. *Canadian Journal of Fisheries and Aquatic Sciences* 38(2): 240–244.
- Mikhail MY, Welch HE. 1989. Biology of Greenland cod, *Gadus ogac*, at Saqvaqujac, northwest coast of Hudson Bay. *Environmental Biology of Fishes* 26: 49–62.
- Mills EL, O'Gorman R, Roseman EF, Adams C, Owens RW. 1995. Planktivory by alewife (*Alosa pseudoharengus*) and rainbow smelt (*Osmerus mordax*) on microcrustacean zooplankton and dreissenid (*Bivalvia: Dreissenidae*) veligers in southern Lake Ontario. *Canadian Journal of Fisheries and Aquatic Sciences* 52: 925–935.
- Morrow JE. 1980. The freshwater fishes of Alaska. University of B.C. Animal Resources Ecology Library. pp 248.
- Percy JA, Fife FJ. 1981. The biochemical composition and energy content of Arctic marine macrozooplankton. *Arctic* 34(4): 307–313.
- Purcell JE, Sturdevant MV 2001. Prey selection and dietary overlap among zooplanktivorous jellyfish and juvenile fishes in Prince William Sound, Alaska. *Marine Ecology Progress Series* 210: 67–83.
- Root RB. 1967. The niche exploitation pattern of the blue-gray gnatcatcher. *Ecological Monographs* 37: 317–350.
- Rosenthal RJ, O'Connell VM, Murphy MC. 1988. Feeding ecology of ten species of rockfishes (Scorpaenidae) from the Gulf of Alaska. *California Fish and Game* 74(1): 16–37.
- Scott WB, Crossman EJ. 1973. Freshwater fishes of Canada. *Bulletin of Fisheries Research Board Canada* 184: 1–966.
- Springer AM, Roseneau DG, Murphy EC, Springer MI. 1984. Environmental controls of marine food webs: food habits of seabirds in the eastern Chukchi Sea. *Canadian Journal of Fisheries and Aquatic Sciences* 41: 1202–1215.
- Tokranov AM. 1985. Feeding in species of sculpins of the genus *Gymnocanthus* (Cottidae) from Kamchatka waters. *Journal of Ichthyology* 25(4): 46–51.
- Tokranov AM, Maksimenkov VV. 1995. Feeding habits of predatory fishes in the Bol'shaya River estuary (West Kamchatka). *Journal of Ichthyology* 35(9): 102–112.
- Valtysson HT. 1995. Feeding habits and distribution of eelpout species (*Lycodes* sp.) (Reinhardt) (Pisces: Zoarcidae) in Icelandic waters. Postgraduate thesis, Department of Biology, University of Iceland, Reykjavik.
- Werner EE, Hall DJ. 1974. Optimal foraging and the size selection of prey by the Bluegill Sunfish (*Lepomis macrochirus*). *Ecology* 55: 1042–1052.
- Wilson MT, Jump CM, Duffy-Anderson JT. 2006. Comparative analysis of the feeding ecology of two pelagic forage fishes: capelin *Mallotus villosus* and walleye pollock *Theragra chalcogramma*. *Marine Progress Ecology Series* 317: 245–258.
- Yang MS, Nelson MW. 1999. Food habits of the commercially important groundfishes in the Gulf of Alaska in 1990, 1993, and 1996. NOAA Technical Memo. NMFS-AFSC 112, pp. 174.

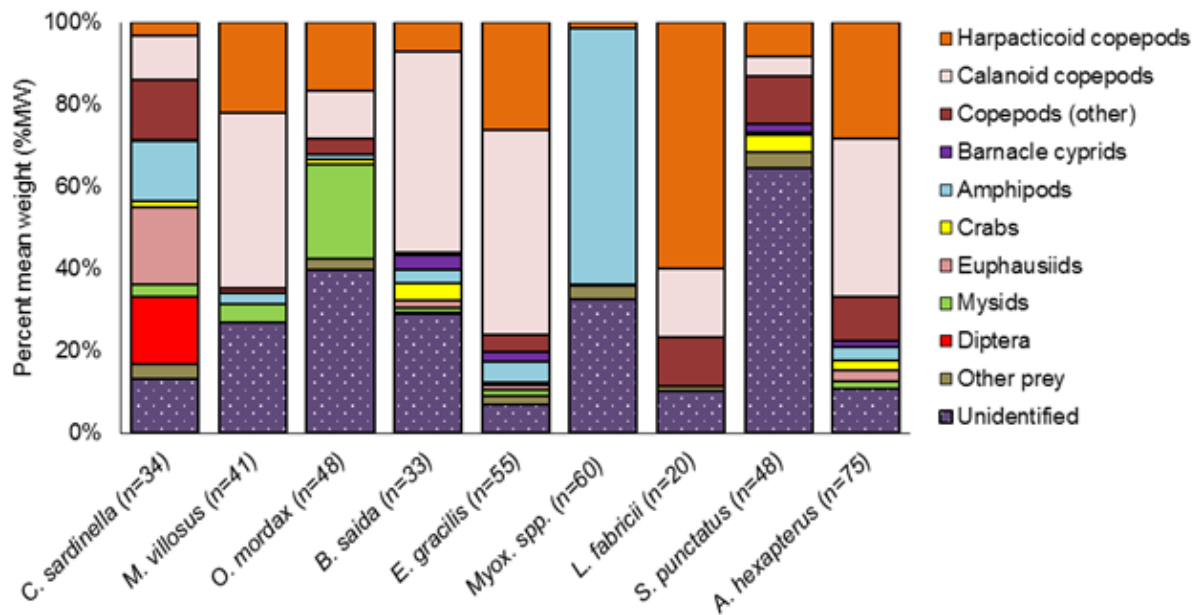


Figure 7.1 Percent mean weight (%MW) of major prey groups (including unidentified prey) consumed by nine fish species collected from Beaufort Sea, Chukchi Sea, and Elson Lagoon regions during ACES 2013 and 2014. The number of non-empty stomachs (n) is listed adjacent to species names. Fish species and prey groups are listed in phylogenetic order.

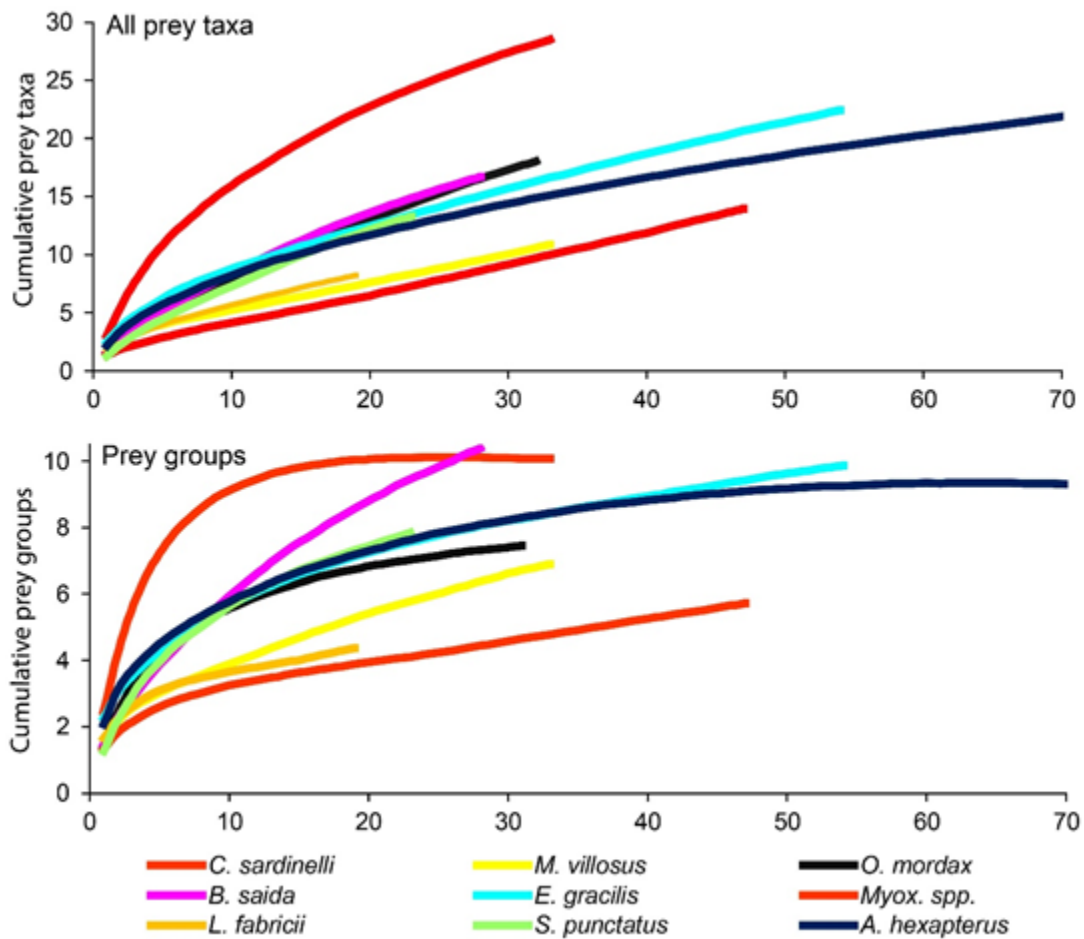


Figure 7.2 Cumulative prey curves summarizing the diet compositions of nine fish species throughout the Beaufort Sea, Chukchi Sea, and Elson Lagoon regions during ACES 2013 and 2014. The upper figure represents the accumulation of all identifiable prey taxa as stomachs were added. The lower figure represents the accumulation of the 10 taxonomically-coarse prey groups as stomachs were added.

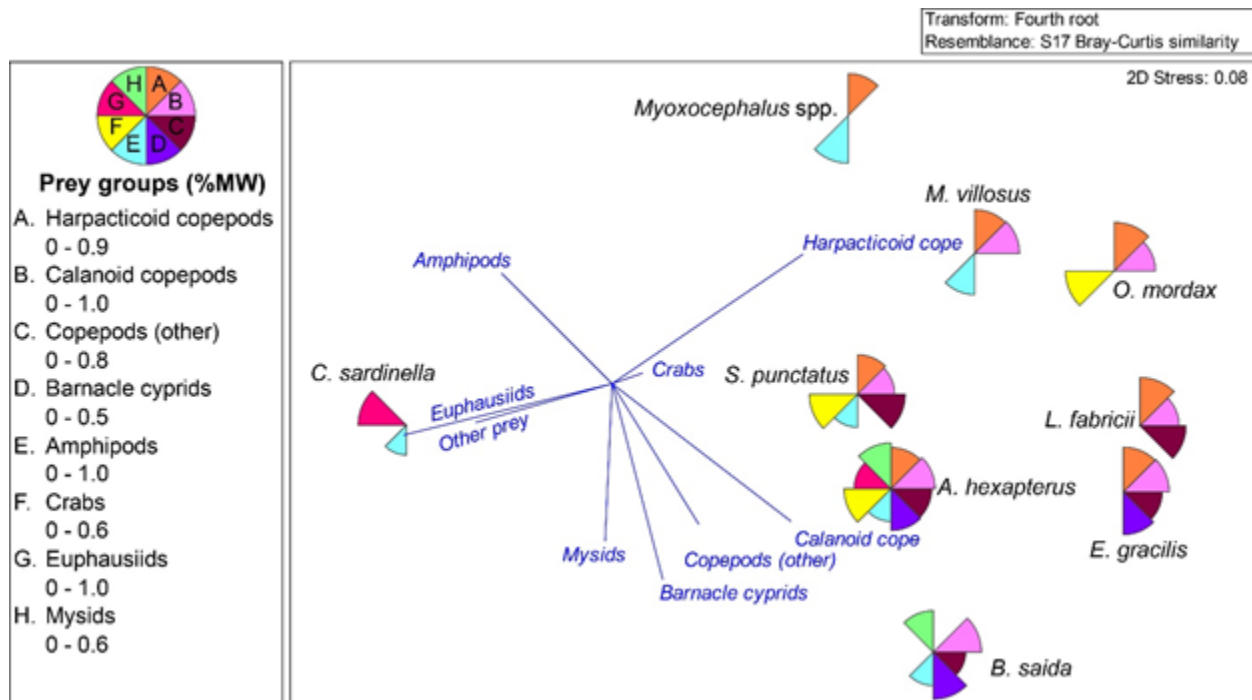


Figure 7.3 Nonmetric multidimensional scaling (nMDS) ordination showing the diet compositions of nine fish species within the Beaufort Sea during ACES 2013 and 2014. Percent mean weight (%MW) values of prey groups are color-coded and listed in phylogenetic order along the left of the figure. Other prey is not listed as to increase visibility among the main prey groups. Points (i.e., fish species) closer together are more similar than those further apart. Overlaid vectors show the specific prey groups driving diet differences, with longer vectors indicating a prey group exerts greater influence within the ordination than shorter vectors. This plot is meant as a visual aid in interpreting the significant interaction between species as determined by PERMANOVA (see text; Tables 6.5 and 6.6).

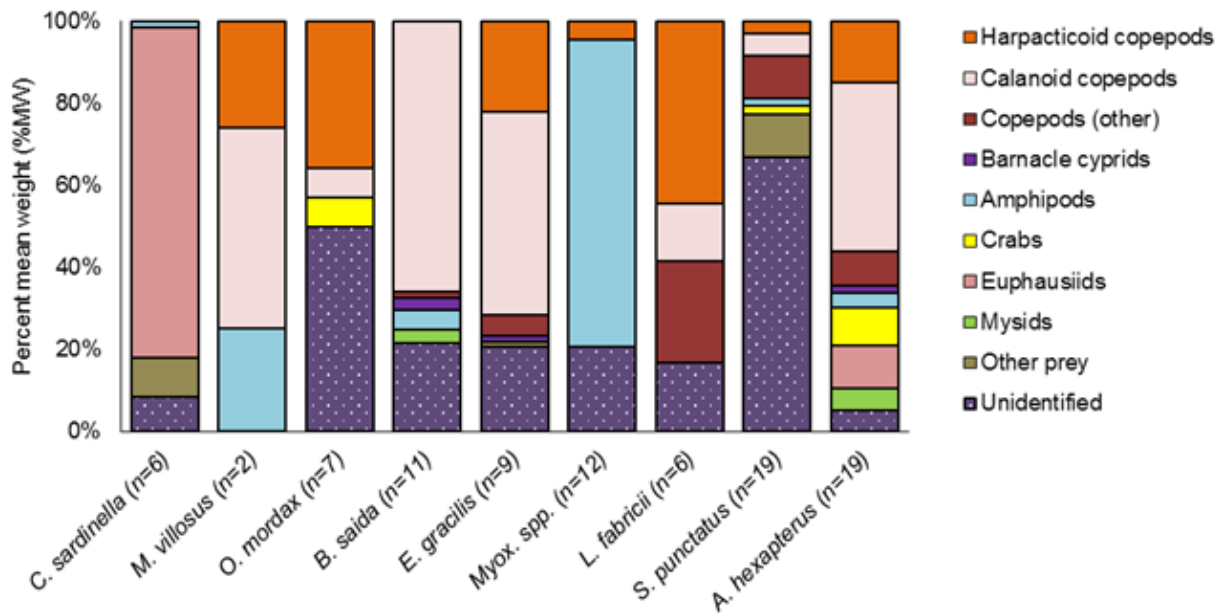


Figure 7.4 Percent mean weight (%MW) of major prey groups (including unidentified prey) consumed by nine fish species collected from the Beaufort Sea during ACES 2013 and 2014. The number of non-empty stomachs (n) is listed adjacent to species names. Fish species and prey groups are listed in phylogenetic order.

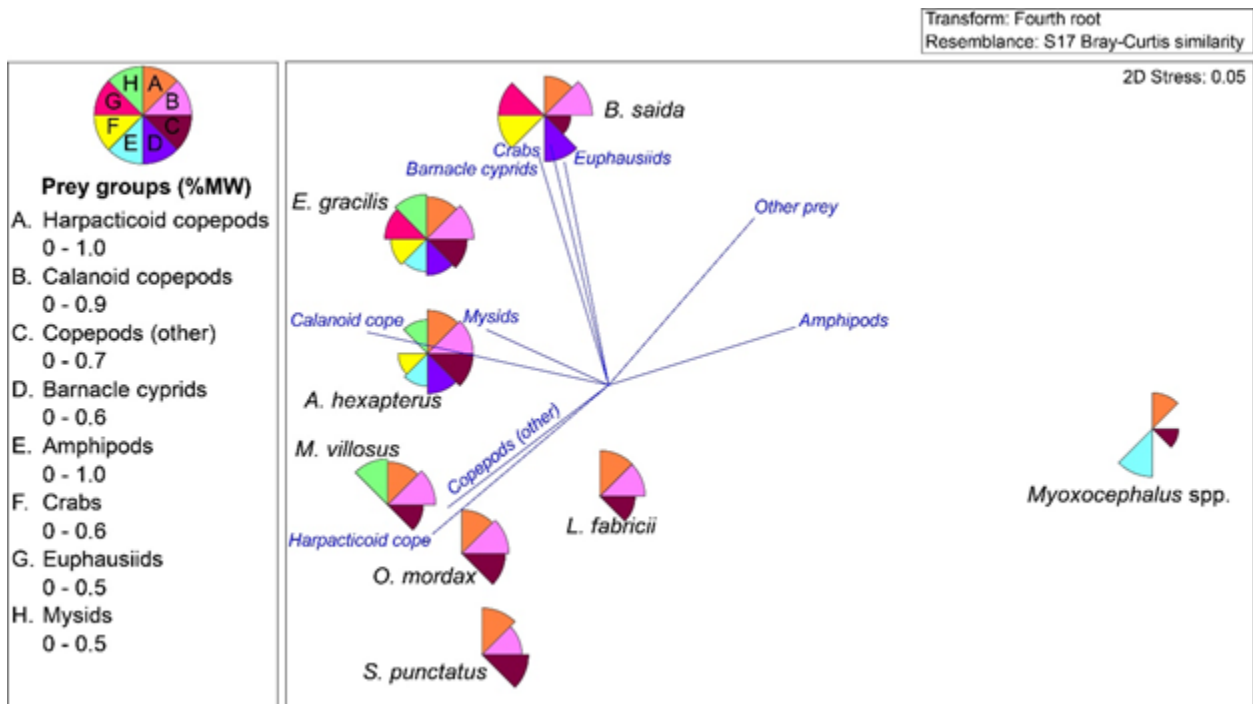


Figure 7.5 Nonmetric multidimensional scaling (nMDS) ordination showing the diet compositions of eight fish species within the Chukchi Sea during ACES 2013 and 2014. Percent mean weight (%MW) values of prey groups are color-coded and listed in phylogenetic order along the left of the figure. Other prey is not listed as to increase visibility among the main prey groups. Points (i.e., fish species) closer together are more similar than those further apart. Overlaid vectors show the specific prey groups driving diet differences, with longer vectors indicating a prey group exerts greater influence within the ordination than shorter vectors. This plot is meant as a visual aid in interpreting the significant interaction between species as determined by PERMANOVA (see text; Tables 6.5 and 6.6).

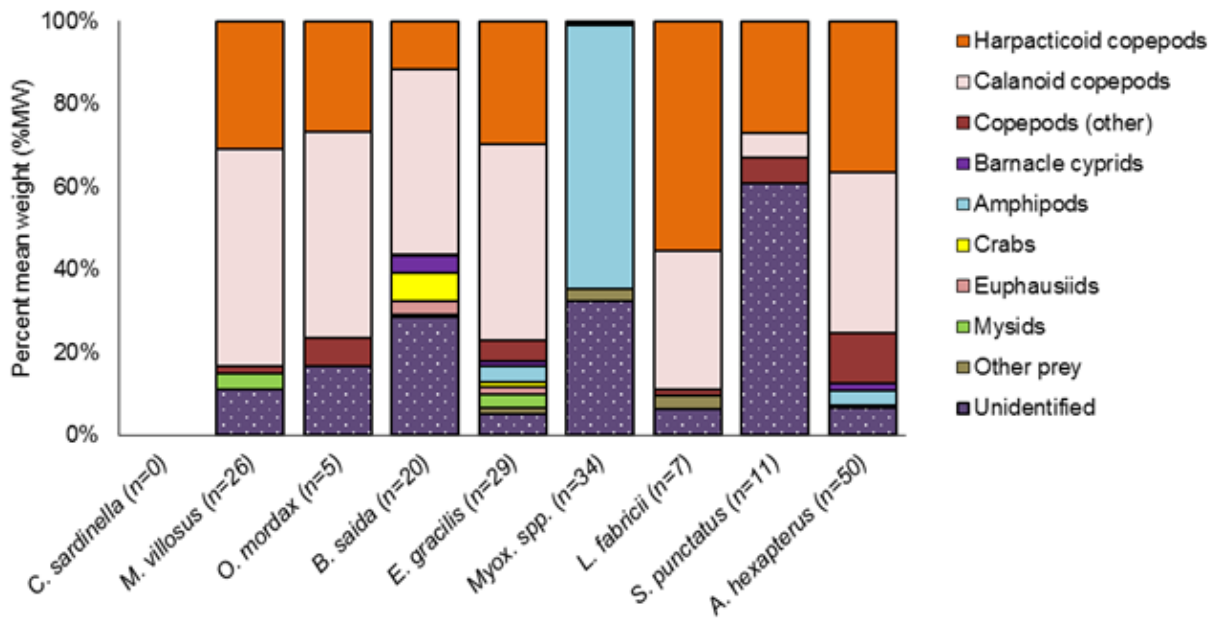


Figure 7.6 Percent mean weight (%MW) of major prey groups (including unidentified prey) consumed by eight fish species collected from the Chukchi Sea during ACES 2013 and 2014. The number of non-empty stomachs (n) is listed adjacent to species names. Fish species and prey groups are listed in phylogenetic order.

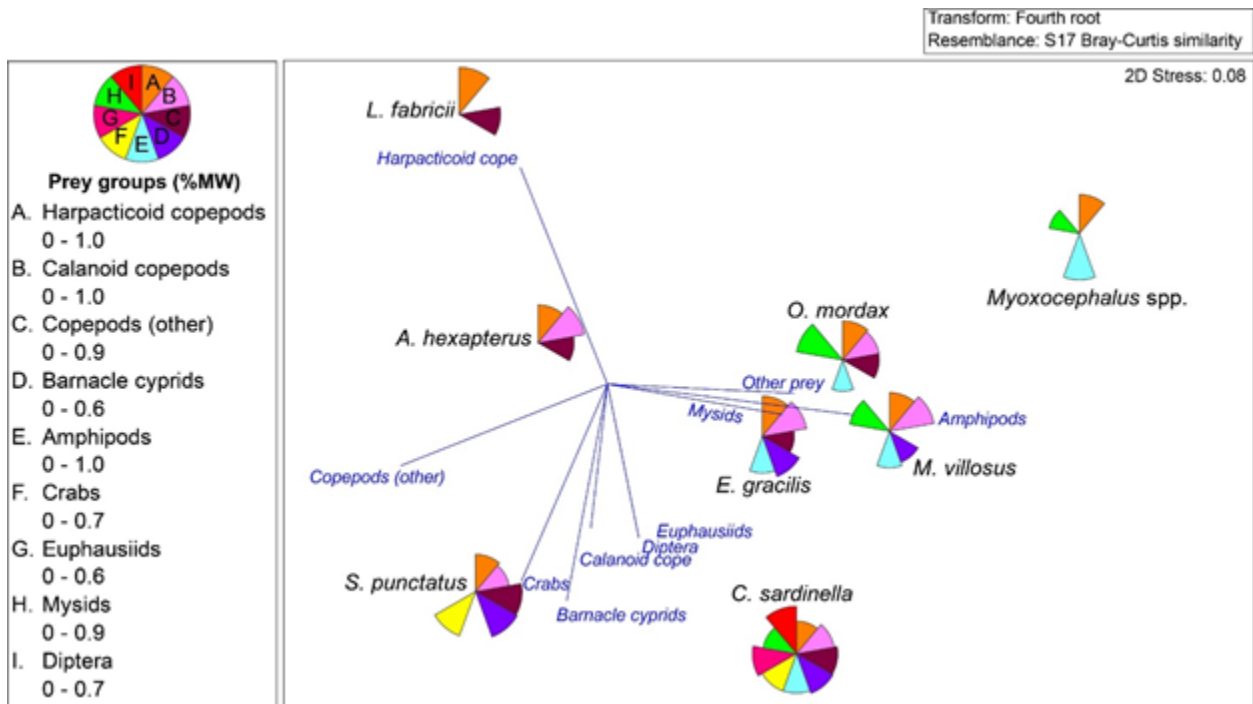


Figure 7.7 Nonmetric multidimensional scaling (nMDS) ordination showing the diet compositions of nine fish species within Elson Lagoon during ACES 2013 and 2014. Percent mean weight (%MW) values of prey groups are color-coded and listed in phylogenetic order along the left of the figure. Other prey is not listed as to increase visibility among the main prey groups. Points (i.e., fish species) closer together are more similar than those further apart. Overlaid vectors show the specific prey groups driving diet differences, with longer vectors indicating a prey group exerts greater influence within the ordination than shorter vectors. This plot is meant as a visual aid in interpreting the significant interaction between species as determined by PERMANOVA (see text; Tables 6.5 and 6.6).

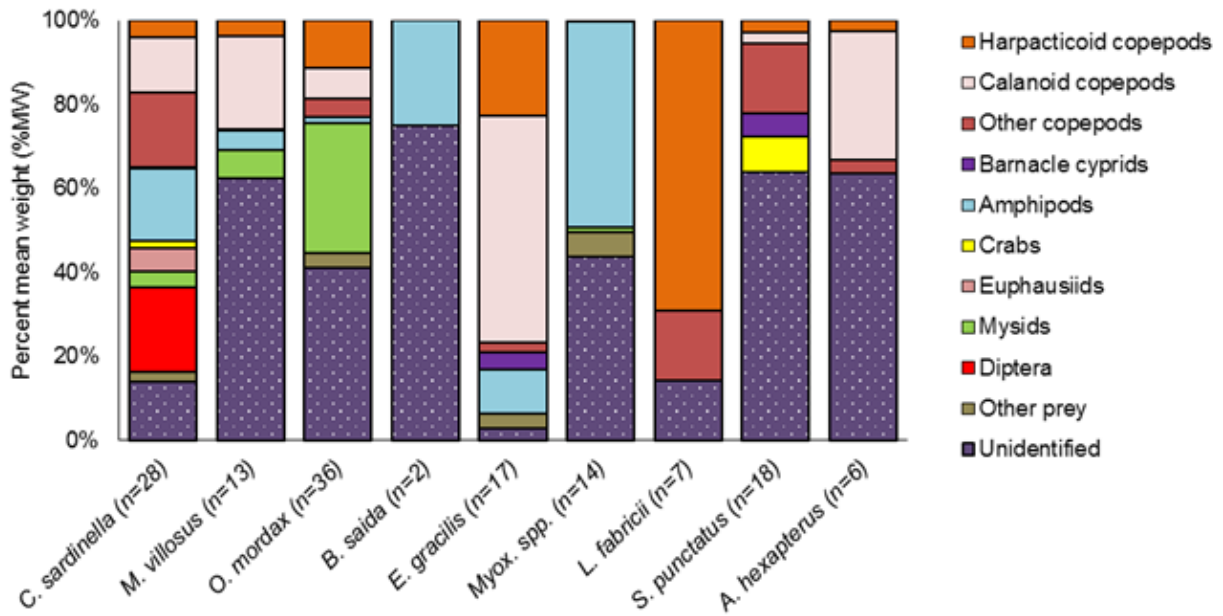


Figure 7.8 Percent mean weight (%MW) of major prey groups (including unidentified prey) consumed by eight fish species collected from Elson Lagoon during ACES 2013 and 2014. The number of non-empty stomachs (n) is listed adjacent to species names. Fish species and prey groups are listed in phylogenetic order.

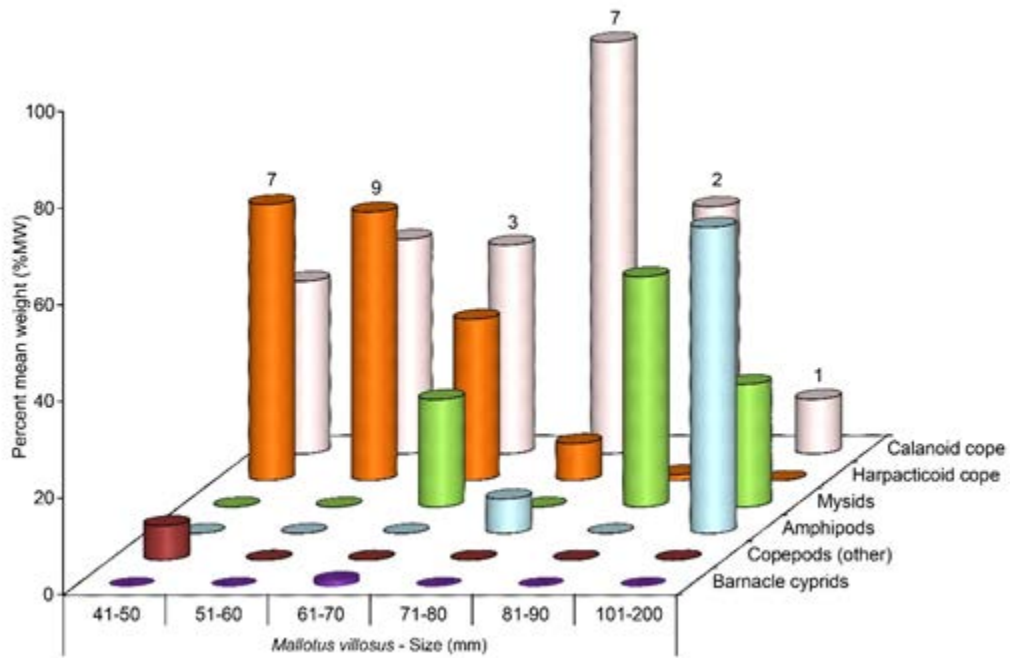


Figure 7.9 *M. villosus* diet composition plotted by 10 to 100 mm size bins to visualize changes in diet with increasing body size. Prey groups along the z-axis are listed from lowest pooled contribution by %MW (front) to greatest pooled contribution by %MW (rear). Only prey groups consumed by *M. villosus* are included along the z-axis. Sample sizes are listed above the rear column.

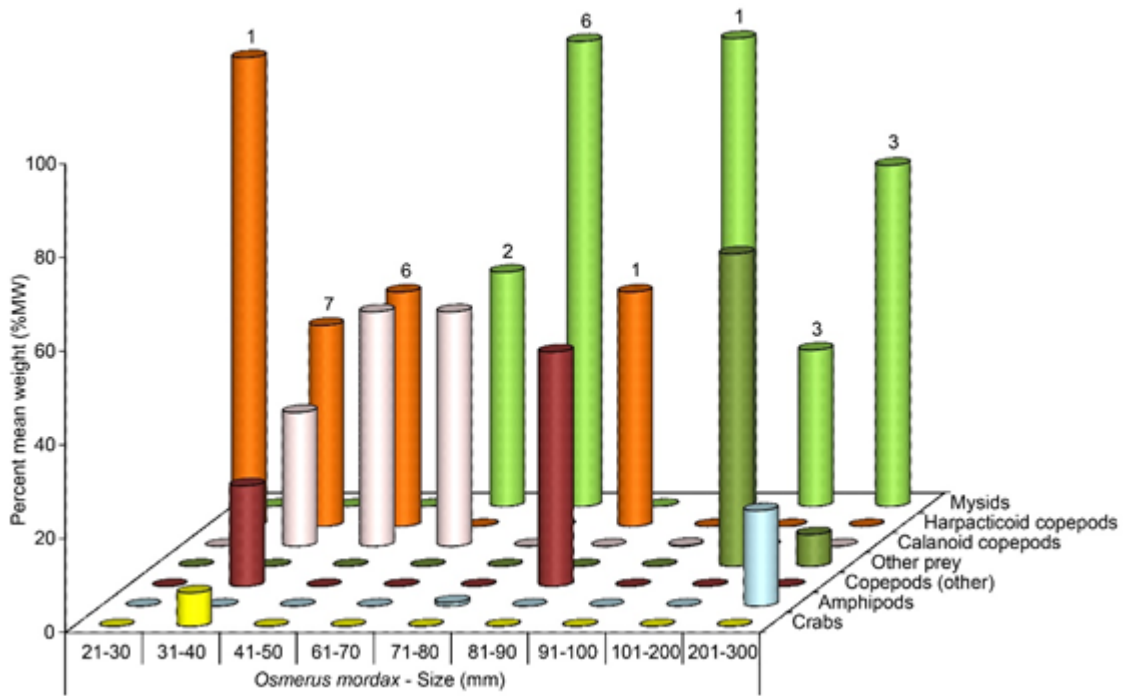


Figure 7.10 *O. mordax* diet composition plotted by 10 to 100 mm size bins to visualize changes in diet with increasing body size. Prey groups along the z-axis are listed from lowest-pooled contribution by %MW (front) to greatest-pooled contribution by %MW (rear). Only prey groups consumed by *O. mordax* are included along the z-axis. Sample sizes are listed above the rear column.

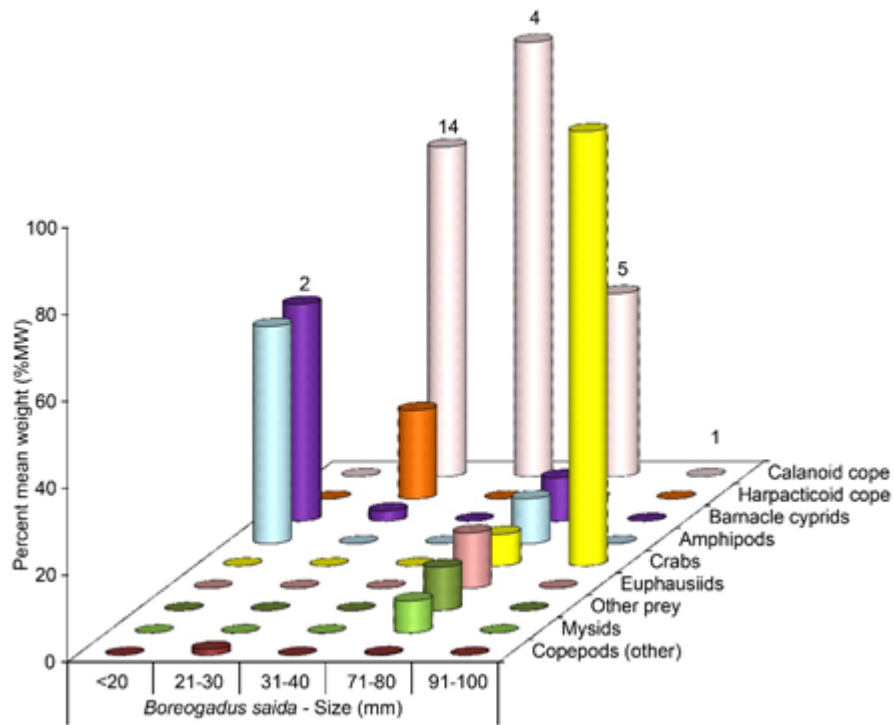


Figure 7.11 *B. saida* diet composition plotted by 10 mm size bins to visualize changes in diet with increasing body size. Prey groups along the z-axis are listed from lowest-pooled contribution by %MW (front) to greatest-pooled contribution by %MW (rear). Only prey groups consumed by *B. saida* are included along the z-axis. Sample sizes are listed above the rear column.

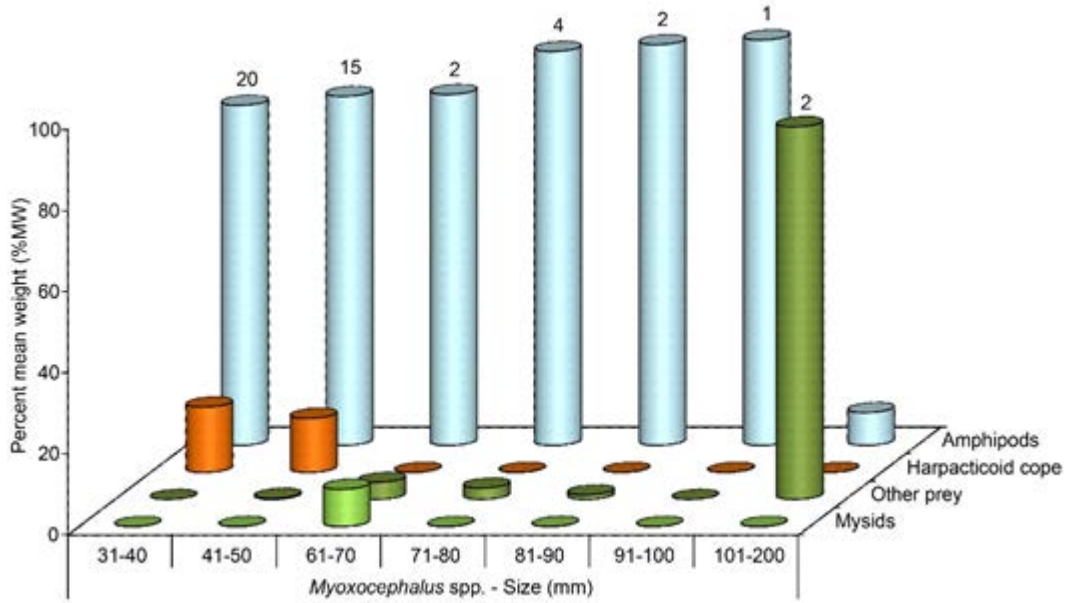


Figure 7.12 *Myoxocephalus* spp. diet composition plotted by 10 to 100 mm size bins to visualize changes in diet with increasing body size. Prey groups along the z-axis are listed from lowest-pooled contribution by %MW (front) to greatest-pooled contribution by %MW (rear). Only prey groups consumed by *Myoxocephalus* spp. are included along the z-axis. Sample sizes are listed above the rear column.

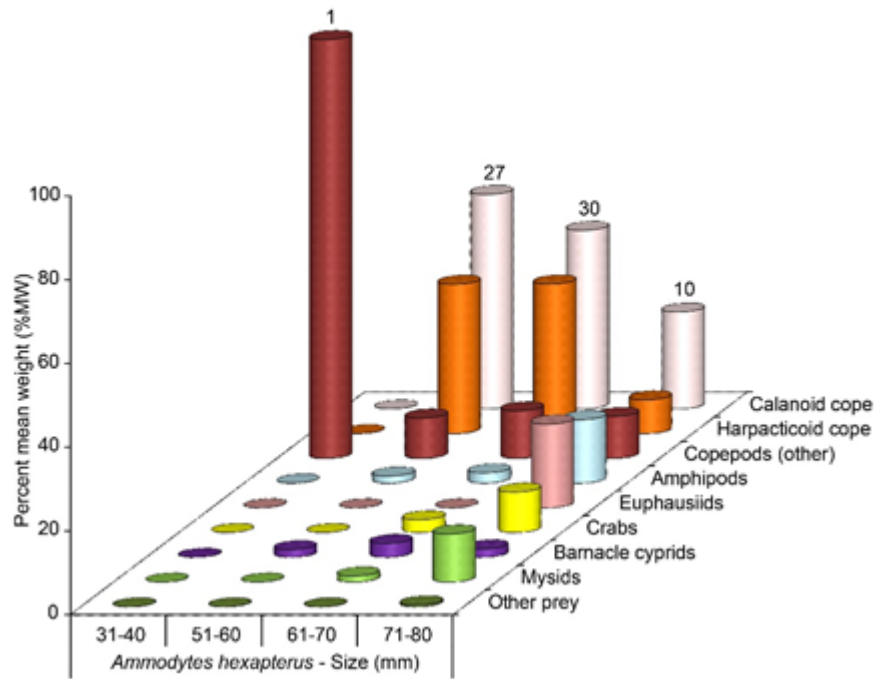


Figure 7.13 A. *hexapterus* diet composition plotted by 10 mm size bins to visualize changes in diet with increasing body size. Prey groups along the z-axis are listed from lowest-pooled contribution by %MW (front) to greatest-pooled contribution by %MW (rear). Only prey groups consumed by *A. hexapterus* are included along the z-axis. Sample sizes are listed above the rear column.

Table 7.1 Common prey items of *C. sardinelli*, *M. villosus*, *O. mordax*, *B. saida*, *E. gracilis*, *Myoxocephalus* spp., *L. fabricii*, *S. punctatus*, and *A. hexapterus* as detailed by historical sources. Each fish species was collected during ACES 2013 and 2014.

Fish species	Common prey	Sources
<i>Coregonus sardinella</i>	Benthic copepods, amphipods, diptera, surface insects.	Mann and McCart 1981; Bond and Erickson 1991
<i>Mallotus villosus</i>	Calanoid copepods, euphausiids, mysids, cladocerans	Kuznetsova 1997; Wilson et al. 2006
<i>Osmerus mordax</i>	Calanoid copepods, amphipods, mysids, cladocerans	Haldorson and Craig 1984; Mills et al. 1995
<i>Boreogadus saida</i>	Calanoid copepods, amphipods, euphausiids, cumaceans, mysids	Lowry and Frost 1981; Craig et al. 1982; Coyle et al. 1997; Gray et al. 2016a
<i>Eleginus gracilis</i>	Benthic amphipods, shrimps, crabs, euphausiids, polychaetes	Coyle et al. 1997; Kuznetsova 1997
<i>Myoxocephalus</i> spp.	Amphipods, crabs, shrimps, polychaetes	Atkinson and Percy 1992, Gray et al. 2016b
<i>Lumpenus fabricii</i>	Benthic copepods, amphipods, polychaetes, bivalve siphons	Atkinson and Percy 1992
<i>Stichaeus punctatus</i>	Calanoid copepods, benthic copepods, euphausiids, polychaetes	Keats et al. 1993
<i>Ammodytes hexapterus</i>	Calanoid copepods, benthic copepods, amphipods, euphausiids	Khudya et al. 1996; Purcell and Sturdevant 2001

Table 7.2 Common predators of *C. sardinelli*, *M. villosus*, *O. mordax*, *B. saida*, *E. gracilis*, *Myoxocephalus* spp., *L. fabricii*, *S. punctatus*, and *A. hexapterus* as detailed by historical sources. Each fish species was collected during ACES 2013 and 2014.

Fish species	Common predators	Sources
<i>Coregonus sardinella</i>	Beluga whales, birds of prey, fishes (e.g., Salmonidae and Gadidae)	Morrow 1980; Dehn et al. 2007; Loseto et al. 2009
<i>Mallotus villosus</i>	Ice seals, seabirds, fishes (e.g., Gadidae, Cottidae, and Zoarcidae)	Jewett 1978; Springer et al. 1984, Tokranov 1985; Valtysson 1995; Dehn et al. 2007
<i>Osmerus mordax</i>	Beluga whales, ice seals, seabirds, shore birds, fishes (e.g., Salmonidae and Percidae)	Scott and Crossman 1973; Springer et al. 1984, Dehn et al. 2007; Loseto et al. 2009
<i>Boreogadus saida</i>	Beluga whales, ice seals, seabirds, fishes (e.g., cannibalism, Pleuronectidae)	Bain and Sekerak 1978; Springer et al. 1984, Bowering and Lilly 1992, Dehn et al. 2007; Loseto et al. 2009
<i>Eleginus gracilis</i>	Beluga whales, ice seals, seabirds, fishes (e.g., Pleuronectidae and Cottidae)	Jewett and Feder 1980; Springer et al. 1984, Tokranov and Maksimenkov 1995; Dehn et al. 2007; Loseto et al. 2009
<i>Myoxocephalus</i> spp.	Seals, seabirds, gadid fishes	Barrett 1991; Hall et al. 1998; Gray et al. 2016b
<i>Lumpenus fabricii</i>	Gadid and pleuronectid fishes	Jewett and Feder 1980; Yang and Nelson 1999
<i>Stichaeus punctatus</i>	Gadid fishes	Mikhail and Welch 1989
<i>Ammodytes hexapterus</i>	Ice seals, seabirds, fishes (e.g., cannibalism, Cottidae, Pleuronectidae, Salmonidae; Sebastidae)	Springer et al. 1984, Rosenthal et al. 1988; Khudya 1993; , Tokranov and Maksimenkov 1995; Yang and Nelson 1999; Dehn et al. 2007

Table 7.3 Percent mean weight (%MW) of prey consumed by nine fish species throughout the Beaufort Sea, Chukchi Sea, and Elson Lagoon regions during ACES 2013 and 2014. Fish species, along with the 10 prey groups, are listed in phylogenetic order. Samples sizes (n) of stomachs containing prey are listed underneath corresponding species. Listed in italics below prey groups are total stomachs (both empty and prey-containing) and counts of empty stomachs.

Prey groups	<i>C. sardinella</i> (n=34)	<i>M. villosus</i> (n=41)	<i>O. mordax</i> (n=48)	<i>B. saida</i> (n=33)	<i>E. gracilis</i> (n=55)
Harpacticoid cope.	4	32	27	10	29
Calanoid cope.	12	57	19	67	53
Copepods (other)	15	2	6	1	5
Barnacle cyprids	3	<1	–	7	3
Amphipods	16	3	2	5	6
Crabs	4	–	2	5	1
Euphausiids	21	–	–	2	1
Mysids	3	6	36	1	2
Diptera	17	–	–	–	–
Other prey	4	–	7	2	2
Unidentified ^b	13	27	40	29	7
<i>Total stomachs^c</i>	<i>34</i>	<i>55</i>	<i>60</i>	<i>34</i>	<i>56</i>
<i>Empty stomachs</i>	<i>0</i>	<i>14</i>	<i>12</i>	<i>1</i>	<i>1</i>

Continued- Prey groups	<i>Myox</i> ^a spp. (n=60)	<i>L. fabricii</i> (n=20)	<i>S. punctatus</i> (n=48)	<i>A. hexapterus</i> (n=75)
Harpacticoid cope	13	66	27	31
Calanoid cope	–	18	10	42
Copepods (other)	<1	15	35	13
Barnacle cyprids	–	–	4	2
Amphipods	82	–	2	4
Crabs	–	–	11	3
Euphausiids	–	–	–	3
Mysids	<1	–	–	2
Diptera	–	–	–	–
Other prey	4	1	11	<1
Unidentified ^b	33	10	64	11
<i>Total stomachs</i> ^c	<i>61</i>	<i>23</i>	<i>63</i>	<i>79</i>
<i>Empty stomachs)</i>	<i>1</i>	<i>3</i>	<i>15</i>	<i>4</i>

^a Includes a combination of sculpin species belonging to the genus, *Myoxocephalus*

^b Unidentifiable prey were not included in percent mean weight calculations so that these values would not deflate the contribution of identifiable prey to the fishes' diets.

^c Includes empty stomachs (if present).

Table 7.4 Counts of prey eaten by nine fish species throughout the Beaufort Sea, Chukchi Sea, and Elson Lagoon regions during ACES 2013 and 2014. Prey counts are summarized by 11 prey groups, including an unidentified category. Samples sizes (n) of stomachs containing prey are listed underneath corresponding species. Percent contribution by number of a particular prey group ((count of prey in a particular group / total number of identifiable prey)*100) is listed in parentheses adjacent to count information. Fish species and prey groups are listed in phylogenetic order.

Prey groups	<i>C. sardinella</i> (n=34)	<i>M. villosus</i> (n=41)	<i>O. mordax</i> (n=48)	<i>B. saida</i> (n=33)	<i>E. gracilis</i> (n=55)
Harpacticoid cope	3,248 (22)	123 (25)	133 (35)	161 (34)	2,553 (66)
Calanoid cope	2,618 (18)	360 (73)	41 (11)	274 (58)	745 (19)
Copepods (other)	7,137 (49)	1 (<1)	5 (1)	9 (2)	395 (10)
Barnacle cyprids	113 (1)	1 (<1)	–	4 (1)	9 (<1)
Amphipods	337 (2)	3 (1)	21 (6)	4 (1)	8 (<1)
Crabs	10 (<1)	–	1 (<1)	13 (3)	3 (<1)
Euphausiids	373 (3)	–	–	2 (<1)	1 (<1)
Mysids	12 (<1)	3 (1)	165 (43)	2 (<1)	3 (<1)
Diptera	609 (4)	–	–	–	–
Other prey	38 (<1)	–	14 (4)	1 (<1)	133 (3)
Unidentified ^b	15	15	25	17	24
<i>Total number of prey</i>	<i>14,510</i>	<i>506</i>	<i>405</i>	<i>487</i>	<i>3,874</i>

Continued- Prey groups	<i>Myox</i> ^a spp. (n=60)	<i>L. fabricii</i> (n=20)	<i>S. punctatus</i> (n=48)	<i>A. hexapterus</i> (n=75)
Harpacticoid cope	68 (34)	952 (97)	74 (63)	2,770 (55)
Calanoid cope	–	14 (1)	3 (3)	1,717 (34)
Copepods (other)	1 (1)	15 (2)	31 (26)	516 (10)
Barnacle cyprids	–	–	1 (1)	24 (<1)
Amphipods	117 (59)	–	1 (1)	11 (<1)
Crabs	–	–	3 (3)	12 (<1)
Euphausiids	–	–	–	6 (<1)
Mysids	1 (1)	–	–	3 (<1)
Diptera	–	–	–	–
Other prey	11 (6)	2 (<1)	4 (3)	5 (<1)
Unidentified ^b	27	5	39	21
<i>Total number of prey</i>	<i>225</i>	<i>988</i>	<i>156</i>	<i>5,085</i>

^a Includes a combination of sculpin species belonging to the genus, *Myoxocephalus*

^b Unidentifiable prey was not included in percent count information so that these values would not deflate the contribution of identifiable prey to the fishes' diets.

Table 7.5 Results from overall permutational multivariate analysis of variance (PERMANOVA) relating fish species and region (Beaufort Sea, Chukchi Sea, Elson Lagoon) to fish diet compositions. Information in the table is abbreviated as follows: df = degrees of freedom, SS = sum of squares, MS = mean sum of squares, Pseudo-F = F statistic analogous to that of ANOVA, P(perm) = p-values (significant <0.05) determined by permutation, perms = number of permutations used in determining p-values. Significant values are bolded.

Source	df	SS	MS	Pseudo-F	P(perm)	Perms
Species	8	232820	29103	14.329	0.001	999
Region	2	10391	5195.7	2.5582	0.017	998
Species:Region	15	74590	4972.7	2.4484	0.001	998
Residuals	312	633660	2031			
Total	337	1047900				

Table 7.6 Results from PERMANOVA and post-hoc comparisons exploring the interaction between regions and species (see Table 6.5). This table details the interspecific differences in diet compositions within the Beaufort Sea, Chukchi Sea, and Elson Lagoon regions. PERMANOVA was used to determine differences between all species' diets within a specific region. Post-hoc comparisons (denoted by a t-value) were developed to determine significant differences in diet compositions between all possible pairs of species within a region. Significant values are bolded, nearly significant values (i.e., $p > 0.05$ but < 0.10) are italicized.

Interspecific analysis	PERMANOVA or post-hoc comparisons					
Within regions – between species (PERMANOVA)	df	SS	MS	Pseudo-F	P(perm)	Perms
Beaufort Sea	8	118290	14787	7.4004	0.001	996
Chukchi Sea	7	146320	20904	12.751	0.001	997
Elson Lagoon	8	115390	14423	5.3297	0.001	998
Post-hoc comparisons within regions – between species						
Species within the Beaufort Sea region				<i>t-value</i>	<i>P(perm)</i>	<i>Perms</i>
<i>Ammodytes hexapterus, Boreogadus saida</i>				2.076	0.005	998
<i>Ammodytes hexapterus, Coregonus sardinella</i>				3.285	0.001	981
<i>Ammodytes hexapterus, Eleginus gracilis</i>				1.079	0.334	998
<i>Ammodytes hexapterus, Lumpenus fabricii</i>				<i>1.573</i>	<i>0.064</i>	962
<i>Ammodytes hexapterus, Mallotus villosus</i>				0.798	0.702	156
<i>Ammodytes hexapterus, Myoxocephalus spp.</i>				3.630	0.001	995
<i>Ammodytes hexapterus, Osmerus mordax</i>				1.185	0.237	729
<i>Ammodytes hexapterus, Stichaeus punctatus</i>				1.687	0.017	997
<i>Boreogadus saida, Coregonus sardinella</i>				8.063	0.001	376
<i>Boreogadus saida, Eleginus gracilis</i>				3.012	0.001	718
<i>Boreogadus saida, Lumpenus fabricii</i>				4.371	0.001	316
<i>Boreogadus saida, Mallotus villosus</i>				2.650	0.021	22

<i>Boreogadus saida, Myoxocephalus spp.</i>	6.193	0.001	205
<i>Boreogadus saida, Osmerus mordax</i>	3.715	0.010	63
<i>Boreogadus saida, Stichaeus punctatus</i>	3.139	0.001	715
<i>Coregonus sardinella, Eleginus gracilis</i>	7.911	0.001	790
<i>Coregonus sardinella, Lumpenus fabricii</i>	4.639	0.003	140
<i>Coregonus sardinella, Mallotus villosus</i>	3.588	0.045	22
<i>Coregonus sardinella, Myoxocephalus spp.</i>	4.438	0.001	189
<i>Coregonus sardinella, Osmerus mordax</i>	3.745	0.002	113
<i>Coregonus sardinella, Stichaeus punctatus</i>	2.601	0.001	621
<i>Eleginus gracilis, Lumpenus fabricii</i>	2.086	0.013	709
<i>Eleginus gracilis, Mallotus villosus</i>	1.179	0.316	45
<i>Eleginus gracilis, Myoxocephalus spp.</i>	5.189	0.001	645
<i>Eleginus gracilis, Osmerus mordax</i>	1.261	0.247	264
<i>Eleginus gracilis, Stichaeus punctatus</i>	2.291	0.003	909
<i>Lumpenus fabricii, Mallotus villosus</i>	0.823	0.477	17
<i>Lumpenus fabricii, Myoxocephalus spp.</i>	3.547	0.001	86
<i>Lumpenus fabricii, Osmerus mordax</i>	0.515	0.788	41
<i>Lumpenus fabricii, Stichaeus punctatus</i>	1.509	0.086	364
<i>Mallotus villosus, Myoxocephalus spp.</i>	1.473	0.084	12
<i>Mallotus villosus, Osmerus mordax</i>	0.405	0.866	8
<i>Mallotus villosus, Stichaeus punctatus</i>	1.045	0.387	37
<i>Myoxocephalus spp., Osmerus mordax</i>	2.807	0.011	27
<i>Myoxocephalus spp., Stichaeus punctatus</i>	2.619	0.002	380

<i>Osmerus mordax</i> , <i>Stichaeus punctatus</i>	1.344	0.113	141
<i>Within the Chukchi Sea region</i>	<i>t-value</i>	<i>P(perm)</i>	<i>Perms</i>
<i>Ammodytes hexapterus</i> , <i>Boreogadus saida</i>	2.501	0.003	999
<i>Ammodytes hexapterus</i> , <i>Eleginus gracilis</i>	1.429	0.121	999
<i>Ammodytes hexapterus</i> , <i>Lumpenus fabricii</i>	0.950	0.416	993
<i>Ammodytes hexapterus</i> , <i>Mallotus villosus</i>	1.795	0.054	999
<i>Ammodytes hexapterus</i> , <i>Myoxocephalus spp.</i>	8.031	0.001	999
<i>Ammodytes hexapterus</i> , <i>Osmerus mordax</i>	0.506	0.759	981
<i>Ammodytes hexapterus</i> , <i>Stichaeus punctatus</i>	1.766	0.054	990
<i>Boreogadus saida</i> , <i>Eleginus gracilis</i>	1.685	0.056	999
<i>Boreogadus saida</i> , <i>Lumpenus fabricii</i>	1.659	0.061	584
<i>Boreogadus saida</i> , <i>Mallotus villosus</i>	1.138	0.253	968
<i>Boreogadus saida</i> , <i>Myoxocephalus spp.</i>	6.035	0.001	997
<i>Boreogadus saida</i> , <i>Osmerus mordax</i>	0.889	0.459	354
<i>Boreogadus saida</i> , <i>Stichaeus punctatus</i>	2.646	0.003	593

Interspecific analysis	PERMANOVA or post-hoc comparisons		
<i>Within the Chukchi Sea region – continued from above</i>	<i>t-value</i>	<i>P(perm)</i>	<i>Perms</i>
<i>Eleginus gracilis</i> , <i>Lumpenus fabricii</i>	0.821	0.533	996
<i>Eleginus gracilis</i> , <i>Mallotus villosus</i>	Negative ^a		
<i>Eleginus gracilis</i> , <i>Myoxocephalus spp.</i>	8.108	0.001	999
<i>Eleginus gracilis</i> , <i>Osmerus mordax</i>	Negative ^a		

<i>Eleginus gracilis, Stichaeus punctatus</i>	2.361	0.008	991
<i>Lumpenus fabricii, Mallotus villosus</i>	0.293	0.826	339
<i>Lumpenus fabricii, Myoxocephalus spp.</i>	6.558	0.001	576
<i>Lumpenus fabricii, Osmerus mordax</i>	Negative ^a		
<i>Lumpenus fabricii, Stichaeus punctatus</i>	1.322	0.211	49
<i>Mallotus villosus, Myoxocephalus spp.</i>	6.947	0.001	996
<i>Mallotus villosus, Osmerus mordax</i>	0.387	0.701	153
<i>Mallotus villosus, Stichaeus punctatus</i>	2.350	0.026	253
<i>Myoxocephalus spp., Osmerus mordax</i>	4.703	0.001	390
<i>Myoxocephalus spp., Stichaeus punctatus</i>	5.966	0.001	428
<i>Osmerus mordax, Stichaeus punctatus</i>	1.699	0.163	41
<i>Within the Elson Lagoon region</i>	<i>t-value</i>	<i>P(perm)</i>	<i>Perms</i>
<i>Ammodytes hexapterus, Coregonus sardinella</i>	1.473	0.036	781
<i>Ammodytes hexapterus, Eleginus gracilis</i>	0.631	0.728	621
<i>Ammodytes hexapterus, Lumpenus fabricii</i>	3.970	0.012	26
<i>Ammodytes hexapterus, Mallotus villosus</i>	0.656	0.752	42
<i>Ammodytes hexapterus, Myoxocephalus spp.</i>	3.140	0.008	68
<i>Ammodytes hexapterus, Osmerus mordax</i>	1.855	0.016	320
<i>Ammodytes hexapterus, Stichaeus punctatus</i>	1.642	0.062	64
<i>Coregonus sardinella, Eleginus gracilis</i>	2.588	0.001	999
<i>Coregonus sardinella, Lumpenus fabricii</i>	2.464	0.002	993
<i>Coregonus sardinella, Mallotus villosus</i>	1.564	0.034	992

<i>Coregonus sardinella, Myoxocephalus spp.</i>	2.512	0.003	999
<i>Coregonus sardinella, Osmerus mordax</i>	2.403	0.001	998
<i>Coregonus sardinella, Stichaeus punctatus</i>	1.255	0.173	998
<i>Eleginus gracilis, Lumpenus fabricii</i>	2.980	0.002	958
<i>Eleginus gracilis, Mallotus villosus</i>	1.250	0.209	964
<i>Eleginus gracilis, Myoxocephalus spp.</i>	4.165	0.001	996
<i>Eleginus gracilis, Osmerus mordax</i>	3.326	0.001	998
<i>Eleginus gracilis, Stichaeus punctatus</i>	2.866	0.001	998
<i>Lumpenus fabricii, Mallotus villosus</i>	3.589	0.017	31
<i>Lumpenus fabricii, Myoxocephalus spp.</i>	4.056	0.003	125
<i>Lumpenus fabricii, Osmerus mordax</i>	2.720	0.001	716
<i>Lumpenus fabricii, Stichaeus punctatus</i>	2.305	0.009	90
<i>Mallotus villosus, Myoxocephalus spp.</i>	3.003	0.001	240
<i>Mallotus villosus, Osmerus mordax</i>	1.739	0.027	790
<i>Mallotus villosus, Stichaeus punctatus</i>	1.968	0.010	234
<i>Myoxocephalus spp., Osmerus mordax</i>	2.990	0.001	993
<i>Myoxocephalus spp., Stichaeus punctatus</i>	2.859	0.001	384
<i>Osmerus mordax, Stichaeus punctatus</i>	2.155	0.008	951

^aPRIMER does not report negative t-values; see Figure 6.5 to approximate differences between these species.

Table 7.7 Percent mean weight (%MW) of prey consumed by nine fish species in the Beaufort Sea during ACES 2013 and 2014. Fish species, along with the 10 prey groups, are listed in phylogenetic order. Samples sizes (n) of stomachs containing prey are listed underneath corresponding species. Listed in italics below prey groups are total stomachs (both empty and prey-containing) and counts of empty stomachs.

Prey groups	<i>C. sardinella</i> (n=6)	<i>M. villosus</i> (n=2)	<i>O. mordax</i> (n=7)	<i>B. saida</i> (n=11)	<i>E. gracilis</i> (n=9)
Harpacticoid cope	–	26	63	–	32
Calanoid cope	–	49	25	86	58
Copepods (other)	–	–	–	2	6
Barnacle cyprids	–	–	–	5	2
Amphipods	2	25	–	5	–
Crabs	–	–	13	–	–
Euphausiids	87	–	–	–	–
Mysids	–	–	–	3	–
Diptera	–	–	–	–	–
Other prey	11	–	–	–	1
Unidentified ^b	8	–	50	22	21
<i>Total stomachs^c</i>	6	2	11	11	9
<i>Empty stomachs</i>	0	0	4	0	0

Continued- Prey groups	<i>Myox</i> ^a spp. (n=12)	<i>L. fabricii</i> (n=6)	<i>S. punctatus</i> (n=19)	<i>A. hexapterus</i> (n=19)
Harpacticoid cope	18	58	12	16
Calanoid cope	–	17	11	42
Copepods (other)	–	25	33	9
Barnacle cyprids	–	–	–	2
Amphipods	82	–	4	4
Crabs	–	–	11	9
Euphausiids	–	–	–	11
Mysids	–	–	–	8
Diptera	–	–	–	–
Other prey	–	–	28	–
Unidentified ^b	21	17	67	5
<i>Total stomachs</i> ^c	<i>12</i>	<i>6</i>	<i>22</i>	<i>20</i>
<i>Empty stomachs</i>	<i>0</i>	<i>0</i>	<i>3</i>	<i>1</i>

^a Includes a combination of sculpin species belonging to the genus, *Myoxocephalus*

^b Unidentifiable prey was not included in percent mean weight calculations so that these values would not deflate the contribution of identifiable prey to the fishes' diets.

^c Includes empty stomachs (if present).

Table 7.8 Percent mean weight (%MW) of prey consumed by nine fish species in the Chukchi Sea during ACES 2013 and 2014. Fish species, along with the 10 prey groups, are listed in phylogenetic order. Samples sizes (n) of stomachs containing prey are listed underneath corresponding species. Listed in italics below prey groups are total stomachs (both empty and prey-containing) and counts of empty stomachs.

Prey groups	<i>C. sardinelli</i> (n=0)	<i>M. villosus</i> (n=26)	<i>O. mordax</i> (n=5)	<i>B. saida</i> (n=20)	<i>E. gracilis</i> (n=29)
Harpacticoid cope	–	36	40	18	31
Calanoid cope	–	58	50	58	50
Copepods (other)	–	2	10	<1	6
Barnacle cyprids	–	–	–	8	1
Amphipods	–	–	–	–	4
Crabs	–	–	–	9	1
Euphausiids	–	–	–	4	2
Mysids	–	4	–	–	3
Diptera	–	–	–	–	–
Other prey	–	–	–	3	2
Unidentified ^b	–	11	17	28	5
<i>Total stomachs^c</i>		<i>27</i>	<i>7</i>	<i>21</i>	<i>30</i>
<i>Empty stomachs</i>		<i>1</i>	<i>2</i>	<i>1</i>	<i>1</i>

Continued- Prey groups	<i>Myox</i> ^a spp. (n=34)	<i>L. fabricii</i> (n=7)	<i>S. punctatus</i> (n=11)	<i>A. hexapterus</i> (n=50)
Harpacticoid cope	9	59	70	38
Calanoid cope	–	36	13	40
Copepods (other)	<1	2	17	14
Barnacle cyprids	–	–	–	3
Amphipods	87	–	–	4
Crabs	–	–	–	<1
Euphausiids	–	–	–	–
Mysids	–	–	–	<1
Other prey	4	4	–	<1
Unidentified ^b	32	6	61	7
<i>Total stomachs</i> ^c	35	7	18	52
<i>Empty stomachs (%O)</i>	1	0	7	2

^a Includes a combination of sculpin species belonging to the genus, *Myoxocephalus*

^b Unidentifiable prey was not included in percent mean weight calculations so that these values would not deflate the contribution of identifiable prey to the fishes' diets.

^c Includes empty stomachs (if present).

Table 7.9 Percent mean weight (%MW) of prey consumed by nine fish species in Elson Lagoon during ACES 2013 and 2014. Fish species, along with the 10 prey groups, are listed in phylogenetic order. Samples sizes (n) of stomachs containing prey are listed underneath corresponding species. Listed in italics below prey groups are total stomachs (both empty and prey-containing) and counts of empty stomachs.

Row Labels	<i>C. sardinella</i> (n=28)	<i>M. villosus</i> (n=13)	<i>O. mordax</i> (n=36)	<i>B. saida</i> (n=2)	<i>E. gracilis</i> (n=17)
Harpacticoid cope	4	17	18	0	23
Calanoid cope	15	57	11	0	55
Copepods (other)	18	0	7	0	2
Barnacle cyprids	4	1	0	0	5
Amphipods	19	11	3	100	11
Crabs	5	0	0	0	0
Euphausiids	6	0	0	0	0
Mysids	4	15	51	0	0
Diptera	21	0	0	0	0
Other prey	3	0	10	0	3
Unidentified ^b	14	62	41	75	3
<i>Total stomachs^c</i>	28	26	42	2	17
<i>Empty stomachs</i>	0	13	6	0	0

Continued- Prey groups	<i>Myox</i> ^a spp. (n=14)	<i>L. fabricii</i> (n=7)	<i>S. punctatus</i> (n=18)	<i>A. hexapterus</i> (n=6)
Harpacticoid cope	18	81	13	14
Calanoid cope	0	0	6	80
Copepods (other)	0	19	50	6
Barnacle cyprids	0	0	13	0
Amphipods	71	0	0	0
Crabs	0	0	19	0
Euphausiids	0	0	0	0
Mysids	2	0	0	0
Diptera	0	0	0	0
Other prey	10	0	0	0
Unidentified ^b	44	14	64	64
<i>Total stomachs</i> ^c	<i>14</i>	<i>10</i>	<i>23</i>	<i>7</i>
<i>Empty stomachs</i> (%0)	<i>0</i>	<i>3</i>	<i>5</i>	<i>1</i>

^a Includes a combination of sculpin species belonging to the genus, *Myoxocephalus*

^b Unidentifiable prey was not included in percent mean weight calculations so that these values would not deflate the contribution of identifiable prey to the fishes' diets.

^c Includes empty stomachs (if present).

Table 7.10 Results from PERMANOVA and post-hoc comparisons exploring the interaction between species and regions (see Table 6.5). This table details the intraspecific differences in diet compositions across the Beaufort Sea, Chukchi Sea, and Elson Lagoon regions. PERMANOVA was used to determine if similar species' diets significantly differed between the three regions. Post-hoc comparisons were developed to determine significant differences in similar species' diet compositions between all possible pairs of regions. Significant values are bolded.

<i>Intraspecific</i>						
<i>Species across regions (PERMANOVA)</i>	<i>df</i>	<i>SS</i>	<i>MS</i>	<i>Pseudo-F</i>	<i>P(perm)</i>	<i>Perms</i>
<i>Coregonus sardinelli</i>	1	23127	23127	7.364	0.001	999
<i>Mallotus villosus</i>	2	4249.7	2124.9	0.937	0.403	838
<i>Osmerus mordax</i>	2	18548	9273.8	2.990	0.009	995
<i>Boreogadus saida</i>	1	5306.6	5306.6	2.884	0.021	884
<i>Eleginus gracilis</i>	2	839.24	419.62	0.309	0.902	998
<i>Myoxocephalus spp.</i>	2	1023.4	511.71	0.391	0.721	998
<i>Lumpenus fabricii</i>	2	3184.6	1592.3	1.716	0.185	544
<i>Stichaeus punctatus</i>	2	16066	8032.8	2.543	0.021	992
<i>Ammodytes hexapterus</i>	2	8759	4379.5	2.242	0.041	998
 <i>Post-hoc comparisons within species – between regions</i>						
<i>Coregonus sardinelli</i>				t-value	P(perm)	Perms
Beaufort, Elson Lagoon				2.713	0.001	997
 <i>Osmerus mordax</i>				t-value	P(perm)	Perms
Beaufort, Chukchi				0.779	0.482	19
Beaufort, Elson Lagoon				1.739	0.035	411
Chukchi, Elson Lagoon				1.904	0.023	581

<i>Boreogadus saida</i>	t-value	P(perm)	Perms
Beaufort, Chukchi	1.698	0.041	901

<i>Stichaeus punctatus</i>	t-value	P(perm)	Perms
Beaufort, Chukchi	1.912	0.008	364
Beaufort, Elson Lagoon	0.898	0.505	386
Chukchi, Elson Lagoon	2.132	0.019	152

<i>Ammodytes hexapterus</i>	t-value	P(perm)	Perms
Beaufort, Chukchi	1.979	0.014	999
Beaufort, Elson Lagoon	0.666	0.854	582
Chukchi, Elson Lagoon	0.864	0.522	796

Table 7.11 Results from PERMANOVA, used to examine the effect of fish body size on diet composition. All specimens were pooled by species, with fish length included as a covariate. A significant difference (boldface) indicates that a species diet differed across the size ranges of individuals collected by this study.

Size-based – PERMANOVA - length as a covariate	Df	SS	Pseudo-F	P(perm)	Perms
<i>Coregonus sardinelli</i>	1	2923.2	0.771	0.576	999
<i>Mallotus villosus</i>	1	9283.6	4.392	0.028	999
<i>Osmerus mordax</i>	1	20959	7.243	0.002	999
<i>Boreogadus saida</i>	1	4736.6	2.967	0.048	998
<i>Eleginus gracilis</i>	1	877.9	0.661	0.495	999
<i>Myoxocephalus spp.</i>	1	5577.7	5.328	0.026	998
<i>Lumpenus fabricii</i>	1	769.3	1.395	0.252	925
<i>Stichaeus punctatus</i>	1	6362.7	1.834	0.136	999
<i>Ammodytes hexapterus</i>	1	7001.5	3.728	0.023	999

8.0 Prey Quality of Arctic Marine Fish

J. Vollenweider, R. Heintz, L. Sousa, R. Bradshaw

8.1 Introduction

Food web modeling will be an integral tool in predicting how Arctic marine ecosystems will change in the light of climate change. The Arctic is warming faster than the rest of the globe as a result of polar amplification and feedback processes associated with melting sea ice, incurring immediate and pronounced climatological effects relative to the rest of the globe (Screen and Simmonds 2010). Warming conditions and cascading environmental effects (ice melting, increases in precipitation, increased storm activity) have already been linked to changes in marine Arctic community composition. Northward range extensions of fish species have been documented in the Chukchi and Beaufort Seas and will likely continue (Rand and Logerwell 2010; Mecklenburg et al. 2007). Arctic fish species are also expected to adapt differentially to changing conditions, with some species such as saffron cod being more resilient to warming conditions, and others such as Arctic cod faring poorly with reductions in growth (Laurel et al. 2016). How changes in fish community composition affect piscivorous fish and their marine mammal and seabird predators is relatively unexplored (See table 6.2). Changes in species composition of fishes may have complex cumulative and synergistic effects that cannot be assessed without the inclusion of bioenergetic considerations. For example, laboratory studies of Steller sea lions and northern fur seals found they were not able to compensate for a lack of high-lipid/high-energy prey by consuming more biomass or a diversity of low-quality prey species (Gomez et al. 2016, Rosen and Trites 2000). Therefore food web modeling will be an important predictive tool to understand predator-prey relationships and energy flow under different scenarios, providing a holistic means to evaluate how Arctic fish and their predators may fare with climate change.

Food web models rely on accurate quantification of fish condition parameters which are sparse to nonexistent. Modeling efforts, in particular for marine mammals, have been forced to rely on literature values from disparate locations (Bluhm and Gradinger 2007). We provide a library of the energetic condition measures of the most abundant Arctic fish species caught in the Chukchi and Beaufort Seas in an effort to provide accurate data for use in food web and other bioenergetic models.

8.2 Methods

8.2.1 Fish Collections

Fish were collected from the U.S. waters of the Chukchi Sea, the western Beaufort Sea and Elson Lagoon between 2005 and 2015 from multiple surveys, including 1) Ecology of Forage Fishes in the Arctic Nearshore (AFF), 2) The Arctic Coastal Ecosystem Survey (ACES), 3) ArcticEis, and 4) Shelf Habitat and EcoLogy of Fish and Zooplankton (SHELFZ) (Figure 8.1). Sampling timing and fishing methodology varied by project (Table 8.1). Greater detail on fishing techniques can be found in Marsh et al. 2016, Norcross et al. 2010, Stauffer 2004, and Thedinga et al. 2013. Generally, five to fifteen fish of each species representative of each catch were retained from each haul/station and frozen. Additional samples were obtained from subsistence collections in Barrow and Kotzebue. In the laboratory, fish were measured, weighed, and stomach contents were removed.

8.2.2 Fish Condition Analyses

Small fish (< 0.5 g) were dried whole to a constant weight then homogenized, while large fish (\geq 0.5 g) were homogenized wet and an aliquot was dried to a constant weight. Drying occurred in either drying ovens set to 60 °C or using a LECO Thermogravimetric Analyzer (TGA) 601 or 701 at 135 °C. A replicate sample was included in each batch of samples when sufficient mass was available, otherwise herring homogenate or purchased meat standards (NIST Meat1546) were replicated (not to exceed 15% from target values). Dried samples were homogenized to a uniform consistency. When fish were too small to accommodate sample sizes needed for chemical analyses, several individuals of relatively similar size were composited by collection.

Energy density (ED; kJ/g dry mass) was measured using bomb calorimetry. Dried homogenates of 30-70 mg (small pellets) or 70-200 mg (large pellets) were pressed into pellets and combusted using a Parr 6725 semi-micro bomb calorimeter using standard instrument operating procedures from the instrument manual. Quality assurance samples with each batch of samples included 1) duplicate benzoic acid standards (not to exceed 0.5% CV for large pellets or 1.5% for small pellets, and 0.5% error from target values for large pellets or 2.0% for small pellets), 2) a sample replicate when sample mass permitted (not to exceed 1.5 STDEV for both large and small pellets), and 3) a tissue reference sample (not to exceed 2.75% error from the target value for large pellets or 3.0% error for small pellets). Energy densities were converted to a wet-mass basis using moisture content. Total energy (kJ) was calculated as energy density x wet mass.

8.3 Results

Pacific herring were the most energy-rich (7.98 ± 0.32 kJ/g wet mass; mean \pm SE) of the 24 species evaluated, having 2.4 times greater energy density than the most energy-deplete Alaska plaice (3.27 kJ/g) (Table 8.2, Figure 8.2). The three species of cisco were also relatively energy-rich, while all other species were similarly low, only varying by 1.7 kJ/g amongst them. Within families, there was little difference in energy density by species, with the exception that Arctic cod were significantly more energy-rich than the other gadids, being 11% more energy-rich than walleye pollock and 24% more energy-rich than saffron cod (ANOVA $p < 0.000$) (Figure 8.3). The cottids also had some differentiation by species, with Arctic staghorn, belligerent, and Arctic sculpins having approximately 17% higher energy density than shorthorn and fourhorn sculpin (ANOVA $p < 0.000$).

As fish catches were comprised primarily of juvenile fish, correlations between energy density and length could only be evaluated for 5 species which spanned relatively large size ranges. In general, there were moderate positive correlations between fish length and energy density (Table 8.3, Figure 8.4). In contrast, energy density of fourhorn sculpin decreased with length. When the effect of water content was removed, correlations between energy density and length increased slightly on a dry mass basis. For a given increase in length, Pacific herring and capelin increased their energy density at more than twice the rate of the 2 gadids. When compared to their counterparts in the Gulf of Alaska during summer months (July–September) Arctic fish accumulated energy at a slower rate than those in the Gulf of Alaska, evidenced by a significant interaction effect ($P = 0.006$) (Figure 8.5). Similarly, Pacific herring in the Arctic accumulated energy at a slower rate than those in the Gulf of Alaska ($P = 0.002$).

Total energy content (kJ) of individual fish integrates size-related changes in energy density and fish size. Arctic cisco had statistically the greatest energy content per individual fish of all the

species ($2,126.9 \pm 381.6$ kJ, $p < 0.000$), followed by the other 2 species of cisco (Bering cisco: $1,273.2 \pm 461.8$ kJ and least cisco: $1,271.8 \pm 73.5$ kJ) (Figure 8.6). Pacific herring and Alaska plaice were also among the top 5 species with the highest energy content. Within families, the ranking of species by total energy content was different than when energy density was compared (Figure 8.7). For example, on a gram-for-gram comparison, Arctic cod have significantly more energy per gram than walleye pollock or saffron cod. But when the energy density is scaled up to the total energy content of a whole fish, saffron cod have the most energy due to their large size.

Of the top 5 species, the ciscos and Pacific herring had the highest energy densities and were also the largest of the fish, culminating in the greatest total energy content (Figures 8.6–8.8). Alaska plaice, however, had the lowest energy density of all species (though only one animal was analyzed), but the relatively large size of the fish overwhelmed the low energy density, resulting in a high total energy content. The importance of fish size became more pronounced as fish size increased, which could be seen by the clear discrimination between Pacific herring and saffron cod larger than 200 mm (Figure 8.9).

8.4 Discussion

When considering the energy density of the Arctic species examined, the most energy-rich species are not highly abundant nor wide-spread (see Arctic Eis results). For example, Pacific herring were not caught in great abundance north of Norton Sound, and cisco species are limited to brackish waters in lagoon habitats. Pacific sand lance, Arctic staghorn sculpin and rainbow smelt were also caught in low abundance. Therefore the most energy-rich species with a wide distribution and large abundance is Arctic cod. Another very abundant and wide-spread species, capelin, was only 5% lower in energy density than Arctic cod. In contrast, another species of great interest because of its' tolerance of warm waters and potential to thrive with ocean temperature increases is saffron cod (Laurel et al. 2016). If Arctic cod were to diminish in abundance coincident with increases in saffron cod, the concern is that saffron cod are a significantly suboptimal prey having 25% lower energy density than Arctic cod. A caveat to this scenario, however, is that saffron cod are distributed close to the coast and it is unknown if their distribution would expand under warming conditions and become available to offshore predators.

Accounting for fish size and scaling energy up to total energy of an individual fish, the fish species with the greatest total energy content are similarly low in abundance with limited distributions. Again, ciscos and herring have the greatest energy content of the species examined but with distribution limitations discussed above. Alaska plaice and eelpouts are low in abundance, leaving saffron cod as the abundant/widespread species with the greatest total energy content per fish, having 4 times the energy content as an Arctic cod or more than 7 times the energy content of a capelin. From these comparisons, it is plain that a combination of abundance, distribution and fish size must be accounted for when determining the value of a prey species for its predators.

There are some similarities and stark differences between the summertime energetics of the 24 Arctic species examined here compared to more southerly species in Alaska. We conducted a similar study in the Gulf of Alaska (GOA) where we analyzed the energy content of the 23 most abundant marine fish species (Vollenweider et al. 2011). The average energy density of the Arctic species examined in this study were very similar to that of the GOA, ranging from 3.27-

7.98 kJ/g wet mass, while those in the GOA ranged from 3.64-9.78 kJ/g. In contrast, the range of average total energy of fish in the GOA was 14 times as great as Arctic fish (Arctic fish: 0.3-2,127 kJ; SEAK: 30-30,624 kJ). This stark difference is due to the large size discrepancy of abundant fish between the two regions, with the Arctic comprised of many juveniles as well as adult fish of diminutive size.

Only 2 species of fish could be directly compared between the Arctic study and the Gulf of Alaska study. Pacific herring and capelin spanning a large size range were caught in both regions. From the energy density-length relationships, we saw slower energy accumulation with size in the Arctic than in the GOA for both species of fish. This is somewhat of a counterintuitive phenomenon, as one might expect Arctic fish to put on energy at a faster rate during the brief summer months in preparation for the longer, colder Arctic winters. On the other hand, Arctic fish in colder water may have significantly reduced metabolic rates and may therefore require less energy to sustain themselves.

This is the most thorough library of Arctic fish condition and prey quality to date. However, a significant limitation of this dataset is the lack year-round sampling due to substantial logistic constraints imposed by Arctic winters. Pelagic fish species in particular, are known to undergo significant seasonal cycles in energy content in relation to their ontogenetic development, food availability and maturation state (Vollenweider et al. 2011). Generally, there is an increase in energy content during productive summer conditions, followed by a decrease in energy over winter when food is scarce and gonad development may concurrently take place in preparation for spawning. Most extreme are Pacific herring for which energy density (on a wet mass basis) can nearly double from spring minima to fall maxima. Demersal species cycle less, likely due to a more steady-state conditions near the sea floor. To what degree the prey quality of Arctic fish species fluctuates seasonally requires further investigation.

8.5 Acknowledgements

We would like to thank the multiple funding sources that payed for fish collections and energetics analysis, including the North Pacific Research Board (NPRB), the Bureau of Ocean Energy Management (BOEM), North Slope Borough (NSB), and the US Fish and Wildlife Service. The NSB also provided invaluable logistical help that made many of these fish collections possible, in particular Todd Sformo, Craig George, Brian Person, Billy Adams, Robert Suydam and Taqulik Hepa. We also thank the scientists and vessel crew of the ACES, AFF2015, SHELFZ, and ArcticEis projects, in particular Kevin Boswell, Brenda Norcross, Alexei Pinchuk, Franz Meuter, Ed Farley, Kris Cieciel, Libby Logerwell, Sandra Parker-Stetter, and Darcie Neff. Additional key field personnel include Mark Barton, Ann Robertson, and Sam George who spent several summers in Barrow, AK running the beach seining effort, as well as Eric Wood, Alyssa Frothingham, Stella Moser, and Wyatt Fournier. Many people in the lab were instrumental in sample analyses, including Stella Mosher, Corey Fugate, Robert Bradshaw, Matt Callahan, Tayler Jarvis, Sarah Ballard, Bryan Cormack, Aswhin Sreenivasan, Hannah Findlay, Kevin Heffern and Casey Debenham.

8.6 References

Bluhm BA, Gradinger R. 2008. Regional variability in food availability for Arctic marine mammals. *Ecological Applications*. 18:S77-S96.

- Gomez MD, Rosen DAS, Trites AW. 2016. Net energy gained by northern fur seals (*Callorhinus ursinus*) is impacted more by diet quality than by diet diversity. *Can J Zool.* 94:123-135.
- Helser, TE, Colman, JR, Anderl DM, Kastle CR. 2017. Growth dynamics of saffron cod (*Eleginus gracilis*) and Arctic cod (*Boreogadus saida*) in the Northern Bering and Chukchi Seas. *Deep Sea Res. II*, 135:66-77.
- Laurel BJ, Spencer M, Iseri P, Copeman LA. 2016. Temperature-dependent growth and behavior of juvenile Arctic cod (*Boreogadus saida*) and co-occurring North Pacific gadids. *Polar Biology.* 39(6):1127-1135.
- Marsh JM, Mueter FJ, Iken K, Danielson S. 2016. Ontogenetic, spatial and temporal variation in trophic level and diet of Chukchi Sea fishes. *Deep-Sea Res. II*, doi:10.1016/j.dsr2.2016.07.010
- Mecklenburg CW, Stein DL, Sheiko BA, Chernova NV, Mecklenburg TA, Holladay BA. 2007. Russian-American long-term census of the Arctic: benthic fishes trawled in the Chukchi Sea and Bering Strait, August 2004. *Northwestern Naturalist.* 88(3): 168-187.
- Norcross BL, Holladay BA, Busby MS, Mier KL. 2010. Demersal and larval fish assemblages in the Chukchi Sea. *Deep-Sea Res. II*, 57(1-2) :57-70.
- Rand KM, Logerwell EA. 2011. The first demersal trawl survey of benthic fish and invertebrates in the Beaufort Sea since the late 1970s. *Polar Biology.* 34(4):475-488.
- Rosen DA, Trites AW. 2000. Pollock and the decline of Steller sea lions: testing the junk-food hypothesis. *Can J Zool.* 78(7): 1243-1250.
- Screen JA, Simmonds I. 2010. The central role of diminishing sea ice in recent Arctic temperature amplification. *Nature.* 464: 1334-1337.
- Stauffer GD. 2004. NOAA protocols for groundfish bottom trawl surveys of the nation's fishery resources. U.S. Dep. Commer., NOAA Tech. Memo. NMFS-SPO-6, 205.
- Theedinga JF, Johnson SW, Neff AD, Hoffman CA, Maselko JM. 2013. Nearshore fish assemblages of the Northeastern Chukchi Sea, Alaska. *Arctic*, 66(3): 257-268.
- Vollenweider, JJ, Heintz R.A, Schaufler L, Bradshaw R. 2011. Seasonal cycles in whole-body proximate composition and energy content of forage fish vary with water depth. *Mar. Bio.* 158(2): 413-427.

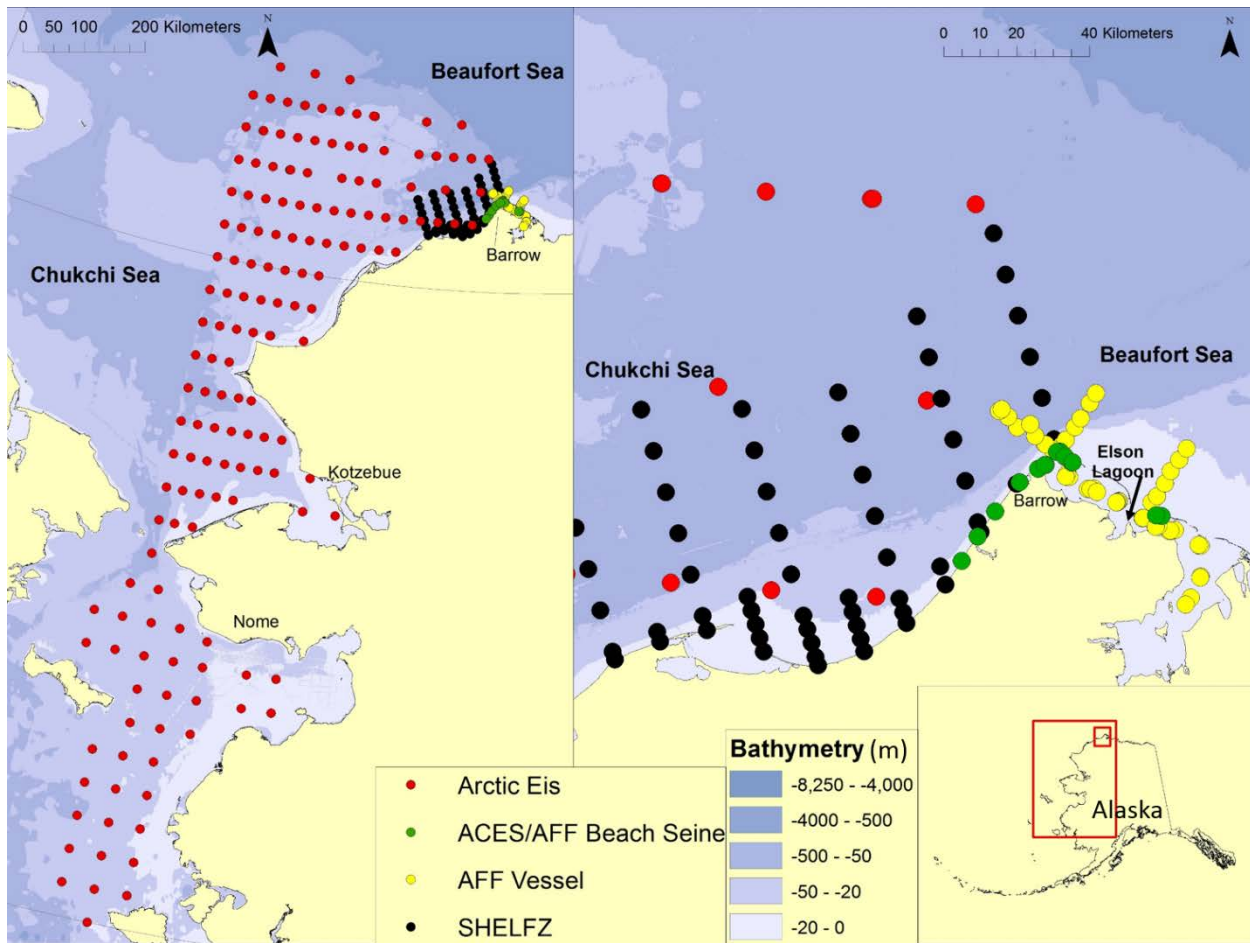


Figure 8.1 Station design of the projects from which samples were obtained , including 1) Ecology of Forage Fishes in the Arctic Nearshore (AFF), 2) The Arctic Coastal Ecosystem Survey (ACES), 3) ArcticEis, and 4) Shelf Habitat and EcoLogY of Fish and Zooplankton (SHELFZ). Additional samples were obtained from subsistence collections in Barrow and Kotzebue.

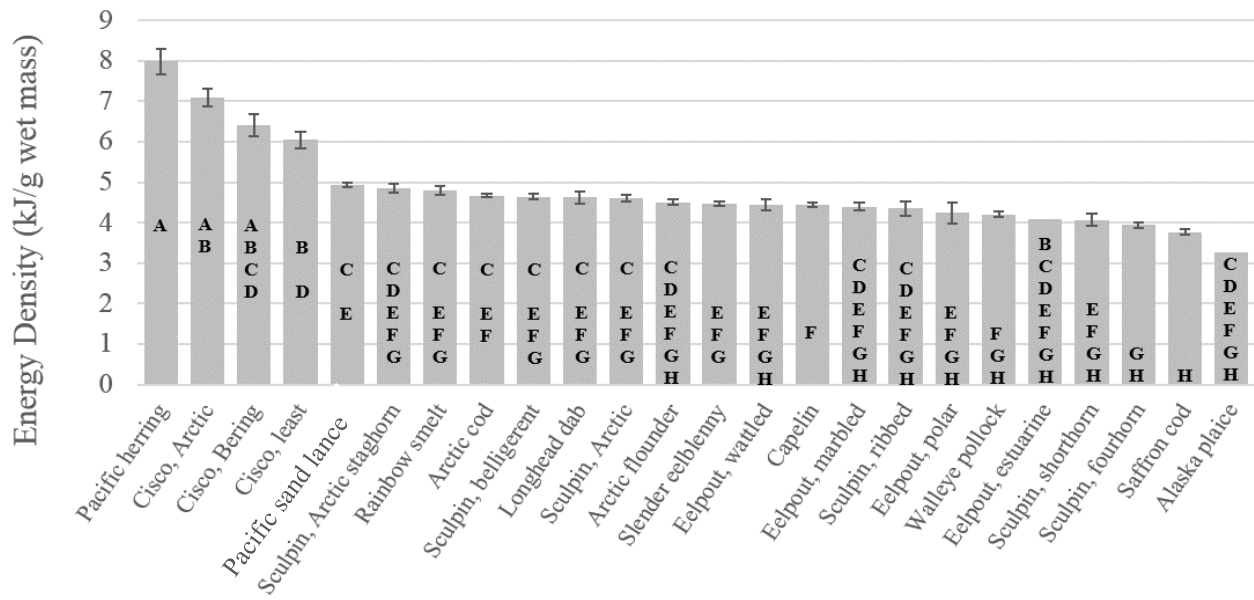


Figure 8.2 Average energy density (kJ/g wet mass) of all sampled Arctic fish species. Like letters indicate statistical similarity determined by ANOVA.

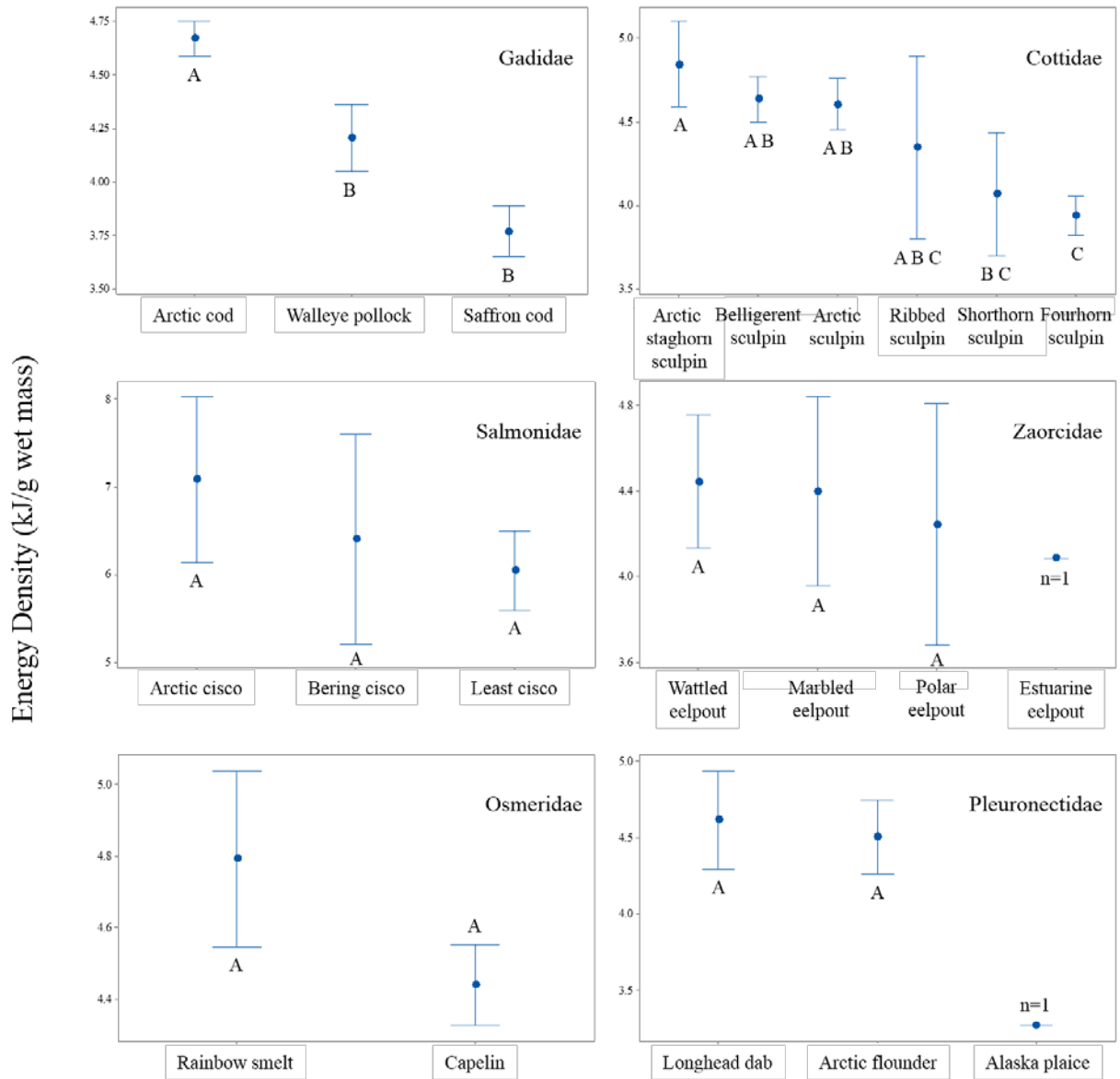


Figure 8.3 Average energy density (kJ/g wet mass) by family of Arctic fish species. Like letters indicate statistical similarity determined by ANOVA.

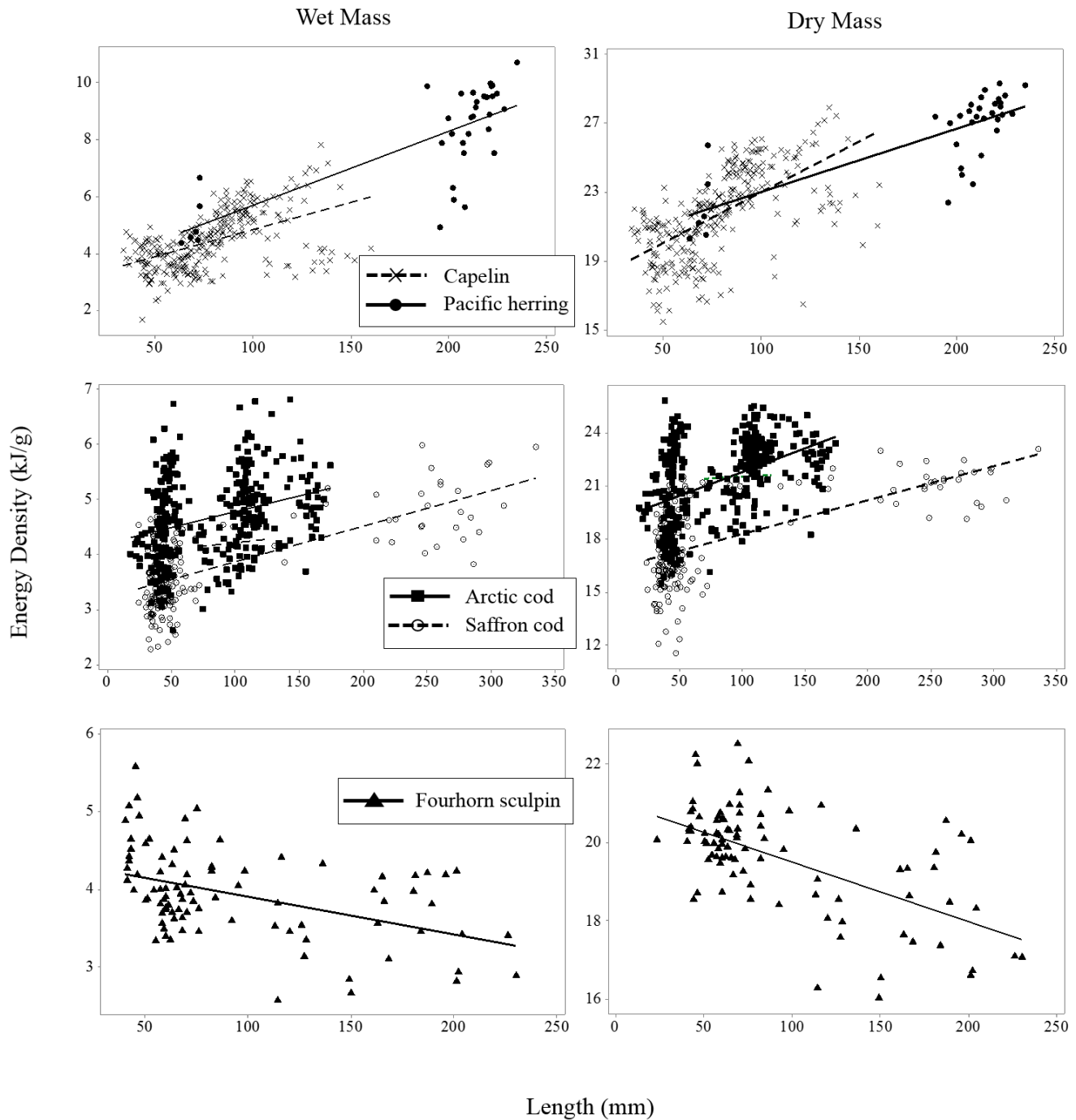


Figure 8.4 Energy density (ED; kJ/g) as a function of length for Arctic fish species. Panels on the left show ED on a wet mass basis (kJ/g wet mass) and panels on the right show ED on a dry mass basis (kJ/g dry mass). The top panels depict linear regressions for capelin ($R^2=0.26$ wet mass, 0.37 dry mass) and Pacific herring ($R^2=0.57$ wet mass, 0.61 dry mass), the central panels depict Arctic cod ($R^2=0.09$ wet mass, 0.20 dry mass) and saffron cod ($R^2=0.47$ wet mass, 0.36 dry mass) and the bottom panels depict fourhorn sculpin ($R^2=0.19$ wet mass, 0.35 dry mass).

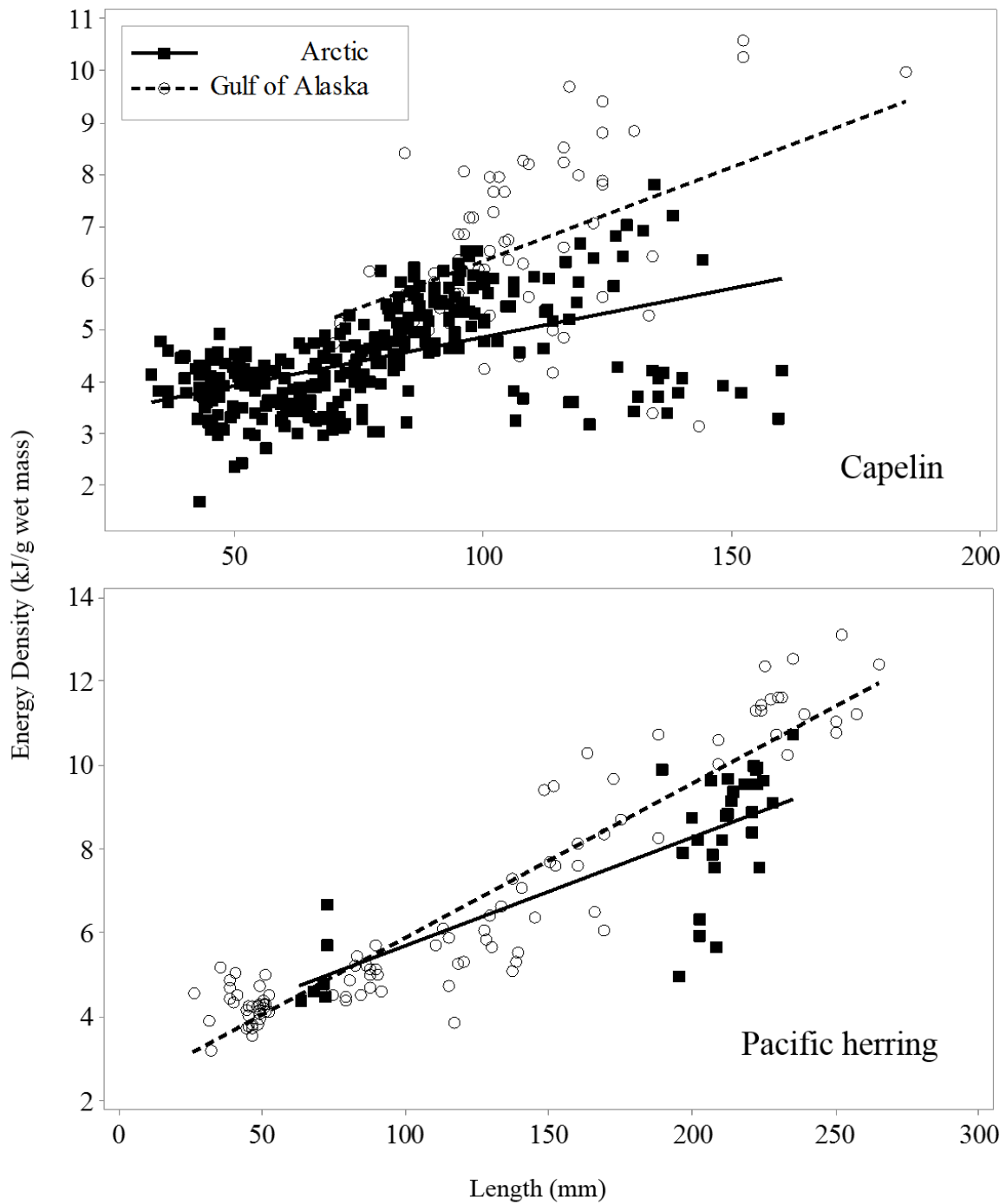


Figure 8.5 Length-energy density relationship of Pacific herring and capelin collected in the summer (July–September) from two Large Marine Ecosystems, the Arctic and the Gulf of Alaska.

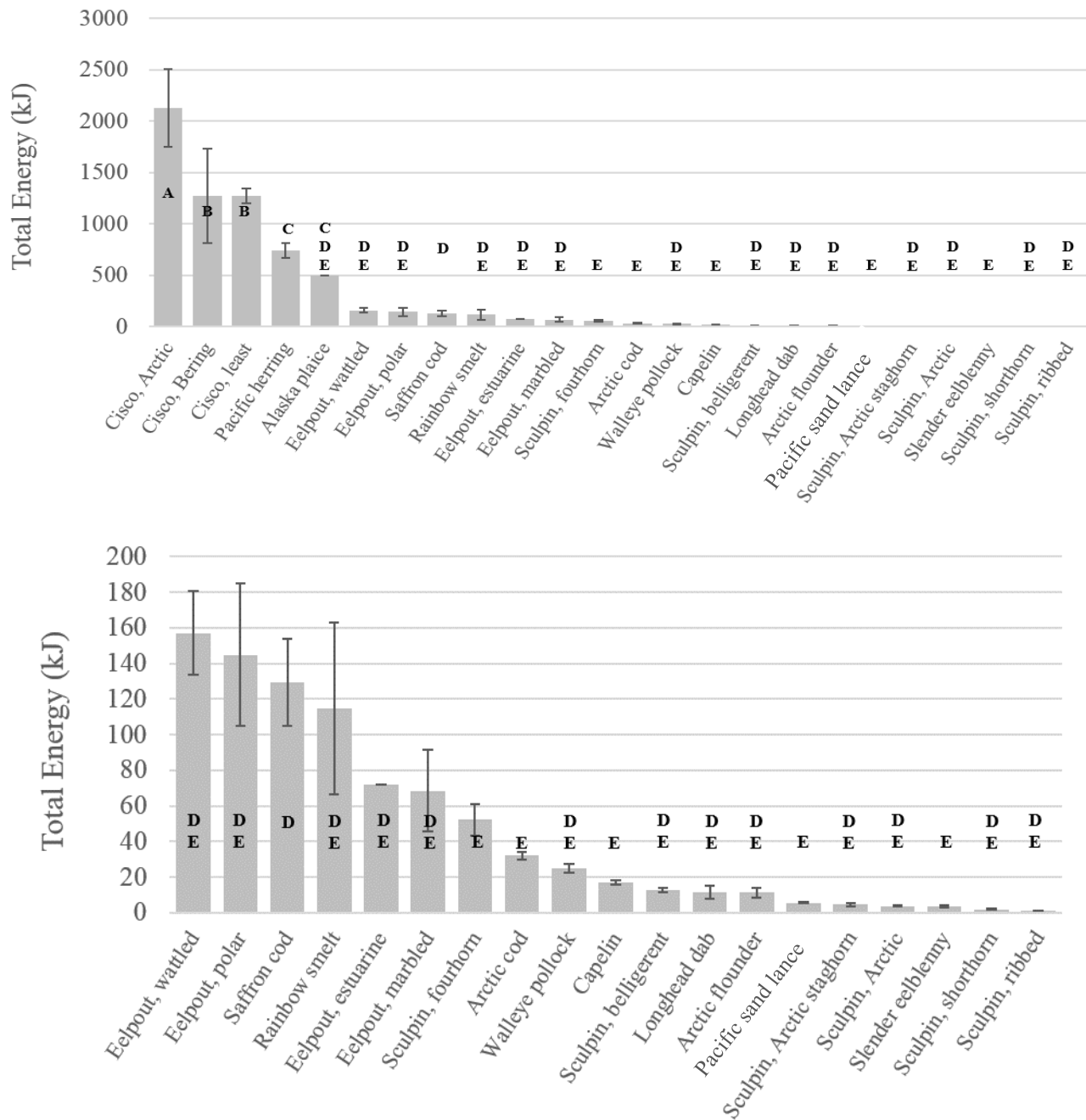


Figure 8.6 Average total energy content (kJ) of all sampled Arctic fish species. Like letters indicate statistical similarity determined by ANOVA. The top panel includes all 24 species evaluated and the bottom panel excludes the top 5 species with the greatest energy content.

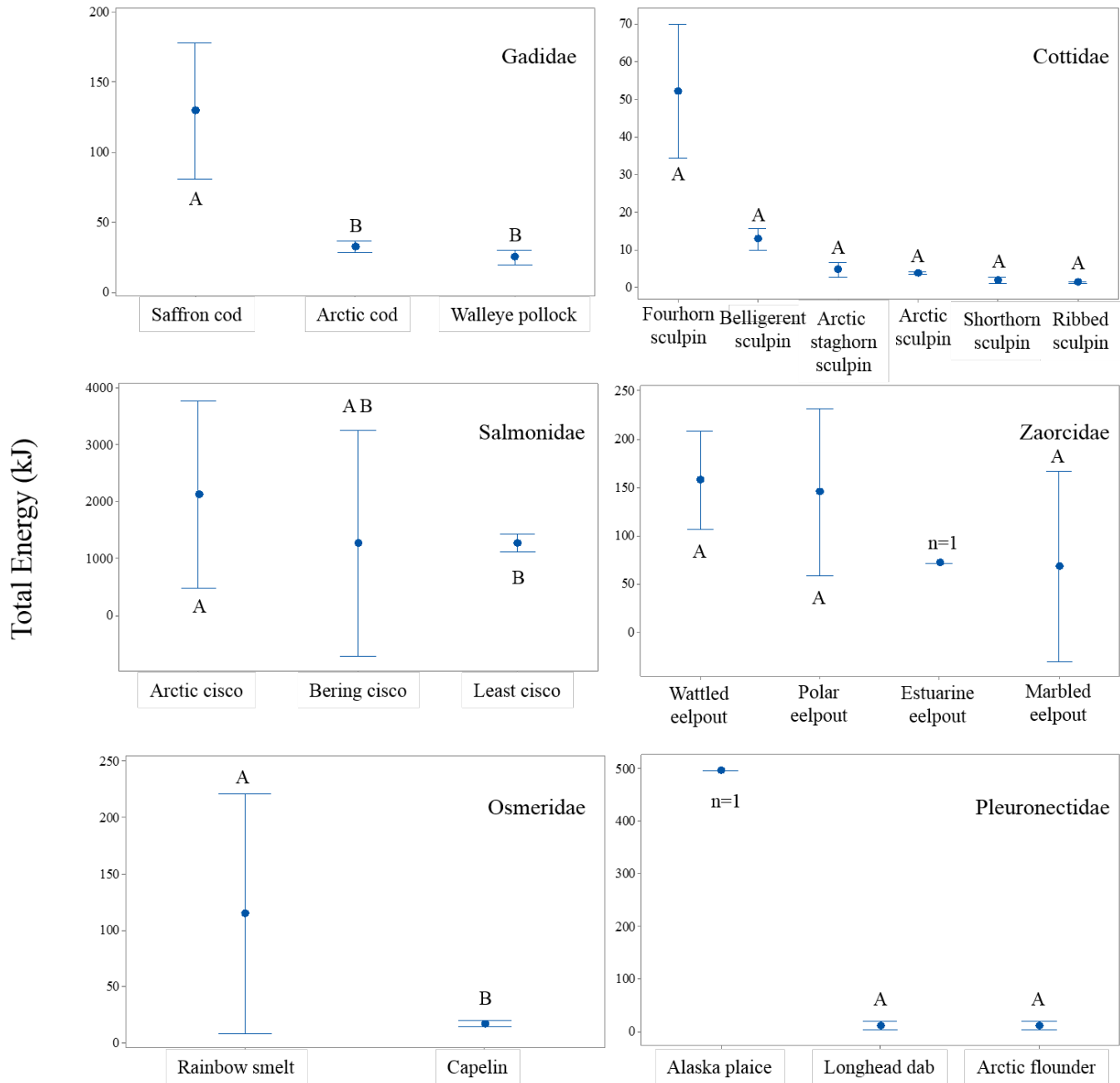


Figure 8.7 Average total energy (kJ) by family of Arctic fish species. Like letters indicate statistical similarity determined by ANOVA.

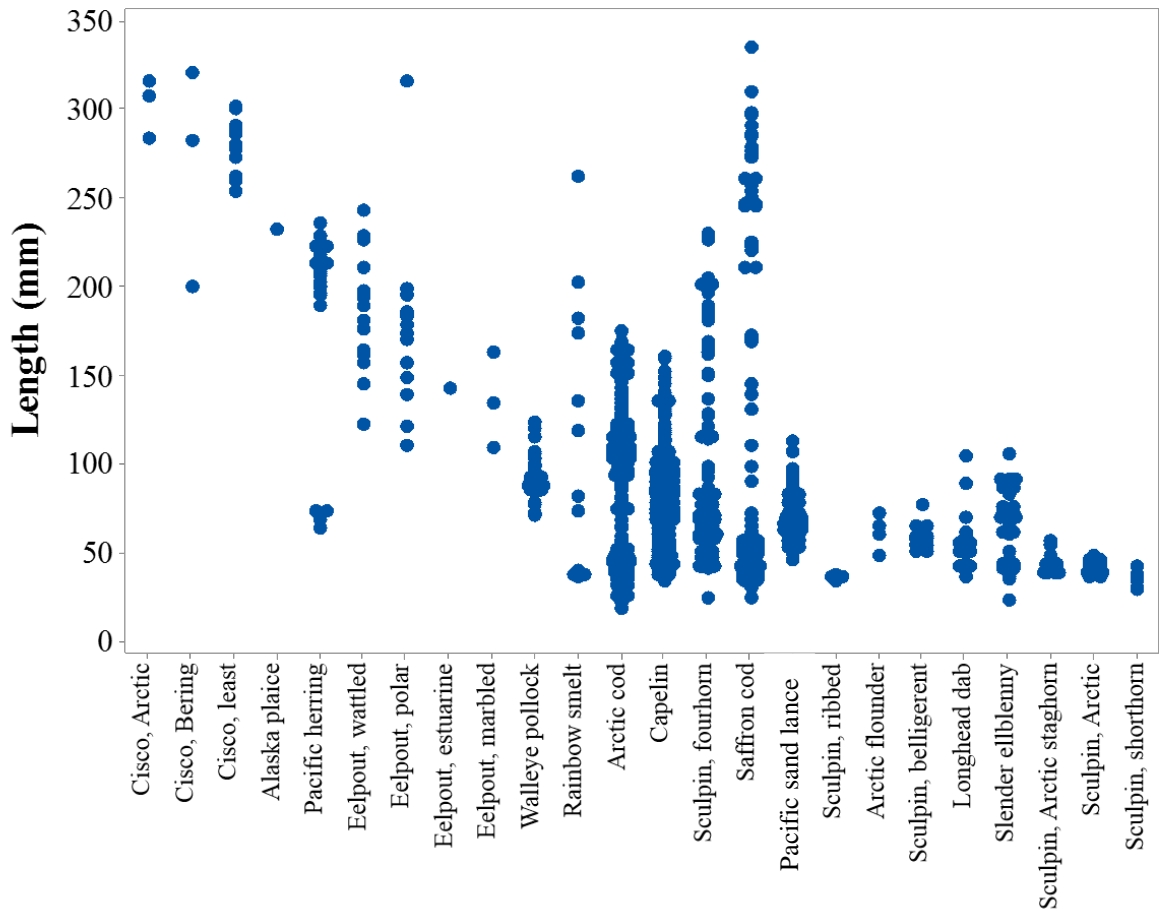


Figure 8.8 Individual value plot of lengths (mm) of Arctic fish evaluated for energetics.

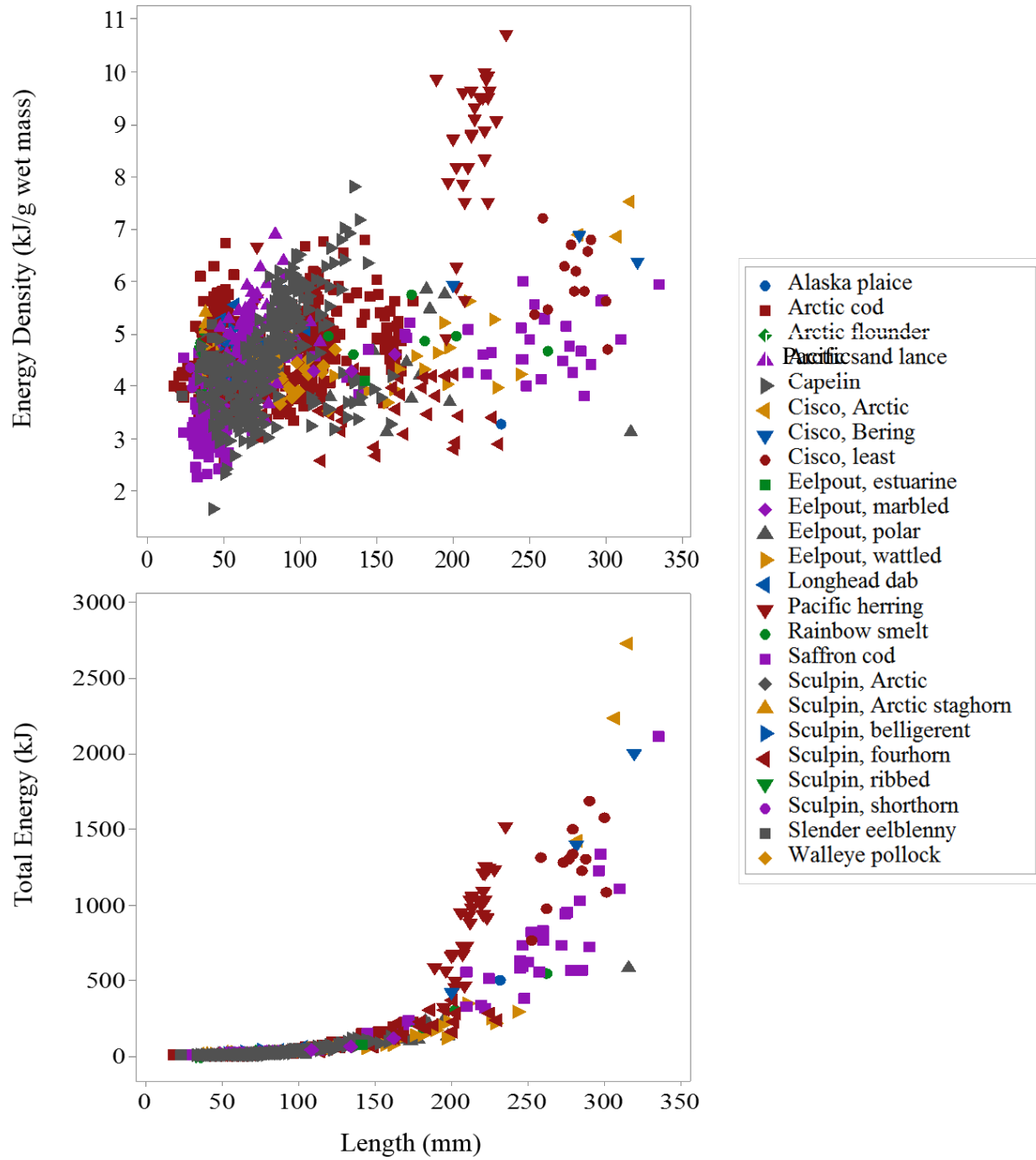


Figure 8.9 Energy density (kJ/g wet mass) in relation to length (mm) (top panel) and total energy content (kJ) in relation to length (bottom panel) of all Arctic species.

Table 8.1 Survey details of the projects from which samples were obtained , including 1) Ecology of Forage Fishes in the Arctic Nearshore (AFF), 2) The Arctic Coastal Ecosystem Survey (ACES), 3) ArcticEis, and 4) Shelf Habitat and EcoLogY of Fish and Zooplankton (SHELFZ).

Project	Year	Months	Fishing Methods
AFF	2015	July - September	1) 37 m variable mesh beach seine 2) 5 x 3.5 m Aluette mid-water trawl 3) 4.7 m Plumb staff beam trawl 4) 2.6 x 1.2 m Otter trawl
ACES	2005, 2007, 2012-2014	July - August	1) 37 m variable mesh beach seine 2) 2.6 x 1.2 m Otter trawl
ArcticEis	2012-2013	August - September	1) 122 m CanTrawl 400/601 mid-water trawl 2) 6.1 x 6.1 m Marinovich mid-water trawl 3) 4.7 m Plumb staff beam trawl 4) 34.1 m 83-112 Eastern otter trawl
SHELFZ	2013	August - September	1) 5 x 3.5 m Aluette mid-water trawl 2) 6.1 x 6.1 m Marinovich mid-water trawl 3) 4.7 m Plumb staff beam trawl 4) 34.1 m 83-112 Eastern otter trawl

Table 8.2 Mean length, mass and energy of Arctic fish species. Values indicate mean + standard error, (sample size).

Common Name	Family	Genus species	Length (mm)	Mass (g)	ED (kJ/g wet)	ED (kJ/g dry)	Total Energy (kJ)
Alaska plaice	Pleuronectidae	<i>Pleuronectes quadrituberculatus</i>	232 (1)	151.65	3.3	17.5	495.7
Arctic cod	Gadidae	<i>Boreogadus saida</i>	80.0±2.1 (361)	6.48±0.43	4.7±0.0	21.2±0.1	32.1±2.2
Arctic flounder	Pleuronectidae	<i>Liopsetta glacialis</i>	60.8±5.0 (4)	2.55±0.60	4.5±0.1	21.0±0.3	11.5±2.8
Pacific sand lance	Ammodytidae	<i>Ammodytes hexapterus</i>	70.9±1.3 (89)	1.16±0.08	4.9±0.1	21.3±0.2	5.7±0.4
Capelin	Osmeridae	<i>Mallotus catervarius</i>	77.9±1.5 (297)	3.52±0.27	4.4±0.1	21.7±0.1	17.0±1.3
Cisco, Arctic	Salmonidae	<i>Coregonus autumnalis</i>	302.0±9.9 (3)	298.20±47.40	7.1±0.2	24.9±0.3	2127±382
Cisco, Bering	Salmonidae	<i>Coregonus laurettae</i>	267.3±35.4 (3)	195.90±70.60	6.4±0.3	23.5±0.4	1273±462
Cisco, least	Salmonidae	<i>Coregonus sardinella</i>	279.0±4.4 (12)	210.60±10.70	6.0±0.2	21.9±0.3	1271.8±73.5
Eelpout, estuarine	Zoarcidae	<i>Lycodes turneri</i>	142.0 (1)	17.52	4.1	20.8	71.8
Eelpout, marbled	Zoarcidae	<i>Lycodes raridens</i>	135.0±15.3 (3)	15.34±4.76	4.4±0.1	21.5±0.2	68.4±22.9
Eelpout, polar	Zoarcidae	<i>Lycodes polaris</i>	174.8±14.0 (13)	36.10±12.50	4.2±0.3	19.9±0.6	145.0±39.7
Eelpout, wattled	Zoarcidae	<i>Lycodes palearis</i>	185.6±8.6 (15)	34.25±4.60	4.4±0.1	20.9±0.3	157.2±23.6
Longhead dab	Pleuronectidae	<i>Limanda proboscidea</i>	56.8±4.4 (16)	2.34±0.74	4.6±0.2	20.0±0.4	11.6±3.9
Pacific herring	Clupeidae	<i>Clupea pallasii</i>	188.1±9.4 (35)	84.58±7.24	8.0±0.3	26.2±0.4	739.2±72.2
Rainbow smelt	Osmeridae	<i>Osmerus mordax</i>	114.5±22.1 (12)	23.40±10.10	4.8±0.1	21.7±0.3	114.9±48.3
Saffron cod	Gadidae	<i>Eleginus gracilis</i>	83.1±6.5 (163)	26.33±4.76	3.8±0.1	14.1±3.5	129.4±24.7
Sculpin, Arctic	Cottidae	<i>Myoxocephalus scorpioides</i>	41.0±0.8 (18)	0.83±0.04	4.6±0.1	20.5±0.2	3.8±0.2
Sculpin, Arctic staghorn	Cottidae	<i>Gymnocanthus tricuspis</i>	43.5±2.1 (10)	0.97±0.18	4.8±0.1	20.8±0.2	4.7±0.9
Sculpin, belligerent	Cottidae	<i>Megalocottus platycephalus</i>	57.5±1.5 (17)	2.76±0.28	4.6±0.1	21.0±0.2	12.9±1.4
Sculpin, fourhorn	Cottidae	<i>Myoxocephalus quadricornis</i>	92.9±5.6 (91)	14.16±2.44	3.9±0.1	19.6±0.1	52.2±9.0
Sculpin, ribbed	Cottidae	<i>Triglops pingelii</i>	35.0±0.8 (4)	0.30±0.01	4.3±0.2	20.2±0.2	1.3±0.1
Sculpin, shorthorn	Cottidae	<i>Myoxocephalus scorpius</i>	34.2±2.1 (6)	0.46±0.08	4.1±0.1	18.2±0.3	1.9±0.3
Slender eelblenny	Stichaeidae	<i>Lumpenus fabricii</i>	58.8±3.0 (44)	0.74±0.11	4.5±0.1	20.1±0.2	3.1±0.6
Walleye pollock	Gadidae	<i>Gadus chalcogrammus</i>	93.2±2.8 (26)	5.89±0.58	4.2±0.1	21.5±0.2	24.8±2.5

Table 8.3 Correlation of energy density (ED; kJ/g) to fish length from linear regression for 5 species of Arctic fish. Energy density (kJ/g) is expressed on both a wet mass and dry mass basis.

Common Name	Regression Equation Wet Mass	Regression Equation Dry Mass
Arctic cod	ED=4.215+0.005706*Length (R ² = 0.09)	ED=19.11+0.02704*Length (R ² = 0.20)
Saffron cod	ED=3.224+0.006485*Length (R ² = 0.47)	ED=16.41+0.01909*Length (R ² = 0.36)
Pacific herring	ED=3.090+0.02599*Length (R ² =0.57)	ED=19.36+0.03660*Length (R ² =0.61)
Capelin	ED=2.952+0.01911* Length (R ² =0.26)	ED=17.15+0.05866* Length (R ² =0.37)
Fourhorn sculpin	ED=4.392-0.004842*Length (R ² =0.19)	ED=21.02-0.01514*Length (R ² =0.35)

9.0 Food Web Analysis (Isotopes)

M. Barton

9.1 Introduction

Polar regions have recently become of interest due to the rapid rate of climate change in these extreme environments (Johannesson et al. 2004; Moline et al. 2008; McMahon et al. 2009). The rapid decrease in sea ice cover has drawn the attention of oil and gas, shipping, and tourism industries looking to capitalize on previously unavailable resources (AMAP 2008; Jones 2012). Though these new opportunities may benefit the world economy, they have equal potential to damage nearby ecosystems. In the past few decades a considerable amount of research has focused on ecosystems of the Arctic Ocean, to establish baselines before these potential threats are realized. However, despite this effort, only a small portion of this research has been focused on coastal regions (Norcross et al. 2004; Bluhm and Gradinger 2008; Iken et al. 2010), and an even smaller portion of that has focused on the very nearshore (shallower than 15 m; Craig et al. 1982; Craig et al. 1985; Dunton et al. 2006; Dunton et al. 2012).

The Arctic nearshore is largely comprised of estuarine lagoon and barrier island systems. Based on knowledge of well-studied lower-latitude systems, these estuaries have the potential to be highly productive and important habitats for the rearing of juvenile fish, foraging grounds for a multitude of protected and endangered marine mammals and birds (Elliott et al. 1990; Beck et al. 2001; Fry et al. 2003; Dunton et al. 2012), as well as an important resource for nearby subsistence villages. Though we presume that these Arctic estuaries function in similar ways as their low-latitude counterparts, we cannot make this assumption without further research.

The study of food webs can offer great insight to the functionality of an ecosystem, and identify crucial prey resources for the survival of the community. Several studies have investigated trophic pathways to high level predators such as polar bears (*Ursus maritimus*), seals and seabirds (Hobson and Welch 1992; Dehn et al. 2006; Dehn et al. 2007), but to date nobody has focused on Arctic nearshore fish communities. Given that sea ice coverage is diminishing, and increased sightings of ice dependent predators in the nearshore in late summer (personal communication with North Slope Borough Department of Wildlife, Barrow, AK), these nearshore fish communities are likely to become important forage as the Arctic climate continues to warm (Bluhm and Gradinger 2008).

The paucity of information about Arctic nearshore foodwebs is in part due to the inherent difficulty of acquiring adequate samples when the water surface is covered by several meters of ice for the majority of the year. Using stomach contents of fish collected only during summer months to determine foodweb structure would result in a biased foodweb model that only represents summer prey selection (Wiens 1989; Hobson and Welch 1992). Stable isotope analysis of carbon and nitrogen is a better suited approach as the isotope ratios within the tissues of fish are a representation of their prey resources across an extended period of time, thus incorporating part of the year when ice cover prevents sample collection (Hobson and Clark 1992; Phillips et al. 2005; Fry 2006; Logan et al. 2006).

We use stable isotope analysis of carbon and nitrogen to investigate foodweb structures across three nearshore habitat types in the Arctic nearshore.

9.2 Methods

9.2.1 Study Area

Point Barrow, AK is a unique area where multiple Arctic nearshore habitat types are found in close proximity to each other. Furthermore, Point Barrow is bordered on the West by the Chukchi Sea (CHS) and to the East by the Beaufort Sea (BFS), with the large estuarine Elson Lagoon (ESL) opening into the Beaufort Sea just 5 km Southeast of Point Barrow (Figure 1.1). These distinct water bodies have distinct conditions that are likely to support different species assemblages. Furthermore, this dynamic area undergoes a great change as it shifts from ice-covered winter to open water summer, and these changes are expected to drive changes in community composition as the seasons progress.

9.2.2 Sample Collection

The communities were sampled using a beach seine at 12 stations (5 CHS, 3 BFS, and 4 ESL) at weekly intervals from July 14th – August 25th (Week 1–6) for three consecutive years (2013–15). The seine was 37 m long with variable mesh sizes (10 m of 32 mm outer panels, 4 m of 6 mm middle panels, and 9 m of 3.2 mm blunt panel). Each set was round-haul style, paid out of a 3 m inflatable zodiac following methods used by Johnson et al. (2010). All collections occurred during daylight hours. The entire catch was put in a Ziploc bag and placed on ice to be processed in the lab. In the case of very large catches (> 1000 fish), fish larger than 40 mm were set aside, the remainder of the catch was weighed in the field, and a 1 liter subsample was placed in a Ziploc bag to be processed in the lab. Once in the lab, all fish were sorted by species and enumerated. In the case of a subsample, the numbers of each species were multiplied proportionally by the weight of the entire sample to estimate their abundances. Fish were frozen after processing to be used in multiple analyses that are not discussed further in this article. Temperature, salinity, and Dissolved Oxygen (DO) were recorded using a YSI EXO2 data sonde at each sampling event. Wind speed, direction and air temperature were recorded using a handheld anemometer. However, these environmental factors and their importance in community composition were discussed in chapter 4.

9.2.3 Analytical Approach

The relationships between $\delta^{13}\text{C}$ and $\delta^{15}\text{N}$ were investigated to identify clustering of species to indicate if certain species may depend on different basal resources. This relationship was also investigated for each separate waterbody (Elson Lagoon, Beaufort Sea, and Chukchi Sea) to identify trophic pathways and the basal resources (terrestrial vs. oceanic carbon) of species found in each of these habitats based on published ranges of phytoplankton and detritus isotopic signatures. Furthermore, the slope of the trophic pathway was compared to known trophic enrichment factors (TEFs) of carbon and nitrogen isotopes to indicate whether these enrichment factors are appropriate for isotope based foodweb models of Arctic nearshore fishes.

9.3 Results

Stable $\delta^{13}\text{C}$ and $\delta^{15}\text{N}$ isotope ratios of 415 samples of 20 common species of nearshore fish and invertebrates were analyzed to identify nearshore Arctic food web structures across three water bodies surrounding Point Barrow, Alaska. Across this range, $\delta^{15}\text{N}$ ranged from 9.55 ‰ to 16.64 ‰ (Mean \pm SD = 13.93 \pm 1.16 ‰), and $\delta^{13}\text{C}$ ranged from -25.47 ‰ to -14.54 ‰ (-18.85 \pm 1.66 ‰). There is no correlation between $\delta^{15}\text{N}$ and $\delta^{13}\text{C}$ in the overall data set, however when the data is broken down by water body it is clear that there is a positive linear relationship in the Beaufort

($R^2 = 0.12$, $p < 0.01$) and the Chukchi ($R^2 = 0.72$, $p < 0.01$; with the Arctic Shanny group removed as an outlier) and a negative linear relationship in the Elson Lagoon ($R^2 = 0.17$, $p = 0.05$; Figure 9.1).

9.4 Discussion

Stable carbon and nitrogen isotopes can be used to identify trophic pathways within a food web. The isotope biplot of all samples indicates that these samples may be bisected into two groups, a possible indication that they may be a part of different trophic pathways (Figure 9.1A). $\delta^{13}\text{C}$ $\delta^{15}\text{N}$ exhibit step-wise additive changes as material is passed on from one trophic level to the next (DeNiro and Epstein 1978; DeNiro and Epstein 1981; Layman et al. 2007). Therefore, a positive linear relationship through trophic levels usually indicates that this food chain is dependent on one basal resource. Though there is not clear linear relationship in the overall data, when broken down by water body a positive linear relationship is seen in the samples of the Chukchi and Beaufort Seas, indicating that fish and macroinvertebrates on the oceanic side of the barrier islands are dependent on single basal resources. In the Elson Lagoon, a negative linear relationship is present, suggesting that fish and macroinvertebrates in the lagoon may be dependent on multiple sources of carbon.

In order to further investigate the trophic structures of these food webs we must first establish an appropriate way to calculate the trophic levels of the species included in the analysis. The linear model of the Chukchi samples had the best fit ($R^2 = 0.72$, $p < 0.01$) producing a line of best fit with an x-coefficient of 0.8 and an y-intercept of 28.8, indicating that $\delta^{13}\text{C}$ and $\delta^{15}\text{N}$ increase trophically at a ratio of 1:1.25. Dunton et al. (2006) indicated that isotopic signatures of marine primary producers in the Arctic are between -22 and -25 ‰ for $\delta^{13}\text{C}$ and between 5 and 7 ‰ for $\delta^{15}\text{N}$, and that terrestrial organic material has a signature between -27 and -23 ‰ for $\delta^{13}\text{C}$ and between 0 and 1.5 ‰ for $\delta^{15}\text{N}$. The model of Chukchi samples would indicate that nitrogen values of 5 to 7 ‰ would be coincident with a carbon values of -30 to -27 ‰. Here we see a carbon signature expected from terrestrial basal resources paired with a nitrogen signature expected from marine primary producers. This pattern is possible if terrestrial detritus is decomposed to release nutrients that are fixed by phytoplankton in the lagoon.

Based on $\delta^{13}\text{C}$ it seems likely that the nearshore fish and macroinvertebrate communities on the oceanic side of the barrier islands near Point Barrow are depending on terrestrially derived basal resources. Dunton et al. (2006) indicated that because the Beaufort Sea is relatively unproductive, it is highly dependent on the productivity of lagoon and barrier island systems. The Chukchi on the other hand was less dependent on terrestrial organic material because *in situ* primary production was significantly higher than in the Beaufort Sea. Perhaps the reason that we see a dependence on terrestrial carbon in both the Beaufort and the Chukchi is because the nearest Chukchi sampling station is merely 5 km away from Eluitkak Pass where the Elson Lagoon connects to the Beaufort. The overall flow of the Alaska Coastal Current (ACC) is East in this region, but regularly reverse during strong wind events (Danielson et al. 2014) and is likely to carry much organic material from the Elson Lagoon into the Chukchi Sea.

In order to investigate the trophic levels within Arctic nearshore fish communities, we must first establish appropriate Trophic Enrichment Factors (TEFs). A trophic enrichment factor is defined as the difference or discrimination of isotopic values between consecutive trophic levels. Past isotopic studies have used broadly accepted average TEFs for carbon and nitrogen isotopes (3.4

‰ for $\delta^{15}\text{N}$, and 1 ‰ for $\delta^{13}\text{C}$), but recent studies have identified that species specific TEFs are necessary in many cases (Logan et al. 2006; Madigan et al. 2012; Rosenblatt and Heithaus 2013). Very few studies have identified TEFs in Arctic species, however Hobson and Welch (1992) and Hobson et al. (1996) identify TEFs for nitrogen of 2.4 ‰ for Arctic seabirds and phocid seals. This value is consistent with an estimated TEF for Arctic sculpin from the Point Barrow region (Barton et al. unpublished). Using the slope of the linear model of Chukchi samples, we estimate that the TEF of $\delta^{13}\text{C}$ would be approximately 3 ‰, and this ratio of $\delta^{15}\text{N}$: $\delta^{13}\text{C}$ TEFs is also consistent with TEFs calculated for Arctic sculpin.

In the Elson Lagoon we found that a negative relationship between $\delta^{13}\text{C}$ and $\delta^{15}\text{N}$, suggesting that there may be multiple source of carbon important in this foodweb. If we use the slope for $\delta^{13}\text{C}$ and $\delta^{15}\text{N}$ calculated from the model of samples in the Chukchi, we find that basal resource with $\delta^{15}\text{N}$ of 5 to 7 ‰ would have $\delta^{13}\text{C}$ values ranging between approximately -24 and -27 ‰. This range of $\delta^{13}\text{C}$ values includes small portions of both terrestrial carbon and marine primary producer signatures identified by Dunton et al. (2006). This would indicate that some of the organisms such as isopods, amphipods, and Belligerent sculpin (*Megalocottus platycephalus*) in the lagoon system are at least in part dependent on marine primary producers that are probably being advected into the lagoon during East winds when the inlet flows into the lagoon (see chapter 2 and 3).

To calculate a range of possible trophic levels for each species, the basal resource values of $\delta^{15}\text{N}$ (5 to 7 ‰) was subtracted from each species average $\delta^{15}\text{N}$, and the remainder was divided by the TEF of 2.4 (Table 9.1). Trophic levels ranged from 2.7 to 4.4 when $\delta^{15}\text{N}$ of basal resources were set at 5 ‰, and 3.5 to 5.3 when $\delta^{15}\text{N}$ of basal resources were set at 7 ‰. Early isotopic investigations identified that Arctic marine foodwebs could be rather long because polar bears make up their own fifth trophic level (Hobson and Welch 1992), but these estimations were dependent on a higher TEF for nitrogen (3.8 ‰) calculated between polar bears and ringed seals. Given that multiple cases have indicated that TEFs for nitrogen may be significantly lower in Arctic foodwebs, we may expect that these foodwebs contain more than five trophic levels. If we assume that there are two trophic levels above those identified in our samples, with seals and seabirds eating fish, and polar bears eating seals, our results would indicate that there are 6 or 7 trophic levels in nearshore Arctic marine foodwebs.

This may be possible because many Arctic species have a tendency to grow much larger than similar species in lower latitudes. Because of this there is a large range of zooplankton sizes in the Arctic ranging from small species of copepods rotifers and small copepods, to large copepods, krill and mysids, to large predatory amphipods. Based on the fact that the size and trophic levels of mysids in the Point Barrow region as similar to some small fish, it seems likely that they feed on smaller zooplankton thus creating a second trophic level within zooplankton. Furthermore, a third trophic level may be present in zooplankton as large predatory amphipods such as *Gammarus wilkitzkii* have been observed feeding on fish and mysids that are approximately the same size as themselves. These amphipods have also commonly been seen in the stomachs of fish caught throughout our survey (see chapter 6). Alternatively, these amphipods may also be increasing their trophic levels by scavenging on the carcasses of higher trophic level organisms. Unlike lower latitudes where there are fewer trophic levels, the extreme cold in the Arctic slows down microbial decomposition. As a result, carcasses of large marine

mammals are relatively abundant for long periods of time allowing scavengers such as amphipods to feed on them.

To summarize, the positive relationships between $\delta^{13}\text{C}$ and $\delta^{15}\text{N}$ in the Beaufort and Chukchi samples indicates that these communities are probably dependent on a single basal resource. Given the $\delta^{13}\text{C}$ values of these species, it is likely that this basal resource is terrestrially derived, and likely being supplied through the Elson Lagoon. The Elson Lagoon on the other hand has a negative relationship between $\delta^{13}\text{C}$ and $\delta^{15}\text{N}$, indicative of more than one basal resource. The species with less depleted $\delta^{13}\text{C}$ and less enriched $\delta^{15}\text{N}$ are probably dependent on basal resource from marine primary producers advected into the lagoon from the Beaufort as well as terrestrial organic matter from tundra runoff. Research by Hobson et al. (1996) and unpublished data (Barton et al. In review) suggests that TEFs in the Arctic marine system may be relatively low for $\delta^{15}\text{N}$ and relatively high for $\delta^{13}\text{C}$. Using these TEFs we estimate that these nearshore ecosystems may have 6 or 7 trophic levels, as opposed to the previously suggested 5 trophic levels. These extra trophic levels are most likely explained by the large range in size and diversity of zooplankton in the Arctic within which 2 or 3 trophic levels may be present. This new information would suggest that the lower trophic levels of Arctic nearshore foodwebs may be far more complex than once believed, and it may be necessary to focus future efforts on understanding these predator-prey relationships further, so that we may establish an accurate baseline to assess how these foodwebs change in the near future.

9.5 References

- Álvarez E, López-Urrutia Á, Nogueira E (2012) Improvement of plankton biovolume estimates derived from image-based automatic sampling devices: Application to FlowCAM. *J Plankton Res* 34:454–469. doi: 10.1093/plankt/fbs017
- AMAP (2008) Arctic oil and Gas. Arctic Monitoring and Assessment Programme, Oslo, Norway
- Beck M, Jr KH, Able K (2001) The identification, conservation, and management of estuarine and marine nurseries for fish and invertebrates. *Bioscience* 51:633–641.
- Benke A, Cushing C (2006) Rivers of North America, First Edit. Elsevier Academic Press, Burlington, MA
- Berkman P, Young O (2009) Governance and environmental change in the Arctic Ocean. *Science* (80-.). 324:339–340.
- Bluhm B, Gradinger R (2008) Regional Variability in Food Availability For Arctic Marine Mammals. *Ecol Appl* 18:S77–S96. doi: <http://dx.doi.org/10.1890/06-0562.1>
- Borer AET, Seabloom EW, Shurin JB, et al (2008) What Determines the Strength of a Trophic Cascade? Published by : Ecological Society of America WHAT DETERMINES THE STRENGTH OF A TROPHIC CASCADE ? 86:528–537.
- Craig P (1984) Fish use of coastal waters of the Alaskan Beaufort Sea: a review. *Trans Am Fish Soc* 113:37–41.
- Craig P, Griffiths W, Haldorson L, McElderry H (1985) Distributional patterns of fishes in an Alaskan arctic lagoon. *Polar Biol* 4:9–18.
- Craig PC, Griffiths B, Griffiths WB, Ffiths WBGR (1982) Ecological Studies of Arctic Cod (*Boreogndus saida*) in Beaufort Sea Coastal Waters, Alaska. *Can Bull Fish Aquat Sci* 39:395–406. doi: 10.1139/f82-057
- Danielson SL, Weingartner TJ, Hedstrom KS, et al (2014) Coupled wind-forced controls of the Bering-Chukchi shelf circulation and the Bering Strait throughflow: Ekman transport,

- continental shelf waves, and variations of the Pacific-Arctic sea surface height gradient. *Prog Oceanogr* 125:40–61. doi: 10.1016/j.pocean.2014.04.006
- Deegan L a. (1993) Nutrient and Energy Transport between Estuaries and Coastal Marine Ecosystems by Fish Migration. *Can. J. Fish. Aquat. Sci.* 50:74–79.
- Dehn L, Follmann E, Thomas D, et al (2006) Trophic relationships in an Arctic food web and implications for trace metal transfer. *Sci Total Environ* 362:103–123. doi: 10.1016/j.scitotenv.2005.11.012
- Dehn L, Sheffield G, Follmann E, et al (2007) Feeding ecology of phocid seals and some walrus in the Alaskan and Canadian Arctic as determined by stomach contents and stable isotope analysis and stable isotope analysis. *Polar Biol* 30:167–181. doi: 10.1007/s00300-006-0171-0
- DeNiro M, Epstein S (1981) Influence of diet on the distribution of nitrogen isotopes in animals. *Geochim Cosmochim Acta* 45:341–351.
- DeNiro MJ, Epstein S (1978) Influence of diet on the distribution of carbon isotopes in animals. *Geochim. Cosmochim. Acta* 42:495–506.
- Dunton KH, Schonberg S V., Cooper LW (2012) Food Web Structure of the Alaskan Nearshore Shelf and Estuarine Lagoons of the Beaufort Sea. *Estuaries and Coasts* 35:416–435. doi: 10.1007/s12237-012-9475-1
- Dunton KH, Weingartner T, Carmack EC (2006) The nearshore western Beaufort Sea ecosystem: Circulation and importance of terrestrial carbon in arctic coastal food webs. *Prog Oceanogr* 71:362–378. doi: 10.1016/j.pocean.2006.09.011
- Elliott M, O'Reilly MG, Taylor CJL (1990) The forth estuary: a nursery and overwintering area for North Sea fishes. *Hydrobiologia* 195:89–103. doi: 10.1007/BF00026816
- Fry B (2006) *Stable Isotope Ecology*, Third edit. Springer, Baton Rouge, LA
- Fry B, Baltz D, Benfield M, et al (2003) Stable Isotope Indicators of Movement and Residency for Brown Shrimp (*Farfantepenaeus aztecus*) in Coastal Louisiana Marshscapes. *Estuaries* 26:82–97.
- Grebmeier J, McRoy C (1989) Pelagic-benthic coupling on the shelf of the northern Bering and Chukchi Seas. III Benthic food supply and carbon cycling . *Mar Ecol Prog Ser* 53:79–91. doi: 10.3354/meps053079
- Grebmeier JM, Mcroy CP, Feder HM (1988) Pelagic-benthic coupling on the shelf of the northern Bering and Chukchi Seas . I . Food supply source and benthic biomass. *Mar Ecol* 48:57–67.
- HECKY RE, FEE EJ (1981) Primary production and rates of algal growth in Lake Tanganyika. *Limnol Oceanogr* 26:532–547. doi: 10.4319/lo.1981.26.3.0532
- Hobson K, Clark R (1992) Assessing avian diets using stable isotopes I: turnover of ^{13}C in tissues. *Condor* 94:181–188.
- Hobson K, Welch H (1992) Determination of trophic relationships within a high arctic marine food web using $\Delta^{13}\text{C}$ and $\Delta^{15}\text{N}$ analysis. *Mar Ecol Prog Ser* 84:9–18.
- Hobson KA, Schell DM, Renouf D, Noseworthy E (1996) Stable carbon and nitrogen isotopic fractionation between diet and tissues of captive seals : Implications for dietary reconstructions involving marine mammals. *Can J Fish Aquat Sci* 53:528–533. doi: 10.1139/cjfas-53-3-528
- Iken K, Bluhm B, Dunton K (2010) Benthic food-web structure under differing water mass properties in the southern Chukchi Sea. *Deep Res Part II Top Stud Oceanogr* 57:71–85. doi: 10.1016/j.dsr2.2009.08.007

- Johannesson OM, Bengtsson L, Miles MW, et al (2004) Arctic climate change : observed and modelled temperature and sea-ice variability. *Tellus* 56:328–341.
- Johnson SW, Thedinga JF, Neff AD, Hoffman CA (2010) Fish Fauna in Nearshore Waters of a Barrier Island in the Western Beaufort Sea , Alaska.
- Johnson WR (1988) Current response to wind in the Chukchi Sea: A regional coastal upwelling event.
- Jones N (2012) Oil exploration ramps up in US Arctic.
- Layman CA, Arrington DA, Montaña CG, et al (2007) Can Stable Isotope Ratios Provide for Community-Wide Measures of Trophic Structure. *Ecology* 88:42–48.
- Loecher M, Ropkins K (2015) Rgooglemaps and loa: Unleashing R Graphics Power on Map Tiles. *J Stat Softw* 63:1–18.
- Logan J, Haas H, Deegan L, Gaines E (2006) Turnover rates of nitrogen stable isotopes in the salt marsh mummichog, *Fundulus heteroclitus*, following a laboratory diet switch. *Oecologia* 147:391–5. doi: 10.1007/s00442-005-0277-z
- Madigan DJ, Litvin SY, Popp BN, et al (2012) Tissue turnover rates and isotopic trophic discrimination factors in the endothermic teleost, pacific bluefin tuna (*Thunnus orientalis*). *PLoS One* 7:e49220. doi: 10.1371/journal.pone.0049220
- McMahon CR, Bester MN, Hindell M a., et al (2009) Shifting trends: Detecting environmentally mediated regulation in long-lived marine vertebrates using time-series data. *Oecologia* 159:69–82. doi: 10.1007/s00442-008-1205-9
- McManus MA, Woodson CB (2012) Plankton distribution and ocean dispersal. *J Exp Biol* 215:1008 – 1016. doi: 10.1242/jeb.059014
- Moline M a, Karnovsky NJ, Brown Z, et al (2008) High latitude changes in ice dynamics and their impact on polar marine ecosystems. *Ann N Y Acad Sci* 1134:267–319. doi: 10.1196/annals.1439.010
- Nemeth M, Priest J, Degan D, et al (2014) Sockeye salmon smolt abundance and inriver distribution: results from the Kvichak, Ugashik, and Egegik rivers in Bristol Bay, Alaska, 2014.
- Norcross BL, Holladay B a., Busby MS, Mier KL (2010) Demersal and larval fish assemblages in the Chukchi Sea. *Deep Sea Res Part II Top Stud Oceanogr* 57:57–70. doi: 10.1016/j.dsr2.2009.08.006
- Norcross BL, Holladay BA, Busby MS, Mier K (2004) RUSALCA – Fisheries Ecology and Oceanography.
- Phillips DL, Newsome SD, Gregg JW (2005) Combining sources in stable isotope mixing models: alternative methods. *Oecologia* 144:520–7. doi: 10.1007/s00442-004-1816-8
- Richlen M, Lobel P (2011) Effects of depth, habitat, and water motion on the abundance and distribution of ciguatera dinoflagellates at Johnston Atoll, Pacific Ocean. *Mar Ecol Prog Ser* 421:51–66. doi: 10.3354/meps08854
- Rosenblatt AE, Heithaus MR (2013) Slow isotope turnover rates and low discrimination values in the american alligator: implications for interpretation of ectotherm stable isotope data. *Physiol Biochem Zool* 86:137–48. doi: 10.1086/668295
- Thedinga J, Johnson S, Neff A, et al (2012) Nearshore Fish Assemblages of the Eastern Chukchi Sea , Alaska. Juneau, AK
- Walsh JJ, Dieterle D a., Chen FR, et al (2011) Trophic cascades and future harmful algal blooms within ice-free Arctic Seas north of Bering Strait: A simulation analysis. *Prog Oceanogr* 91:312–343. doi: 10.1016/j.pcean.2011.02.001

- Wiens J (1989) Spatial scaling in ecology. *Society* 3:385–397. doi: 10.2307/2389612
- York N (1980) Fairbridge, R. 1980. The estuary: its definitions and geodynamic cycle, pp. 1-35.
In: E Olausson and I Cato (eds.), *Chemistry and Biochemistry of Estuaries*. Wiley, New York.

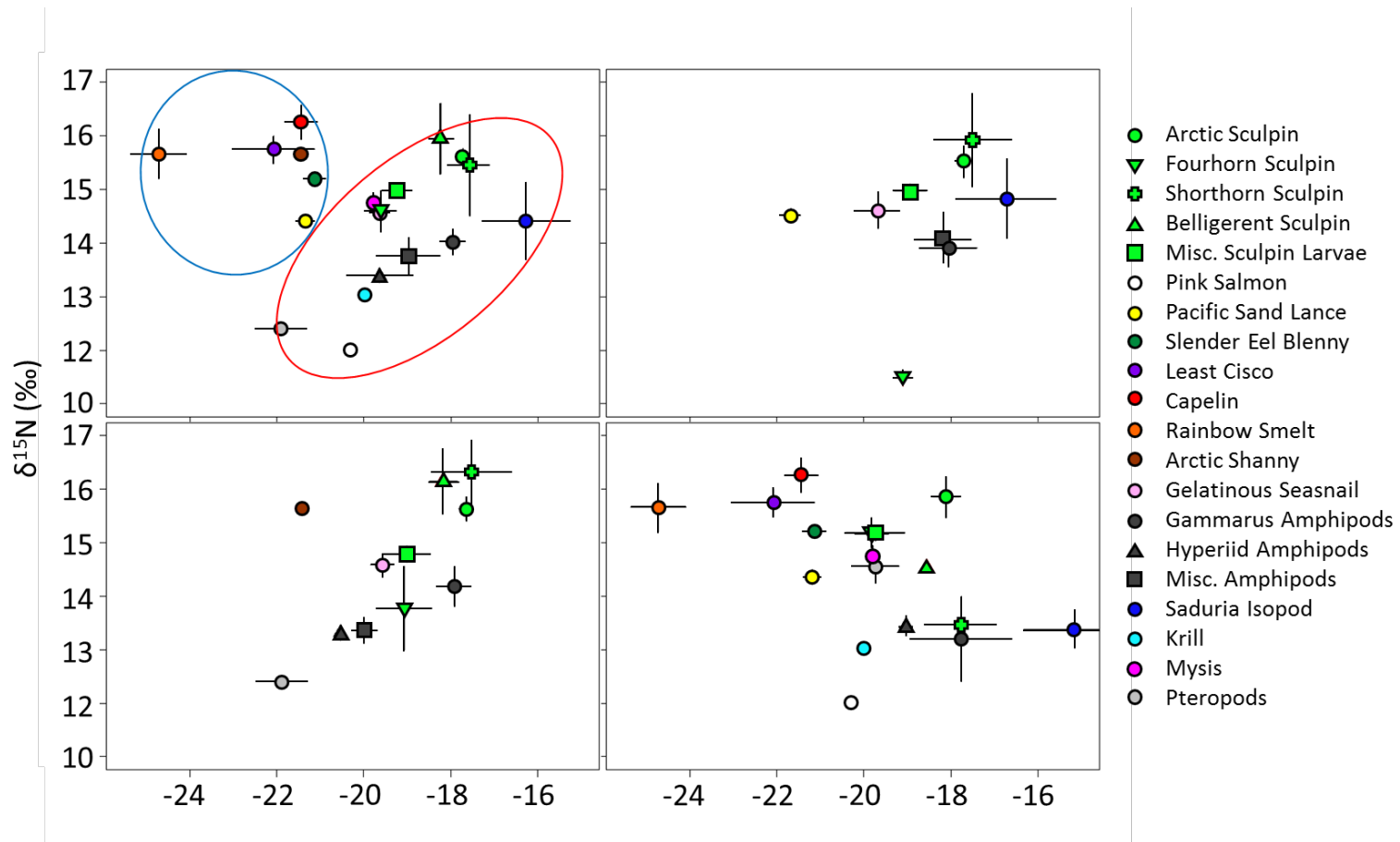


Figure 9.1 Stable isotope biplots of all samples (A), Beaufort Sea (B), Chukchi Sea (C), Elson Lagoon (D). Different colors represent different species groups. Points with the same color represent similar species, and shapes differentiate between them. Error bars represent standard error for $\delta^{13}\text{C}$ (x-axis) and $\delta^{15}\text{N}$ (y-axis).

Table 9.1 A summary of isotopic data by species or species group. Carbon and nitrogen isotopes are given as the average $\delta^{13}\text{C}$ and $\delta^{15}\text{N}$ with standard error. These are the same values used to produce Figure 9.1. Trophic level ranges were calculated using a trophic enrichment factor for $\delta^{15}\text{N}$ of 2.4 per mil, and basal resources of 5 and 7 per mil.

Group Name	Species	$\delta^{15}\text{N} \pm \text{SE}$	$\delta^{13}\text{C} \pm \text{SE}$	Trophic Level Range
Amphipod Gammarus		13.02 \pm 0.11	-17.95 \pm 0.14	2.51 - 3.34
Amphipod Hyperiid		12.39 \pm 0.06	-19.63 \pm 0.37	2.25 - 3.08
Amphipod Misc		12.76 \pm 0.18	-18.98 \pm 0.37	2.40 - 3.23
Arctic Sculpin		14.61 \pm 0.08	-17.71 \pm 0.06	3.17 - 4.00
Arctic Shanny		14.64	-21.4432	3.18 - 4.02
Belligerent Sculpin		14.95 \pm 0.34	-18.22 \pm 0.15	3.31 - 4.15
Capelin		15.27 \pm 0.16	-21.45 \pm 0.18	3.44 - 4.28
Fourhorn Sculpin		13.61 \pm 0.20	-19.61 \pm 0.18	2.75 - 3.59
Gelatinous seasnail		13.58 \pm 0.07	-19.64 \pm 0.11	2.74 - 3.58
Isopod Saduria		13.41 \pm 0.37	-16.26 \pm 0.51	2.67 - 3.50
Krill		12.03	-19.97	2.10 - 2.93
Least Cisco		14.75 \pm 0.13	-22.07 \pm 0.48	3.23 - 4.06
Mysis Shrimp		13.73 \pm 0.11	-19.78 \pm 0.07	2.80 - 3.64
Pacific Sand Lance		13.41 \pm 0.06	-21.36 \pm 0.10	2.67 - 3.50
Pink Salmon		11.01	-20.30	1.67 - 2.50
Pterapods		11.41 \pm 0.05	-21.91 \pm 0.29	1.84 - 2.67
Rainbow Smelt		14.66 \pm 0.23	-24.73 \pm 0.32	3.19 - 4.03
Sculpin Larvae		13.98 \pm 0.05	-19.24 \pm 0.17	2.91 - 3.74
Shorthorn Sculpin		14.47 \pm 0.47	-17.58 \pm 0.23	3.11 - 3.94
Slender Eel Blenny		14.21 \pm 0.04	-21.14 \pm 0.13	3.01 - 3.84

10.0 Latitudinal dependence of body condition, growth rate, and stable isotopes of juvenile capelin (*Mallotus villosus*) in the Bering and Chukchi Seas

M. Barton, J. Moran, J. Vollenweider, R. Heintz, K. Boswell

10.1 Introduction

Latitudinal variation exists across seascapes and some species found across a wide range of climatic conditions have different feeding and life-history strategies according to the conditions they face (Conover 1988; Post and Parkinson 2001; Shoji et al. 2011; Rypel 2012). Life-history strategy is defined as the allocation of energy throughout a lifetime to optimize growth, survival, and reproduction (Noordwijk and Jong 2014). Energy allocation in juvenile fish is particularly important, when there are concurrent energetic demands to grow (predator avoidance, increase accessibility to prey) and store energy to survive their first winter (Mogensen and Post 2012). Fish condition is often used as a parameter to examine survival potential and recruitment processes (Heintz et al. 2013) and is often expressed as measures of energy density (kJ/g), which is driven by lipid content (Anthony et al. 2000). Stable isotopes have become a popular method for examining dietary sources and trophic structure within species and their ecosystems (DeNiro and Epstein 1978, 1981; Hobson and Welch 1992; Layman et al. 2007a; Peterson and Fry 2014). Many trophic studies focus on carbon and nitrogen isotopes, but they rarely consider simultaneous measures of energetic condition and growth. These latter measures offer important information describing the quality of prey items and consequently diet implications for fish condition and optimality of habitats within a system (Sherwood et al. 2007). Thus, food web structures and carbon sources that maximize productivity can be identified by combining isotopic analysis with indices of growth and energetic condition. This is important in the Arctic and sub-Arctic where marine conditions are changing rapidly (Grebmeier et al. 2006), and those changes are likely to affect prey availability and quality.

As coastal waters in the Arctic become increasingly warmer and ice-free due to shifting climate conditions, it is likely that species will extend, restrict, or shift their ranges as a function of changing tolerable conditions, eliciting change in coastal food web structures of northern oceans (Grebmeier et al. 2006; Moline et al. 2008; Eisner et al. 2013). These coastal food webs provide critical subsistence fisheries and serve as a food source for numerous endangered and protected marine mammals and sea birds (Hobson and Welch 1992). With these changes occurring, high-latitude species may see intrusions from lower-latitude species, introducing new predators and competition for resources and space (Gilman et al. 2010; Sorte et al. 2010; Grebmeier 2012; Litzow and Mueter 2014). The lifehistory strategies of species that have wide tolerance of environmental conditions may serve as proxies to examine fish condition with changes in food web structure across extensive spatial domains and offer insight into predicting how these important forage fish may fare in the Arctic as climatic conditions change.

The Western Coast of Alaska is bordered by the Bering Sea in the southwest and the Chukchi Sea in the northwest. The high-nutrient, high-salinity Bering Shelf Water (BSW) and the freshwater runoff and wind-driven Alaska Coastal Current (ACC) run along the entire length of

these coasts, and the front between them typically occurs between 30 and 60 km from shore (Stabeno et al. 1995; Steele et al. 2010). The front between these two distinct water masses may generate optimal growth conditions to support an abundance of planktivorous fish in coastal waters (Coyle and Pinchuk 2005; Weingartner et al. 2005; Hopcroft et al. 2010; Eisner et al. 2013). Because of the extensive latitudinal range of this persistent front, it presents the opportunity to study the effects of latitude on trophic interactions and energy allocation strategies of coastal planktivorous fish. This water mass provides gradients of temperature and freshwater influx, two primary conditions that are expected to increase significantly with climate change (Peterson et al. 2002; Chan et al. 2011; Dunton et al. 2014). The proximity of this coastal current to land allows for the examination of fish trophodynamics and condition in response to freshwater/terrestrial influence.

Capelin (*Mallotus villosus*) are an abundant planktivorous forage fish found throughout western Alaskan waters and serve as an important link between lower and higher trophic levels (Gjørseter and Bamstedt 1998; Johnson et al. 2010; Sherwood et al. 2007). Capelin's wide geographical distribution suggests plasticity in its life-history strategies. Because of capelin's trophic position and value as a prey resource, their ability to adapt to different conditions and prey resources will probably play an important role in the response of larger, economically important or endangered members of higher trophic levels, including fish, marine mammals, and sea birds. Previous research has shown that great variability exists in planktonic assemblages throughout the ACC and BSW (Schell et al. 1998; Dunton et al. 2006; Eisner et al. 2013) and it is likely that distinct planktonic assemblages coincide and interact with distinct food webs. Capelin can be used as a model species for the adaptability of mid trophic levels (forage fish) to changing climatic conditions in the Arctic by examining their energy allocation patterns and trophodynamics across gradients in climate and latitudes in which they are abundant.

Past studies have examined the latitudinal dependence of energy allocation strategies of fish, but to date they have largely been restricted to smaller scales or closed freshwater and have not incorporated stable isotope analysis (SIA) to examine the effects of variations in diet (Shoji et al. 2011; Mogensen and Post 2012; Rypel 2012; Siddon et al. 2013). The use of a combination of energetics and stable isotope data may offer further insight into the adaptability and sensitivity of these coastal food webs to changing conditions throughout the Alaskan coastline. We aim to quantify energy density, growth rates, and isotope ratios among juvenile capelin along the entire west coast of Alaska within a single water body, the ACC/BSW front, to examine how variation in condition and growth rate varies as a function of latitude, temperature, riverine influence, and trophic and dietary composition.

10.2 Materials and Methods

10.2.1 Fish Collections

Juvenile capelin ($n = 62$) were collected during the summer fall of 2012 using three different vessels spanning 13.9 of latitude (57.5° N– 71.4° N; Fig. 10.1). Capelin were selectively subsampled from expansive fish surveys from stations between 25 and 75 km from the coastline (with exception of the stations in Bristol Bay that were approximately 100 km from the coast) and thus likely to be near the ACC/BSW front (Stabeno et al. 1995; Steele et al. 2010). Capelin analyzed for this project are also limited to those <100 mm length and are assumed to be juveniles based on their size (Vesin et al. 1981; Hop and Gjørseter 2013) and lack of adult

pigmentation. Capelin were sampled using a 198-m-long surface trawl towed behind a 54.9-m chartered fishing vessel between August 8 and September 21, 2012. The trawl had hexagonal mesh on the wings and body, a 1.2 cm mesh cod end liner, and a 50 m x 25 m mouth (horizontal x vertical). Each tow lasted for 30 min at approximately 8.3 km h⁻¹ at stations within a 103 km² grid along the western Alaskan coast between 60° N and 71.4° N. Four more sites were sampled using the same methods by the NOAA ship Oscar Dyson between 57.5° N and 60° N (August 20–October 9, 2012). Capelin along the nearshore were sampled with beach seines near Barrow, AK (~71° N), during August 7–20, 2012. The seine was 37 m long with variable mesh sizes (10 m of 32 mm outer panels, 4 m of 6 mm middle panels, and 9 m of 3.2 mm blunt panel). Each set was round-haul style, paid out of a 7-m skiff following methods used by Johnson et al. (2010). All collections occurred during daylight hours. Physicochemical parameters from offshore stations were averaged from the top 20 m of the water column using a CTD at each sampling station at the time of collection. Water temperature and salinity from beach seine sites were measured from the top 0.5 m of water using a thermometer and refractometer. Fish were measured to fork length (FL) and kept frozen until analyzed in the laboratory.

Individual capelin were randomly subsampled within each site (Table 10.1). In the laboratory, individual fish wet weights were measured, stomach contents removed, and a sample of white muscle of ~0.01 g was dissected and frozen (-80 °C) for RNA/DNA analysis. Individual capelin were dried to a constant weight using a LECO Thermogravimetric Analyzer (TGA) 601/701 and homogenized using mortar and pestle until a uniform consistency was reached. Dry homogenates of individual juvenile capelin were stored in a desiccator prior to SIA and bomb calorimetry analyses.

10.2.2 Bomb Calorimetry

Energy density of juvenile capelin (kJ g⁻¹ dry mass) was quantified using bomb calorimetry. A Parr Instrument 6725 semi-micro bomb calorimeter was used to combust pellets of dry fish homogenate following standard instrument operating protocols from the manufacturer. Precision and accuracy of measurements were assessed by evaluating duplicate benzoic acid standards, replicate samples, and a tissue reference material of Pacific herring or walleye pollock homogenate. Error limits were set for the quality assurance samples, where precision from replicate benzoic acid standards was not allowed to vary by more than 1.5 % coefficient of variation and must have been within 2.0 % of the target value. Sample replicates were not allowed to vary by more than 1.5 standard deviations, and tissue reference samples were not allowed to vary by more than 3.0 % from target reference values.

10.2.3 RNA/DNA Analysis

Instantaneous growth rates were estimated from RNA/ DNA ratios following methods outlined in Sreenivasan (2011). A ~10 mg of frozen muscle sample was taken from each fish. RNA/DNA ratios were quantified fluorometrically using one dye and two enzymes (RNase and DNase; Caldarone et al. 2001). Nucleic acids were isolated from the smaller muscle samples and dyed using 75 µL ethidium bromide (5 lg ml⁻¹) according to the protocol outlined by Caldarone et al. (2001). Total fluorescence at excitation and emission wavelengths of 355 and 600 nm, respectively, was recorded, then the samples were sequentially treated with RNase and DNase, and the resulting reduced fluorescence was measured to obtain RNA and DNA fluorescence, respectively. Standard curves were constructed using serial dilutions of 18 s–28 s rRNA (Sigma R-0889) and calf thymus DNA (Sigma D-4764) standards. DNA concentrations in tissues are

stable, but RNA concentrations vary greatly depending on the rate of protein synthesis where a high RNA/DNA ratio indicates a high growth rate (Weber et al. 2003).

10.2.4 Stable Isotopes Analysis

SIA of carbon and nitrogen is used to examine the origins and type of dietary sources assimilated by fish (DeNiro and Epstein 1978, 1981). All subsamples of dried fish homogenate were weighed to 0.55 ± 0.15 mg. In between every four samples, a standard or duplicate sample was analyzed to examine precision of measurements. Samples were analyzed at the Florida International University SERC Stable Isotope Laboratory using elemental analysis–isotope ratio mass spectrometry (EA-IRMS), with a NA1500 NC (EA) coupled to a Delta C (IRMS). Error based on internal glycine standards ranged $0.09\text{--}0.21$ ‰ for $\delta^{15}\text{N}$ and $0.07\text{--}0.10$ ‰ for $\delta^{13}\text{C}$.

Lipid corrections were computed using C/N ratios (4.45 ± 0.66) following “Eq. 1” outlined by Logan et al. (2008). This equation requires the assumption that the difference between bulk $\delta^{13}\text{C}$ and lipid-free $\delta^{13}\text{C}$ approximates 6 ‰ as suggested by McConnaughey and McRoy (1979). Later work by Post et al. (2007) pointed out that these methods are suitable for organisms with 15 % or less lipid content, and that caution should be used at higher lipid contents because they had insufficient samples with such high-lipid content to adequately model the relationship. Thus, using the relationship presented by Post et al. (2007), we estimate that approximately 82 % of our samples contain less than 15 % lipids, 15 % of our samples contain <17.5 % lipid, and the remaining 3 % contain <20 % lipid. Based on this information, we deemed this method of lipid correction appropriate for our samples.

10.2.5 Stomach Contents

Prey from the stomach contents of juvenile capelin was identified to species and life-history stage where possible using methods outlined by Sturdevant et al. (2012). Adult Calanus spp. were classified by size: small B 2.4 mm in length, medium = 2.5–2.9 mm, and large C 3 mm. Aggregate wet weights of separated prey groups were measured from each fish. Weights were converted into percent contributions to the total mass of prey found in each stomach to standardize against the unevenness in fullness. Percent contributions from individual capelin were averaged over regional groups (see Data analysis section below) to standardize against unevenness in sample size.

10.2.6 Data Analysis

The 62 juvenile capelin from 17 sampling stations were separated into 7 regional groups (Table 10.1) based on latitude and distance from each other (Fig. 10.1). General Additive Models (GAMs) were used for qualitative assessment to identify patterns of dependent variables with latitude as the independent variables. Linear regressions were used to assess the relationship between dependent variables ($\delta^{15}\text{N}$, $\delta^{13}\text{C}$, energy density, RNA/DNA ratios, length, and weight) and to offer a quantitative approach to assessing the relationships of energetics and SIA with latitude.

10.3 Results

10.3.1 Energy Allocation

Across the sample set, energy density ranged from 20.77 to 26.49 kJ g⁻¹ (Mean \pm SD = 22.85 ± 1.33 kJ g⁻¹). RNA/ DNA ratios ranged from 13.10 to 31.61 (22.89 ± 4.33). Linear regression

indicated a weak positive correlation between energy density and RNA/DNA ($R^2 = 0.32$, $p < 0.0001$; Fig. 10.2a). Energy density increased significantly with latitude, but RNA/DNA did not (energy density: estimated degrees of freedom [edf] = 4, $R^2 = 0.34$, $p < 0.0001$, Fig. 10.3a; RNA/DNA: edf = 4, $R^2 = 0.14$, $p = 0.01$, Fig. 10.3b). The models for energy density and RNA/DNA suggest that the Point Barrow group may be an outlier relative to other samples, as the values rapidly decrease at this region group. In addition, capelin from Point Barrow were significantly smaller than all other groups (FL: $p = 0.0002$; wet weight: $p < 0.0001$) and were the only fish collected by beach seines in the very near shore. When the Point Barrow group was removed from the analysis, energy density was linearly correlated with latitude ($R^2 = 0.36$, $p < 0.0001$, Fig. 10.4a); however, the linear model between RNA/DNA and latitude was not significant ($R^2 = 0.06$, $p = 0.05$, Fig. 10.4b). Furthermore, linear regressions indicated that energy density was strongly positively correlated with fish length (FL: $R^2 = 0.47$, $p < 0.0001$) and full body wet weight ($R^2 = 0.63$, $p < 0.0001$).

In contrast, GAM models using sea surface temperature as a predictor indicated that more variability in RNA/DNA ratios was explained by surface temperature than in energy density (RNA/DNA: edf = 3, $R^2 = 0.28$, $p < 0.0001$; energy density: edf = 4, $R^2 = 0.15$, $p < 0.0001$, Fig. 10.5a– b); however, both models suggest that these measures vary slightly with increasing temperature until a threshold of approximately 9 °C is reached, at which point they both decreased rapidly. In turn, a GAM using surface temperature with latitude as the predictor indicates that these factors have a nonlinear relationship (edf = 4, $R^2 = 0.29$, $p < 0.0001$, Fig. 10.6).

10.3.3 Stable Carbon and Nitrogen Isotopes

Stable $\delta^{13}\text{C}$ and $\delta^{15}\text{N}$ isotope ratios of juvenile capelin were analyzed to identify changes in the origins of dietary material and trophic position across latitudes. Across this range, $\delta^{13}\text{C}$ ranged from -22.47 to 17.89 ‰ (mean \pm SD = -20.33 ± 1.10 ‰) and $\delta^{15}\text{N}$ ranged from 11.76 to 17.09 ‰ (14.31 ± 1.29 ‰). The linear correlation between $\delta^{13}\text{C}$ and $\delta^{15}\text{N}$ was strongly negative ($R^2 = 0.67$, $p < 0.0001$; Fig. 10.2B).

The relationships between $\delta^{13}\text{C}$ and $\delta^{15}\text{N}$ with latitude were highly significant, and much of the variability in both SIA measures could be explained by latitude ($\delta^{13}\text{C}$: edf = 3, $R^2 = 0.54$, $p < 0.0001$; $\delta^{15}\text{N}$: edf = 3, $R^2 = 0.67$, $p < 0.0001$; Fig. 10.3C-D). Linear regressions indicated that $\delta^{13}\text{C}$ was positively correlated and $\delta^{15}\text{N}$ was negatively correlated with latitude ($R^2 = 0.55$, $p < 0.0001$; $R^2 = 0.75$, $p < 0.0001$, respectively; Fig. 10.4c–d) when anomalies at the northernmost sampling stations (Point Barrow group) and the southernmost sampling stations (Bristol Bay group; Fig. 10.1) are removed. A similar pattern for each isotope was seen with temperature, suggesting that peak energy content and growth rate at the high latitudes coincide with feeding at higher trophic levels and incorporation of depleted $\delta^{13}\text{C}$.

10.3.4 Stomach Contents

Juvenile capelin diets were dominated by *Calanus spp.* copepods, with the average proportion of copepods in nonempty stomachs being 79.8 %. Stomach contents in Bristol Bay consisted solely of large- and medium-sized *Calanus spp.* copepods, but stations near the Bering Strait had increased prey diversity, including important contributions from decapod larvae, and smaller contributions of small copepods, cladocerans, and chaetognaths. At the Point Barrow stations, the diets consist completely of small copepods and *Themisto libellula*, a predatory hyperiid

amphipod (Auel and Werner 2003; Pinchuk et al. 2013). Of the capelin caught at Point Barrow, 56 % of them had empty stomachs, while empty stomachs were not observed at any other station (Fig. 10.7).

10.4 Discussion

10.4.1 Energy Allocation

Given that capelin occupy a wide latitudinal range, it is expected that they exhibit plasticity not only in their diet but also the allocation of energy obtained to cope with differences in climatic conditions. When prey resources are limited, we expect to see a trade-off between energy storage and growth rate as energy availability is generally not great enough to allow for concurrent processes of high growth rates and energy storage in juvenile fish (Post and Parkinson 2001). We saw evidence for increased energy provisioning for more severe winters in juvenile capelin in higher latitudes, with a positive correlation between energy density and latitude. This phenomenon has been observed for other fish species where the longer high-Arctic winters require a larger store of energy to survive than shorter, lowlatitude winter locations (Biro et al. 2005).

It is also plausible that though the fish were sampled at approximately the same time of year, season could play a factor in the greater energy densities at higher latitudes. Many species of fish undergo seasonal changes in their energy content as a factor of ontogenetic changes and maturation, particularly pelagic species such as capelin (Vollenweider et al. 2011). In general, fish increase energy during summer periods of high productivity, peak in the fall, and decline overwinter when prey can be scarce and gametes start developing for later spawning. The onset of winter will come much sooner to the fish in the Arctic. Therefore, it could be that higher energy densities observed at higher latitudes are a factor of the accelerated onset of winter, while further to the south there is additional time to prepare.

Increased energy storage at high latitudes could be expected to impair growth rates relative to southern areas. Another reason to expect lower growth rates in the Arctic is that capelin, as are many species of fish, are smaller at age at higher latitudes (Chambers and Leggett 1987; Chambers et al. 1989; Olsen et al. 2005). However, measurements of RNA/DNA remained relatively constant across latitudes. In concert, higher energy densities in the Arctic and equivalent RNA/DNA across latitudes imply that fish in higher latitudes have greater accessibility to energy resources that can be simultaneously allocated to growth and energy storage. An alternate explanation is that RNA/ DNA ratios in juvenile capelin are driven more by sea surface temperature. Comparisons across a temperature range have been shown to require laboratory-based calibration studies (Caldarone et al. 2001). Without these studies to validate the temperature effect on RNA/DNA and growth relationship, it is conceivable that temperature is confounding our use of RNA/DNA as an index to growth.

However, RNA/DNA ratios varied with temperature and were greatest just above 9 °C, which occurred in the middle range of the Chukchi coast near Wainwright Inlet. This indicates that RNA production is maximized at this temperature. However, it is unclear whether this translates to increased growth. It is possible that increased RNA synthesis is a compensation for reduced efficiency in protein synthesis enzymes (Houlihan et al. 1995; Smith and Ottema 2006). Coincidentally, this is also the location where energy density reached a maximum. This could

suggest that growing conditions are maximized at 9 °C. High growth rates near the end of the growing season have been associated with increased lipid reserves in high-latitude perch and subsequent winter survival (Huss et al. 2008). A summer-long sampling effort of capelin in the Point Barrow region during icefree periods in 2013 and 2014 shows that capelin were more abundant at 8–9 °C (Barton et al. unpublished data). Capelin distribution, abundance, and diet are impacted by water temperature. In cold years (1–2 °C below average), capelin are distributed across a much broader area in higher numbers in the Bering Sea, and energy-rich *Calanus* spp. are important diet items (Andrews et al. pers. comm.). In warm years (1–1.5 °C above average), capelin distribution is relatively restricted to the cooler, northern reaches of the Bering Sea, and energy-poor *Pseudocalanus* spp. and *Oikopleura* spp. were more abundant in their diet. During August 2012, when these samples were collected, an average temperature anomaly near Point Barrow stations of 5 to 7.5 °C above average was measured, suggesting that an abundance of energy-poor prey items was likely present (Parkinson and Comiso 2013).

Similarly, capelin distribution in Glacier Bay in Southeast Alaska was highly correlated with water temperatures, but in contrast to our results, these capelin were most abundant in the colder (6–7 °C) glacial waters over warmer (7–8 °C) estuarine central bay waters (Arimitsu et al. 2008). In this case, the glacial waters must have offered an advantage over the central bay waters. Glacial runoff brings with it high concentrations of nutrients (Hood and Scott 2008) and creates stratification by forming a freshwater lens, thus promoting plankton blooms to occur and providing an abundant food source for resident capelin. Additionally, Arimitsu et al. (2008) demonstrated that these waters were highly turbid, which may offer protection from sight-based predation, and increased feeding opportunities for capelin. Though we expect that temperature plays an important role in the life-history strategies of capelin, different temperature preferences in Southeast Alaska compared to the Western coast of Alaska in our study suggest that other factors such as predator abundance, prey availability, and turbidity may be more important drivers than temperature.

10.4.2 Stable Carbon and Nitrogen Isotopes

Relationships between $\delta^{13}\text{C}$ and $\delta^{15}\text{N}$ can be used to identify a number of factors that describe the variation of assimilated materials obtained through capelin diets as a function of latitude. It is common to observe positive correlations between $\delta^{13}\text{C}$ and $\delta^{15}\text{N}$ isotope ratios because both become enriched ($\delta^{13}\text{C} \approx +1 \text{ ‰}$; $\delta^{15}\text{N} \approx +3.8 \text{ ‰}$) with increasing trophic level provided that the basal resources remain the same (Hobson and Welch 1992; Layman et al. 2007a). The negative correlation seen in our results may suggest that within a single species, carbon sources and trophic structure may differ spatially. In order to better understand these differences in dietary composition of juvenile capelin, $\delta^{13}\text{C}$ and $\delta^{15}\text{N}$ ratios across the latitudinal range must be investigated individually.

10.4.3 Stable Carbon Isotopes

Basal resources in the BSW and Anadyr Water (AW) are mostly derived of pelagic production, but in the ACC basal resources consist mostly of terrestrial materials contributed by freshwater runoff (Grebmeier et al. 1988). This concept is consistent with the pattern of $\delta^{13}\text{C}$ throughout our sampling stations, suggesting that the majority of the variation in $\delta^{13}\text{C}$ may be explained by riverine inputs along the path of the ACC. It is expected that the ACC is less depleted in $\delta^{13}\text{C}$ when entering Bristol Bay as it is derived from relatively marine waters from the Gulf of Alaska moving through Unimak Pass (Kline 1999). As it travels north between 58° and 63° N, a number

of rivers discharge a substantial amount of fresh water into the ACC, including the Kvichak, Nushagak, Kuskokwim, and Yukon which cumulatively average 310 km³ year⁻¹ (40 % of the average annual freshwater runoff into the ACC; Fig. 10.1) (Weingartner et al. 2005; Benke and Cushing 2006). As these rivers discharge, $\delta^{13}\text{C}$ -depleted labile organic material accumulates and is incorporated into primary producers and eventually secondary consumers like capelin (Dunton et al. 2005; Helfield and Naiman 2016). As the ACC continues northward, it converges and mixes with the benthic-derived marine BSW and the AW (Grebmeier et al. 1988; Dunton et al. 2005), causing isotopic ratios to become less depleted again. The lack of major rivers that drain into the southern Chukchi coast of Alaska limits riverine inputs of terrestrial organic material north of the Bering Strait, and $\delta^{13}\text{C}$ continues to become less depleted as the ACC travels further north.

The pattern described above might suggest that $\delta^{13}\text{C}$ correlates with salinity; however, when this relationship was investigated, we found neither discernible patterns nor any significant correlation. This may be explained by the relative differences of salinity and isotopic content between riverine waters and ACC waters. We posit that the difference in salinity between riverine and coastal waters may be relatively small compared to the difference in abundance of materials that may be incorporated as basal resources, thus explaining why riverine discharge may elicit a change in $\delta^{13}\text{C}$, but not in salinity. Given that the ACC is known to be driven by freshwater discharge and has relatively low levels of in situ production (Grebmeier et al. 1988; Weingartner et al. 2005), this phenomenon may serve as a possible explanation for the observed trends.

Freshwater inputs support observations for $\delta^{13}\text{C}$ between 58° and 70° N, but an anomaly exists at the northernmost regional groups (Wainwright Inlet and Point Barrow) of the data set where $\delta^{13}\text{C}$ becomes more depleted again. It is possible that this could be attributed to the incorporation of high-lipid content in prey items that are depleting the carbon signature. However, if this were the case we would expect capelin in these regions to show an increase in energy density, which is not the case. A more likely explanation is that the series of small streams and rivers along the Chukchi coast of the North Slope of Alaska, as well as two substantial estuaries (Wainwright Inlet and Peard Bay) that are likely to carry large loads of labile terrestrial carbon from permafrost meltwater runoff into coastal waters, could be responsible for the depletion of $\delta^{13}\text{C}$ ratios in capelin at the northernmost stations (Dutta et al. 2006; Schuur et al. 2008). Though this runoff is relatively small compared to major rivers in the Bering Sea, when combined, these terrestrial inputs may be large enough to cause a significant shift in dietary $\delta^{13}\text{C}$ of capelin.

10.4.4 Stable Nitrogen Isotope

$\delta^{13}\text{C}$ and $\delta^{15}\text{N}$ have inverse relationships with latitude, where $\delta^{15}\text{N}$ is less enriched in Bristol Bay, and then rapidly becomes more enriched at Nunivak Island (17.1 ‰). The ratios became gradually less enriched with latitude, reaching a minimum at Point Hope (11.8 ‰), at which point they become enriched again at the northernmost groups (Wainwright Inlet and Point Barrow). When investigating carbon isotope patterns, we found that our results resembled broad-scale patterns described by Schell et al. (1998); however, the fluctuations we found in nitrogen isotopes do not. The difference between our maximum and minimum $\delta^{15}\text{N}$ surpasses the commonly accepted trophic enrichment value of 3.8 ‰ (Hobson and Welch 1992; Post 2002; Hansen et al. 2012) and suggests that capelin along this latitudinal gradient are feeding at different trophic levels. When this pattern is compared to that of $\delta^{13}\text{C}$, it becomes clear that $\delta^{15}\text{N}$

is more enriched where terrestrial inputs are increased. This difference may be attributed to one or both of two scenarios: (1) The prey that capelin feed on are depending on different basal resources; (2) and capelin are feeding on different prey types in relation to latitude.

One possible explanation is that the basal resources vary with latitude and may elicit a cascading effect on the isotopic ratios of capelin. Fractionation of $\delta^{15}\text{N}$ differs depending on the type of nitrogen compounds used by primary producers. Atmospheric nitrogen (N^2) fixers such as phytoplankton generally have a small range of $\delta^{15}\text{N}$ (-2 to 2 ‰), whereas nitrate, nitrite, ammonia, and ammonium fixers such as benthic marine plants and terrestrial plants have a much greater range (-8 to 3 ‰), leading to a wide range of possible values of coastal basal resources (Fry 2007). As mentioned previously, the relationship between $\delta^{13}\text{C}$ and $\delta^{15}\text{N}$ suggests that $\delta^{15}\text{N}$ becomes more enriched where terrestrial inputs are highest. It is likely that the increased diversity in basal resources caused by the increased terrestrial inputs led to an increase in trophic level variation, thus supporting more trophic levels than areas with less terrestrial input (Layman et al. 2007b). This suggests that Arctic coastal food webs may gain complexity and productivity as Arctic warming continues to increase the magnitude of freshwater discharge (Peterson et al. 2002).

This logic leads us to consider the types of prey items being consumed as an explanation for patterns in nitrogen isotopes. The majority of capelin analyzed may be classified into the lower half of the size class defined as juveniles (75–100 mm) by Vesin et al. (1981), a life stage at which gape and stomach size limits consumable prey items and variability in their diet. Dietary composition of these small capelin was dominated by *Calanus* copepods, with the average proportion of copepods in non-empty stomachs being 79.8 % (Fig. 10.7). Less common prey items including decapod larvae, chaetognaths, and the hyperiid amphipod *T. libellula* are only seen at the Point Barrow group. Isotopic ratios of different size copepods are not likely to differ greatly because of their low trophic position (Schell et al. 1998), but decapod larvae, chaetognaths, and *T. libellula* feed on copepods, thus adding a trophic level between capelin and copepods (Saito and Kiørboe 2001; Auel and Werner 2003). The inclusion of these less common prey types may be responsible for the enrichment observed in $\delta^{15}\text{N}$. Feeding data suggest that at the latitudes where $\delta^{15}\text{N}$ became suddenly enriched (Nunivak Island and Point Barrow), capelin included less common prey items in their diet that would be expected to feed at higher trophic levels (chaetognaths and *T. libellula*, respectively; Fig. 10.7). These results suggest that higher trophic level prey items are present where terrestrial nutrients are abundant and are at least partially responsible for variations in $\delta^{15}\text{N}$ with latitude.

Fish collected at Point Barrow were anomalous in all dependent variables ($\delta^{13}\text{C}$, $\delta^{15}\text{N}$, energy density, and RNA/ DNA). These fish were collected with beach seines and thus are inhabitants of the very nearshore where conditions can be extremely variable in comparison to the coastal offshore waters where the other fish were collected with surface trawls. If these nearshore samples are comparable with the offshore samples in lower latitudes, we may expect that the energy density of sub-Arctic forage fish in the Arctic may increase as future high-latitude conditions change to resemble current lower-latitude conditions. This may offer an alternate high-quality prey source for Arctic piscivores as climate change continues.

However, it is also possible that these nearshore fish are not comparable with offshore samples and thus were removed from most analyses as they were significantly smaller in size than all other samples. The Point Barrow fish were significantly lower in energy density ($p = 0.0004$) and RNA/DNA ($p = 0.0004$) than capelin examined from other areas. When examining the other regional groups, energy density increases from Bristol Bay to Wainwright Inlet and RNA/DNA remains relatively constant; however, at Point Barrow both of these measures fell to some of the lowest values observed. Furthermore, diet data indicate that most of the nearshore fish had empty stomachs (61 %) suggesting that prey are sparsely distributed, and these fish may be undernourished or have difficulty locating prey. The anomalous enrichment of $\delta^{15}\text{N}$ in these fish may support this premise. During starvation, animals will metabolize their own fat and muscle tissue to survive; in essence, they are eating themselves. This causes trophic fractionation and will make it appear as though they are feeding at a higher trophic level (Vander Zanden and Rasmussen 2001). The combination of poor condition and growth, coupled with evidence of low food availability and potential starvation, suggests that the Arctic nearshore habitats near Barrow may not be an optimal environment for juvenile capelin.

If these nearshore habitats are suboptimal, why were capelin highly abundant? These had the highest surface temperatures (11 °C) and were much higher than the optimal growth temperatures (~9 °C), which is not likely to motivate capelin to inhabit these waters. One explanation for their abundance is that these shallow and turbid nearshore waters offer an advantage over nearby habitats such as refuge from abundant local predators (belugas, seals, and sea birds), which are commonly observed feeding in the nearshore. However, it is also possible that juvenile capelin are blown or advected into suboptimal nearshore areas by strong wind and currents, and therefore, their presence in the Arctic nearshore near Barrow is not by choice.

10.5 Conclusions

The combination of growth and condition indices with SIA is a useful method to understand how isotopic food sources contribute to fish production. We suggest that capelin may be an ideal species for such analysis and can provide insight into how the ecosystem may restructure under different climate scenarios, as they have a key trophic position in the ecosystem and a wide latitudinal range. A benefit of using a wide-ranging species such as capelin is that their response to different environmental conditions can be considered a natural experiment; however, as we have pointed out, this also requires additional information to interpret at regional scales. The Chukchi Sea is a sink for biota advected from the Bering Sea, and therefore, communities associated with warm conditions in the Bering Sea may serve as proxies to examine Arctic community level dynamics in the face of warming conditions (Walsh et al. 2004; Woodgate et al. 2012; Coyle et al. 2013). Consequently, examining the response of capelin to a range of physiological conditions may offer a better understanding of how populations of these important forage fish and the community in the Chukchi will respond to climate change. This study has revealed large-scale variation in condition of capelin, but the mechanisms behind this variation need to be further explored.

Varying terrestrial inputs are one mechanism that likely affected capelin condition. Habitats with greater terrestrial inputs are likely to have higher trophic diversity and more basal resources based on ranges of isotopic ratios. This is an important premise as freshwater inputs are expected to increase with climate change, and thus, we may expect to see more complex and more productive Arctic coastal food webs to develop in response. Two important questions arise from

our results: (1) Will climate change lead to higher energy density of sub-Arctic forage fish in the Arctic and offer alternate high-quality forage to nearshore piscivores? (2) Are capelin utilizing suboptimal nearshore habitats near Barrow to avoid predation, or are they advected there through their ontogeny? We suggest that additional studies be developed to examine energetics and SIA of capelin in Arctic and sub-Arctic habitats to better elucidate the mechanisms that underlie these patterns.

10.6 Acknowledgements

We thank Franz Mueter and the rest of the Arctic EIS crew for providing samples, as well as the scientists and crewmen aboard the R/V Oscar Dyson. Special thanks to Craig George, Leandra de Sousa, Todd Sformo, Robert Suydam, and the North Slope Borough Division of Wildlife, who provided significant logistical support for collection of samples in Barrow. Additional thanks to those NOAA affiliates who processed samples in the bioenergetics laboratory, including A Robertson, M Callahan, A Sreenivasan, E Fergusson, J Weems, and H Findley. Funding was provided in part by the North Pacific Research Board to KM Boswell (Project 1229) and in part from BOEM Interagency Agreement Contract Nos. M12PG00024 (ACES) and M12PG00018 (Arctic EIS) of the US Department of the Interior, Bureau of Ocean Energy Management (BOEM), Alaska Outer Continental Shelf Region, Anchorage Alaska as part of the BOEM Environmental Studies Program. This report is funded in part with qualified outer continental shelf oil and gas revenues by the Coastal Impact Assistance Program, Fish and Wildlife Service, US Department of the Interior under Agreement Number 10-CIAP-010, F12AF00188. This is contribution No. 18 from the Marine Education and Research Center in the Institute for Water and Environment at Florida International University.

10.7 References

- Álvarez E, López-Urrutia Á, Nogueira E (2012) Improvement of plankton biovolume estimates derived from image-based automatic sampling devices: Application to FlowCAM. *J Plankton Res* 34:454–469. doi: 10.1093/plankt/fbs017
- AMAP (2008) Arctic oil and Gas. Arctic Monitoring and Assessment Programme, Oslo, Norway
- Beck M, Jr KH, Able K (2001) The identification, conservation, and management of estuarine and marine nurseries for fish and invertebrates. *Bioscience* 51:633–641.
- Benke A, Cushing C (2006) Rivers of North America, First Edit. Elsevier Academic Press, Burlington, MA
- Berkman P, Young O (2009) Governance and environmental change in the Arctic Ocean. *Science* (80-.). 324:339–340.
- Bluhm B, Gradinger R (2008) Regional Variability in Food Availability For Arctic Marine Mammals. *Ecol Appl* 18:S77–S96. doi: <http://dx.doi.org/10.1890/06-0562.1>
- Borer AET, Seabloom EW, Shurin JB, et al (2008) What Determines the Strength of a Trophic Cascade? Published by : Ecological Society of America WHAT DETERMINES THE STRENGTH OF A TROPHIC CASCADE ? 86:528–537.
- Craig P (1984) Fish use of coastal waters of the Alaskan Beaufort Sea: a review. *Trans Am Fish Soc* 113:37–41.
- Craig P, Griffiths W, Haldorson L, McElderry H (1985) Distributional patterns of fishes in an Alaskan arctic lagoon. *Polar Biol* 4:9–18.
- Craig PC, Griffiths B, Griffiths WB, Ffiths WBGR (1982) Ecological Studies of Arctic Cod (*Boreogndus saida*) in Beaufort Sea Coastal Waters, Alaska. *Can Bull Fish Aquat Sci* 39:395–406. doi: 10.1139/f82-057

- Danielson SL, Weingartner TJ, Hedstrom KS, et al (2014) Coupled wind-forced controls of the Bering-Chukchi shelf circulation and the Bering Strait throughflow: Ekman transport, continental shelf waves, and variations of the Pacific-Arctic sea surface height gradient. *Prog Oceanogr* 125:40–61. doi: 10.1016/j.pocean.2014.04.006
- Deegan L a. (1993) Nutrient and Energy Transport between Estuaries and Coastal Marine Ecosystems by Fish Migration. *Can. J. Fish. Aquat. Sci.* 50:74–79.
- Dehn L, Follmann E, Thomas D, et al (2006) Trophic relationships in an Arctic food web and implications for trace metal transfer. *Sci Total Environ* 362:103–123. doi: 10.1016/j.scitotenv.2005.11.012
- Dehn L, Sheffield G, Follmann E, et al (2007) Feeding ecology of phocid seals and some walrus in the Alaskan and Canadian Arctic as determined by stomach contents and stable isotope analysis and stable isotope analysis. *Polar Biol* 30:167–181. doi: 10.1007/s00300-006-0171-0
- DeNiro M, Epstein S (1981) Influence of diet on the distribution of nitrogen isotopes in animals. *Geochim Cosmochim Acta* 45:341–351.
- DeNiro MJ, Epstein S (1978) Influence of diet on the distribution of carbon isotopes in animals. *Geochim. Cosmochim. Acta* 42:495–506.
- Dunton KH, Schonberg S V., Cooper LW (2012) Food Web Structure of the Alaskan Nearshore Shelf and Estuarine Lagoons of the Beaufort Sea. *Estuaries and Coasts* 35:416–435. doi: 10.1007/s12237-012-9475-1
- Dunton KH, Weingartner T, Carmack EC (2006) The nearshore western Beaufort Sea ecosystem: Circulation and importance of terrestrial carbon in arctic coastal food webs. *Prog Oceanogr* 71:362–378. doi: 10.1016/j.pocean.2006.09.011
- Elliott M, O'Reilly MG, Taylor CJL (1990) The forth estuary: a nursery and overwintering area for North Sea fishes. *Hydrobiologia* 195:89–103. doi: 10.1007/BF00026816
- Fry B (2006) *Stable Isotope Ecology*, Third edit. Springer, Baton Rouge, LA
- Fry B, Baltz D, Benfield M, et al (2003) Stable Isotope Indicators of Movement and Residency for Brown Shrimp (*Farfantepenaeus aztecus*) in Coastal Louisiana Marshscapes. *Estuaries* 26:82–97.
- Grebmeier J, McRoy C (1989) Pelagic-benthic coupling on the shelf of the northern Bering and Chukchi Seas. III Benthic food supply and carbon cycling . *Mar Ecol Prog Ser* 53:79–91. doi: 10.3354/meps053079
- Grebmeier JM, Mcroy CP, Feder HM (1988) Pelagic-benthic coupling on the shelf of the northern Bering and Chukchi Seas . I . Food supply source and benthic biomass. *Mar Ecol* 48:57–67.
- HECKY RE, FEE EJ (1981) Primary production and rates of algal growth in Lake Tanganyika. *Limnol Oceanogr* 26:532–547. doi: 10.4319/lo.1981.26.3.0532
- Hobson K, Clark R (1992) Assessing avian diets using stable isotopes I: turnover of ¹³C in tissues. *Condor* 94:181–188.
- Hobson K, Welch H (1992) Determination of trophic relationships within a high arctic marine food web using Delta-¹³ C and Delta-¹⁵ N analysis. *Mar Ecol Prog Ser* 84:9–18.
- Hobson KA, Schell DM, Renouf D, Noseworthy E (1996) Stable carbon and nitrogen isotopic fractionation between diet and tissues of captive seals : Implications for dietary reconstructions involving marine mammals. *Can J Fish Aquat Sci* 53:528–533. doi: 10.1139/cjfas-53-3-528

- Iken K, Bluhm B, Dunton K (2010) Benthic food-web structure under differing water mass properties in the southern Chukchi Sea. *Deep Res Part II Top Stud Oceanogr* 57:71–85. doi: 10.1016/j.dsr2.2009.08.007
- Johannesson OM, Bengtsson L, Miles MW, et al (2004) Arctic climate change : observed and modelled temperature and sea-ice variability. *Tellus* 56:328–341.
- Johnson SW, Thedinga JF, Neff AD, Hoffman CA (2010) Fish Fauna in Nearshore Waters of a Barrier Island in the Western Beaufort Sea , Alaska.
- Johnson WR (1988) Current response to wind in the Chukchi Sea: A regional coastal upwelling event.
- Jones N (2012) Oil exploration ramps up in US Arctic.
- Layman CA, Arrington DA, Montaña CG, et al (2007) Can Stable Isotope Ratios Provide for Community-Wide Measures of Trophic Structure. *Ecology* 88:42–48.
- Loecher M, Ropkins K (2015) Rgooglemaps and loa: Unleashing R Graphics Power on Map Tiles. *J Stat Softw* 63:1–18.
- Logan J, Haas H, Deegan L, Gaines E (2006) Turnover rates of nitrogen stable isotopes in the salt marsh mummichog, *Fundulus heteroclitus*, following a laboratory diet switch. *Oecologia* 147:391–5. doi: 10.1007/s00442-005-0277-z
- Madigan DJ, Litvin SY, Popp BN, et al (2012) Tissue turnover rates and isotopic trophic discrimination factors in the endothermic teleost, pacific bluefin tuna (*Thunnus orientalis*). *PLoS One* 7:e49220. doi: 10.1371/journal.pone.0049220
- McMahon CR, Bester MN, Hindell M a., et al (2009) Shifting trends: Detecting environmentally mediated regulation in long-lived marine vertebrates using time-series data. *Oecologia* 159:69–82. doi: 10.1007/s00442-008-1205-9
- McManus MA, Woodson CB (2012) Plankton distribution and ocean dispersal. *J Exp Biol* 215:1008 – 1016. doi: 10.1242/jeb.059014
- Moline M a, Karnovsky NJ, Brown Z, et al (2008) High latitude changes in ice dynamics and their impact on polar marine ecosystems. *Ann N Y Acad Sci* 1134:267–319. doi: 10.1196/annals.1439.010
- Nemeth M, Priest J, Degan D, et al (2014) Sockeye salmon smolt abundance and inriver distribution: results from the Kvichak, Ugashik, and Egegik rivers in Bristol Bay, Alaska, 2014.
- Norcross BL, Holladay B a., Busby MS, Mier KL (2010) Demersal and larval fish assemblages in the Chukchi Sea. *Deep Sea Res Part II Top Stud Oceanogr* 57:57–70. doi: 10.1016/j.dsr2.2009.08.006
- Norcross BL, Holladay BA, Busby MS, Mier K (2004) RUSALCA – Fisheries Ecology and Oceanography.
- Phillips DL, Newsome SD, Gregg JW (2005) Combining sources in stable isotope mixing models: alternative methods. *Oecologia* 144:520–7. doi: 10.1007/s00442-004-1816-8
- Richlen M, Lobel P (2011) Effects of depth, habitat, and water motion on the abundance and distribution of ciguatera dinoflagellates at Johnston Atoll, Pacific Ocean. *Mar Ecol Prog Ser* 421:51–66. doi: 10.3354/meps08854
- Rosenblatt AE, Heithaus MR (2013) Slow isotope turnover rates and low discrimination values in the american alligator: implications for interpretation of ectotherm stable isotope data. *Physiol Biochem Zool* 86:137–48. doi: 10.1086/668295
- Thedinga J, Johnson S, Neff A, et al (2012) Nearshore Fish Assemblages of the Eastern Chukchi Sea , Alaska. Juneau, AK

- Walsh JJ, Dieterle D a., Chen FR, et al (2011) Trophic cascades and future harmful algal blooms within ice-free Arctic Seas north of Bering Strait: A simulation analysis. *Prog Oceanogr* 91:312–343. doi: 10.1016/j.pocean.2011.02.001
- Wiens J (1989) Spatial scaling in ecology. *Society* 3:385–397. doi: 10.2307/2389612
- York N (1980) Fairbridge, R. 1980. The estuary: its definitions and geodynamic cycle, pp. 1-35. In: E Olausson and I Cato (eds.), *Chemistry and Biochemistry of Estuaries*. Wiley, New York.

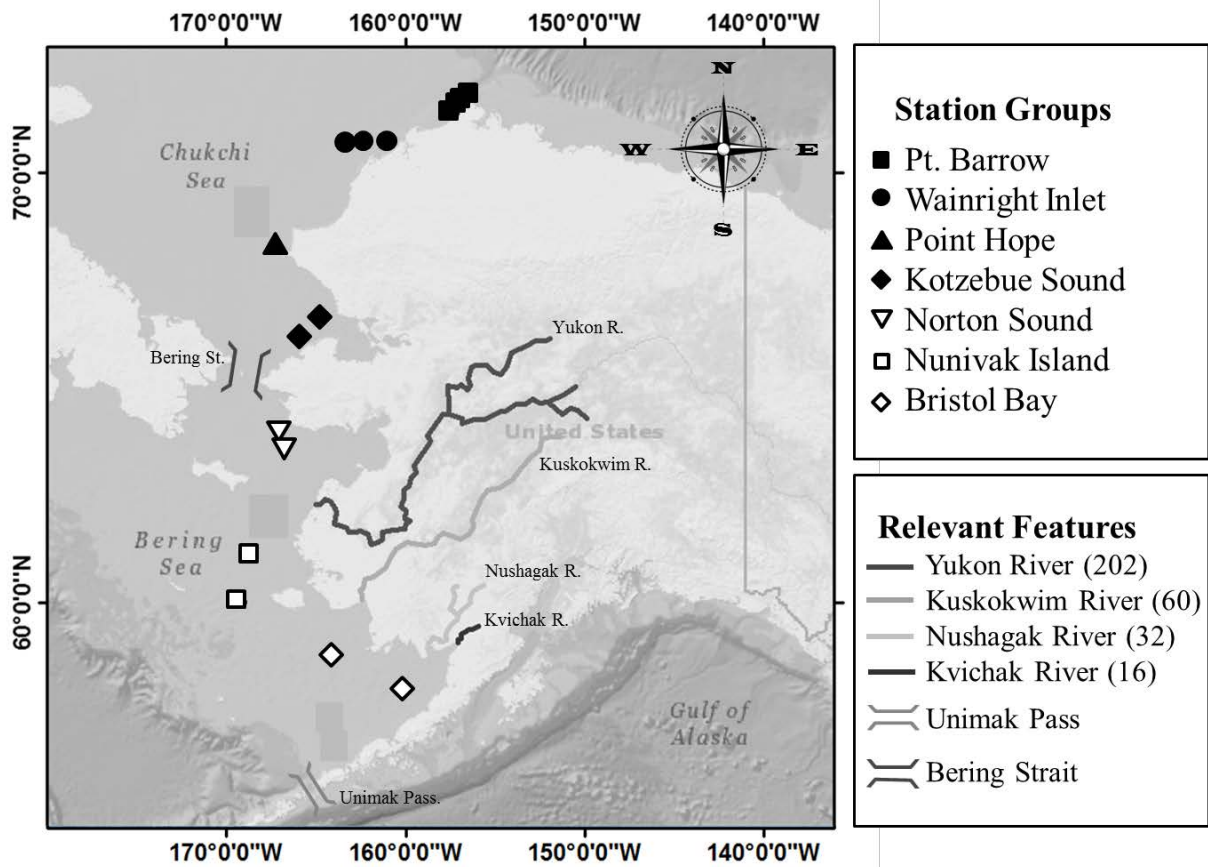


Figure 10.1 Map of Alaskan waters showing sampling locations of juvenile capelin collected. Filled shapes represent the Chukchi Sea stations, open shapes represent Bering Sea stations. Like symbols represent regional groups of fish at similar latitudes. The numbers in parentheses after each river represent the individual annual discharge ($\text{km}^3 \text{ yr}^{-1}$) of each river (Benke and Cushing 2006; Nemeth et al. 2014). This map was produced with the CRAN-R package “Rgooglemaps” (Loecher and Ropkins 2015).

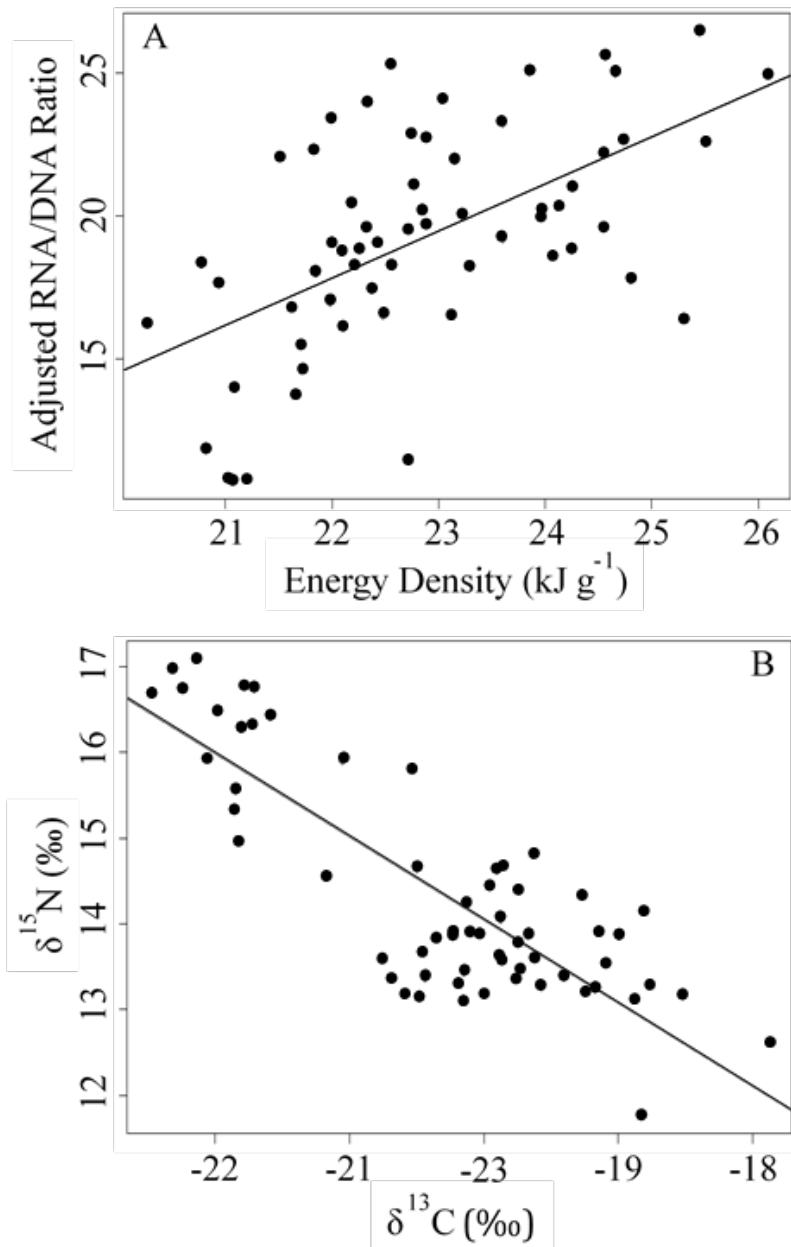


Figure 10.2 Linear regression between energy density and RNA/DNA ratios were strongly correlated (A; $R^2=0.3163$, $p<0.0001$). A linear regression between $\delta^{13}\text{C}$ and $\delta^{15}\text{N}$ shows a strong negative correlation (B; $R^2=0.6747$, $p<0.0001$).

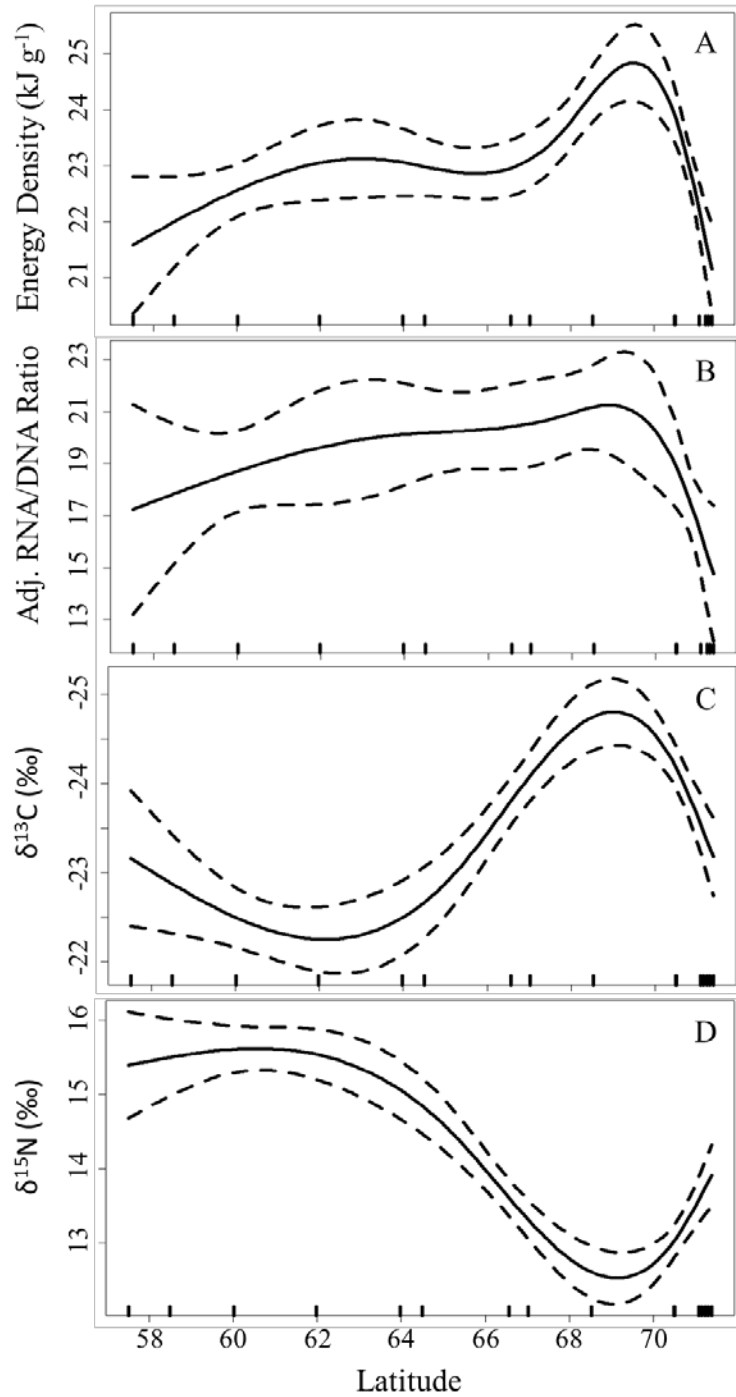


Figure 10.3 General Additive Models for energy density (A), RNA/DNA Ratios (B), $\delta^{13}\text{C}$ (C) and $\delta^{15}\text{N}$ (D) for all juvenile capelin with a smoothing function on latitude. All models were created using cubic splines were used with 5 knots ($\text{edf} = 4$) for Energy Density and RNA/DNA ratios, and 4 knots ($\text{edf} = 3$) for $\delta^{13}\text{C}$ and $\delta^{15}\text{N}$. The dashed lines represent the 95% confidence interval. Each model was significant with varying levels of deviance explained (A: $R^2 = 0.34$,

$p < 0.0001$; B: $R^2 = 0.14$, $p = 0.01$; C: $R^2 = 0.54$, $p < 0.0001$; D: $R^2 = 0.67$, $p < 0.0001$). The bold tick marks above the x-axis represent latitudes at which fish samples were collected.

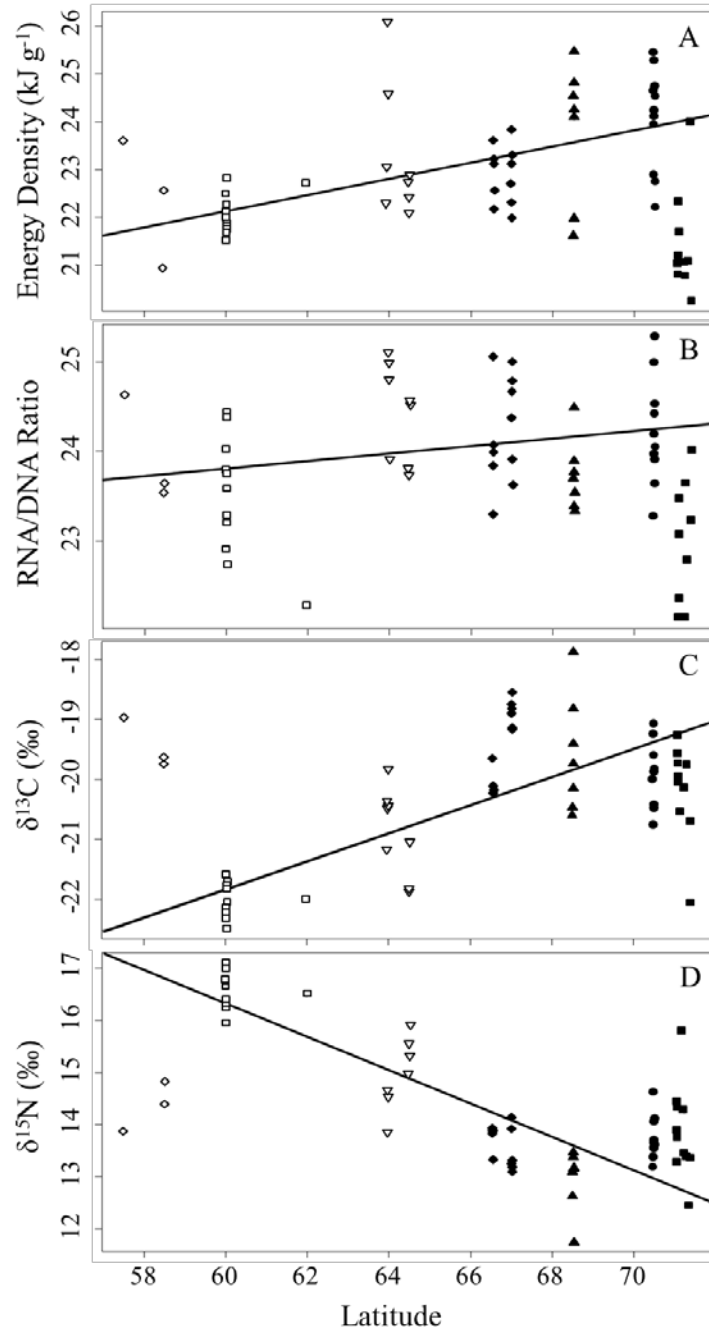


Figure 10.4 Linear regressions of energy density (A), RNA/DNA Ratios (B), $\delta^{13}\text{C}$ (C) and $\delta^{15}\text{N}$ (D) with latitude. The northern-most sampling stations (Point Barrow group: ■) and the southern-most sampling stations (Bristol Bay group: ◇) were removed as outliers for the analysis. Energy density was strongly correlated ($R^2=0.36$, $p<0.0001$) with latitude, but RNA/DNA ratios were not ($R^2=0.06$, $p=0.05$). $\delta^{13}\text{C}$ is negatively correlated and $\delta^{15}\text{N}$ is positively correlated with latitude ($R^2=0.55$, $p<0.0001$; $R^2=0.75$, $p<0.0001$; respectively). Station symbology: Wainwright inlet (●), Point Hope (▲), Kotzebue Sound (◆), Norton Sound (▽), and Nunivak Island (□).

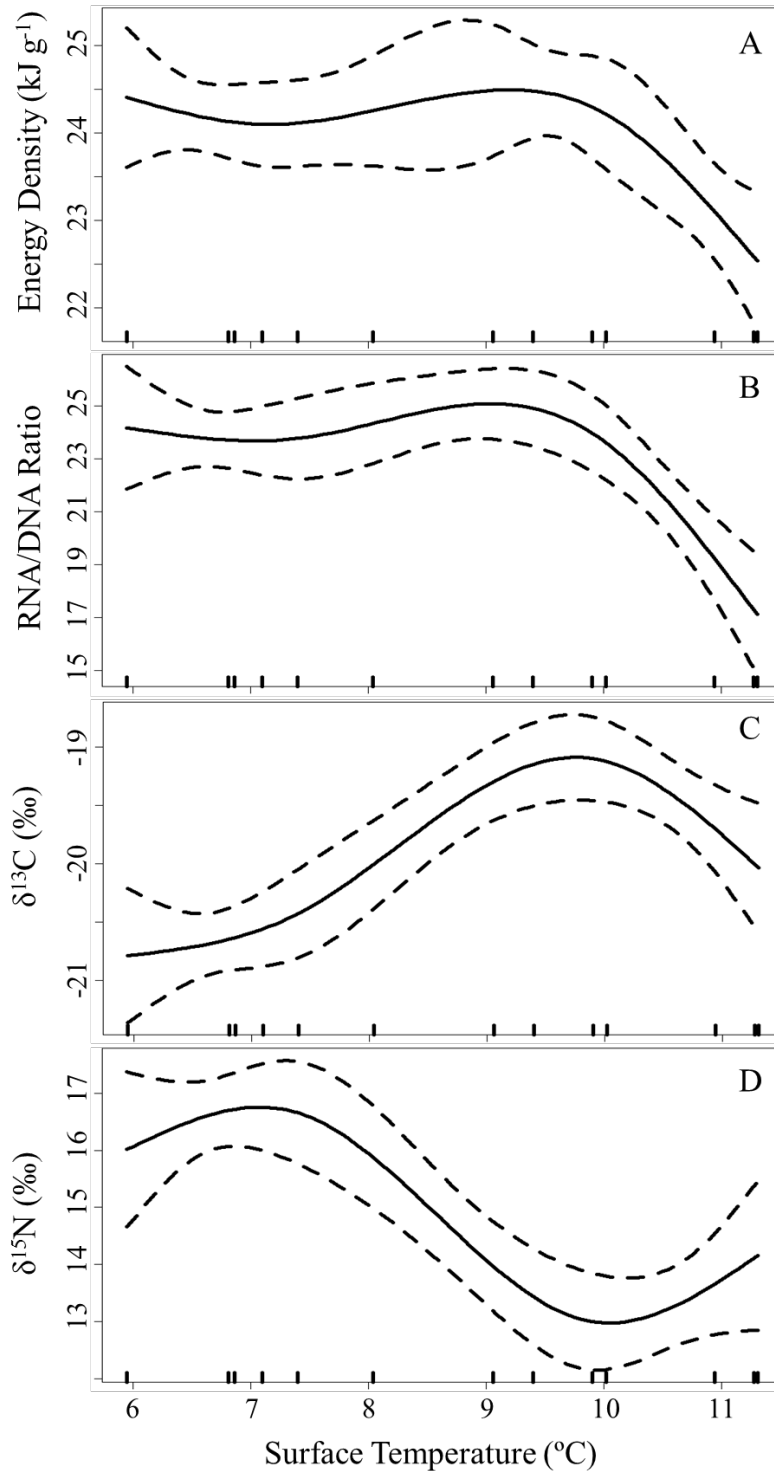


Figure 10.5 General Additive Models for energy density (A), RNA/DNA Ratios (B), $\delta^{13}\text{C}$ (C) and $\delta^{15}\text{N}$ (D) for all juvenile capelin with a smoothing function on temperature. All models were created using cubic splines were used with 5 knots (edf = 4) for Energy Density, and 4 knots (edf = 3) for RNA/DNA ratios, $\delta^{13}\text{C}$ and $\delta^{15}\text{N}$. The dashed lines represent the 95% confidence interval. All models were significant with varying levels of deviance explained (A: $R^2 = 0.15$,

$p < 0.0001$; B: $R^2 = 0.28$, $p < 0.0001$; C: $R^2 = 0.31$, $p < 0.0001$; D: $R^2 = 0.30$, $p < 0.0001$). The bold tick marks above the x-axis represent latitudes at which fish samples were collected.

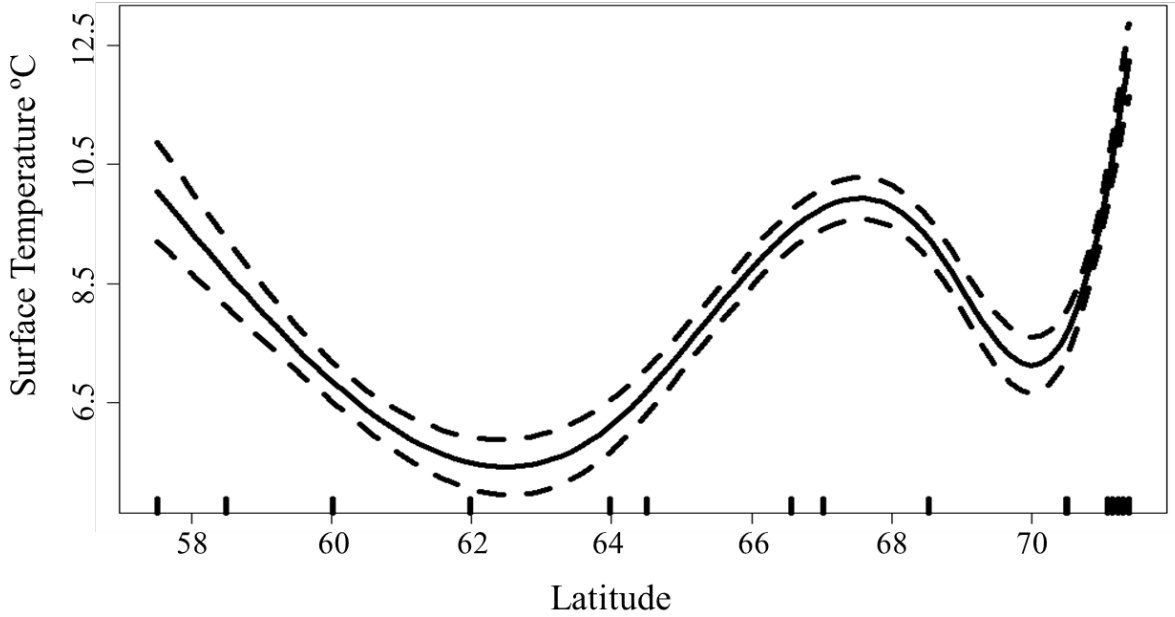


Figure 10.6 GAM of surface temperature with a smoothing function on latitude. The non-linear relationship shows that there is no discernable trend between surface temperature and latitude. The dashed lines represent the 95% confidence intervals. Cubic splines were used with 5 knots ($edf = 4$), the GAM explains 28.8% of the deviance and the relationship was found to be significant ($p < 0.0001$). The bold tick marks above the x-axis represent latitudes at which fish samples were collected.

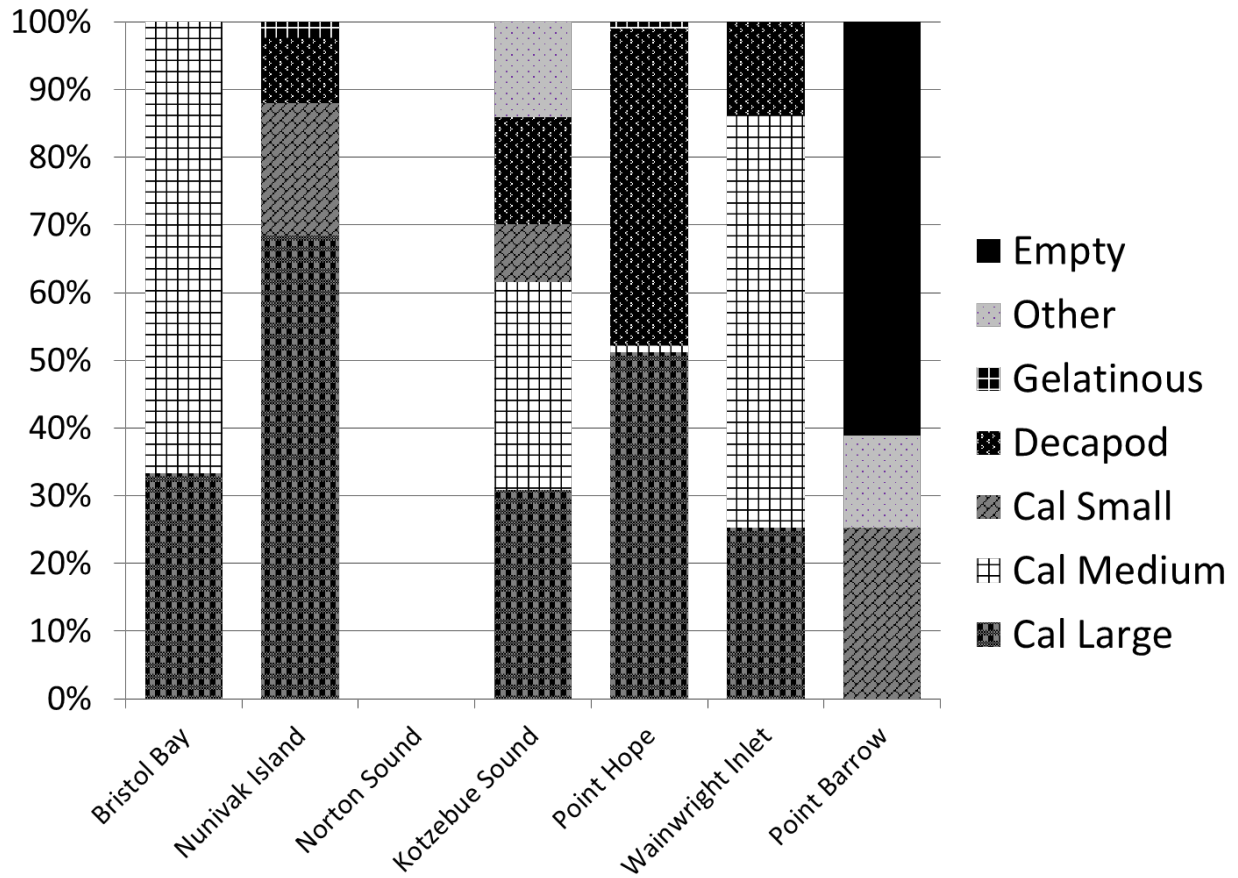


Figure 10.7 Average contributions by weight of prey type in the stomach contents of the analyzed capelin for 6 of the 7 regional groups identified in Table 1. Cal = *Calanus spp.* copepod. No stomach contents data was available for the Norton Sound Group.

Table 10.1 Details of sample sizes and regional group differentiation. Throughout this paper, “regional group” refers to the 7 groups differentiated by symbols.

Group Name	Symbol	Sample Date	Sample Gear	Latitude Range (° N)	N Fish	N Stations	Fish Length (mm) Mean (SD)	SST (°C) Mean (SD)
Pt. Barrow	■	Aug 18–19	Beach Seine	71.09–71.39	11	5	72.8 (8.1)	11.2 (0.2)
Wainwright Inlet	●	Aug 19–20	Surface Trawl	70.50–70.52	11	3	88.4 (7.3)	7.3 (0.6)
Point Hope	▲	Aug 13–14	Surface Trawl	68.54	7	1	89.7 (6.0)	9.9 (-)
Kotzebue Sound	◆	Aug 8–10	Surface Trawl	66.57–67.04	11	2	89.5 (8.0)	9.5 (0.5)
Norton Sound	▽	Sept 12–14	Surface Trawl	63.97–64.51	8	2	85.4 (10.9)	5.95 (0.0)
Nunivak Island	□	Sept 10–20	Surface Trawl	60.01–61.98	11	2	82.2 (7.9)	7.1 (0.1)
Bristol Bay	◇	Aug 21–26	Surface Trawl	57.52–58.49	3	2	81.3 (7.8)	8.7 (0.9)

11.0 Patterns in Basal Resources and Suspended Particulate Matter Compositions in Arctic habitats

M. Barton, K. Abel

11.1 Introduction

Declining sea ice coverage in the Arctic has drawn the attention of global industries such as oil and gas exploration, tourism, and shipping industries (Berkman and Young 2009). These industries have the potential to benefit the global economy by providing jobs and important resources; however, they also pose a potential threat to surrounding ecosystems. Much research effort has been put forth to establish baseline information that can be used to assess the impacts of these potential changes (Norcross et al. 2004; Norcross et al. 2010), but to date there has been little effort in the lagoon and barrier island chains that comprise much of the Arctic nearshore (Craig 1984; Craig et al. 1985; Johnson et al. 2010; Thedinga et al. 2012; Dunton et al. 2012). Though we presume that these habitats have similar importance in coastal ecosystems as well-studied lower latitude estuaries (York 1980; Elliott et al. 1990; Deegan 1993), we cannot assume this without further research.

These estuaries are likely to be important nurseries and foraging grounds for a multitude of fish, birds and marine mammal species as well as an important resource for local subsistence villages. In the event of a disturbance, small organisms and particles are likely to be affected most rapidly. (McManus and Woodson 2012) Given that these small particles make up the base of the food web, these effects are likely to cascade trophically thus affecting all organisms that depend on these resources (Borer et al. 2008; Walsh et al. 2011).

Since microscopic organisms and detritus have high turnover rates, suspended particulate matter (SPM) content can vary greatly at fine temporal scales (McManus and Woodson 2012). In order to account for temporal variability it is important to obtain a sufficient number of samples over an extended period of time (Wiens 1989). Furthermore, SPM content may vary greatly over fine spatial scales and may be greatly affected by physical processes and conditions. For example, high turbulence caused by intense weather conditions or currents can stir up fine particles from the substrate such as detritus, sand and benthic diatoms (Hecky and Fee 1981). On the other end of the spectrum, low turbulence conditions can lead to stratification and settlement of denser particles, leading to a high phytoplankton content and low sediment and detrital content. By focusing on SPM we will be able to identify different patterns in basal resource availability through space and time, providing important information that will help improve predictions of how these ecosystems may change in the face of Arctic climate change.

Identifying SPM content can be time consuming, tedious, and costly making it difficult to collect and process a sufficient number of samples in the field. A Fluid Imaging Flowcam can process these samples rapidly by taking pictures of individual particles as they water sample flows through a digital camera's field of view (Álvarez et al. 2012). These images are saved and can be processed at a later time after the field season, making it possible to focus field effort on sample collection. We aim to use SPM content collected in the Point Barrow region to identify spatiotemporal patterns that will help create a solid baseline that can be used to assess potential

future impacts of climate change, oil and gas exploration, tourism, and shipping in Arctic nearshore ecosystems.

11.2 Methods

11.2.1 Study Area

Point Barrow, AK is a unique area where multiple Arctic nearshore habitat types are found in close proximity to each other. Furthermore, Point Barrow is bordered on the West by the Chukchi Sea (CHS) and to the East by the Beaufort Sea (BFS), with the large estuarine Elson Lagoon (ESL) opening into the Beaufort Sea just 5 km Southeast of Point Barrow. These distinct water bodies have distinct conditions that are likely to support different food web structures. Furthermore, this dynamic area undergoes a great change as it shifts from ice-covered winter to open water summer, and these changes are expected to drive changes in basal resources and prey availability as the seasons progress, offering an opportunity to study spatiotemporal patterns in SPM.

11.2.2 Sample Collection and Lab Processing

Suspended particulate matter was sampled at 12 stations (5 CHS, 3 BFS, and 4 ESL) at a rate of two samples per week in each water body from July 14th – August 25th (Week 1–6) in 2014 surrounding Point Barrow. Samples were collected using from surface waters and poured through a stack of nitex mesh sieves (300, 100, and 20 μm). Water was filtered until the 20 μm mesh became clogged and the total volume was recorded (Richlen and Lobel 2011). Particles retained by the 20 and 100 μm meshes were retained for further analysis in a Fluid Imaging Flowcam, whereas the 300 μm mesh prevented large debris from entering the flowcam samples. Flowcam samples were collected by flushing the nitex mesh with filtered seawater (filtered through a 1 μm mesh), and collecting the runoff in a 50 ml centrifuge tube. This process was continued until the 50 ml was full (Johnson et al. 2010)(Johnson et al. 2010)(Johnson et al. 2010)(Johnson et al. 2010) collections occurred during daylight hours. Once returning to the lab, a 2 ml aliquot of the 50 ml samples (20 and 100 μm) was enumerated and analyzed in the flowcam, and the images were saved for further analysis.

Given the large number of particles encountered by the flowcam, random subsamples of 10% of the total particles (100 particles for samples with a total less than 1000) were taken. The images were then categorized into six categories: detritus, phytoplankton, zooplankton, sediment, miscellaneous and deleted using Fluid Imaging's Visual Spreadsheet. All counts were corrected by the volume of water sampled to get # of Particles/L to ensure comparability between samples. A detailed description of physical traits that were used to categorize the particles is outlined in Table 11.1. The deleted category was used to correct total enumerations so that Catch Per Unit Effort (CPUE) would be comparable across all samples.

After samples from all six weeks were categorized the relative contributions of each category was calculated, as well as a comparable CPUE (particles/L). Patterns in CPUE and relative composition were analyzed using visual representations of the data (Figure 11.1–11.2).

11.3 Results

During the six week sampling period, a total of 30 samples were enumerated from the three water bodies, 10 in BFS, 6 in CHS, and 14 in ESL. A total of 17,744 particles were collected. Average particles/L differed between water bodies as well as within water bodies: BFS 341 ± 256 (mean \pm SD), CHS 196 ± 39 , ESL 940 ± 691 . Particles in collected in the 20 μm mesh were high in the first week, but dropped to a low the next week, following a steady increase until the end of the sampling period (Figure 11.1). There was no distinguishable pattern in particle content for the 100 micron mesh size. Week four ESL in the 100 μm sample had the highest CPUE recorded at 1154 particles/L (Figure 11.2). In week 6 all three water bodies had relatively high particle content and all three were dominated by detritus. Elson lagoon over all had the highest average particles/L of all three water bodies but also had the highest variance. The Chukchi Sea had the lowest average and variance of the three and was primarily dominated by detritus. The Beaufort Sea varied between detritus and phytoplankton, and the particle content was in between the Chukchi and Elson Lagoon.

11.4 Discussion

Phytoplankton and particulate matter content was particularly high in the Elson Lagoon when compared to the Beaufort and Chukchi Seas. This difference in high abundance of phytoplankton and particulate matter in general collected in the Elson Lagoon over the other two water bodies can be explained by multiple environmental factors occurring during the 6 week sampling period. Elson Lagoon is blocked off from direct currents coming from the Chukchi and Beaufort Sea by a barrier island chain. Due to the relative isolation and lack of circulation in the Elson Lagoon waters tend to become easily stratified leading to warmer temperatures and high productivity (Hecky and Fee 1981). Meltwater runoff from the nearby tundra is likely to intensify stratification by creating a freshwater lens as well as supply ample nutrients to support a high phytoplankton abundance and terrestrial organic material that contributes to the detrital content. Both Beaufort and Chukchi had low SPM particles compared to ESL, this is probably due to the constant flow of the Alaska Coastal Current (ACC) preventing settling of particles. In contrast, the ESL is likely to have higher sedimentation rates, and much of these particles are resuspended and deposited whenever a wind event causes vertical mixing. This concept seems to be supported by the medium SPM in the BFS, which has a direct connection to the ESL, whereas the CHS with low SPM lacks this connection.

Previous works have suggested that the Chukchi Sea is significantly more productive than the Beaufort Sea (Grebmeier et al. 1988; Norcross et al. 2010)(Grebmeier and McRoy 1989), yet the data suggests the opposite with the Chukchi having the lowest SPM of the three water bodies. This contradictory pattern may be explained by a patchy distribution in primary productivity that was missed by our relatively fine sampling. The Chukchi borders the Northeast bound ACC on the Southeastern side, suggesting that wind direction between North to East would favor upwelling after the Coriolis effect is taken into account (Johnson 1988). However, during 2014 the dominant wind direction was South. This may explain why the Chukchi Sea seemed to be less productive compared to the Elson Lagoon and Beaufort Sea during this sampling season. Perhaps, if our sampling design were expanded to larger spatial and temporal scales the CHS would have been realized as the more productive water body (NOAA ESRL Weather Station at Wiley-Post International Airport, Barrow, AK).

Another pattern noted was the difference in particle composition content between the 20 μm and 100 μm mesh. Week 1 and 3 were similar, but weeks 2, 4, 5, and 6 had stark differences between the two mesh sizes. The 20 μm started high in the week 1 then rapidly decreased the following week and continued to increase steadily throughout the sampling period, while the 100 μm was more erratic and did not show any discernable temporal pattern. The pattern seen in the 20 μm mesh may be explained by increasing primary productivity throughout the summer. Summer temperature and stratification create optimal conditions for phytoplankton to bloom. The initial decrease in particles collected in the 20 μm mesh may be a result of zooplankton grazing. Zooplankton abundance often has a delayed response to phytoplankton blooms as the bloom must first reach a biomass capable of supporting a growing zooplankton population.

Following the same predator-prey response logic, we might also expect the particles collected by the 100 μm mesh to increase throughout the summer, but this pattern is not realized in our data. This is likely because our methods of collection are biased to non-motile organisms, and may not be representative of the zooplankton community. In future efforts it would be best to include a plankton tow to collect larger and more motile plankton species so that a more comprehensive dataset can be constructed.

11.5 References

- Álvarez E, López-Urrutia Á, Nogueira E (2012) Improvement of plankton biovolume estimates derived from image-based automatic sampling devices: Application to FlowCAM. *J Plankton Res* 34:454–469. doi: 10.1093/plankt/fbs017
- AMAP (2008) Arctic oil and Gas. Arctic Monitoring and Assessment Programme, Oslo, Norway
- Beck M, Jr KH, Able K (2001) The identification, conservation, and management of estuarine and marine nurseries for fish and invertebrates. *Bioscience* 51:633–641.
- Benke A, Cushing C (2006) Rivers of North America, First Edit. Elsevier Academic Press, Burlington, MA
- Berkman P, Young O (2009) Governance and environmental change in the Arctic Ocean. *Science* (80-.). 324:339–340.
- Bluhm B, Gradinger R (2008) Regional Variability in Food Availability For Arctic Marine Mammals. *Ecol Appl* 18:S77–S96. doi: <http://dx.doi.org/10.1890/06-0562.1>
- Borer AET, Seabloom EW, Shurin JB, et al (2008) What Determines the Strength of a Trophic Cascade? Published by : Ecological Society of America WHAT DETERMINES THE STRENGTH OF A TROPHIC CASCADE? 86:528–537.
- Craig P (1984) Fish use of coastal waters of the Alaskan Beaufort Sea: a review. *Trans Am Fish Soc* 113:37–41.
- Craig P, Griffiths W, Halderson L, McElderry H (1985) Distributional patterns of fishes in an Alaskan arctic lagoon. *Polar Biol* 4:9–18.
- Craig PC, Griffiths B, Griffiths WB, Ffiths WBGR (1982) Ecological Studies of Arctic Cod (*Boreogndus saida*) in Beaufort Sea Coastal Waters, Alaska. *Can Bull Fish Aquat Sci* 39:395–406. doi: 10.1139/f82-057
- Danielson SL, Weingartner TJ, Hedstrom KS, et al (2014) Coupled wind-forced controls of the Bering-Chukchi shelf circulation and the Bering Strait throughflow: Ekman transport, continental shelf waves, and variations of the Pacific-Arctic sea surface height gradient. *Prog Oceanogr* 125:40–61. doi: 10.1016/j.pocean.2014.04.006

- Deegan L a. (1993) Nutrient and Energy Transport between Estuaries and Coastal Marine Ecosystems by Fish Migration. *Can. J. Fish. Aquat. Sci.* 50:74–79.
- Dehn L, Follmann E, Thomas D, et al (2006) Trophic relationships in an Arctic food web and implications for trace metal transfer. *Sci Total Environ* 362:103–123. doi: 10.1016/j.scitotenv.2005.11.012
- Dehn L, Sheffield G, Follmann E, et al (2007) Feeding ecology of phocid seals and some walrus in the Alaskan and Canadian Arctic as determined by stomach contents and stable isotope analysis and stable isotope analysis. *Polar Biol* 30:167–181. doi: 10.1007/s00300-006-0171-0
- DeNiro M, Epstein S (1981) Influence of diet on the distribution of nitrogen isotopes in animals. *Geochim Cosmochim Acta* 45:341–351.
- DeNiro MJ, Epstein S (1978) Influence of diet on the distribution of carbon isotopes in animals. *Geochim. Cosmochim. Acta* 42:495–506.
- Dunton KH, Schonberg S V., Cooper LW (2012) Food Web Structure of the Alaskan Nearshore Shelf and Estuarine Lagoons of the Beaufort Sea. *Estuaries and Coasts* 35:416–435. doi: 10.1007/s12237-012-9475-1
- Dunton KH, Weingartner T, Carmack EC (2006) The nearshore western Beaufort Sea ecosystem: Circulation and importance of terrestrial carbon in arctic coastal food webs. *Prog Oceanogr* 71:362–378. doi: 10.1016/j.pocean.2006.09.011
- Elliott M, O'Reilly MG, Taylor CJL (1990) The forth estuary: a nursery and overwintering area for North Sea fishes. *Hydrobiologia* 195:89–103. doi: 10.1007/BF00026816
- Fry B (2006) *Stable Isotope Ecology*, Third edit. Springer, Baton Rouge, LA
- Fry B, Baltz D, Benfield M, et al (2003) Stable Isotope Indicators of Movement and Residency for Brown Shrimp (*Farfantepenaeus aztecus*) in Coastal Louisiana Marshscapes. *Estuaries* 26:82–97.
- Grebmeier J, McRoy C (1989) Pelagic-benthic coupling on the shelf of the northern Bering and Chukchi Seas. III Benthic food supply and carbon cycling . *Mar Ecol Prog Ser* 53:79–91. doi: 10.3354/meps053079
- Grebmeier JM, Mcroy CP, Feder HM (1988) Pelagic-benthic coupling on the shelf of the northern Bering and Chukchi Seas . I . Food supply source and benthic biomass. *Mar Ecol* 48:57–67.
- HECKY RE, FEE EJ (1981) Primary production and rates of algal growth in Lake Tanganyika. *Limnol Oceanogr* 26:532–547. doi: 10.4319/lo.1981.26.3.0532
- Hobson K, Clark R (1992) Assessing avian diets using stable isotopes I: turnover of ¹³C in tissues. *Condor* 94:181–188.
- Hobson K, Welch H (1992) Determination of trophic relationships within a high arctic marine food web using Delta-¹³ C and Delta-¹⁵ N analysis. *Mar Ecol Prog Ser* 84:9–18.
- Hobson KA, Schell DM, Renouf D, Noseworthy E (1996) Stable carbon and nitrogen isotopic fractionation between diet and tissues of captive seals : Implications for dietary reconstructions involving marine mammals. *Can J Fish Aquat Sci* 53:528–533. doi: 10.1139/cjfas-53-3-528
- Iken K, Bluhm B, Dunton K (2010) Benthic food-web structure under differing water mass properties in the southern Chukchi Sea. *Deep Res Part II Top Stud Oceanogr* 57:71–85. doi: 10.1016/j.dsr2.2009.08.007
- Johannesson OM, Bengtsson L, Miles MW, et al (2004) Arctic climate change : observed and modelled temperature and sea-ice variability. *Tellus* 56:328–341.

- Johnson SW, Thedinga JF, Neff AD, Hoffman CA (2010) Fish Fauna in Nearshore Waters of a Barrier Island in the Western Beaufort Sea , Alaska.
- Johnson WR (1988) Current response to wind in the Chukchi Sea: A regional coastal upwelling event.
- Jones N (2012) Oil exploration ramps up in US Arctic.
- Layman CA, Arrington DA, Montaña CG, et al (2007) Can Stable Isotope Ratios Provide for Community-Wide Measures of Trophic Structure. *Ecology* 88:42–48.
- Loecher M, Ropkins K (2015) Rgooglemaps and loa: Unleashing R Graphics Power on Map Tiles. *J Stat Softw* 63:1–18.
- Logan J, Haas H, Deegan L, Gaines E (2006) Turnover rates of nitrogen stable isotopes in the salt marsh mummichog, *Fundulus heteroclitus*, following a laboratory diet switch. *Oecologia* 147:391–5. doi: 10.1007/s00442-005-0277-z
- Madigan DJ, Litvin SY, Popp BN, et al (2012) Tissue turnover rates and isotopic trophic discrimination factors in the endothermic teleost, pacific bluefin tuna (*Thunnus orientalis*). *PLoS One* 7:e49220. doi: 10.1371/journal.pone.0049220
- McMahon CR, Bester MN, Hindell M a., et al (2009) Shifting trends: Detecting environmentally mediated regulation in long-lived marine vertebrates using time-series data. *Oecologia* 159:69–82. doi: 10.1007/s00442-008-1205-9
- McManus MA, Woodson CB (2012) Plankton distribution and ocean dispersal. *J Exp Biol* 215:1008 – 1016. doi: 10.1242/jeb.059014
- Moline M a, Karnovsky NJ, Brown Z, et al (2008) High latitude changes in ice dynamics and their impact on polar marine ecosystems. *Ann N Y Acad Sci* 1134:267–319. doi: 10.1196/annals.1439.010
- Nemeth M, Priest J, Degan D, et al (2014) Sockeye salmon smolt abundance and inriver distribution: results from the Kvichak, Ugashik, and Egegik rivers in Bristol Bay, Alaska, 2014.
- Norcross BL, Holladay B a., Busby MS, Mier KL (2010) Demersal and larval fish assemblages in the Chukchi Sea. *Deep Sea Res Part II Top Stud Oceanogr* 57:57–70. doi: 10.1016/j.dsr2.2009.08.006
- Norcross BL, Holladay BA, Busby MS, Mier K (2004) RUSALCA – Fisheries Ecology and Oceanography.
- Phillips DL, Newsome SD, Gregg JW (2005) Combining sources in stable isotope mixing models: alternative methods. *Oecologia* 144:520–7. doi: 10.1007/s00442-004-1816-8
- Richlen M, Lobel P (2011) Effects of depth, habitat, and water motion on the abundance and distribution of ciguatera dinoflagellates at Johnston Atoll, Pacific Ocean. *Mar Ecol Prog Ser* 421:51–66. doi: 10.3354/meps08854
- Rosenblatt AE, Heithaus MR (2013) Slow isotope turnover rates and low discrimination values in the american alligator: implications for interpretation of ectotherm stable isotope data. *Physiol Biochem Zool* 86:137–48. doi: 10.1086/668295
- Thedinga J, Johnson S, Neff A, et al (2012) Nearshore Fish Assemblages of the Eastern Chukchi Sea , Alaska. Juneau, AK
- Walsh JJ, Dieterle D a., Chen FR, et al (2011) Trophic cascades and future harmful algal blooms within ice-free Arctic Seas north of Bering Strait: A simulation analysis. *Prog Oceanogr* 91:312–343. doi: 10.1016/j.pcean.2011.02.001
- Wiens J (1989) Spatial scaling in ecology. *Society* 3:385–397. doi: 10.2307/2389612

York N (1980) Fairbridge, R. 1980. The estuary: its definitions and geodynamic cycle, pp. 1-35.
In: E Olausson and I Cato (eds.), *Chemistry and Biochemistry of Estuaries*. Wiley, New York.

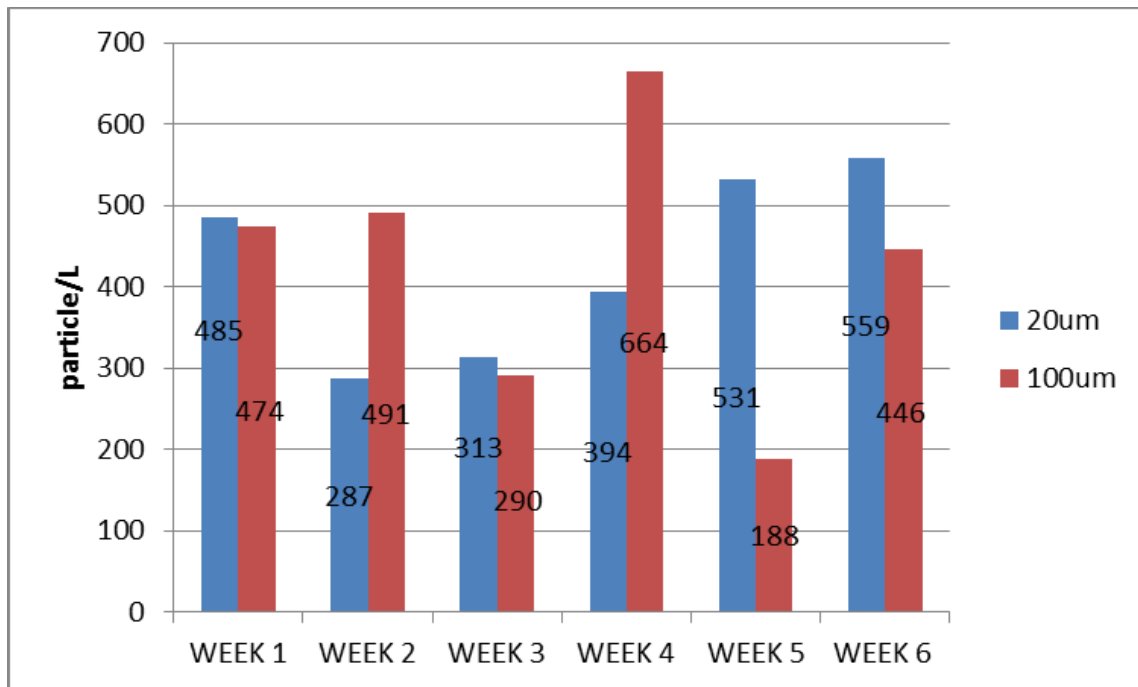


Figure 11.1 Graphical representation of CPUE for each size class separated by week. CPUE is given as Particles/L. Mesh size 20 μm includes particles between 20–100 μm in length, and mesh size 100 μm represents particles between 100–300 μm in length.

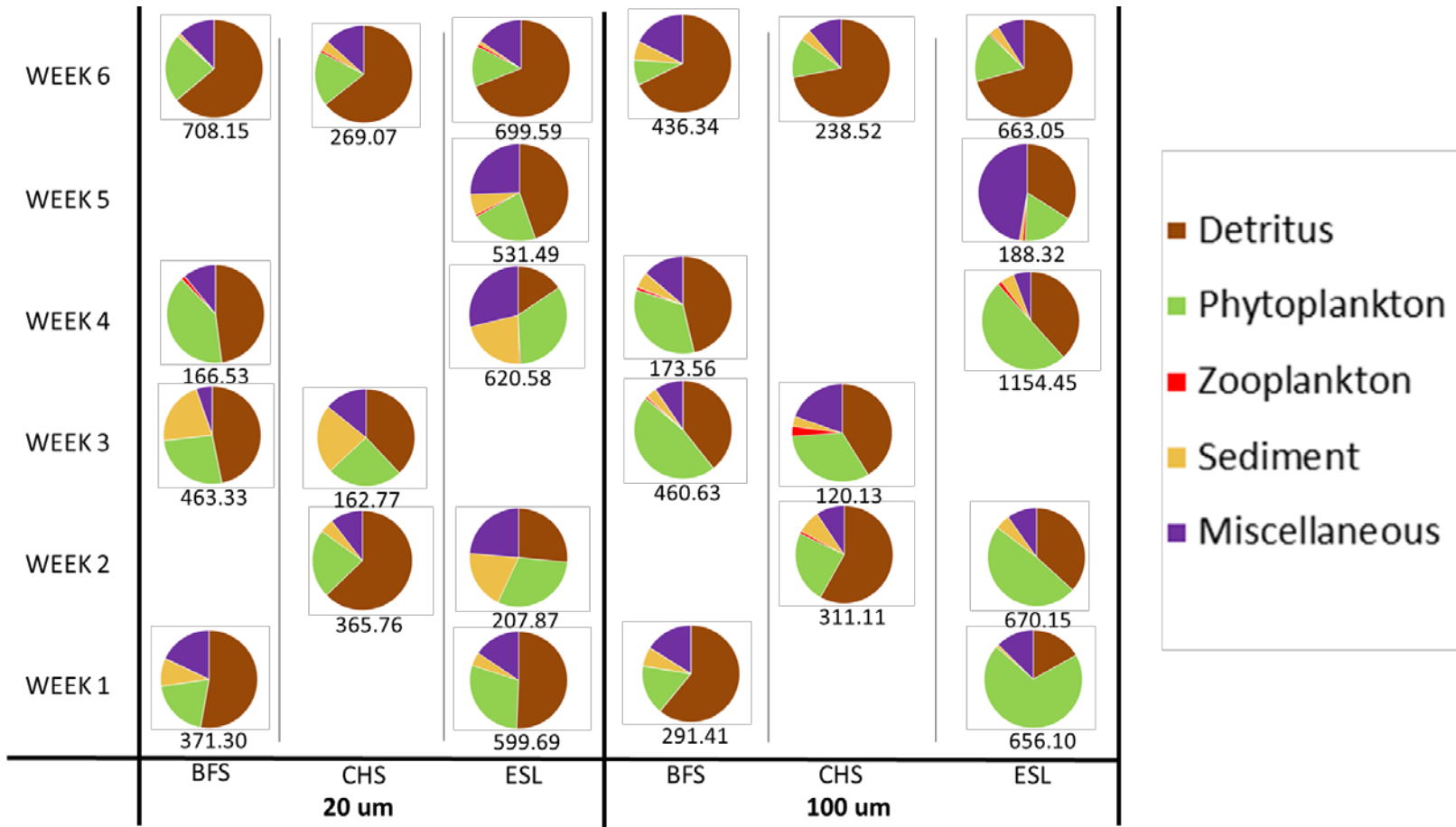
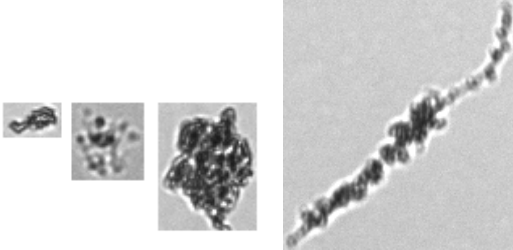
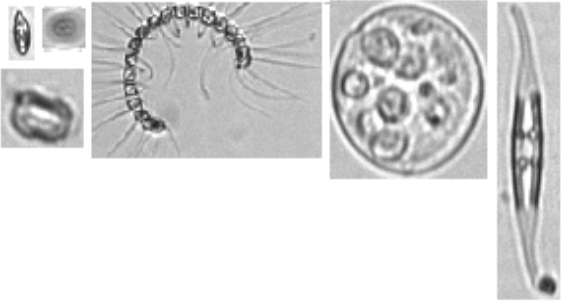


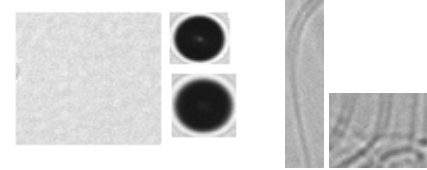


Figure 11.2 Relative abundance of Suspended Particulate Matter (SPM) divided by water body and size class on the X-axis and sampling week on the y-axis. The number under each pie chart is the CPUE for that week in Particles/L. Mesh size 20 µm includes particles between 20–100 µm in length, and mesh size 100 µm represents particles between 100–300 µm in length.

Table 11.1 Physical attributes used to categorize particles in the Flowcam images. Images are provided.

Categories	Physical Attributes
<p>Detritus</p> 	<ul style="list-style-type: none"> • High intensity (high light absorption) • Asymmetrical • No organelles or defined structures • variable sizes
<p>Phytoplankton</p> 	<ul style="list-style-type: none"> • Symmetry • Defined/deliberate shape • Organelles and/or bristles • Size range: >20 μm
<p>Zooplankton</p> 	<ul style="list-style-type: none"> • Symmetry • mobile appendages • Differentiated tissues and/or organs
<p>Sediment</p> 	<ul style="list-style-type: none"> • Low intensity (low light absorption) • Defined outline • No organelles or appendages • Can occur in small clusters
<p>Deleted</p> 	<ul style="list-style-type: none"> • Bubbles: black perfect circle, often with a light outline and/or a light center • Blanks: false identification of a particle when no particle is present • Appendages without a body mass
<p>Miscellaneous</p>	

12.0 Conclusions

We found that nearshore Arctic habitats are dominated by juveniles and therefore function as nursery areas similar to other nearshore areas in the rest of the globe. Arctic nearshore areas are “reset” every year through ice scouring. Direct evidence of this was observed from fine-scale habitat mapping. As the summer ice-free season progresses, fish move into the newly available habitat as the ice melts and species diversity and abundance increases. Within a summer, periods of sustained wind force oceanographic currents and consequently structure nearshore fish communities of juvenile fish with relatively poor swimming ability. Chukchi sites were most different from the other water bodies, with annual differences in the fish community likely stemming from influences from the adjacent Alaska Coastal Current. Elson Lagoon showed no annual differences in fish community composition as it is more of an enclosed system. The Beaufort sites appear to be a complex mixing zone between the Chukchi and Elson water bodies, with interannual differences in fish communities every year. Annual differences in fish communities were associated with changes in water temperature and pervasive storm conditions.

Specifically, we assessed the “seasonal” composition and variation in nearshore fish communities and the degree of connectivity between three water bodies (Chukchi Sea, Beaufort Sea, Elson Lagoon) near Barrow, Alaska during the summer ice-free season (early July – late August) of 2013 and 2015. Through weekly beach seining, concurrent oceanographic measurements, catch analysis, and laboratory processing of fish samples, we evaluated the following hypotheses:

H₁: There will be no difference in the spatial patterns or habitat association of fish and invertebrate communities as a function of habitat designation or along functional habitat gradients (depth, salinity, temperature).

Conclusions: Species composition, species richness and abundance are different in the three waterbodies surrounding Point Barrow: Chukchi Sea, Beaufort Sea, and the extensive Elson Lagoon.

- Nearshore habitats are reset annually due to ice scouring of sea ice, evidenced by finescale habitat maps.
- Fish appear to take advantage of lagoon resources early in summer as the habitat is available first with early sea ice melting, then abundance shifts to the Beaufort and Chukchi as summer progresses.
- Fish species richness and abundance increase significantly between weeks as fish move into the newly available habitats. Fish communities do not vary on a daily scale.
- Sculpin are present in all 3 water bodies consistently throughout the summer period. Because of their continued presence and high site fidelity, they could be considered a “biomonitor for environmental change”.
- Sand lance are more abundant in the 2 marine water bodies, while capelin and cisco are more abundant in Elson Lagoon.
- Biodiversity in the Beaufort and Chukchi Seas is dominated by pulses of sub-Arctic forage fish (capelin, sand lance, slender eelblenny), and it is likely that their patchy distribution leads to an underrepresentation of their abundance.

- There is a strong, predictive correlation between the wind velocity and the water flow in and out of Elson Lagoon through Plover Pass near Point. Because fish in the nearshore are predominantly juveniles, their reduced swimming capacity subjects them to prevailing ocean currents.
- Fish community composition was significantly influenced by wind speed and direction, with some influence of temperature and salinity. (38% of the variance in community composition can be explained with only 7 variables: Wind speed and direction at 12 hr lag time, surface salinity, air temperature, 2 principle components of euclidean distance, and year).
- Annual differences were detected in fish communities, depending on the water body. In Elson Lagoon, fish community composition was similar in all 3 years (2013-2015). In the Chukchi Sea, 2014 and 2015 had similar community composition, but 2013 was markedly different, which was a year in which the Alaska Coastal Current (just offshore of our sampling area) had a partial shut-down. In the Beaufort Sea, there were differences in community composition in all 3 years, suggesting a more complicated structure likely because it's a mixing zone between the Chukchi, Elson Lagoon and the Eastern Beaufort.
- Forage fish are more abundant in warmer calmer years (2013), whereas no forage fish (including Arctic cod) are abundant in cold and windier years (2014), suggesting that warming conditions may lead to higher abundance of forage in the nearshore initially.

H₂: Size, energy content, feeding ecology, and age structure of targeted species will not vary among habitats.

Conclusions: The high degree of connectivity of between the three habitats and the relatively small distance between sampling sites (80 km distance between furthest sites) contributed to the failure to detect distinct differences in energy content of fish. Rather, all the nearshore areas of this study showed relatively depressed energy content relative to offshore areas from which samples were obtained from other projects.

H₃: There will be no detectable linkages in productivity pathways between lagoon and nearshore habitats based on energetics, growth, and isotopic composition of fishes.

Conclusions: The Beaufort and Chukchi Seas display a relationship between $\delta^{13}\text{C}$ and $\delta^{15}\text{N}$ typical of a food web that depends on a single basal resource. Elson Lagoon appears to be dependent on multiple basal resources. The majority of the nearshore foodweb is dependent on terrestrial carbon and nitrogen fixed by primary production, however a few species in the lagoon appear to be dependent on marine derived carbon. Increasing evidence that Arctic trophic systems may have lower than typical trophic enrichment factors for nitrogen suggest that these systems may have 1-2 more trophic levels than previously believed.

Additional Findings:

1. The most abundant species caught in nearshore areas include sculpin species, Pacific sand lance, capelin, eelblennies, and to a lesser degree Arctic cod, saffron cod, snailfish, flatfish and cisco.

2. The majority of fish in nearshore areas are juveniles.
3. Analysis of local weather data in Barrow showed that average air temperature increased sharply in the last decade.
4. There were some extended periods of several weeks with relatively sustained wind speed and direction, but at other times wind speed and direction is highly volatile changing on a daily basis. Wind speeds influenced fish community composition, with Pacific sand lance associated with periods of strong, persistent Easterly winds, while Arctic cod were associated with strong, persistent westerlies. This phenomenon is similar to the Krill Trap described by Steve Okkenen and Carin Ashjian further offshore.
5. Fine scale habitat mapping showed that strong storms restructured benthic habitat.
6. Latitudinal patterns in energy content of capelin are probably complex due to variability in seasonal cycles in different habitats. Latitudinal patterns in growth rate are highly dependent on water temperature. Latitudinal patterns in carbon isotopes are dependent on freshwater discharge transporting allochthonous terrestrial carbon into nearby foodwebs. Latitudinal patterns in nitrogen isotopes are likely related to increased productivity near estuaries due to the influx of high trophic level nitrogen from decaying salmon carcasses as well as the inclusion of higher trophic level prey items. The Arctic nearshore may be a suboptimal habitat for capelin as suggested by low energy density, low growth rates, empty stomachs and enriched nitrogen signatures that are indicative of starvation.
7. Of the 23 marine Arctic fish species measured, the top 5 most energy dense (kJ/g wet mass) fish species were Pacific herring, Arctic/Bering/least cisco, and Pacific sand lance. Arctic cod are the most energy dense of the abundant and widely distributed species. On a relative mass basis, saffron cod have 25% less energy density than Arctic cod.
8. When accounting for fish size, saffron cod can be significantly larger than Arctic cod, conferring a total energy content per fish nearly 4 times as much as Arctic cod or 7 times that of capelin.
9. When considering prey quality of Arctic fish, energy density, fish size and fish distribution need to be considered.

Future considerations:

1. Research: Improve our understanding of the entire Elson Lagoon hydrodynamics with a oceanographic measurements from all passes simultaneously.
2. Research: measure seasonal energy content (winter) and condition of important fish prey species, including Arctic cod, capelin and fourhorn sculpin. Document age, diet, and maturation stage in relation to energy content.
3. Research: develop a long-term index of the nearshore community dynamics and identify linkages with variation in abiotic factors.

13.0 Synthesis

R. Heintz, J. Vollenweider

13.1 Summary

The nearshore ecotone around Point Barrow, Alaska is bordered by the biological communities and processes associated with the adjacent Chukchi Sea, Beaufort Sea and Elson Lagoon. The area is physically complex; Barrow Canyon transects the Chukchi shelf to the west of Point Barrow while the Beaufort Sea shelf to the east is broad and shallow. Along the Beaufort coast a series of barrier islands demarks the seaward boundary of the extensive Elson Lagoon (~200 km², Chapter 2) which receives riverine inputs via Dease Inlet. This geography sets up oceanographic processes modulated by the Alaska Coastal Current, the Beaufort Gyre, density gradients and prevailing easterly winds (Phillips and Reiss 1985; Aagaard and Roach 1990; Ashjian et al. 2010). Fish communities in the region include species representative of coastal estuarine systems (nearshore residents), anadromous populations associated with nearby rivers and deeper dwelling populations characteristic of the more saline waters over the continental shelf and shelf break. The interactions between physical drivers and biological communities are evident in the relatively small area we studied near Point Barrow between 2012 and 2015 (Chapter 1). Here we summarize the findings described in earlier chapters after providing a more detailed description of our study area. We follow this with a brief discussion of the potential agents of change in the region.

13.2 Study area

Benthic substrates found near Point Barrow are characterized by a low gradient bottom covered with Quaternary deposits ranging from sand to gravel (Chapter 1). Benthic habitats inside Elson Lagoon are overlaid with flocculent particulates derived from eroded tundra. Climatic events can influence benthic structure. Ice scour remodels the benthic habitat annually and the effects were clearly evident in our multi-beam surveys (Chapter 1). In addition, large scale wind events result in storm surge and wave activity that rework benthic substrates.

The low gradient bottom results in shallow water depths near Point Barrow, particularly in Elson Lagoon (3 m, Chapter 2). Erosion of tundra produces terrestrially-derived particulates in Elson Lagoon and these are frequently resuspended by wind resulting in turbid waters (Chapter 10). In addition, the shallow Elson Lagoon is fed by large volumes of freshwater discharged into Dease Inlet, which sets up a density-driven front whose position moves along the east-west axis of the lagoon. Waters in the lagoon communicate with those of the Beaufort Sea via a series of openings found among a chain of barrier islands. The connecting waterway between Elson Lagoon and the Beaufort Sea closest to Point Barrow (Eluitkak Pass) is narrow with a deep channel (16 m) while the entrances further east are shallower and much broader (Chapters 1 and 2).

The oceanography near Point Barrow results from a complex hydrodynamic interaction between the Chukchi and Beaufort Seas, and their respective coastal currents, which produces a physically and biologically dynamic environment. The Alaska Coastal Current (ACC) is compressed along the Chukchi coast and transports water and material northward from the Bering Strait to Point Barrow (Figure 1; Danielson et al. 2006). It intersects the westward flowing Beaufort gyre at the outlet of Barrow Canyon and Coriolis forces turn it eastward into the western Beaufort Sea. As the ACC moves along the Beaufort coast it sets up a boundary with

the Beaufort gyre. Adjacent to this boundary is the strong tidally- and storm-driven flow between the Beaufort Sea and the Elson Lagoon system (Chapters 2 and 3) which connects to the Beaufort via Eluitkak Pass (Chapter 1). In summer, predominantly strong, easterly winds drive the warm brackish water out of the lagoon and along the Beaufort coast towards Point Barrow (Chapter 2). These easterlies can be sufficiently energetic to reverse the ACC (Okkonen 2008; Weingartner et al. 2009), which causes deep water from the Beaufort shelf break to upwell onto the shelf transporting nekton and nutrients towards shore (Ashjian et al. 2010). The energetic and continually adjusting flows around Point Barrow support productive waters (Watanabe et al. 2012) and a relatively high density of pelagic forage fish can be found there (Crawford 2009).

13.3 The Point Barrow Ecotone

13.3.1 The Alaska Coastal Current connects the Chukchi Sea to the Beaufort Sea
The ACC is a density-driven current characterized by relatively brackish and warm waters during the ice free season. Density driven currents are a common feature along the perimeter of the Arctic Basin and are referred to as the riverine coastal domain (RCD) (Carmacks et al. 2015). Important components of the RCD include relatively warm temperatures, low salinity and high concentrations of particulates and colored dissolved organic material (CDOM) (Carmacks et al. 2015). These conditions are optimal for anadromous species occupying the RCD including coregonids and osmerids that prefer low salinity waters (Thorstenson and Love 2016, Roux 2016).

Our analysis of the waters near Point Barrow is consistent with the general RCD model. Salinities in the very nearshore varied widely from a low of 4 ppt to 35 ppt. Similarly, temperatures ranged from -0.3 °C to 12 °C (Chapter 1). Li et al. (Chapter 2) demonstrates how a strong counter wind current at the Eluitkak Pass connects waters of Elson Lagoon to the Beaufort Sea. When there is northeasterly wind, the subtidal current at the pass moves against the wind and water flows out of the Lagoon, while water moves into the lagoon through the much wider openings on its eastern side. The whole lagoon with its multiple openings works as a system that can “amplify” the wind effect so that the pressure gradient established by the wind stress can be relieved through relatively strong flows in the narrow pass. Consequently, wind drives the movement of water-borne material in and out of Elson Lagoon. The importance of this connection is emphasized by our observations (Chapter 10) of elevated numbers of phytoplankton particles in Elson Lagoon relative to the Beaufort Sea and Chukchi Sea, which suggests that stratified nutrient-rich waters of Elson Lagoon can be a source of carbon for pelagic organisms residing in shallow coastal waters.

13.3.2 Species composition and ages reveal connections between nearshore and offshore

The communities of fish caught near Point Barrow were representative of two major ecological groups: a “lagoon” group and a “marine” group. Each group’s frequency of occurrence and relative abundance depended on water body (Chapter 3). Species from the “lagoon” group were primarily encountered in Elson Lagoon. While species from the marine group could be found in Elson Lagoon they were more frequently encountered and most abundant in marine waters. Species typical of the lagoon group included anadromous species such as Ciscoes, Rainbow Smelt and Salmon as well as Fourhorn Sculpin, Plain Sculpin and Arctic Flounder. Marine species, such as Arctic Cod, Saffron Cod, and Pacific Sand lance were most frequently caught in

the marine water bodies. Capelin and Slender Eelblennies were found just as frequently in Elson Lagoon and the marine waters, but their abundance was greatest in marine waters. It is important to note that catches in all locations were dominated by species from the family Cottidae. This was the most speciose family caught throughout the study area. However, there were species were found in different locations. For example, Hairhead, Shorthorn and Arctic Sculpins were associated with the marine group while Fourhorn Sculpin were associated with the “lagoon” type.

Fish abundance and diversity was influenced by temperature. In 2014, the coldest year, the catch per unit effort (CPUE) in all water bodies (Chapter 4) was approximately one quarter that of 2013 and half of 2015. Not only was CPUE depressed in the cold year, but the fewest number of species was observed in 2014. Species apparently unaffected by cold temperatures included Fourhorn Sculpin, Arctic Cod, Alligator Fish and Pacific Sand Lance as demonstrated by constant frequencies of occurrence across years. Fish most frequently encountered in warm years included Arctic Flounder, Capelin, Arctic Shanny, Tubenose Poacher and Slender Eelblennies. An important finding was that the fish representative of the marine species, such as Arctic Cod, were primarily larvae and juveniles. Arctic Cod, Saffron Cod, and Capelin were predominately age-0 fish in all catches (Chapter 5). While older fish were captured, the median size of these species was within the range of those aged 0. For example, more than one third of the Arctic Cod captured in beach seines were less than 27 mm long. In comparison, very few Arctic Cod that small (2% of the catch) were caught in a coincident offshore survey in 2013, though the smallest Arctic cod caught offshore was 19 mm. In addition, many of the near shore resident species such as Arctic Shannies, Slender Eelblennies, Sculpins and Pacific Sand lance were also dominated by juvenile size classes (Chapter 5, Robards et al. 2002) with relatively few adult forms. Conversely, the amphidromous species were dominated by adult forms including Rainbow Smelt and the Ciscoes. These data indicate that the amphidromous species are using the Point Barrow area as a feeding ground while offshore “marine” species and nearshore residents were using these very nearshore habitats as a nursery.

13.3.3 Feeding histories through diet analysis and isotopes reveal large scale spatial trends

Fishes near Point Barrow exploited a wide variety of pelagic zooplankton and benthic macroinvertebrates effectively linking prey of differing qualities to upper trophic level predators. The variety of prey is evident from the cumulative prey curves which indicated that more than 20 stomachs were needed to adequately characterize a given species’ diet, even when their prey were lumped into broad categories (Chapter 6). Much of the variety related to the size of the fish sampled. Pacific Sand lance, Capelin, Rainbow Smelt, Arctic Cod and Cottids all changed diet as they grew. For the non-Cottids these shifts included decreasing consumption of copepods in favor of larger prey such as amphipods and mysids. In contrast, Cottids focused primarily on amphipods and switched to piscivory at around 100 mm. The importance of this piscivory to the remaining species is currently unknown, but Cottids were the most frequently caught group and are known predators of Capelin and Pacific Sand lance (Chapter 6). While less than 1% of the Cottids caught in beach seines were larger than 100 mm, nearly 60% of the Cottids caught in slightly deeper water (>2 m) were larger than 100 mm (Chapter 5) indicating small fish in nearshore habitats may be an important source of nutrition to local Cottids.

Isotopic analysis indicated that carbon sources associated with riverine inputs were much less important to organisms from the nearshore areas around Point Barrow than in nearshore areas further south and east. A known feature of the waters near Point Barrow is the enrichment of $\delta^{13}\text{C}$ relative to the eastern Beaufort Sea (Suape et al. 1989, Schell et al. 1998, Dunton et al. 2006) and Bering Strait (Schell et al. 1998; Chapter 9). Enrichment of $\delta^{13}\text{C}$ along these coasts is believed to relate to the diminishing influence of riverine inputs as the area is bracketed by the McKenzie River to the east and the Yukon River to the south. We observed a similar effect among mysids, sculpins and blennies sampled from Elson Lagoon compared with reports from the eastern Beaufort Sea (Chapter 8; Dunton et al. 2012). Similarly, capelin become progressively enriched with $\delta^{13}\text{C}$ from the Bering Strait northward to Point Barrow (Chapter 9). Further offshore the westward enrichment of $\delta^{13}\text{C}$ was less pronounced (McTigue et al. 2014; Marsh et al. 2017). Thus there is a diminishing influence of terrestrial productivity in marine organisms as distance increases from river mouths and more so offshore.

Despite the diminished role of riverine carbon, multiple carbon sources are integral to the maintenance of the different fish communities around Point Barrow. Levels of $\delta^{15}\text{N}$ were inversely related to $\delta^{13}\text{C}$ in biota collected from Elson Lagoon (Chapter 8) because higher trophic level consumers apparently derived carbon from a variety of sources. Carbon in the diets of Cottids was most enriched with $\delta^{13}\text{C}$ consistent with lower trophic biota (e.g. mysids, gammarids, hyperids, and isopods) (Chapter 8). Pacific Sand lance, Capelin and Slender Eelblennies had intermediate levels of $\delta^{13}\text{C}$ enrichment (Chapter 6) which was consistent with reports of $\delta^{13}\text{C}$ in copepods from the northeastern Chukchi (Marsh et al. 2017). Fish consuming the sources most depleted in $\delta^{13}\text{C}$ were Rainbow Smelts and Least Ciscoes. The low levels of $\delta^{13}\text{C}$ in Rainbow Smelt are less than those of phytoplankton (McTigue et al. 2014) or suspended particulate organic matter (SPOM) in the northeastern Chukchi (Marsh et al. 2017). Carbon becomes enriched with $\delta^{13}\text{C}$ as trophic levels increase, hence Rainbow Smelt must have been consuming a diet that was derived from an even more depleted source than the nearby marine environment offered. Perhaps terrestrially derived prey, such as the dipterans observed in the diets of Least Ciscoes (Chapter 6), are also important to Rainbow Smelt.

For pelagic species the source of carbon may not have much bearing on their condition. No difference was detected in the energy densities of fish from the different water bodies (Chapter 7). On a broader scale than addressed in this study, we note $\delta^{13}\text{C}$ in Capelin tissues become enriched with latitude in the Alaska Coastal Current along the length of the Chukchi coast, as does their energy density (Chapter 9). However, Capelin sampled in the very nearshore waters around Point Barrow contradicted this rule by having relatively low energy densities. Comparisons of the energy density of herring in the Arctic nearshore with those from the Gulf of Alaska failed to reveal differences in condition (Chapter 7). It could be that fishes sampled in the very nearshore near Point Barrow had lower energy densities because nearshore temperatures were elevated (Chapter 9), fish were diverting energy to growth rather than storage (Martin et al. 2017), or that the nutritional rewards of the nearshore are less than those offshore.

13.4 Sources of change

Warming conditions in the Arctic are likely to have a variety of direct and indirect impacts on the nearshore. Prolonged ice-free periods are motivating increased transportation and resource development in the region. Development of nearshore areas would have a direct effect on the availability of habitat. Nearshore fish are accustomed to annual remodeling of the benthic habitat

as a result of ice scour (Chapter 1; Shapiro et al. 1991), but impacts during the summer ice-free season are expected to increase from increasing storms (Chapter 1) and human development. Anthropogenic contamination of benthic habitats, particularly by petroleum hydrocarbons is another potential direct effect of increased human activity. Petroleum hydrocarbons can exert effects on juvenile fish through a wide range of metabolic pathways resulting in narcosis, teratogenic effects and carcinoma (Incardona et al. 2005). Moreover, these effects may be differentially expressed among species (e.g. Jung et al. 2015) potentially altering community structure. This may be important because the Arctic nearshore appears to be an important nursery for many forage species.

Change in the nearshore around Point Barrow directly related to climate conditions will include warming temperatures, alterations in ice phenology, shoreline erosion, and increased freshwater discharge. Warming air temperatures are evident in the area around Point Barrow since the 1940's (Chapter 1). Similarly, water temperature of the Chukchi Sea has gradually increased over the last 80 years. During this time, interannual variability in water temperature resulting in "warm" and "cold" conditions in the marine waters around Point Barrow (Luchin and Pantelev 2014) preview the impending changes to the region. Warm conditions are characterized by the northeastward flow of warm Pacific waters "down" through Barrow Canyon while cool conditions divert Pacific waters further from shore through Herald Canyon causing cold Arctic basin waters to move in the opposite direction "up" into Barrow Canyon (Luchin and Pantelev 2014). Cold conditions were observed during offshore surveys near Point Barrow in 2013. However in the nearshore 2014 was the coolest year studied (Chapter 1) and the lower temperatures were associated with changes in fish community structure and reduced abundance (Chapter 4). Each of these conditions brings its own zooplankton community into the waters around Point Barrow (Pinchuk et al. 2017), which will affect food web structure. Increased frequency of warm conditions will alter the fish community structure in the area around Point Barrow, as indicated by effect of sampling year on our analysis of community composition (Chapter 4). This was primarily due to the presence of forage species associated with Pacific waters (Capelin, Pacific Sand lance) in 2013, the warmest and calmest of the three years surveyed (Chapter 1).

Changing ice conditions are a conspicuous feature of the nearshore around Point Barrow. The ice-free period is increasing asymmetrically. The timing of ice breakup in the spring/summer is remaining relatively constant while the timing of ice-up is becoming progressively delayed (C. George, personal communication; Chapter 1). It is unclear how this might affect the nearshore fish communities around Point Barrow. We observed a distinct temporal pattern to species richness (Chapter 4). Regardless of the temperature and timing of ice retreat we consistently observed a peak in richness four to five weeks after shore-fast ice was gone. Abundance of juvenile gadids was highest in the week immediately following ice retreat in all years. This is consistent with observations that age-0 Arctic Cod are following the ice edge as it retreats. We were unable to evaluate fish community structure more than 7 weeks following ice retreat due to conflicts with local whaling operations. However, models of beluga whale foraging by Hauser et al. (2017) suggest movement of sea ice is likely to affect whale habitat selection. The implication is that sea ice location may be influencing the distribution of their forage which includes Saffron Cod, Arctic Cod, and Pacific Sand lance (Quakenbush et al. 2015). More work will be required to understand the impacts of prolonging the ice free period on the nearshore fish communities.

Along with warming conditions freshwater discharge can be expected to increase in the Arctic with concomitant impacts on density driven currents and the distribution of density fronts in nearshore areas. Freshening is likely to have a direct impact on the quality of forage for nearshore fishes. Freshening conditions influence the size of the particles in the phytoplankton bloom (Li et al., 2009), producing profound effects on food web structure (Li et al., 2009). Our studies revealed an increased range of salinities in 2013, the warmest year. This resulted in a broader temperature/salinity envelope which increased the range of conditions available to nearshore fishes (Chapter 1). Thus, the frequency with which amphidromous species were observed outside Elson Lagoon was greater in 2013 than 2014 or 2015 (Chapter 1, Chapter 3). Conversely, Arctic Cod were caught most frequently when salinity was highest. Coincidentally, interannual variation was an important explanatory variable in the Canonical Correspondence Analysis (Chapter 4), accounting for 15% of the variability in community structure, which was about half that of the combined effects of air temperature, salinity, and wind conditions. A similar analysis also determined that salinity was a more important driver of community composition than temperature in the Husky Lakes area on the coast of the Canadian Beaufort (Roux et al. 2015).

The ecotone around Point Barrow is dynamic and complex. Its proximity to Utqiavik (formerly known as Barrow) makes it a prime location for subsistence harvest of birds, marine mammals and fish. The forage base for these species comprises the species evaluated in this study. The availability and quality of these prey will likely change as warming continues in the region. This will have direct impacts on the ability of local hunters to provision their community. This study provides important baseline information on their abundance, distribution, diets, condition and age structure that can be used to assess change in the future. Currently our understanding of this area is too limited to produce predictions of how change will occur. However, our results can lead to more specific questions about the fate of the little fish residing in the Point Barrow nearshore.

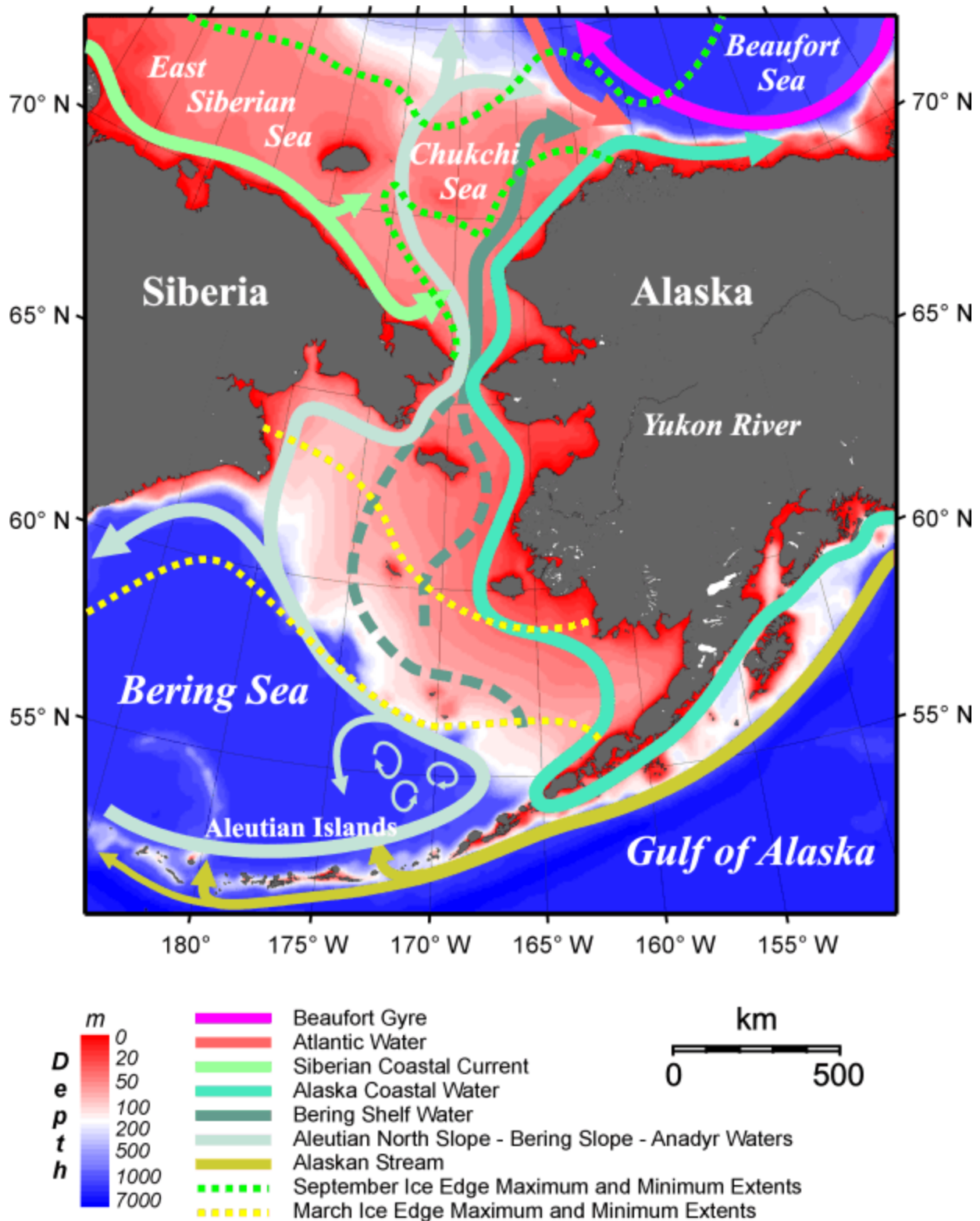


Figure 13.1 Schematic of ocean currents converging at Point Barrow (taken from Danielson et al. 2006).

13.5 References

- Aagaard, K., and A. T. Roach. 1990. Arctic ocean-shelf exchange: Measurements in Barrow Canyon. *Journal of Geophysical Research* 95(C10):18163–18175.
- Ashjian, C. J., S. R. Braund, R. G. Campbell, J. C. George, J. Kruse, W. Maslowski, S. E. Moore, C. R. Nicolson, S. R. Okkonen, B. F. Sherr, B. E. Sherr, Y. H. Spitz. 2010. Climate variability, oceanography, bowhead whale distribution, and Iñupiat subsistence whaling near Barrow, Alaska. *Arctic*. 63(2):179–194.
- Carmack, E., P. Winsor, and W. Williams. 2015. The contiguous panarctic Riverine Coastal Domain: A unifying concept. *Progress in Oceanography* 139:13-23.
- Crawford, R. E. 2009. Forage fish habitat distribution near the Alaskan coastal shelf areas of the Beaufort and Chukchi seas. Prince William Sound Oil Spill Recovery Institute, Project 09-10, Cordova, Alaska.
- Danielson, S., K. Aagaard, T. Weingartner, S. Martin, P. Winsor, G. Gawarkiewicz, and D. Quadfasel. 2006. [*The St. Lawrence polynya and the Bering shelf circulation: New observations and a model comparison*](#). *Journal of Geophysical Research* 111(C9).
- Dunton, K. H., T. Weingartner, and E. C. Carmack. 2006. The nearshore western Beaufort Sea ecosystem: circulation and importance of terrestrial carbon in arctic coastal food webs. *Progress in Oceanography* 71(2):362-378.
- Dunton, K. H., S. V. Schonberg, and L. W. Cooper. 2012. Food web structure of the Alaskan nearshore shelf and estuarine lagoons of the Beaufort Sea. *Estuaries and Coasts* 35(2):416-435.
- Hauser, D. D., K. L. Laidre, H. L. Stern, S. E. Moore, R. S. Suydam, and P. R. Richard. 2017. Habitat selection by two beluga whale populations in the Chukchi and Beaufort seas. *PloS one* 12(2):e0172755.
- Incardona, J.P., M. G. Carls, H. Teraoka, C. A. Sloan, T. K. Collier, and N. L. Scholz. 2005. Aryl hydrocarbon receptor-independent toxicity of weathered crude oil during fish development. *Environmental Health Perspectives*, 113(12), p.1755.
- Jung, J. H., M. Kim, U. H. Yim, S. Y. Ha, W. J. Shim, Y. S. Chae, H. Kim, J. P. Incardona, T. L. Linbo, and J. H. Kwon. 2015. Differential toxicokinetics determines the sensitivity of two marine embryonic fish exposed to Iranian Heavy Crude Oil. *Environmental science & technology* 49(22):13639-13648.
- Li, C., E. Weeks, and J. L. Rego. 2009. In situ measurements of saltwater flux through tidal passes of Lake Pontchartrain estuary by Hurricanes Gustav and Ike in September 2008. *Geophysical Research Letters* 36(19).
- Luchin, V., and G. Panteleev. 2014. Thermal regimes in the Chukchi Sea from 1941 to 2008. *Deep Sea Research Part II: Topical Studies in Oceanography* 109:14-26.
- Marsh, J. M., F. J. Mueter, K. Iken, and S. Danielson. 2017. Ontogenetic, spatial and temporal variation in trophic level and diet of Chukchi Sea fishes. *Deep Sea Research Part II: Topical Studies in Oceanography* 135:78-94.
- Martin, B. T., R. Heintz, R., Danner, E.M., and Nisbet, R.M., 2017. Integrating lipid storage into general representations of fish energetics. *Journal of Animal Ecology*.
- McTigue, N. D., and K. H. Dunton. 2014. Trophodynamics and organic matter assimilation pathways in the northeast Chukchi Sea, Alaska. *Deep Sea Research Part II: Topical Studies in Oceanography* 102:84-96.
- Okkonen, S. R., and Alaska Outer Continental Shelf Region. 2008. Exchange between Elson Lagoon and the nearshore Beaufort Sea and its role in the aggregation of zooplankton.

- US Department of Interior, Minerals Management Service, Alaska Outer Continental Shelf Region, Final Report M06PX00011. Fairbanks, Alaska.
- Phillips, R. L., and T. E. Reiss. 1985. Nearshore marine geologic investigations, Point Barrow to Skull Cliff, northeast Chukchi Sea. US Department of the Interior, Geological Survey, Report 85-50. Menlo Park, California.
- Pinchuk, A. I. and L. B. Eisner. 2017. Spatial heterogeneity in zooplankton summer distribution in the eastern Chukchi Sea in 2012–2013 as a result of large-scale interactions of water masses. *Deep Sea Research Part II: Topical Studies in Oceanography* 135:27-39.
- Robards, M. D., G. A. Rose, and J. F. Piatt. 2002. Growth and abundance of Pacific sand lance, *Ammodytes hexapterus*, under differing oceanographic regimes. *Environmental Biology of Fishes* 64(4):429-441.
- Quakenbush, L. T., R. S. Suydam, A. L. Bryan, L. F. Lowry, K. J. Frost, and B. A. Mahoney. 2015. Diet of beluga whales (*Delphinapterus leucas*) in Alaska from stomach contents, March–November. *Marine Fisheries Review* 77:70-84.
- Roux, M. J., L. A. Harwood, X. Zhu, and P. Sparling. 2016. Early summer near-shore fish assemblage and environmental correlates in an Arctic estuary. *Journal of Great Lakes Research* 42(2):256-266.
- Saupe, S. M., D. M. Schell, and W. B. Griffiths. 1989. Carbon-isotope ratio gradients in western arctic zooplankton. *Marine Biology* 103(4):427-432.
- Schell, D. M., B. A. Barnett, and K. A. Vinette. 1998. Carbon and nitrogen isotope ratios in zooplankton of the Bering, Chukchi and Beaufort seas. *Marine Ecology Progress Series* 162:11-23.
- Shapiro, L. H., and P. W. Barnes. 1991. Correlation of nearshore ice movement with seabed ice gouges near Barrow, Alaska. *Journal of Geophysical Research:Oceans* 96(C9):16979–16989.
- Thorsteinson, L. K., and M. S Love. 2016. Alaska Arctic marine fish ecology catalog. U.S. Geological Survey, Report 2016-5038 (OCS Study, BOEM 2016-048). Anchorage, Alaska.
- Watanabe, E., M. J. Kishi, A. Ishida, and M. N. Aita. 2012. Western Arctic primary productivity regulated by shelf-break warm eddies. *Journal of Oceanography* 68(5):703-718.
- Weingartner, T. J., S. L. Danielson, J. L. Kasper, and S. R. Okkonen. 2009. Circulation and water property variations in the nearshore Alaskan Beaufort Sea (1999 – 2007). Publications of the US Geological Survey, Paper 88.

14.0 Management and Policy Implications

In February 2009 the North Pacific Fishery Management Council (NPFMC) voted to proactively protect fishery resources in the federally-managed waters in the Arctic by banning commercial fishing from the Bering Strait to the U.S.-Canadian border. That area includes all waters in the U.S. Exclusive Economic Zone of the Chukchi and Beaufort Seas from 3 to 200 nmi from land. Fishing industry and environmental advocates approved of the council's decision because all agreed that even in 2009, prior to the lowest recorded sea ice in 2012, the melting of sea ice outpaced regulators' ability to manage Arctic Ocean waters. At the time of the unprecedented decision to ban U.S. commercial fishing in the Arctic Ocean, there was no fishing of any major scale occurring in the Arctic. However, the NPFMC decided to write an Arctic Fishery Management Plan (FMP) to control commercial fisheries if they should develop. The NPFMC ruled that scientists and policymakers must be able to better assess resources in the region before allowing fishing. Following that historic decision, an Arctic Fishery Management Plan (FMP) that prohibits new commercial fishing in Beaufort Sea waters was adopted by the NPFMC and approved by the Secretary of Commerce.

In August 2015, the five Arctic countries with coastlines bordering the Arctic Ocean, Canada, Denmark, Norway, Russia and the U.S., signed a non-binding voluntary agreement to bar commercial fishing in the Central Arctic Ocean (Hoag 2016). The nations agreed to keep commercial fishing vessels out of the region until scientists have improved their understanding of the region and can produce science-based assessments of the fish stocks and distribution. Experts from those countries are examining the links between fish stocks and the adjacent ecosystems. In December 2015 there was discussion of a binding agreement on Arctic fisheries. Those talks included not only the five Arctic nations, but also other governments (China, Japan, South Korea, Iceland, and the European Union) that are interested in fishing in the international waters of the central Arctic (Sturzik 2016). A binding agreement has yet to be reached.

The US Arctic FMP closes the Arctic management area to commercial fishing so that unregulated fishing does not occur until sufficient information is accrued to allow fishing to be conducted sustainably, and with due concern for other ecosystem components (NPFMC 2009). The FMP as currently written could allow the area to be opened in the future. However no fishing would be approved until research shows that fisheries could be conducted sustainably and without harm to the ecosystem, i.e., including seabirds, seals, and whales, in consultation with Native residents. The FMP states that knowledge of the current status of fish populations in the Arctic is necessary to identify fish species potentially vulnerable to oil and gas exploration, their life stages, essential fish habitat, and to inform the new emphasis on food web modeling and Arctic climate change issues. The results of this study inform some of those objectives.

Valuable life stage and habitat information was amassed at multiple spatial and temporal scales around Barrow, Alaska during this study. It is apparent that abundance and distribution of fishes is dependent upon species and life stage. The largest Least Cisco, Rainbow Smelt and Saffron Cod were found in Elson Lagoon, indicating the lagoon is essential fish habitat for adults of these species. However, younger smaller Rainbow Smelt and Saffron Cod were also found in the lagoon, with fewer numbers outside the lagoon. In contrast, another important forage fish, Arctic Cod, was very abundant and large in the Chukchi, although age-0 and age-1 Arctic Cod were

captured in the Chukchi and Beaufort Seas as well as in Elson Lagoon. Sculpins of all ages and sizes were collected in all three regions. Some species were small in all three areas, e.g., Arctic Shanny (<40 mm) and Pacific Sand Lance (<100 mm). This information can be compared with collections across the Chukchi and Beaufort Seas to establish a benchmark of the importance of very nearshore and lagoon areas as essential fish habitat for Arctic fish species.

A compelling reason for the U.S. and the other Arctic nations to prevent commercial fishing in the Arctic is the very real concern about warming, loss of sea ice, and potential impacts on the ecosystem, specifically the food web. This project examined food dynamics and diets of fishes in the nearshore environment. As with abundance and distribution, diets varied with fish species and life stage. Interestingly, diet varied for some species among the three regions, indicating feeding is more dependent on food availability than preference in these nearshore areas. Results of this study indicate that food webs may be longer and more complex than previously believed, meaning ecosystem changes due to a warming Arctic could either be dampened because of redundancies or exacerbated by multiple point of vulnerability.

One of the arguments for the Arctic FMP in 2009 was that the science needs to catch up with the rate of change in the Arctic (Hoag 2016). That is still true, but the paucity of knowledge about fishes in the Arctic that was recognized by the North Pacific Fisheries Management Council (NPFMC 2009) has been lessened by the contributions of this study.

14.0 References

- Barnes, P. W., D. M. Schell, E. Reimnitz. 1984. The Alaskan Beaufort Sea: Ecosystems and environments. Academic Press, Inc. Orlando. 466 p.
- Bouchard, C., L. Fortier. 2011. Circum-Arctic comparison of the hatching season of polar cod *Boreogadus saida*: A test of freshwater winter refuge hypothesis. *Prog. Ocean.* 90(4): 105-116.
- Hoag, H. 2016. Nations negotiate fishing in Arctic high seas. *Arctic Deeply*, 28 April 2016, <https://www.newsdeeply.com/arctic/articles/2016/04/28/nations-negotiate-fishing-in-arctic-high-seas> (accessed 31 August 2016)
- Logerwell, E., M. Busby, C. Carothers, S. Cotton, J. Duffy-Anderson, E. Farley, P. Goddard, R. Heintz, B. Holladay, J. Horne, S. Johnson, B. Lauth, L. Moulton, D. Neff, B. Norcross, S. Parker-Stetter, J. Seigle, T. Sformo. 2015. Fish communities across a spectrum of habitats in the western Beaufort Sea and Chukchi Sea. *Prog. Ocean.* 136: 115-132.
- NPFMC. 2009. Fisheries Management Plan for Fish Resources of the Arctic Management Area. North Pacific Fishery Management Council. 605 West 4th Ave, Suite 306, Anchorage, AK.
- Struzik, E. 2016. Welcome to the Arctic, fish. *Hakai Magazine*, 22 August 2016, <https://www.hakaimagazine.com/article-long/welcome-arctic-fish> (accessed 31 August 2016)



The Department of the Interior Mission

As the Nation's principal conservation agency, the Department of the Interior has responsibility for most of our nationally owned public lands and natural resources. This includes fostering sound use of our land and water resources; protecting our fish, wildlife, and biological diversity; preserving the environmental and cultural values of our national parks and historical places; and providing for the enjoyment of life through outdoor recreation. The Department assesses our energy and mineral resources and works to ensure that their development is in the best interests of all our people by encouraging stewardship and citizen participation in their care. The Department also has a major responsibility for American Indian reservation communities and for people who live in island territories under US administration.



The Bureau of Ocean Energy Management

As a bureau of the Department of the Interior, the Bureau of Ocean Energy Management (BOEM) primary responsibilities are to manage the mineral resources located on the Nation's Outer Continental Shelf (OCS) in an environmentally sound and safe manner.

The BOEM Environmental Studies Program

The mission of the Environmental Studies Program (ESP) is to provide the information needed to predict, assess, and manage impacts from offshore energy and marine mineral exploration, development, and production activities on human, marine, and coastal environments.